ANALYSIS OF GEOLOGICAL, TECHNICAL AND ECONOMIC ASPECTS OF GEOTHERMAL RESOURCE POTENTIAL IN AQUACULTURE APPLICATION IN BALTIC SEA REGION: LITHUANIAN CASE

Prof. Dr. Mayur Pal – Kaunas Technology University, Lithuania

Dr. Sigitas Petrauskas – Lithuanian Geothermal Association LGA, Lithuania

Prof. Dr. Saulius Sliaupa – Nature Research Centre, Lithuania

Contents

1. Glossary of Geothermal Terms

Shallow geothermal – depth of 150 m (based on the history of exploitation in Lithuania). For comparison: 500 m in Switzerland, 400 m in Germany, and 300 m in Austria.

Geothermal water - water heated within the earth by natural phenomenon to a temperature of 30°C or more

Heat flow – the movement of heat from within the Earth to the surface, where it is dissipated into the atmosphere, surface water, and space by radiation

Thermal water - is groundwater with a surface temperature of 20°C gushing from natural springs or exploited with production wells

Thermal gradient - the rate of increase or decrease in the Earth's temperature relative to depth (°C/m). Commonly used °C/100 m

Salinity - a measure of the quantity or concentration of dissolved salts in water. Water classification (https://www.fao.org/4/T0667E/T0667E00.htm):

Water class	Salt concentration (mg/l)
Non-saline	< 500
Slightly saline	500 – 1500
Moderately saline	1500 – 7000
High saline	7000 – 15000
Very high saline	15000 – 35000
Brine	>35000

Total dissolved solids (TDS) – the term used to describe the amount of solid materials in water

Potable and service water - drinking water is sweet water with a very high degree of purity, so it is suitable for human consumption

Aquitard - large rock formation with low permeability, not capable of yielding groundwater.

Geothermal field/system - a discrete area where geothermal energy is known to be found and includes all areas that are hydrologically linked

Permit area - anybody, who wants to explore geothermal energy in an area free for mining needs a concession. Anybody, who wants to exploit geothermal energy needs authorization or the mine's property.

Calculation of installed capacity - data of installed geothermal power and used energy are of particular interest to the general public. The installed geothermal capacity must be calculated. The basis is initially the installed geothermal capacity:

(1) $P = \varrho F * cF * Q * (Ti - To)$

with

P installed geothermal capacity [W]
ϱF density of the fluids [kg m^{-3}]
cF (isobar) specific heat capacity [J kg^{-1} K^{-1}]

Q flow rate in operation [m^3 s^{-1}]
Ti, To (input resp. output) temperature [°C].

Deep geothermal - consists of systems that exploit geothermal energy with deep boreholes and using the energy directly, without raising its temperature

Doublet - for hydrothermal utilization, water will be hoisted from deep water-bearing aquifers and a heat exchanger accumulates the geothermal energy. The cooled water will be reinjected into the aquifer by a second borehole at a sufficient distance from the production borehole (doublet operation). In general is a combination of a number of production and reinjection boreholes possible

Singlet - the geothermal exploitation with a single well system or singlet only needs a production well because the extracted water will not be reinjected. This is the case for example in the balneological utilization

Re-injection wells - are drilled to dispose of fluids derived from geothermal resources into an underground reservoir. This is done in consideration of the environment and it also maintains the pressure of the geothermal reservoir.

Deep vertical heat exchanger - deep vertical heat exchangers are closed systems, installed in wells with more than 400 m depth. The used technique is similar to the technique of a shallow borehole heat exchanger. In the closed system of the deep vertical heat exchanger circulates a heat carrier medium down to 3000 m depth. The transfer of the heat of the rocks to the circulating fluids in the heat exchanger goes through the backfilling material and the casing of the borehole. The cold fluid is piped down in the annular space of the double tube system (coaxial tube) regulated by quantities. It will be heated up convectively because of its slow motion (5 – 66 m/min) and rise to the surface in the isolated internal pipe. Deep vertical heat exchangers are not relying on good permeable aquifers.

Drilling Fluid - drilling fluid is a complex gas or liquid mixture that is primarily used to suspend and remove cuttings from the well during drilling. This mixture includes water, clay and other additives. It is also known as drilling mud.

Deimena RSt.- refers to the Deimena Regional Stage, a geological unit within the Cambrian period of the Baltic basin.

Fm - is an abbreviation for **"Formation."** A formation is a fundamental unit of stratigraphy, used to describe a distinct layer of rock or sediment that has consistent characteristics and can be mapped across a geographic area.

Well casing - the installation of a string of steel metal to the well bore. This is done to give stability to the well bore, prevent the influx of groundwater, provide support for drilling equipment, support the permanent well head (on completion of drilling) and provide a channel through which steam flows to the surface.

A well test - a fluid flow test conducted to obtain data and information on the properties of the reservoir and the well. Well tests are done before tapping the reservoir, but also after a period of production, to see whether and how much the reservoir properties have changed.

Drawdown - reduction of the water level in a well and in its surrounding groundwater body due to water extraction

Geothermal potential - the fraction of geothermal heat available in the subsurface which can be extracted by technical measures like open and closed loop systems

Aquifer -A permeable rock layer that holds groundwater or geothermal fluids, often targeted for energy extraction due to its ability to store and transmit heat.

Binary Cycle Power Plant -A type of geothermal power plant where geothermal fluid heats a secondary fluid with a lower boiling point in a heat exchanger, which vaporizes and drives a turbine to generate electricity.

Cambrian Aquifer -A significant geothermal aquifer located in Lithuania, characterized by high temperatures suitable for various applications like aquaculture and district heating.

Coaxial Closed-Loop System -A geothermal system where a coaxial pipe configuration is used to circulate working fluid underground, allowing heat exchange without direct contact with geothermal fluids.

Direct-Contact Heat Exchanger -A heat exchanger that enables direct interaction between geothermal fluid and a working fluid, typically used in binary cycle power plants for efficient energy transfer.

Directional Drilling -A drilling technique that allows wells to be angled to reach geothermal resources not directly beneath the drilling site, enhancing flexibility and access to remote geothermal reservoirs.

Enhanced Geothermal Systems (EGS) - A method of creating artificial geothermal reservoirs by injecting water into hot, dry rock formations, which allows for heat extraction through engineered fractures.

Geothermal Gradient -The rate at which Earth's temperature increases with depth, typically around 25–30°C per kilometer, crucial for identifying viable geothermal energy sites.

Geothermal Heat Pump (GHP)- A system using stable underground temperatures to provide heating or cooling for buildings, offering a highly efficient and environmentally friendly alternative to conventional heating.

Heat Load Calculation-The process of determining the amount of heat energy needed to maintain a target temperature, used in geothermal systems for accurate energy planning and efficiency.

Horizontal Well-A type of well drilled horizontally or at an angle, increasing the reservoir exposure for enhanced geothermal fluid extraction and heat transfer efficiency.

Lithology-The study of rock characteristics, including mineral content and formation history, important for assessing geothermal reservoir properties like porosity and permeability.

Porosity-A measure of the void spaces in rock, reflecting a reservoir's capacity to store fluids such as geothermal water or brine.

Permeability-The ability of rock to allow fluids to flow through it, a critical factor in determining the efficiency of geothermal extraction from reservoirs.

Shell and Tube Heat Exchanger-A surface heat exchanger design where one fluid flows through a shell and another through tubes, commonly used in large geothermal power plants.

Submersible Pump-A type of pump installed inside a geothermal well to extract fluids from deep underground, typically used for higher-temperature geothermal resources.

Tornado Chart-A graphical representation used in sensitivity analysis to show the impact of different variables on a model's output, commonly used in geothermal reservoir assessments.

Two-Phase Fluid System-A geothermal fluid system containing both liquid and vapor phases, requiring specific handling and equipment to manage pressure and maximize energy output.

Vertical Well-A well drilled straight down, often used in geothermal applications where resources are directly below the drilling site.

Well Doublet-A configuration involving two wells—one for injection and one for production—used to circulate geothermal fluid within a closed system to extract heat efficiently.

Executive Summary

This study provided detailed aspect of the following elements:

- **Analysis of geothermal resources in Lithuania**
  - Provide available information on the distribution of geological layers, their depths and thicknesses, and their geothermal resources.
  - Provide current available information on the quantities of geothermal water and thermal energy.
  - Collect and present hydro chemical data on water: temperature and mineralization (provide numerical values for temperature and mineralization for the different layers), other parameters if available.

- **Overview of the use of geothermal resources**

  - Provide a summary of the current geothermal exploitation in Lithuania and worldwide, what are the trends.
  - A general overview of geothermal resource extraction technologies (heat and water/brine): drilling methods, pumps, heat exchangers, etc;
  - Overview of geothermal resource users in Lithuania and in neighboring (at least three) countries, their exploited resource characteristics, scope and technology.

- **Assessment of the potential of Western Lithuanian geothermal resources for aquaculture use**
  - Analysis of the potential opportunities for the exploitation of the resources of Western Lithuania Geothermal Anomaly: economic and technical aspects of resource exploitation, legal framework for resource extraction. Analysis of available information on existing wells in Lithuania.
  - Evaluate three potential/suitable technologies for heating water in closed aquaculture systems up to 30°C using geothermal resources (evaluate the maintenance of water temperature for 1000 to 10000 m^3 water volume with 2% renewal rate).
  - Evaluation of the economic, technical aspects of extracting 30 ppt, 100 ppt and 200 ppt salinity brines, including extraction from existing boreholes: investment, technology and operating costs, wastewater management. Prevalence and accessibility of 30 ppt and 30-degree geothermal brine.

1 Introduction

Geothermal energy is increasingly being recognized as a sustainable and renewable resource, with significant potential for reducing dependence on fossil fuels and supporting energy transition goals. In the Baltic Sea region, Lithuania stands out for its unique geothermal potential due to its geological setting within the Baltic Artesian Basin. This basin, characterized by various geothermal aquifers such as the Cambrian and Devonian formations, presents an opportunity for utilizing geothermal resources for various applications, including aquaculture, district heating, and energy generation.

This study focuses on the geological, technical, and economic aspects of geothermal resource potential in Lithuania, particularly in the context of aquaculture. With rising interest in renewable energy and sustainable development, understanding the geothermal resources' distribution, depth, temperatures, and economic feasibility becomes essential for harnessing this energy source effectively. The analysis includes an assessment of geothermal aquifers, reservoir characteristics, and their potential for direct use in heating systems, alongside an evaluation of the technical challenges associated with resource extraction.

By exploring the geothermal capabilities of Lithuania, this study aims to provide critical insights into the possibilities for utilizing geothermal energy in aquaculture, a growing sector that requires efficient and sustainable energy solutions. Moreover, the research will help guide future developments in geothermal energy use in Lithuania, aligning with the country's renewable energy objectives.

This document is structured to provide a comprehensive analysis of geothermal resource potential in Lithuania, particularly for aquaculture applications. It begins with an overview of the geological setting of the Baltic Sea region, detailing the geothermal aquifers' distribution, depth, and temperature profiles. Following this, the geothermal resources of Lithuania are examined, focusing on their current exploitation and potential uses.

The subsequent sections explore the technical aspects of geothermal extraction, including drilling methods, well types, and the technologies used for energy generation and storage. The economic evaluation covers cost estimates for different geothermal systems, along with an assessment of potential geothermal sites in Western Lithuania.

Finally, the document concludes with a discussion of the environmental and economic implications of geothermal energy use, offering insights into the feasibility of integrating geothermal resources into Lithuania's energy strategy, particularly for aquaculture.

The study is organized into three parts, part 1 consists of section 1-5, which gives Geothermal Resources overview in Lithuanian. Section 6-8 provided an overview of the geothermal resources users and technologies, and section 9 onwards provided the details of potential western Lithuania geothermal resources for aquaculture. Conclusions follow in section 22.

2 Analysis of Geothermal Resources in Lithuania

2.1 Classifications of geothermal resources

Geothermal energy works on the principle of harnessing the Earth's interior heat to generate power, provide heating and other industrial applications. Geothermal technologies thus represent a promising alternative to conventional energy sources, with substantial potential for both electricity generation and direct heating applications. The continuous improvement in

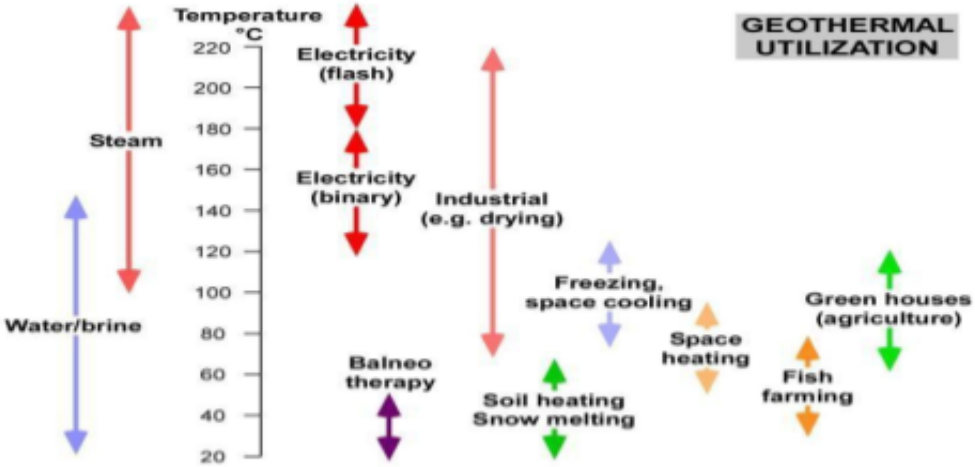

Figure SEQ Figure * ARABIC 1: *Geothermal Energy Resource by Temperature*

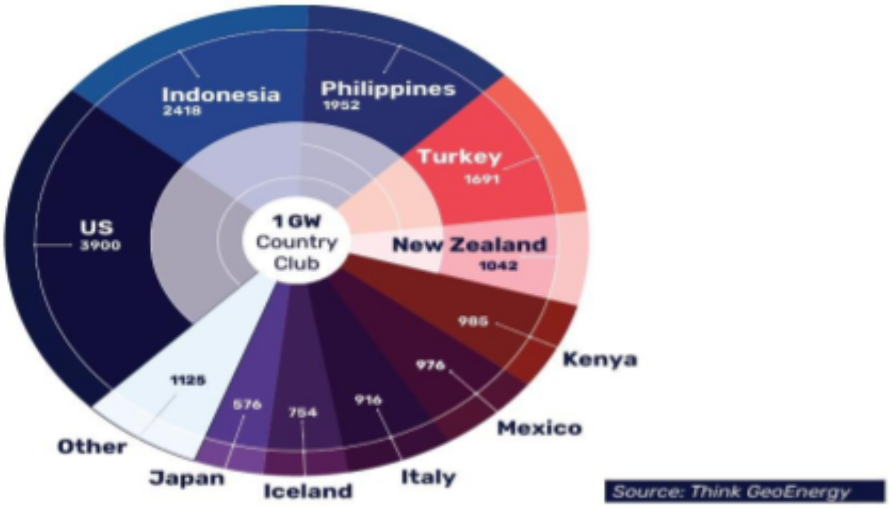

Figure SEQ Figure * ARABIC 2: *Figure showing top 10 Geothermal power use by countries in the word.*

technological advancements enhances the feasibility and efficiency of geothermal energy, positioning it as an increasingly vital component of the global renewable energy portfolio. Geothermal energy by resource temperatures, see **Figure 1.**

The Earth's core has a temperature of about 5000 °C and this energy originates from the core and travel through various subsurface layers depending on the geological conditions and depth of the heat source. Thus, the utilization mode of a geothermal resource is determined by its temperature and depth. For medium to deep geothermal resources, the temperature of the earth

increases with depth at an average rate of 25–30°C per kilometer. In contrast, for shallow geothermal resources, the temperature is approximately constant. Based on the amount of heat travel in the subsurface, different geothermal resource systems are classified as given in **Table 1**.

Table 1 *Categories of geothermal resource system [1].*

Category		Temperature (T)	Production enthalpy (h)
Hot water		T < 220°C	h < 943 kJ/kg
Two-phase, liquid-dominated	Low enthalpy	220°C < T < 250°C	943 kJ/kg < h < 1100 kJ/kg
	Medium-enthalpy	250°C < T < 300°C	1100 kJ/kg < h < 1500 kJ/kg
	High enthalpy	250°C < T < 330°C	1500 kJ/kg < h < 2600 kJ/kg
Two-phase, vapor-dominated		250°C < T < 330°C	2600 kJ/kg < h < 2800 kJ/kg

Geothermal resource extraction technologies are diverse and are specific resource characteristics based on the applications. The geothermal exploration and development are similar to mining and oil and gas field development. However, the development and production of geothermal resources, involving hot fluids, draw from the methods used in the oil/gas industry, with necessary modifications.

2.2 Geological setting of the baltic sea region

The Baltic Sedimentary Basin is the largest tectonic feature defined in the western margin of the Eastern European Platform (Paškevičius, 1997; Stripeika, 1999). The Fennoscandian Shield (some called also the Baltic Shield). the Latvian Saddle (linking Baltic and Moscow sedimentary basins), and the Mazury–Belarus High (Anteclise) are surrounded by positive largest-scale structures. The Baltic sedimentary basin is cut by the Trans-European Suture Zone (including the smaller Sorgenfrei-Tornquist and Teisseyre-Tornquist Zones) (**Figure *3***).

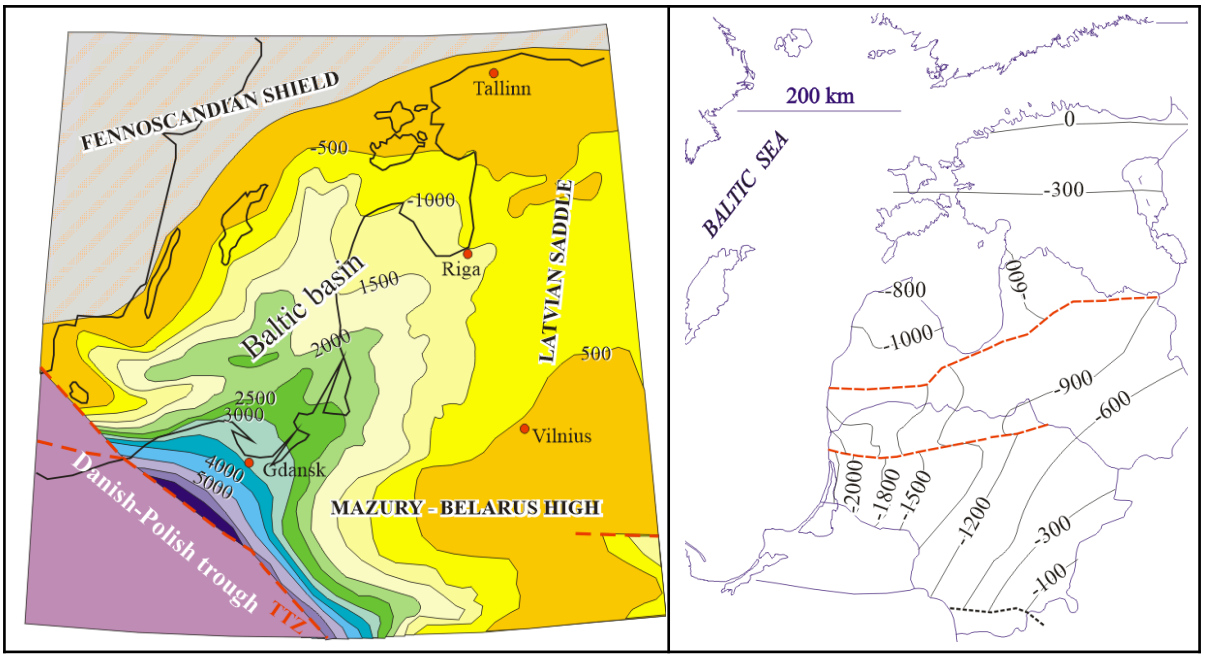

Figure 3. *Depth of the Baltic basin (top of crystalline basement) and depth of the Cambrian aquifer, figure on the left shows the different basements, and figure on right shows the depths.*

The subsidence rates and geometry of the Baltic basin have changed throughout the Phanerozoic, *e.g.*, Caledonian, Variscan, Alpine tectonic stages (Poprawa et al., 1999; Šliaupa et al.. 2006). In incipient stage of the Baltic basin, the Cambrian and Ordovician deposition took place in a passive margin setting with total subsidence of 150-300 m. The geodynamic situation gradually changed during the Silurian time and is classified as the converging and accumulated to up to 4-5 km thick shales and carbonaceous. In Lithuania, the thickness ranges from 50 m in east Lithuania (Tverečius-336) to 850 m in the borehole Nida-1. Intense subsidence persisted during the Devonian up to 1-1.3 km thick terrigenous and calcareous sediments accumulated in the central basin, tectonic mechanism of which is not well understood (Šliaupa et al., 2007). Subsidence drastically decelerated during the earliest Carboniferous giving way to uplift and erosion during the Carboniferous to earliest Permian. Furthermore, the Mazury-Belarus High warmed up in the south, amplitude of which was assessed 1-2 km (Mokrik, 1999) and exposed the crystalline basement (Stirpeik, 1997). Numerous diabase intrusions penetrated the Silurian shales (significant mechanical boundary) in the central part of the Baltic Sea in the central Baltic Sea and one well Girkaliai-2 in west Lithuania in the early Carboniferous (Šliaupa et al., 2011; 2015). It considerably increased the heat flow of the lithosphere (about 30 Ma as determined by shale transformation in Poland) (Kowalska et al., 2019). During the succeeding Alpine tectonic stage (uppermost Permian-Quaternary), the southern and western parts of the basin were involved in the thermal subsidence in the range 1-2 km in the Mazury-Belarus High (**Figure 4, Figure 5**).

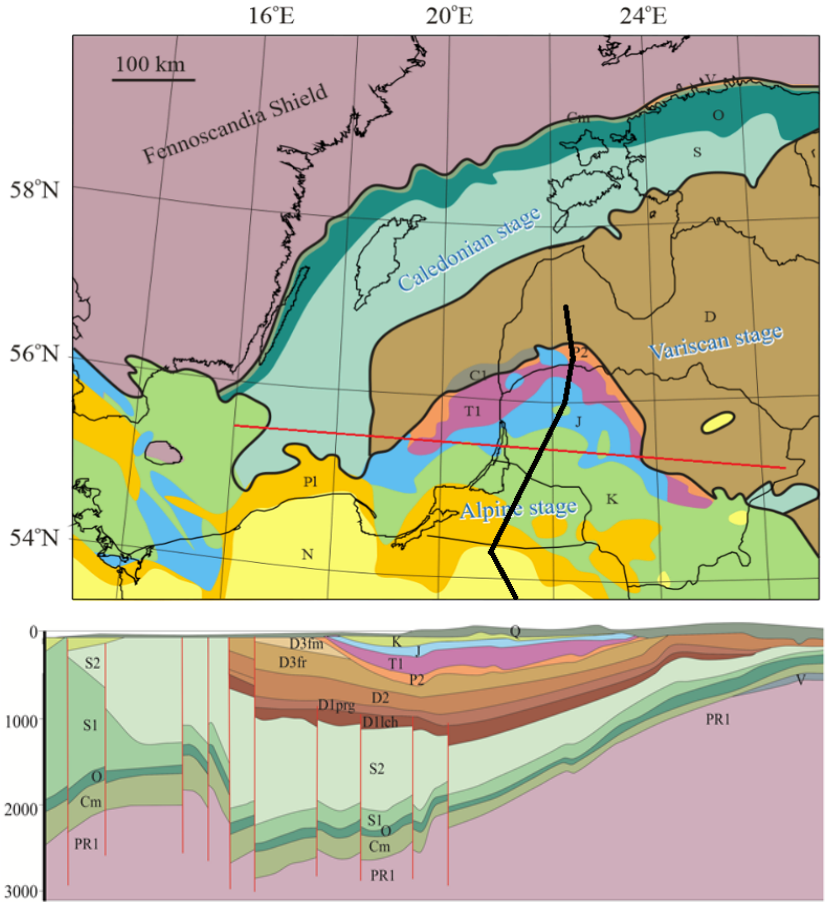

Figure 4. *Geological sub-crop map (Pre-Quaternary level) and cross-section west-east of the Baltic region (Šliaupa and Hot. 2011)*

The Baltic sedimentary basin is considered as the Baltic Artesian Basin (Juodkazis, 1979; Mokrik, 1999). The three major saline geothermal aquifers are defined in the Baltic Artesian Basin

(**Figure 6**). The Cambrian sedimentary deposits overly the crystalline basement of the early pre-Cambrian consolidation. The Kemeri and Šventoji-Upninkai are defined in the Devonian succession (**Figure 7**(Jodkazis et al.. 1997; Rapolienė et al., 2023).

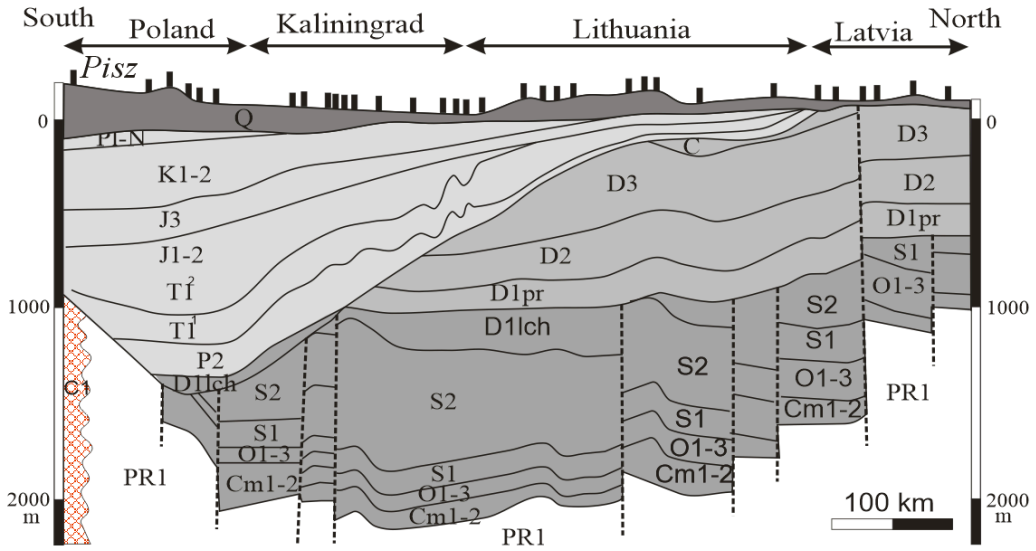

Figure 5. *Regional cross-sections north-south of the Baltic region (Šliaupa et al.. 2015)*

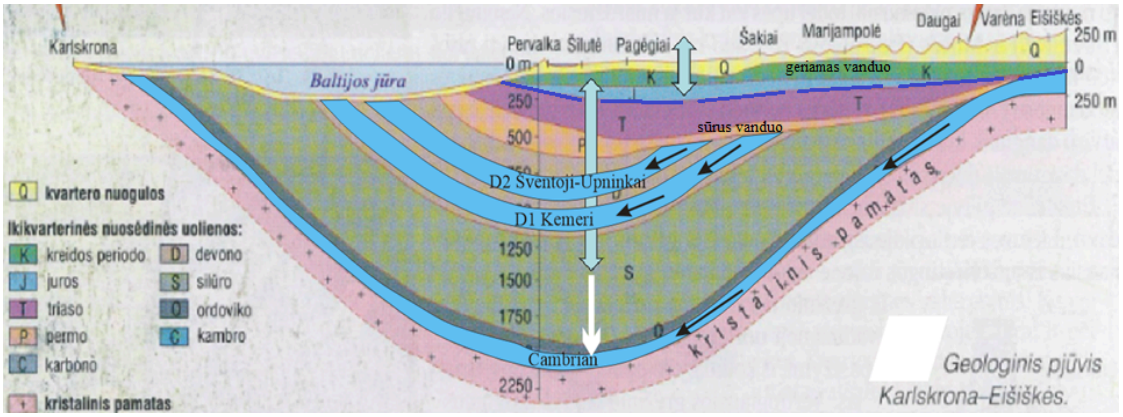

Figure 6. *Regional profile from Sweden to southeast Lithuania across the Baltic Sea. The bottom of the potable water is distributed at a depth of <250 m (maximum depth 650 m was registered in northwest Lithuania). 3 major aquifers are marked below.*

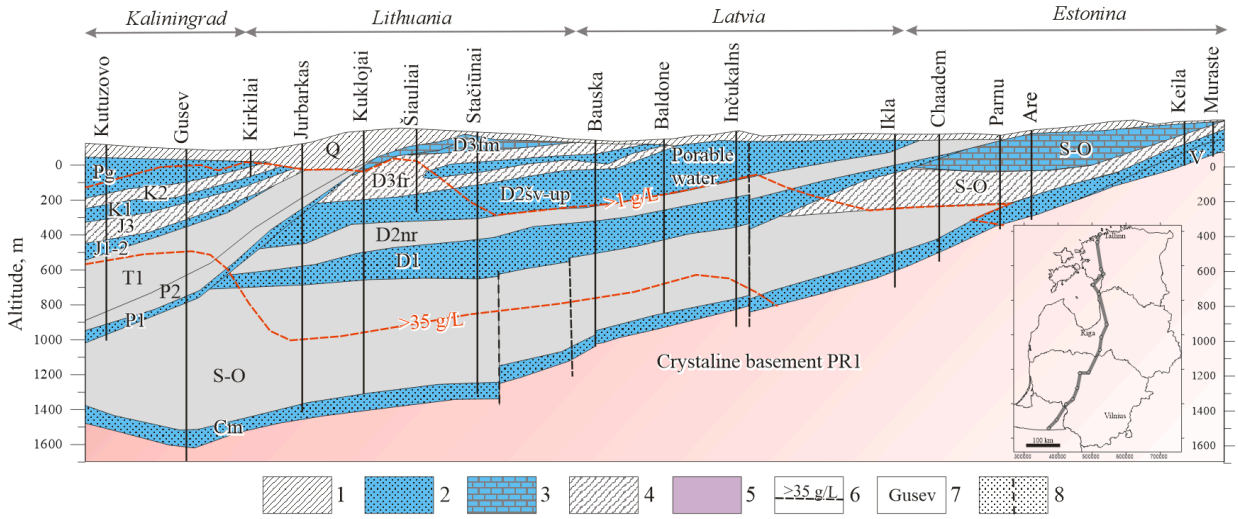

Figure 7. *Major aquifers and temperatures of Lithuania. profile extending N-S. Symbols: 1-Quaternary hydrogeological complex. 2-sandstones (major aquifers are marked in blue). 3-carbonates. 4-aquitards. 5-crystalline basement. 6-major hydrochemical boundaries. 7-reference wells. 8-wells (Juodkazis et al.. 1997. with modifications)*

The Cambrian aquifer of 15-78 m thick is underlain by the Ordovician-Silurian aquitard in Lithuania. The salinity ranges from 1 g/L to salinity 203 g/L (TDS). The temperature varies 14°C to 94°C. The Silurian shales compose the largest aquitard of the Baltic artesian basin which leads to the highest water salinity of the aquifer in the artesian basin.

The Kemeri (lower Devonian) aquifer shows much lower temperatures (up to 45°C) and lower water salinity (100 g/L) in west Lithuania. The thickness varies from 90 m in southwest and 180 m in northwest Lithuania (Jelgava depression). In should be noted, the Kemery aquifer extends to overlying the Rezekne Fm. up to 65 m thick in Latvia and 85 m in Estonia of similar composition (fine friable sandstones comprising subordinated interlayers of shales). In Lithuania, sandstones of the Rezekne RSt. recorded in only the in the Visaginas area northeastern most corner of Lithuania. The aquifer is crowned by the Pärnu Fm. of 8-30 m thick in Lithuania. The section is composed of the strongly cemented by dolomite sandstones, shales, and dolostones. Therefore, this unit is not considered to a part of the Lower Devonian aquifer in Lithuania, while Latvian and Estonian boreholes show excellent reservoir potteries in the northern periphery of the artesian basin.

The Šventoji-Upninkai aquifer (correlated to global Givetian and lowermost Frasnian Stages) is isolated by 75-120 m thick Narva aquitard composed of dolomitic marlstones and dolomites. The Šventoji-Upninkai aquifer ranges from potable water in the eastern part of Lithuania and grades to high-salinity brine in west (35 g/L). The highest temperature was measured at 35°C.
The temperature at interface of crystalline basement and sedimentary pile varies from 11°C (Drūkšiai area studied for Ignalina NPP site; exploration of building stone material in the Kabeliai area in Varėna area) to 94°C close to Šilutė Town (**Figure 8**). The Lithuanian Geothermal Anomaly was defined owing to extensive oil exploration in western part of Lithuania and geothermal data were systematized in late eighties and early nineties (Suveizdis and Rastenienė, 1994; Kepežinskas et al., 1994).

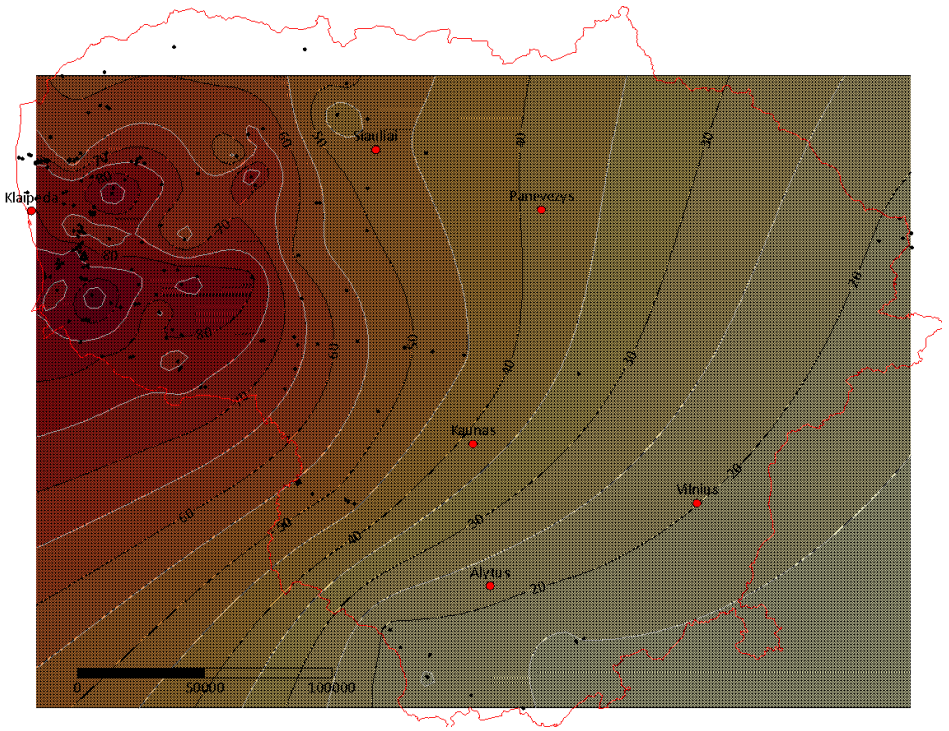

Figure 8. *Temperature of top of the crystallin basement / base the sedimentary cover.*

3 Temperatures and geothermal database

A set of geothermal maps was compiled for Lithuanian territory by Lithuanian Geological Survey (Šliaupa, 2002). Temperature maps at the top of major aquifers: K, J, P_2, D_3žg, D_3st, D_3ys, D_3šv-D_2up, D_1km, D_1gr, Cm, and V (Ediacaran), The crystalline basement map represent the base of the sedimentary deposits of the Baltic basin. The temperatures of top of aquitards T_1, D_3pm, D_2nr, and S are important boundaries of the artesian basin. The alternative Geothermal Atlas of Lithuania was updated by (Rastenienė and Puronas, 2005).

Maps of the temperature distribution at the depths of 100, 200, 500, 1000, 1500, 1750, and 2000 m were compiled at the same scale (7 maps).

The heat flow map of Lithuania was compiled based on thermal measurements in the deep boreholes and measured thermal conductivity data (1 map).

The geothermal gradient ranges from 2.3°C/100m in the southeast to 4.5°C/100m in the southwest in Lithuania. Due to the significant range in thickness of the sedimentary cover and heat flow intensity, the temperature of the Cambrian reservoir varies from 11-22°C in the shallow basin periphery (Vilnius, Varėnos, Lazdijų, Drūkšiai regions) to 80-94°C in the west (Gargždai oil field zone, Ž.Naumiestis geothermal anomaly confined to the "hot" granites, Klaipėda "hot" granites).

The temperature was measured in deep wells in western half of Lithuania owing to extensive oil exploration in west Lithuania (**Figure 9**). The "shallow" boreholes were measured as a part of the geological mapping in east Lithuania (*e.g.*, reference mapping wells, mapping of the crystalline basement of southeast Lithuania, Ignalina NPP area in northeast Lithuania). Few geothermal wells were studied in west Lithuania (Vydmantai, Klaipeda).

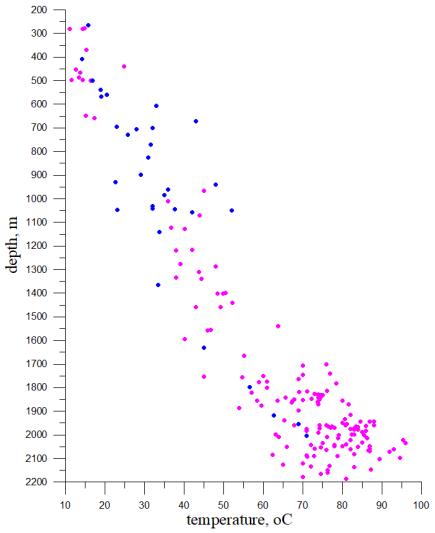

Figure 9. *Temperature measured in deep wells in Lithuania (depth vs. temperature) (Šliaupa. 2002). Pink dots indicate Cambrian succession. Blue wells show bottom depth drilled to other layers. Please note that temperature scattering is crucial for the economic models in the peculiar areas.*

The geothermal database includes 204 boreholes (**Figure 10**). A total of 118 thermal logs have been digitalized. The first thermal measurement experiment was carried out in the well Vilnius in 1949. The shallowest borehole studied is located in the Varėna region (geological mapping borehole Marcinkonys-2, depth to 260 m) and deepest well reached the depth of 2562 m in Kretinga region (geothermal borehole Vydmantai-1). The highest temperature was measured 104°C in the well Vabalai-1 (Šilutė geothermal anomaly) that penetrated Mesozoic quartz monco-diorites to as deep as 2301 m.

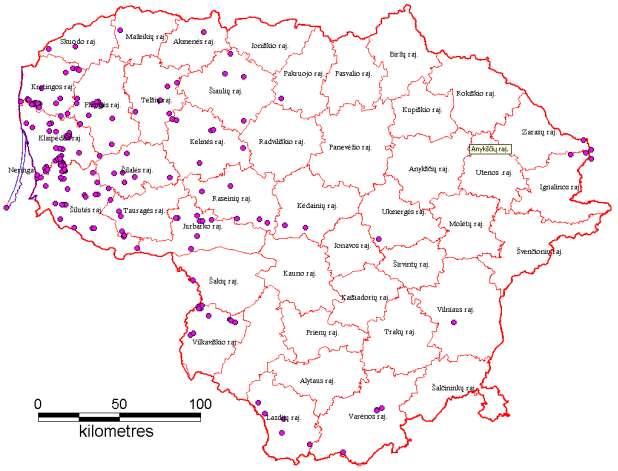

Figure 10. *Temperature measurements were carried out in 204 deep wells (Sliaupa. 2002). Temperatures were measured in most of the oil exploration wells in the western part of Lithuania. while only scarce deep geological mapping boreholes were studied in the east.*

The geothermal gradient ranges from 2.3ºC/100m in the southeast to 4.5ºC/100m in the southwest in Lithuania and is mainly accounted for (1) the heat generation of the crustal lithologies of the crystalline basement (Šliaupa and Rastenienė, 2000) and (2) thermal blanketing of the sedimentary cover of the basin. Also, active infiltration of the meteoric water (most essential in Minsk High. Baltic High including Mozury. Sūduva. Dzūkija and Aukštaičiai Highs). vertical water flow along the faults (Drūkšiai wells). etc.

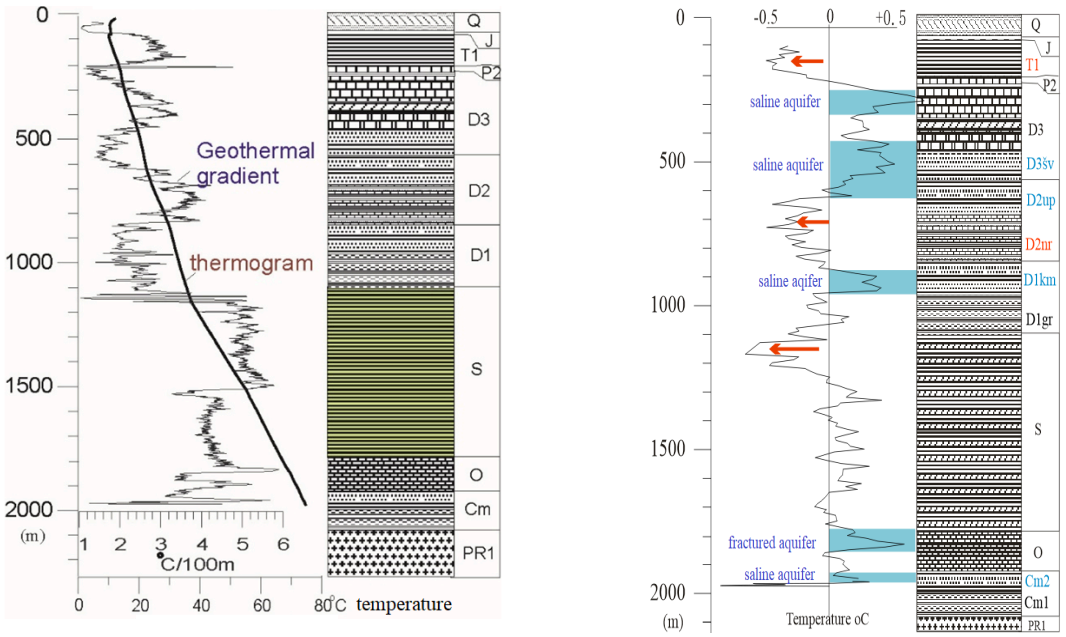

Figure 11. A *- Typical thermogram (temperature and gradients) geothermal well Vydmantai-1. Geothermal gradient reflects the sensitivity of sedimentary lithologies;* ***B*** *– thermal logging indicates the deviation of downhole temperatures measured in 1993 (after 15 days after drilling) and 2004 wells was opened for thermal logging; it marks major aquifers (up to +0.7°C) and shales (up to -0.7°C. Four saline (brain) aquifers are well discernible showing long-term disequilibrating of sandstones and carbonate reservoirs (Deimena RSt of Cambrian. Kemeri Fm. of lower Devonian. Šventoji-Upninkai Fms. of middle-uppermost Devonian. and Upper Devonian. Please note the fractured limestones in the upper part of the Ordovician succession should be classified as the fractured reservoir. The positive and negative delta anomalies are accounted*

for slight dis-equilibration of the geothermal field during the first campaign and were restored during the second measurement campaign.

The temperature logging is an excellent tool to register the thermal conductivity of the sedimentary pile (Vydmantai-1 illustration) (**Figure 11**). However, most of the thermograms are of moderate quality which reduces the geothermal field study application in the particular deep wells. The lowest thermal gradient is registered 0.2-0.4°C/100 m in sandstones (Quaternary, Devonian aquifers) and carbonates (Upper Permian) to 5.0°C/100 m (Upper Silurian graptolitic shales).

Very different parameters are accounted for the high variations of the underground temperatures, *e.g.*, terrestrial heat flow ranging from 19 mW/m^2 the Ovisi-94 in Kurseme Peninsula in Latvia to 94 mW/m^2 in the well Vabalai-1 in southwest Lithuania; heat generation varies from 0.88 $\mu W/m^3$ in mafic intrusions to 4-22 $\mu W/m^3$ in "hot" Proterozoic granitoids; variable hydrodynamic regime in the active inflow the meteoric water and compaction water flow; large-scale blanketing of aqtesian basin (best recognized in the Silurian shales); paleo climate correction (*e.g.*, Suwalki anomaly in NE Poland); upward water flow (were recognised in the Visaginas wells in the Ignalina NPP area). Most studies were carried out by Belarus colleagues (Zui, Urban, Zhuk, Cybulia – *reference below*). The heat flow map was updated by (Šliaupa, 2002).

4 Parameters of the major geothermal aquifers: Cambrian geothermal aquifer: Distribution. depth. and thickness of the Cambrian succession

4.1 Regional background

The shallow marine Baltic basin invited the western margin of the east European Craton that accounted for the breaking apart Baltic continent in the Cambrian. The most intense tectonic extension is defined in the western part of the basin (**Figure 12**) (Poprawa et al.. 2001; Šliaupa et al.. 2007). The anomalous thickness of the Cambrian is related to the attenuated thinned margin of the craton (thickness >250 m) while the vast territory of the Baltic region was involved in the slow subsidence in the east.

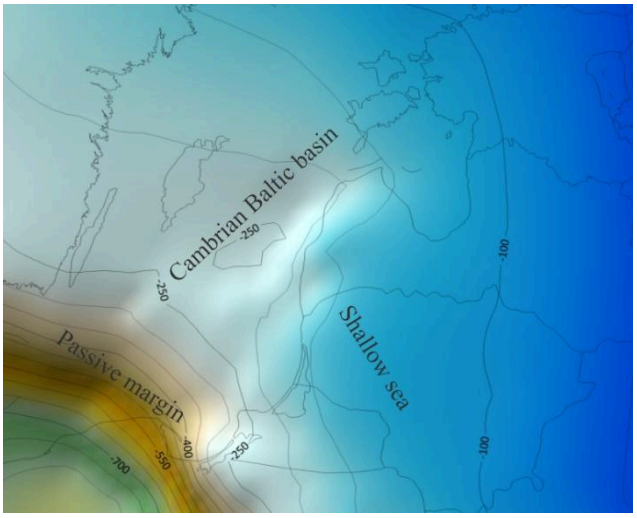

Figure 12. *Thickness and geometry of the Cambrian succession in the Baltic basin. Please note the bending of the western part of the craton. The eroded margins of the Basin are restored.*

The Cambrian succession is distributed in the Lithuanian territory, except the southern part of the country due to deep erosion in the Mazury-Belarus High in the Carboniferous-lower Permian time (**Figure 13**). The depth of the top of the Cambrian reservoir ranges from -290 m (MSL) in south-eastern Lithuania to -2140 m in the Klaipėda depression. The tilting of the Cambrian strata shows general inclination to the southwest (**Figure 13)**.

The deposition of the platform cover was initiated in the Moscow basin in the Ediacaran (local Vendian Stage) time in the east. The basin the eastern part of Lithuanian territory in the latest Proterozoic time, when the grabens overstepped limits of the high-thickness clastic deposits and volcanic effusive rocks. The incipient sedimentary cover (up to 180 m chick greywackes and sandstones) covered the eastern part of Lithuania.
The coarse-grain sediments of the Vendian Series gave way to clays in the earliest Cambrian time (Rovno RSt and Lontova RSt of the Blue Clays). The depositing boundary is restricted by the Nemunas River and Nevėžis River in the east. The largest thickness was documented in the geological mapping borehole Tverečius-336 (Ignalina region).

The second depocentre of the Vendian-lowermost Cambrian age was mapped in north Poland along the western margin of the Baltic Craton (Jaworowski and Sikorska, 2003). By contrast of the Moscow basin, no fossils were documented in the fluvial sandstones of the Żarnowiec Fm. The proximal part of alluvial fans and distal alluvial fans and braid-and-sheet flood plain facies

were identified based on detailed sedimentological inspection of deep boreholes. Equivalents of the Żarnowiec Fm. are probably the Nexö sandstones on the Bornholm Island and the Adlergrund Sandstein Fms. in the well G14-1/86 (Rügen Island.

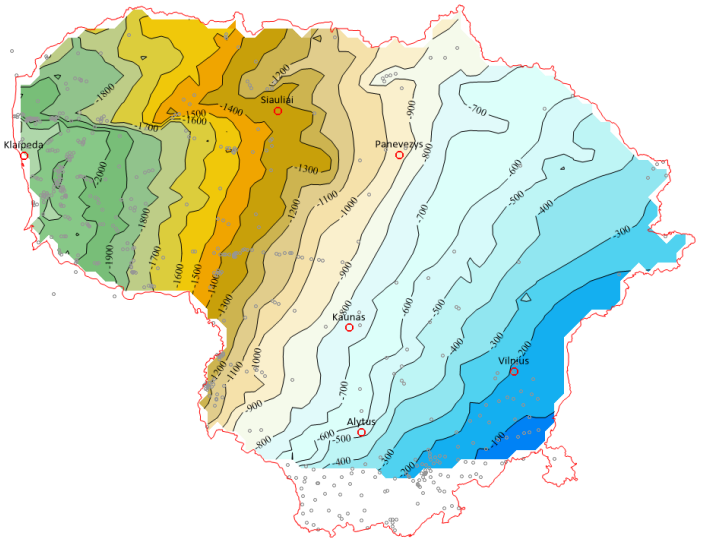

Figure 13. *Depth (m, MLS) of the top of the Cambrian succession of Lithuania. Deep wells (grey circles). Tectonic faults are not indicated on the map.*

The drastic rearrangement of the subsidence pattern is marked by the establishment of the Baltic sedimentary basin in the western periphery of the East European Carton (**Figure 14**). The thickness of the Cambrian succession ranges from 8 m meters (borehole Tverečius-336) in the east to 178 m in the west of Lithuania (wells Žemytė-1,-2). The thickness of the Cambrian succession shows only regional-scale tectonic structure with no discernible tectonic activity at the deposition time accounted to the passive margin tectonic regime. At the regional scale, the west Lithuanian territory was involved in the relative uplift compared to Latvia and the adjacent Kaliningrad District area.

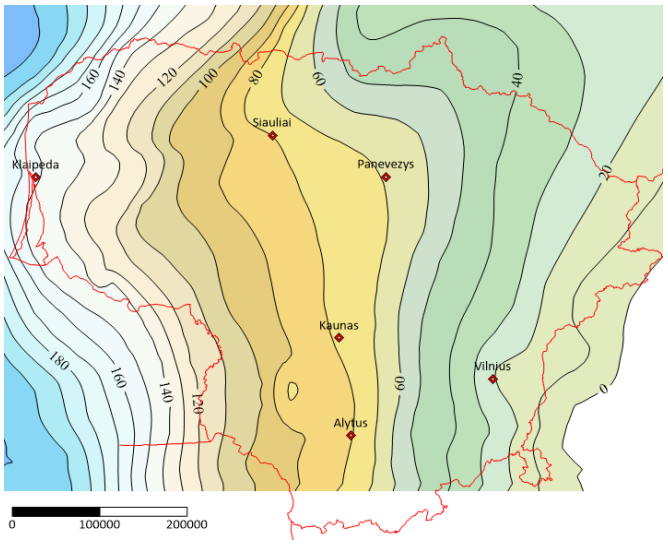

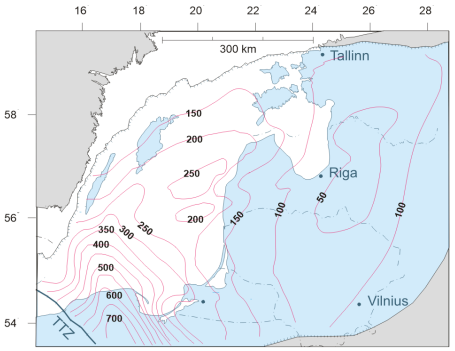

Baltic Cambrian basin
The map shows the total thickness of the Cambrian succession referred to as the Caledonian tectonic stage (without the oldest Moscow basin deposits in the east)

Figure 14. *Thickness of the Cambrian succession of the Baltic basin. Please note the slightly uplifted structure in west Lithuania on both maps.*

The "exotic" structures were defined in Lithuania and classified as the drape structures complicating the peneplane of the crystalline basement (Stirpeika, 1997; Šliaupa and Hot, 2011). They evidence the crustal breaking apart of a western margin of the Baltic craton. The peneplane

was sub-merged by a vast marine basin in the Baltic region in Dominopole RSt (Cambrian Stage 3). They compose the isolated high-amplitude islands, some as high as 113 m (Plungė uplift). The largest "islands" were mapped by a detailed seismic survey and some structures were drilled by a number of oil exploration wells (Veiviržėnai, Baubliai, Pociai, etc.) (Grindaitė et at., 2022; 2023). These "exotic" uplifts are not indicated on the attached map. Furthermore, "drape" structures are drilled also in Kaliningrad district and Estonia. Most numerous small uplifts were defined in the offshore sector of Latvia due to excellent quality of offshore seismic survey.

4.2 Stratigraphy of the Cambrian aquifer in Lithuania

The invasion of the Cambrian shallow marine basin into the Baltic basin started as an elongated NE-SW trend "Baltic Sea". The Baltic basin initiated in the early Cambrian Stage 3 and correlates to the Dominopol RSt. (**Figure 15**). The unified stratigraphic chart of Lithuania is based by (Jankauskas, 2004). They are composed of clayey fine-grained sandstones and siltstones. Due to the low reservoir quality, these terrigenous deposits are classified as aquitard (Šliaupa and Hoth. 2011) (**Figure 15** showing offshore well D1-1.).

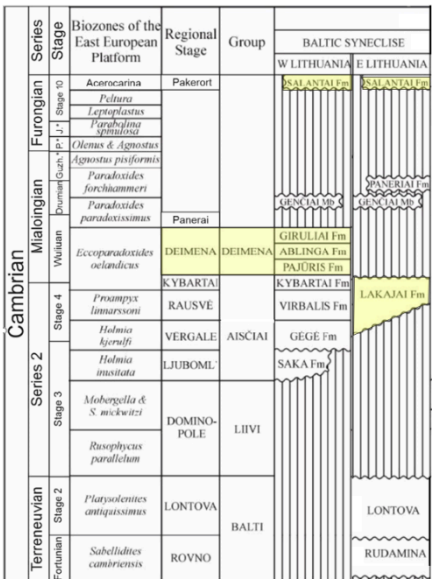

Figure 15. *Cambrian stratigraphic chart of the Baltic Eastern region (Jankauskas. 2004. modified based on adapted stratigraphic chart). The Dominapole RSt marks a new transgression of the Baltic Sedimentary Basin distributed in the axial part of the present Baltic Sea (see* ***Figure 16****). The widest transgression of the shallow marine basin invaded the Baltic countries. The key Cambrian reservoir was accumulated in the Deimena RSt (yellow). In the east, the reservoir grades to the Lajai Fm. of older age. Also, the Deimena sandstones are overlain by about 0.2 m thick Salantai Fm. marking transition from Cambrian to the Ordovician.*

The maximum transgression of the Baltic basin is correlated to the Cambrian Stage 4 on the global stratigraphic chart (Jankauskas and Lendzion, 1992) (**Figure 17-Figure 19**). The Aisčiai Group comprises the Gėgė, Virbalis, and Kybartai Fms of up to 78 m thick in westmost Lithuania and represents the regional scale aquitard (Mokrik, 1997) consisting of shales with subordinate sandstones. The largest thickness of the group was documented in the wells Žemytė-1,-2 in northwest Lithuania and thickness increased to 132 m in the offshore wells D6-1 and D5-1. It should be noted that the sandstone percentage gradually increases to the east and grades to the aquifer of the Virbalis Fm which is an important sandstone body discussing the geothermal energy potential in the Vilkyčiai region (Rastenienė, V. 1994. Assessment of the Cambrian geothermal and balneological conditions of the hydrogeothermal complex in Vilkaviškis city. Geological Institute Archive, Vilnius).

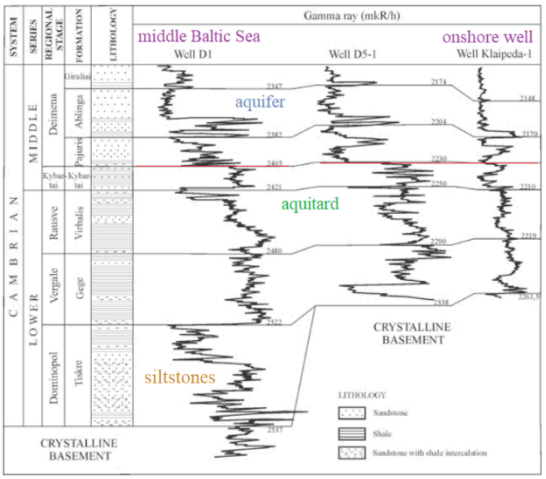

Figure 16. *Stratigraphic interpretation of the gamma-ray log curves. Two offshore wells and well Klaipėda. The Dominopole aquitard (marked brown) was deposited in the axial part of the present Baltic Sea and onlapping Aisčiai aquitard (green colour) and the Deimena aquifer (blue colour) (Šliaupa and Hot, 2011).*

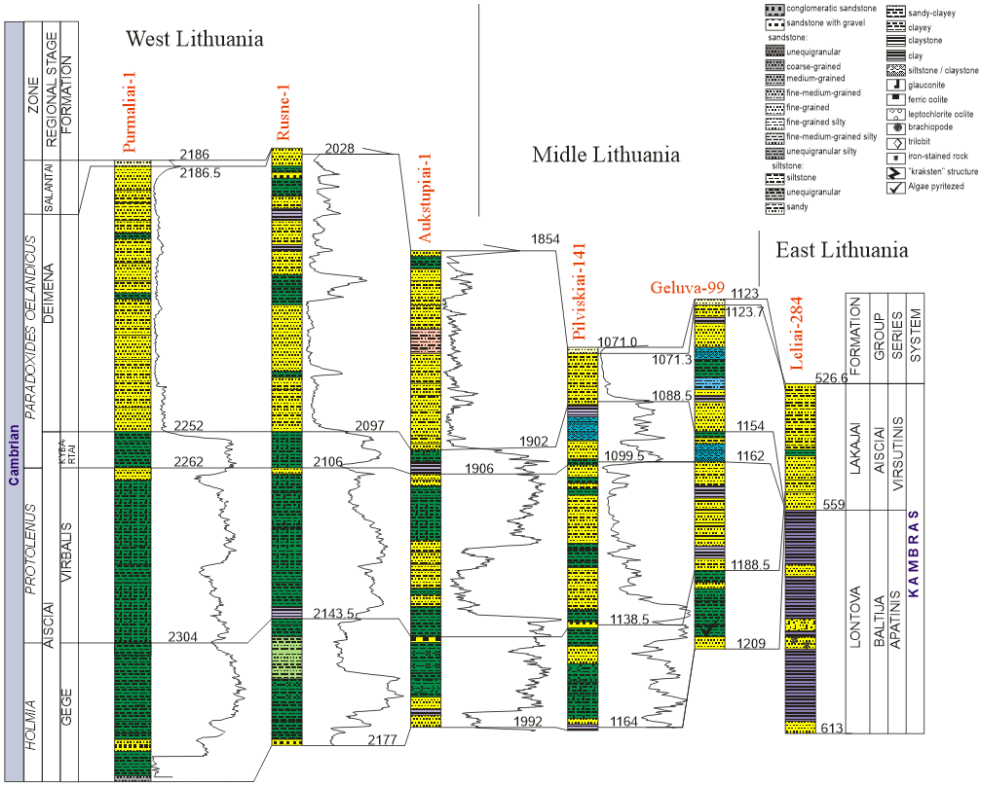

Figure 17. *Lithology and stratigraphical sub-division of the Cambrian deposits along the profile crossing Lithuania "West-East". The Aisčiai Group shows progressive shallowing of sedimentation depth from mud plane facies in the west to intercalation of sandstones and shales in the middle Lithuania. It grades to the Lakajai shoreface sandstones in east Lithuania. Please note, that the well Leliai-284 is located in the western periphery of the Moscow basin. The Aisčiai Group is overlain by a regressive succession of the Deimena reservoir. Some several metre thick shales complicate the architecture of the reservoir implying increasing compartmentalization of the reservoir, essentially in westernmost Lithuania. Please note the Syderiai Fm. was deposited after a long break in sedimentation at the transition zone of the Cambrian and Ordovician sandstones.*

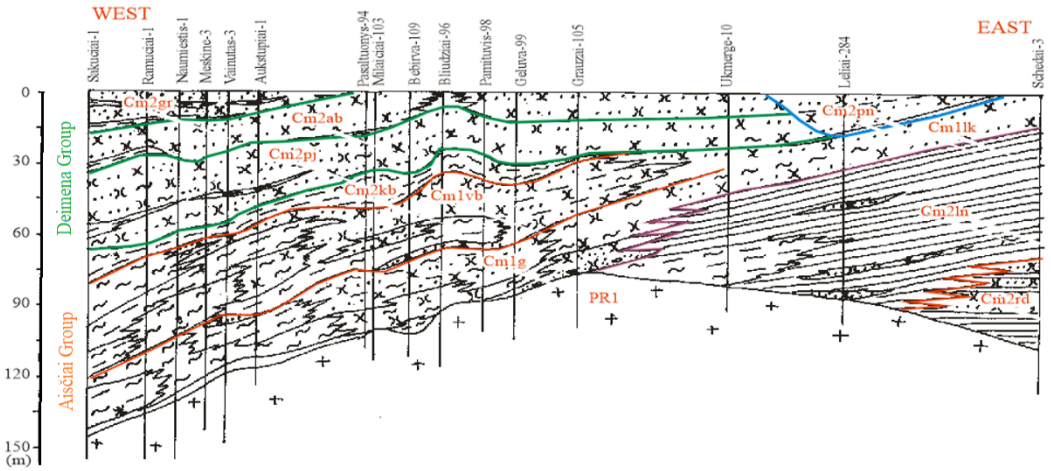

Figure 18. *The same lithological profile (hand drawing) (see Figure 17). The Roduka and Lontova RSts are attributed to the western periphery of the Moscow basin in the east. The Baltic basin was established in the Dominpole RSt (not shown in the profile). The most extensive transgression took place in the Gėgė Fm. and overlain by the Virbaliai highstan systems tracкt. This aquitard is crowned by the Kybartai Fm. clays. This package is unified as the common Aisčiai Group. The Deimena Group (RSt) represents the major and widest-distributed reservoir in the Baltic basin. Please note three formations – Pajūris, Ablinga. and Giruliai Fms. which compartmentalize the reservoir that complicates the exploitation of sandstones.*

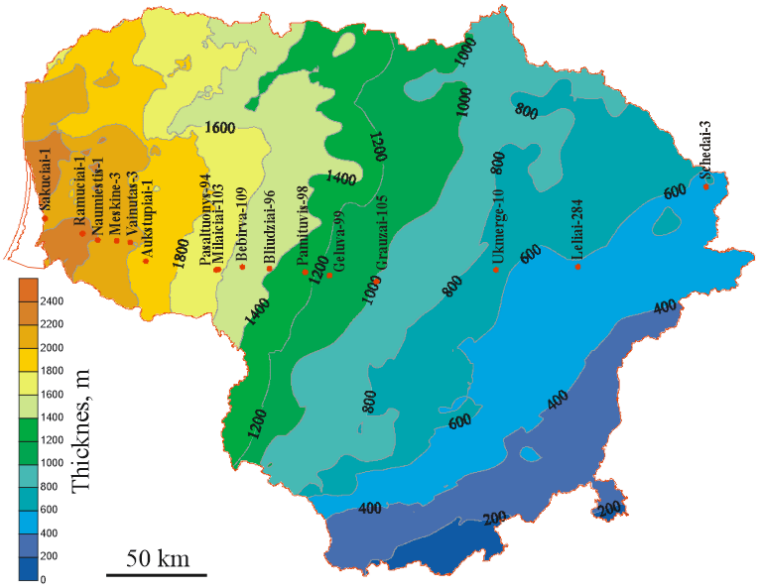

Figure 19. *Depth of the crystalline basement and location wells of profile West-East.*

The Aisčiai Group gives way to fine-grained quartz sandstones attributed to the Lakajai Formations in the eastern periphery of the basin (**Figure 18**). They correlate with the Cirma sandstones in east Latvia and Ruhnu sandstones in Estonia. The largest thickness 88 m was recorded in the geological mapping borehole Lazdijai-6 drilled in southeast Lithuania (depth 720 m).

The Deimana RSt is distributed in the west and middle Lithuania. The thickness reaches 78 m in westernmost Lithuania (**Figure 20**), while the eastern boundary of the reservoir is not well delineated (no fossil record). The most complete stratigraphy of the Deimena RSt is defined in westernmost Lithuania and arranged as a sequence of the Pajūris, Ablinga, and Giruliai Fms. (**Figure 18**). The upper part of the Deimena RSt shows a regressive off-lapping geometry of the reservoir.

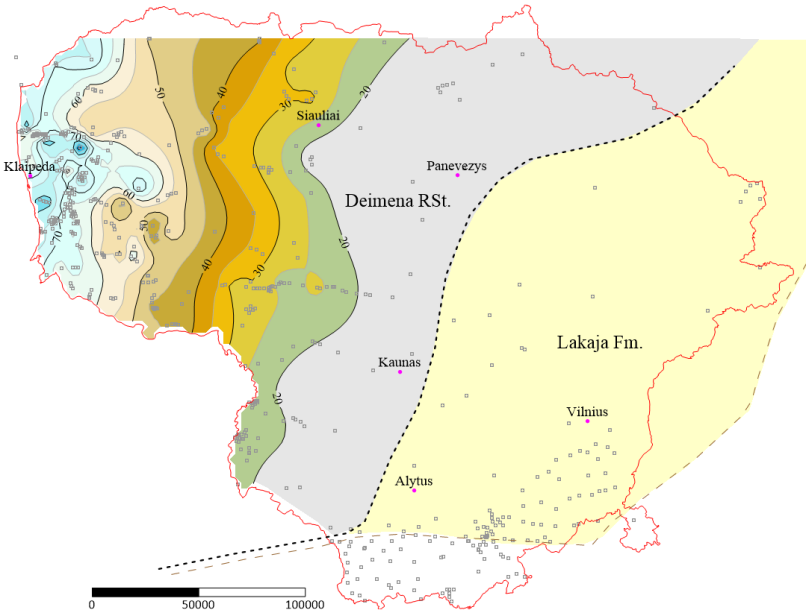

Figure 20. *Distribution and thickness of the Deimena RSt. The older Lakaja Fm. sandstones sub-cropping in the east (yellow). Deep wells are shown (open circles).*

4.3 Reservoir properties of the Cambrian sandstones

The reservoir properties show a clear burial depth control from the eastern periphery of the Baltic basin to deeply buried deposits in the central part of the basin. A common trend *porosity* vs. *permeability* cloud with no discernible "offsets" of the database (**Figure 21**).
No petrophysical data is available on the Lakajai Fm. sandstones (no specific focused study was carried out). The database covers a depth range from 970 m in middle Lithuania to 2250 m in the west (**Figure 21**). Samples were mostly obtained from the Deimena RSt and scarce sandstone and siltstone interlayers present in the Aisčiai Group.

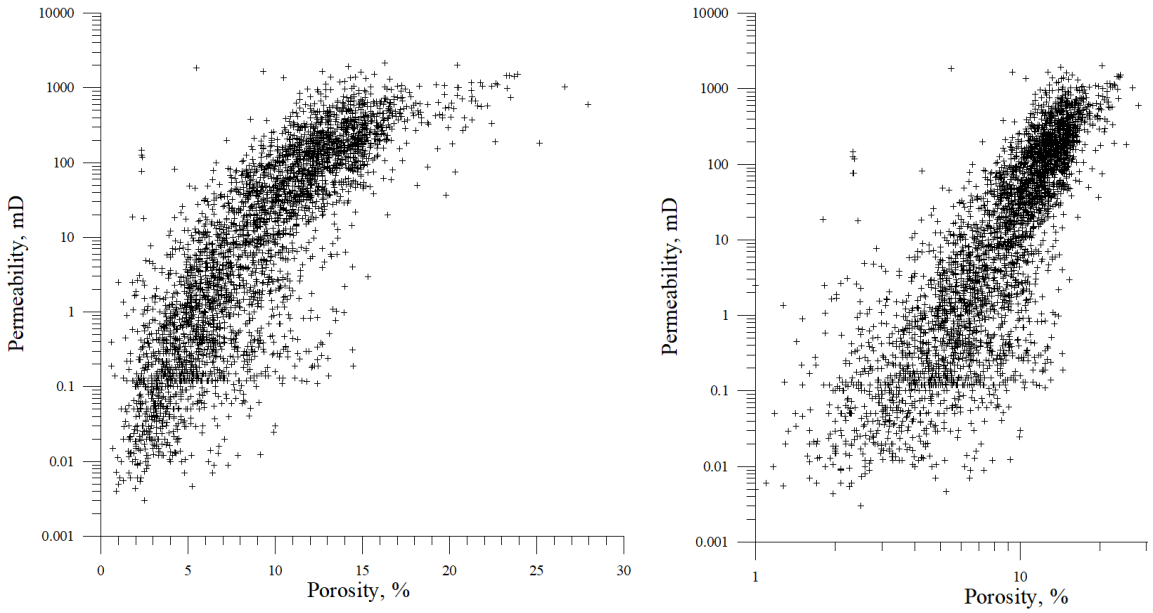

Figure 21. *Porosity vs. permeability of sandstones of middle and west Lithuania. The same database, log-normal and log-log regression trends are recognised. N=5795 samples. Average porosity is calculated 9.0% and the average permeability is 100 mD.*

The three distinct burial depth boundaries are recognized in the petrophysical database (**Figure 22, Figure 23**). As mentioned above, there are no sorted petrophysical parameters of the Lakajai sandstones.

The obscure information is available on the petrophysical properties collected from east Lithuanian boreholes. The same is recorded in Latvia and Estonia (Šliaupa et al., 2003). Based on the petrographic studies of drill cores, the Lakai sandstones are cemented by carbonates which show patchy distribution. Also, only a minor admixture of clay minerals is recognised. No systematic study was carried out on the Lakajai sandstones. Most of the samples collected from the eastern part of Lithuania and Latvia were focused on the Blue Clay formation accumulated on the western periphery of the Moscow basin. The relatively decreased porosity 17-20% of sandstones is related to increased clay admixture in sandstones, while the permeability was documented as high as up to 2400 mD (Visaginas geological mapping wells in the Ignalina NPP area).

The shallowest inspected oil exploration well Akmenynai-149 as well as boreholes Vaškai-1-5 in Pasvalys region indicates incipient authigenic quartz cementation (few percent) (depth 900-980 m) (**Figure 22, Figure 23**). The calcite cement predominates in sandstones. The second important message is the occurrence of gypsum cement in the Vilkaviškis region. The precipitation of gypsum is reasonably accounted for by the downward penetration of the heavy brine from the Zechstein basin (present depth c. 700 m of the Upper Permian and distributed at the depth of 1050-1350 m in the Cambrian sandstones).

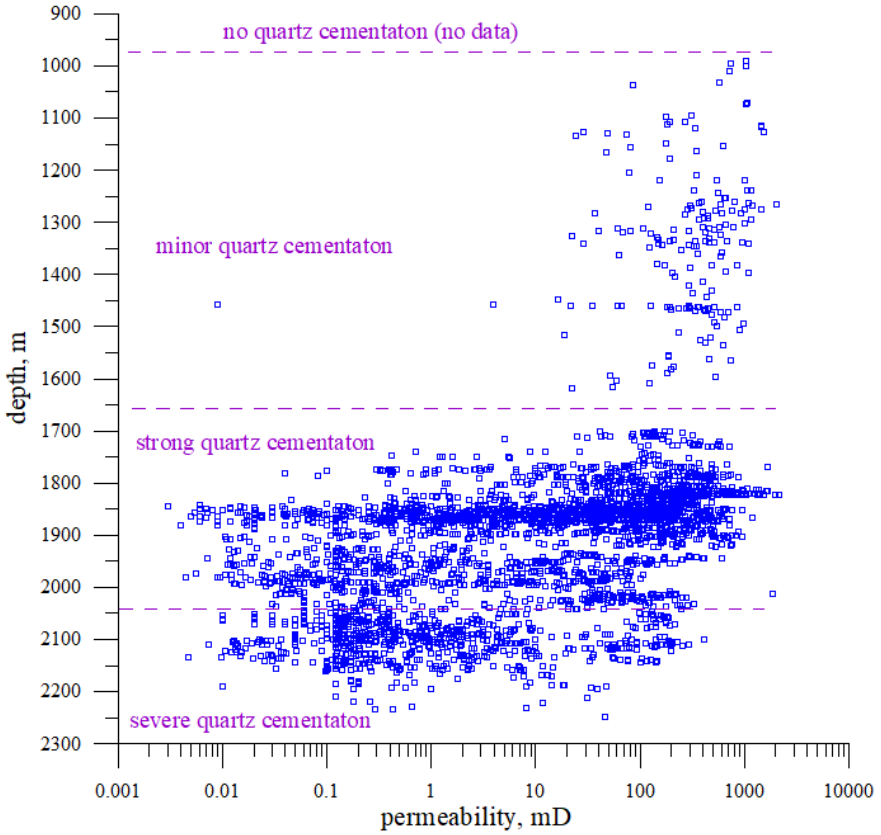

Figure 22. *Permeability vs. depth of the Cambrian sandstones of middle and west Lithuania. Three temperature controlled sharp transition boundaries are noted as discussed below (samples 6240).*

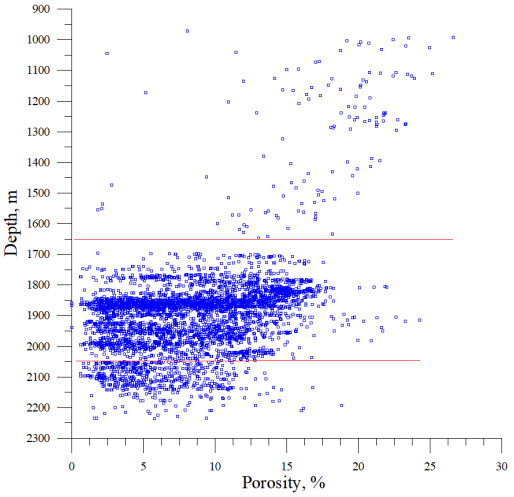

Figure 23. *Porosity vs. depth of Cambrian sandstones (samples 6240).*

The "minor quartz cementation" zone (as indicated in **Figure 22**) shows a rather minor variation in permeability c. 650 mD, while quartz cementation reduces porosity from 20-22% in the Vilkaviškis, Šakiai, Šiauliai to 12-15% (Tauragė. Telšiai) (**Figure 23**).

A sharp petrophysical boundary defined at the depth of about 1650 m shows a drastic decrease in the reservoir quality in the Cambrian sandstones that is primarily related to the intense quartz cementation ("strong cementation zone" in **Figure 22, Figure 23**). Furthermore, this petrophysical boundary is confined to the limit of the West Lithuanian Geothermal Anomaly (Šliaupa, 2005). The average depth of this "strong cementation zone" varies from 1650 m to 2050 m. The average porosity of sandstones is calculated 12.5% and the permeability 172 mD. It should be noted, that drastic variations in reservoir properties of sandstones are strongly controlled by the deposition facies (Molanaar et al., 2007).

The most cemented sandstones of the Deimena RSt are defined in the oil exploration wells along the Baltic Sea shoreline (Sakučiai, Traubai, Purmaliai, Klaipėda) (**Figure 22. Figure 23**).

The "strong quartz cementation zone" shows a peculiar mineralogical composition: 1) authigenic quartz predominates in sandstones; 2) minor content of late diagenetic carbonates of only c. 0.5%. 3) miserable admixture of clay minerals represented by illite, kaolinite, and chlorite. The most intense quartz cementation is confined to the thin-bedded (decimetre scale) facies deposited in the inner shelf environment to less cemented thick-bedded (decimetre-meter) facies accumulated in the distal shoreface environment. Several key publications discussed the role of the authigenic quartz cementation in the reservoir quality as shown, for example, in the diagram *porosity* vs. *quartz cementation* (**Figure 24. Figure 25**) (Molanaar et al., 2007).

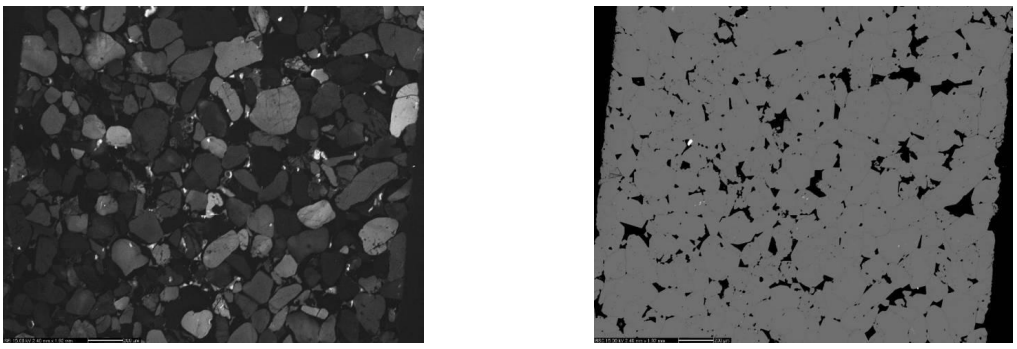

Figure 24*. Sandstone sample was collected from the well Girkaliai-5, depth of 2054 m. Cathodoluminescence microphotograph and back-scatter electron images illustrates increased porosity of the Pajūris sandstone, while poor reservoir quality is defined in the middle and upper part of the Deimena reservoir (discussed below concerning the Vydmantai geothermal boreholes).*

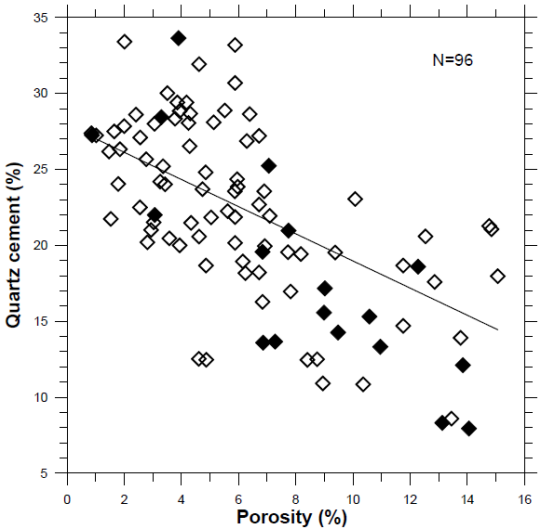

Figure 25. *Porosity vs. quartz cementation intensity of sandstones, depth of samples >1700 m (Molenaar et al., 2007).*

4.4 Temperature distribution in the Cambrian geothermal aquifer

The temperature gradient varies from 1.3-1.7°C/100 m in the east to 3.5-4.5°C/100 m in the west. The temperature of the Cambrian geothermal aquifer increases westwards with increasing burial depth. In the eastern periphery of the basin, the temperature of the Cambrian sandstones is as low as 11-14°C. The West Lithuanian Anomaly is the most peculiar feature recognised on the geothermal map mapped and shows temperatures of the Cambrian geothermal aquifer reaches 65-94°C (**Figure 26, Figure 27**). It should be stressed that the West Lithuanian Anomaly is confined to the major petrophysical boundary showing the worst reservoir quality.

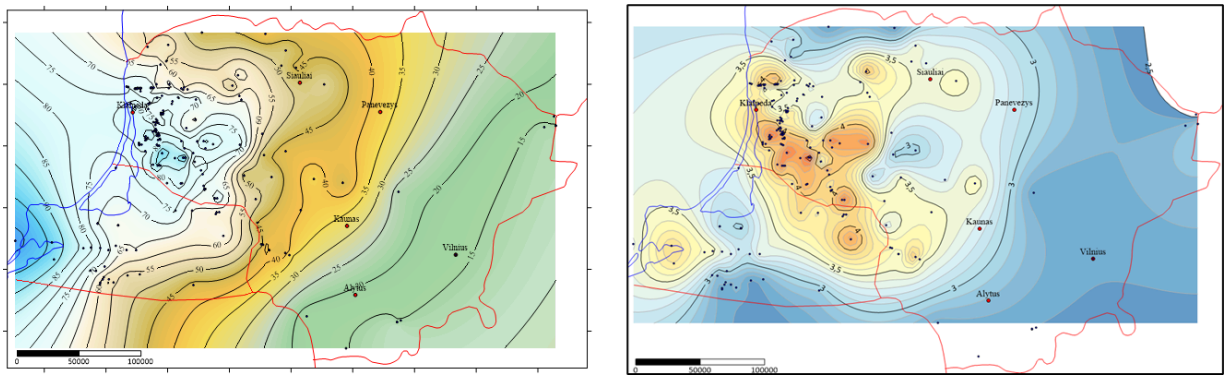

Figure 26. *Temperature of top of the Cambrian aquifer and temperature gradient (Kaliningrad district data were added).*

The thermal conductivity of the Cambrian sandstones varies from 1.76 to 6.7 W/mK (**Figure 27**). The highest values are recorded in the most intensely quartz-cemented sandstones in west Lithuania that is important in parameter for geothermal modelling of the reservoir.

4.5 Geothermal potential of the Cambrian reservoir

The geothermal potential of the Cambrian reservoir is basically governed by 1) temperature and 2) quality of the reservoir quality (*e.g.*, porosity and permeability).
The effective thickness of the Lakajai Fm increases to the west, sandstones are of excellent reservoir quality. However, the temperatures vary from 14°C to about 35°C in the Lakai Fm which is considered below the economic interest (**Figure 28**).

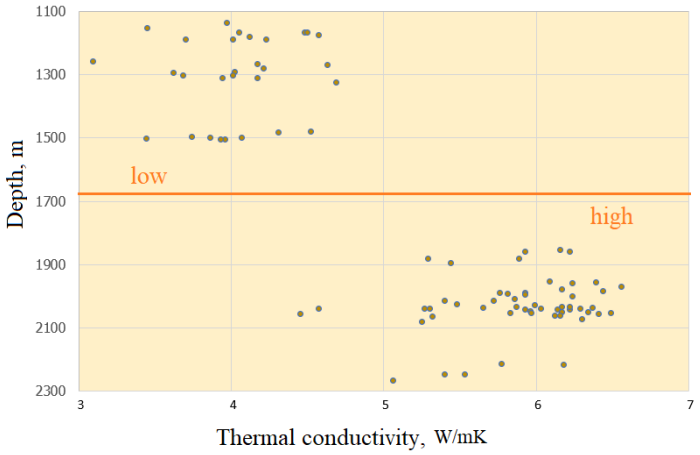

Figure 27. *Thermal conductivity vs. depth of the Cambrian sandstones of middle and west Lithuania.*

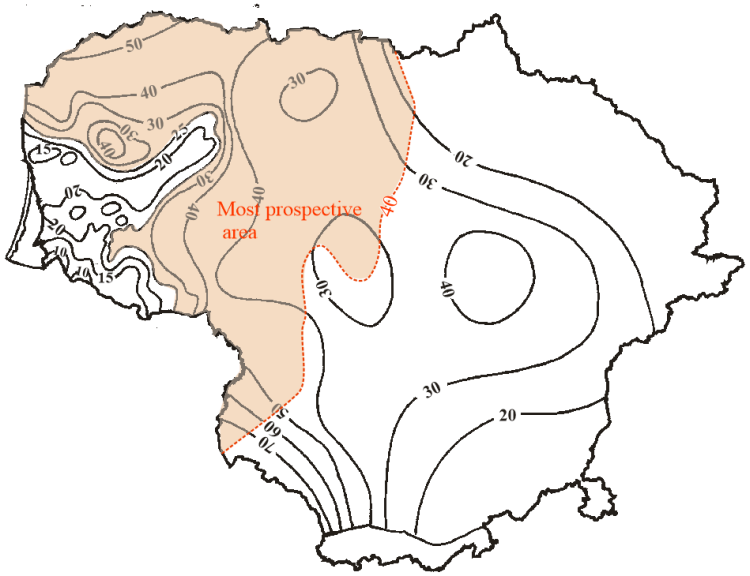

Figure 28. *Effective thickness of the Cambrian geothermal aquifer. The red line shows 40°C isotherm*

The Deimena RSt shows very variable geothermal potential. The most prospective area is characterized by 1) a temperature of 40-70°C and 2) an effective thickness 25-42 m (**Figure 28**). The effective thickness sharply decreases in the southwest owing to severe quartz cementation.
There are different approaches to assessing the geothermal potential of particular sites or areas. The methodology was adopted by (Šliaupa and Kezun, 2011; Šliaupa et al., 2019), as described below:
The shale content was estimated using gamma ray logging data:
$Vsh = (GR - GRmin) / (GRmax - GRmin)$ (1)
here Vsh is the fraction of shale in the rock. GR is the gamma-ray intensity (microR/hr). The open porosity was calculated:
$\Omega = [(DT - DT_{matrix}) / (DT_{fluid} - DT_{matrix})] \times [1 - V_{sh}]$ (2)

here DT is the sonic velocity (μs / m), DTmatrix is the matrix sonic velocity (assumed 170 μs/m). DT_{fluid} is the fluid sonic velocity (assumed 600 μs/m). The effective thickness of the Cambrian reservoir was estimated from logging and drill core data.
The well production (injection) rate was calculated:

$$Q = \frac{2 \cdot \pi \cdot k \cdot m \cdot \Delta P}{\mu \cdot \left[\ln\left(\frac{r_e}{r_w}\right) - \frac{1}{2} + S \right]}, \qquad (3)$$

here Q is the production (injection) rate (m^3/s), k is the permeability (m^2), m is the effective thickness (m), ΔP is the depression (assumed 4 000 000 Pa), μ is water viscosity which depends on temperature and salinity (Pa×s), r_w is the borehole diameter (assumed 0.123 m), r_e is the borehole drainage diameter (assumed 400 m), S is the Skin effect (assumed as +5).
The heat potential of a well was assessed:

$$Qth = c \times Q \times \varrho \times (t_1 - t_2). \qquad (4)$$

here Q_{th} is the heat potential (GJ). c is the specific heat of the water (J/kg × K), Q is water volume (m^3), ϱ is water density (kg/m^3), t_1 and t_2 (assumed 11°C) are temperatures of produced and treated water (°C).

The western part of Lithuania has the potential for geothermal district heating (**Figure 29**). The best conditions are defined in southwest Lithuania (*e.g.*, Vilkaviškis, Šakiai, Jurbarkas, Tauragė). The lowest potential was assessed in Šilutė, Gargždai, etc. Also, the westernmost regions have high potential in the Kemeri geothermal aquifer (**Figure 29**).

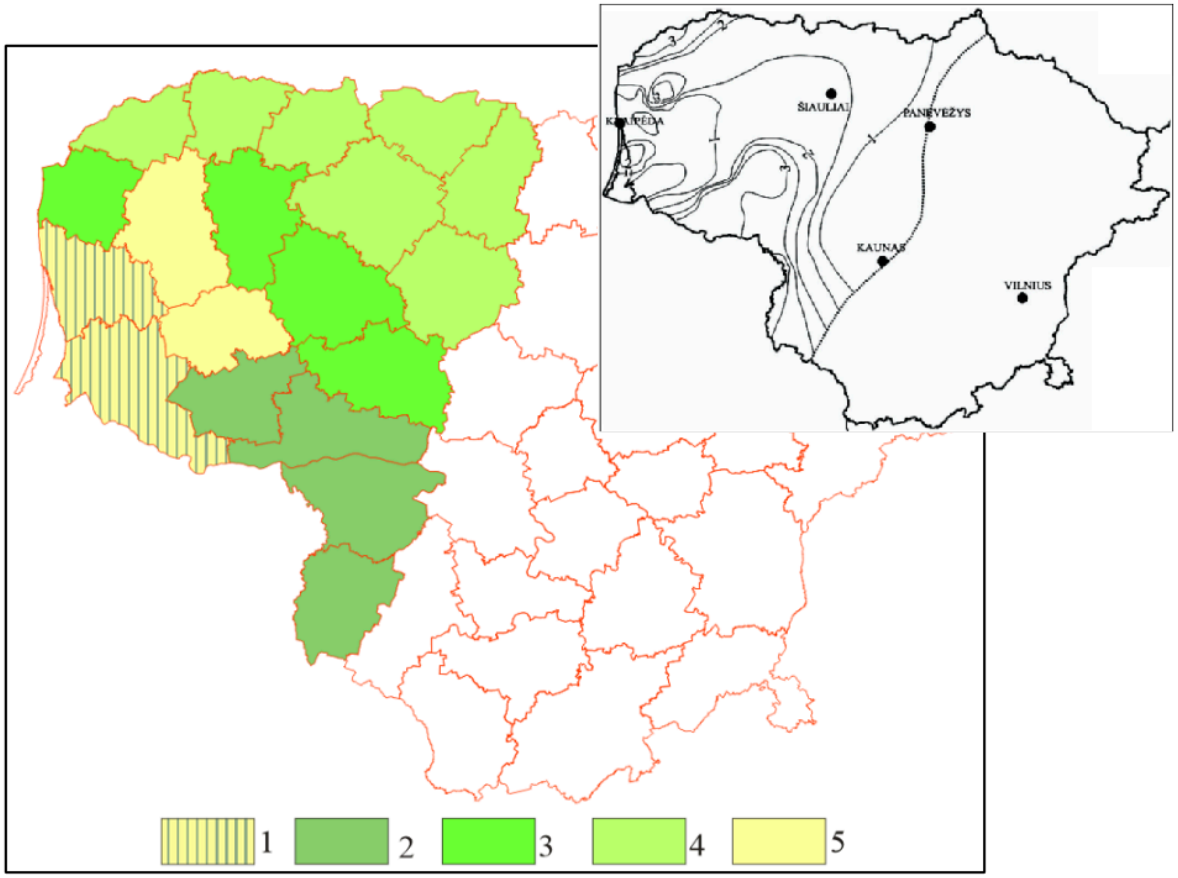

Figure 29. *Geothermal potential rating.*

Geothermal capacity of a geothermal doublet (MW_{th}). 1 – Lower Devonian prospective HD systems (borehole doublet of the 4-8 MWh_{th}); Deimena RSt: 2 – capacity >3-1.5 MWh_{th}. 3 – capacity 1.5-1.0 MWh_{th}. 4 – capacity 1-0.5 MWh_{th}. 5 – capacity <0.5 (Šliaupa, 2008).

Table 2. *Capacity of a geothermal doublet in 9 towns in west Lithuania:*

City	Doublet MW
Klaipėda	0,6
Mažeikiai	1,6
Šilutė	0,4
Tauragė	3,4
Plungė	1,5
Radviliškis	1,3
Raseiniai	2,0
Šakiai	2,0
Šilalė	1,5

4.6 Hydro chemical zonation of the Cambrian geothermal aquifer

The Cambrian aquifer comprises high potable water resources in north Estonia and grades to the saline aquifer up to 203 g/L mineralization (**Figure 30**). The potentiometric surface ranges from +150 m in borehole Tverečius-336 in easternmost Lithuania to +42 m in Palanga mineral water exploration boreholes implying regional water flow directed from the east to the west. Furthermore, the Klaipėda geothermal wells are affected by local water flow directed from the southwest (Mazury High hydrodynamic zone).

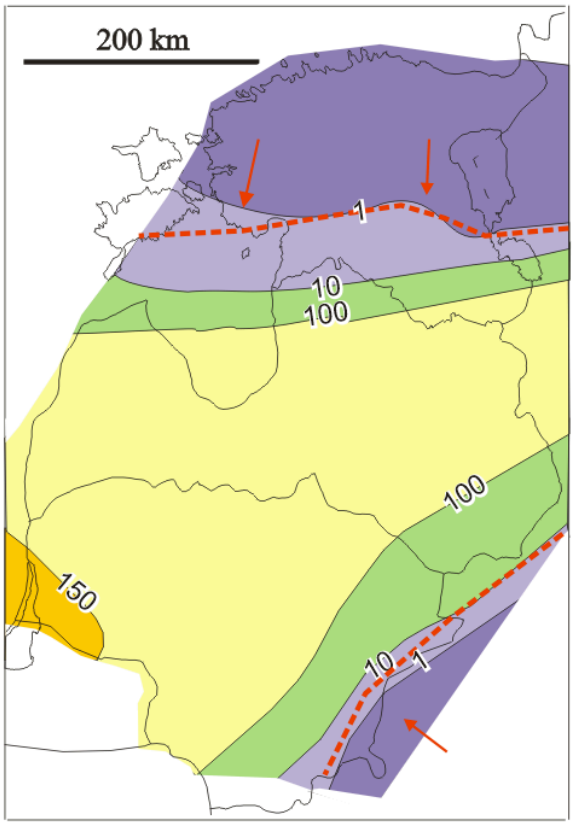

Figure 30. *Water salinity of Cambrian reservoir. g/L (Sliaupa et al.. 2003).*

The lowest mineralization is defined in southeasternmost Lithuania (potable water 0.23 g/L in boreholes Poškos-75, Barčiai-61 in the Šalčininkai region) to 8.0 TDS (borehole Rudmina-713) that is affected by the most intense meteoric water infiltration. It is interesting to note that the mineral water borehole A.Panerių-299 ("Vokė" bottled water) was exploited in this zone close to

Vilnius. The salinity increases sharply from 10 to 100 g/L and is mapped within the 40-50 km wide zone marking the hydrodynamic collision between the compactional water flow in the west and the meteoric water flow in the east (**Figure 31**). There is a low variation in the salinity 100-120 g/L observed in the middle part of Lithuania. The West Lithuanian Geothermal Anomaly (**Figure 26**) is confined to the systematic increase of mineralization to the southwest delineated salinity >120 g/L and reaches as high as 203 g/L close to Šilutė.

Three water type zones are mapped (1) Ca-HCO_3 (<1 g/L), (2) Ca-Na-Cl-SO_4 (1-120 g/L), (3) Na-Cl (120-200 g/L) type. The neutral water (pH=8.1-7.5) is distributed in the shallow aquifer to acidic (pH=5.5-4.0) in the deep part of the basin.

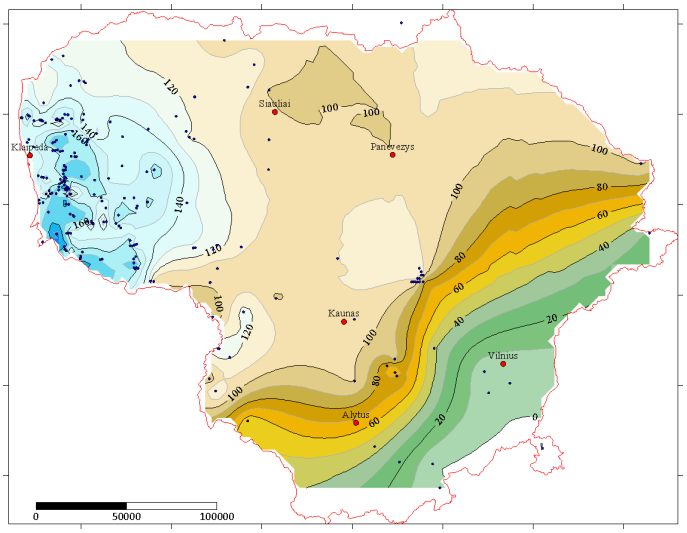

Figure 31. *Mineralization of the Cambrian aquifer. Studied wells are indicated (samples N=279).*

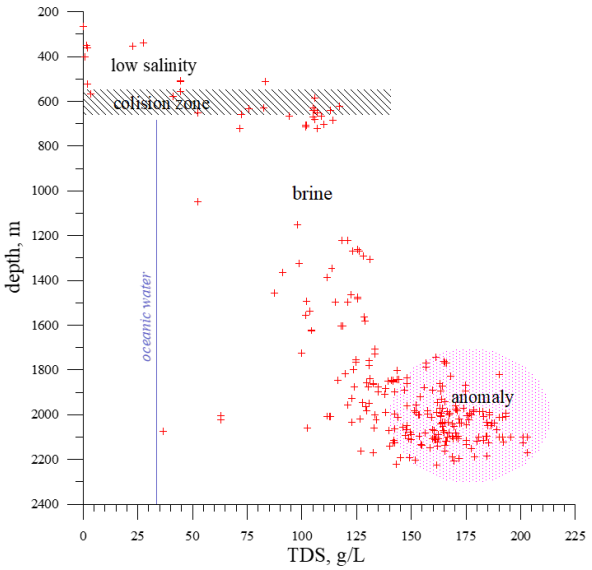

Figure 32. *Mineralization vs. depth of the Cambrian aquifer (number of samples 296). Explanation remarks are discussed in the text. The oceanic water TDS is indicated shoeing very high relative salinity of teh Cambrian formation water.*

The water salinity diagram illustrates three major hydrochemical boundaries in Lithuania (**Figure 32**). The hydrochemical transition zone is defined at a depth of c. 600 m, which is also interpreted as the hydrodynamic boundary. The active meteoric water inflow is defined in the east, while the low-activity (compactional) (Kreitler, 1989). The paleo-hydrochemical

reconstruction of the hydrogeological regime was modelling along the regional-scale profile crossing the Baltic basin that implies migration of the collision zone in the east of Lithuania (Puronas and Šliaupa. 2005).

The cation concentration of the Cambrian aquifer water follows the calcite-natrium trend (**Figure 33**). Several samples are plotted on the calcium field collected from east Lithuanian wells (meteoric water influenced zone). Several anomalies might have accounted for technical errors documenting the laboratory results (*e.g.*, seven wells in the Namiestis oil field?). The anion diagram shows a very strong chloride-suphate trend. Several wells represent meteoric water influx in east Lithuanian. A very strong enrichment in SO_4 (about 5 g/L) is documented in the Lakajai aquifer marking the collision zone and gradually reducing to the west.

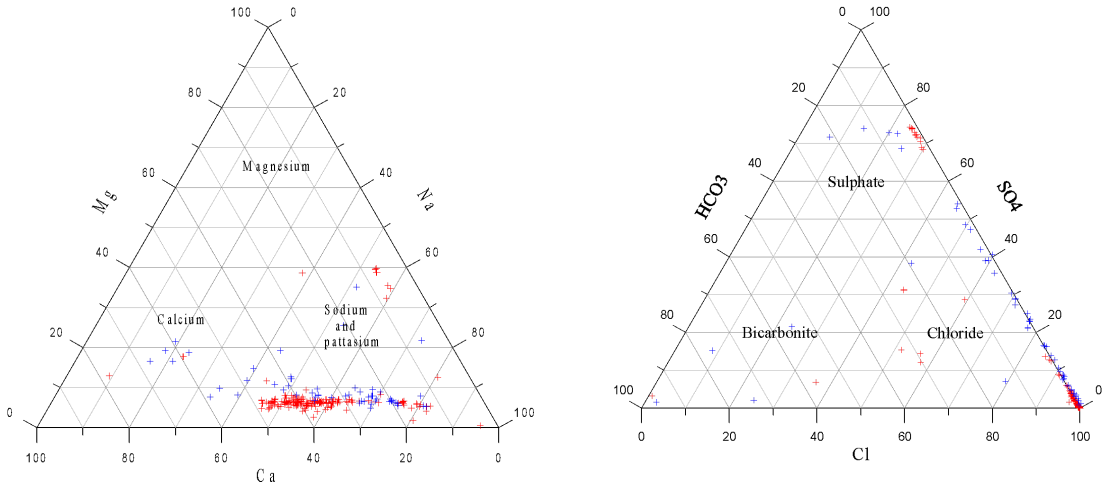

Figure 33. *The cation and anion ternary diagrams show the major trends of the Cambrian and Kemeri (discussed below) water composition.*

The sulphate enrichment is the most spectacular evidence of the hydrogeological system of the Cambrian aquifer. Four hydro chemical zones are distinguished in Lithuania (**Figure 34**). The collision zone is the most sharp boundary defined on the diagram (depth of about 600 m). Notable, the highest sulphate concentration is documented along this boundary (reaching 5.0-5.37 g/L). The concentration of sulphates increases systematically to the west. The "transzonal" zone is defined on the graph, the depth 1300-1650 m. The depletion of sulphates is the most peculiar phenomenon of the Cambrian aquifer in the deepest part of Lithuania (to as low as 10 mg/L). The concentration in the Baltic Sea and Global Ocean are most similar to the middle part of Lithuania.

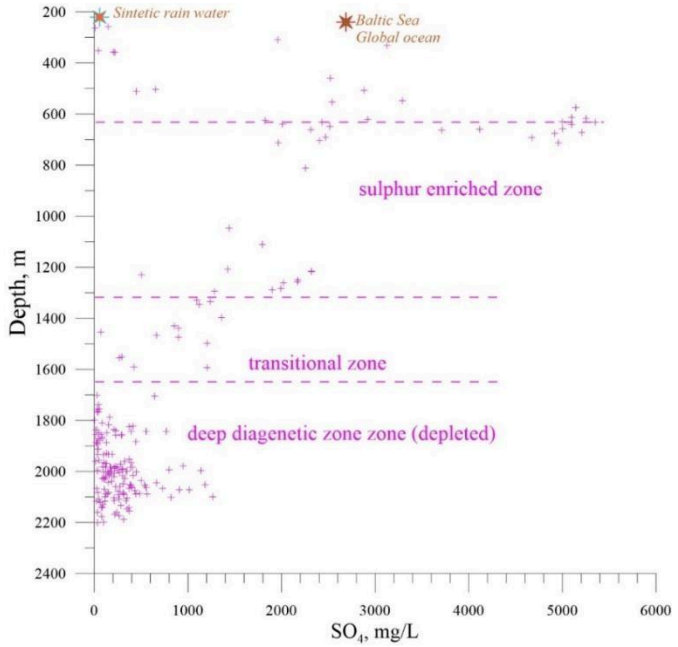

Figure 34. *Enrichment and depletion concentration in SO_4 with depth. 4 hydrochemical zones are defined.*

The chlorite shows a steady increase with depth and riches maximum value of 12.1 g/L in the Degliai wells (for comparison - oceanic water 18.9 g/L), while the carbonate concentration shows no definite trend with a depth of about 0.20 g/L. The amount of sodium increases with the depth and reaches 42.5 g/L in the borehole Geniai-1 (oceanic water 10.55 g/L) and potassium maximum value 2.4 g/L (in well Šiupariai-1), calcium 3.9 g/L (well Barzdėnai-1) and magnesium 5.2 g/L (well Lašai-1). All the wells, characterised by the highest concentration of chemical bulk elements, are restricted to the West Lithuania Geothermal Anomaly. The chemical composition of the water is a paramount parameter for fish and shrimp farming. The most important chemical elements are listed by (Mostafa Shamsuzzaman and Kumar Biswas. 2012): Phosphorus, Copper, Zinc, Magnesium (up to 2,3 g/L in the Ž.Namiestis wells), Calcium (up to 3.9 g/L in the well Barzdėnai1), Potassium (up to 5.3 g/L in the well Baubliai-1), Iron (varies from 6.3 mg/L in Tverečius-336 up to 62 mg/L in the well Rusnė-1), Manganese, pH (3.0 in the Aisčiai Group aquitard to 5.1 in geothermal anomaly to 7.4 in the potable water in the well Poškus-75).

Therefore, the deep wells provide a variety of chemical compositions for selecting most prospective sites in Lithuania. The database collected in Lithuania shows the flexibility for the management of the geothermal-hadrochemical conditions.
The overlapping technique of two maps, temperature and water mineralization, shows the close correlation between the two parameters (**Figure 35**). The proximal parameters to the Baltic Sea indicate (1) the highest temperature which, however, is a negative parameter due to very low reservoir quality and (2) peculiar chemical composition of the pore water of the aquifer. The prospective area is defined in middle Lithuania.

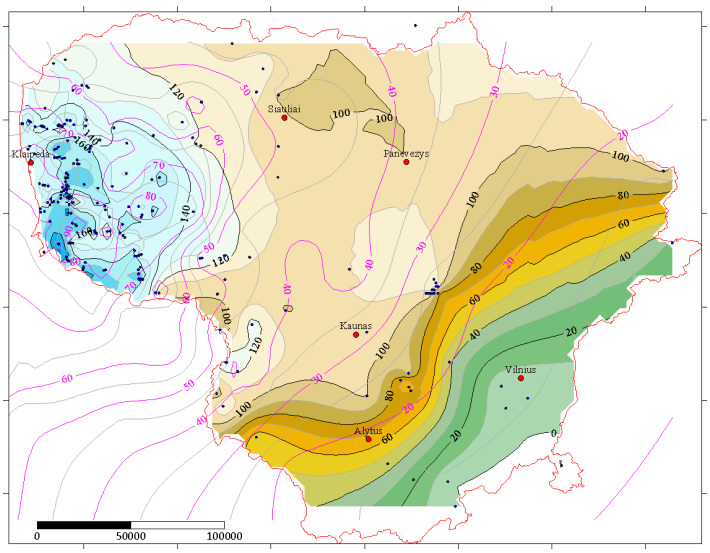

Figure 35. *Temperature overlying the salinity map of the Cambrian aquifer. Studied wells are indicated, see contour lines.*

4.7 Review of the geothermal wells Vydmantai-1,-2

The boreholes Vydmantai-1 and Vydmantai-2 were drilled, basically, seeking to assess petrothermal (hot dry rock) resources in west Lithuania. Also, the drilling with coring was carried out in the Kemeri sandstones and the Cambrian sedimentary rocks. The drill cores:

I. 439-737 m (Upninkai-Šventoji aquifer)
II. 839-1004 m (Kemeri Fm.)
III. 1972-22015.5 m (Cambrian)
IV. 2015.5-2564 m (crystalline basement)

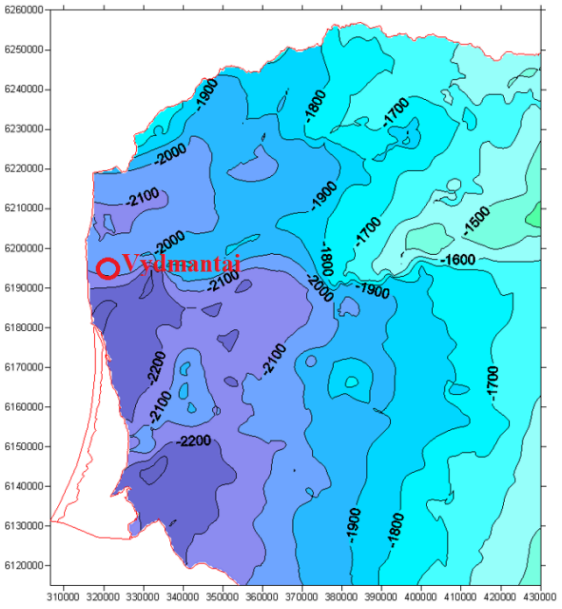

Figure 36. *Depth of the top of the Cambrian reservoir, see contour lines.*

Two boreholes were drilled close to the Vydmantai village. The borehole completion:
Vydmantų-1 – exploitation casing 5.7“ (146 mm) to 2141 m. open boreholes in the crystalline basement 7.5“ (190 mm) to as deep as 2564.

Vydmantu-2 - exploitation casing 5.7“ (146 mm) to 2140.8 m. open crystalline basement 5“ (127 mm) to as deep as 2150.

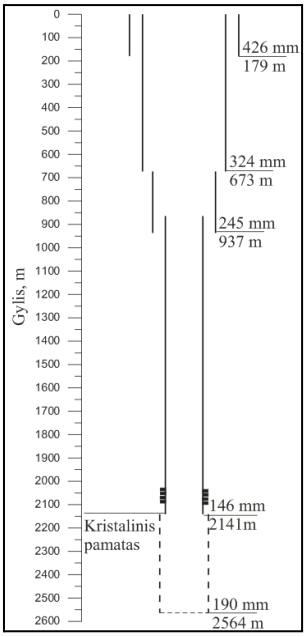

Figure 37. *Borehole conceptual plot*

Crystalline basement parameters indicated on the plot (borehole Vydmantai-1):

I. Drill core recovery (%) (rather poor due to the old drilling rig. also suggesting fracturing)
II. Geological index (old indexing; updated dating 1.84 Ga).
III. Comments and symbols:
IV. *Base of Cambrian sandstones (base of sedimentary cover)*
V. *Vval – weathering crust (inconsistent interpretation; interpreted as saprolite)*
VI. *++ - enderbites (granulitic facies). Int. 2013-2485 m*
VII. *~~ - biotitic shists (sheared zone). Int. 2485-2562 m (thickness of the shear zone 400 m)*
VIII. *Others (e.g. granite veins).*
IX. Thermal conductivity (W/mK)
X. Fractures – vertical and high-angle (19) and sub-horizontal (20) and breccia (21)
XI. Slicking sites (23)

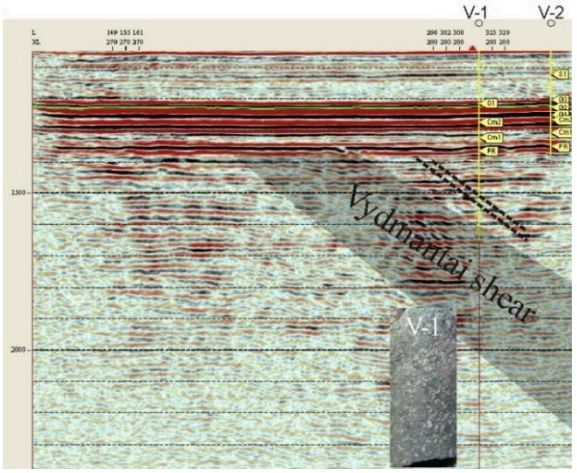

Figure 38. *3D seismic profile crossing the boreholes Vydmantai-1 and Vydmantai-2. Vydmantai shear zone is clear by disturbance of seismic reflectors. Sheared mylonite is shown.*

The **Cambrian** sandstones (Deimena RSt) were drilled by drilled sampling. In the borehole Vydmantai-1, the Deimena RSt was defined at the depth 1972.0-2034.8 m, and borehole Vydmantai-2 – int. 1959.0-2027.0 m. The well logging was carried out in both boreholes. The "hot" shales represent the reference level at the base of the Silurian shales. The thickness of the Ordovician succession is estimated at 125.5 m. The thickness of the Deimena RSt is defined 62.8 m in the borehole Vydmantai-1 and 68.0 m in in the borehole Vydmantai-2. The well loggin implies some disturbance between two wells in the Pajūris Fm. (*e.g.*, peneplain undulations).

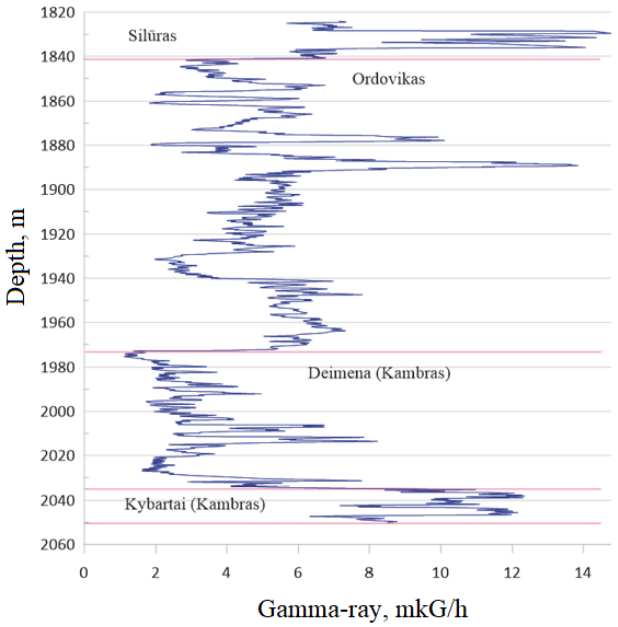

Figure 39. *Gamma-ray log (mkR/h). lowermost Silurian. Ordovician. and Cambrian. borehole Vydmantai-1. The sands were deposited in the distal shelf that was severely affected by high-temperature diagenesis (authigenic quartz cementation). The Cambrian sandstones are overlain by the Ordovician shales and carbonates 132 m thick.*

The Pajūris, Ablinga, and Giruliai Fms are well correlated wo the adjacenent wells (closest are located Girgaliai oil field). The main sandstone is defined in the middle and lower part of the Pajūris Fm.

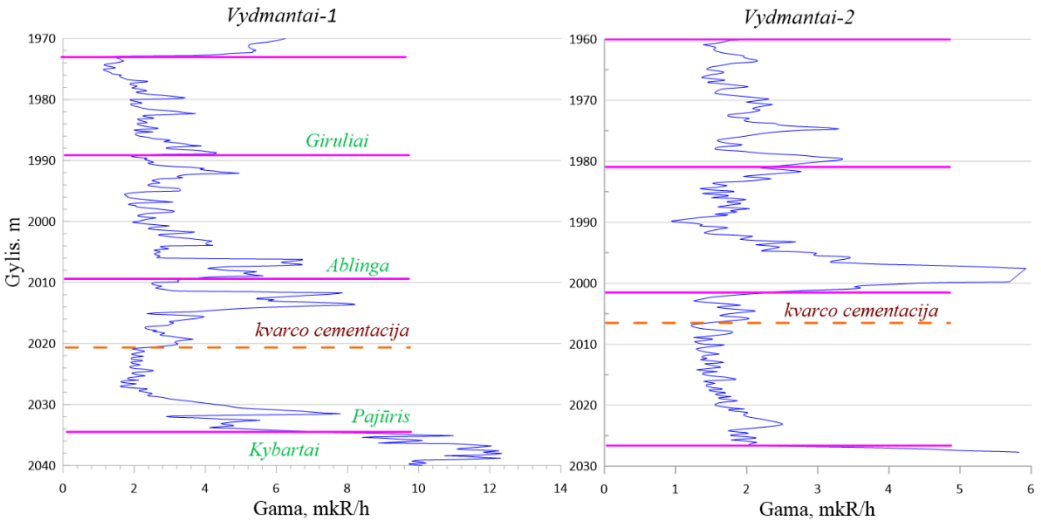

Figure 40. *Gama-ray (mkR/h) well log of boreholes Vydmantai-1, -2. The authigenic quartz cementation is defined at the depth of 2020.3 m in the borehole Vydmantai-1 and 2006.0 m in the borehole Vydmantai-2. Please note the larger thickness of the Cambrian succession in the borehole Vydmantai-2 (basement undulation). The specific details document variations of the sin-sedimentation features.*

A number of samples were collected to measure the petrophysical properties of the Deimena sandstones. Porosity of the the Giruliai ir Ablinga Fms sandstones was measured very 3-8% and permeability 0.1-1 mD. In general, the reservoir properties are controlled by the natural fracturing of sandstones. The lower part of the reservoir is attributed to the Pajūris Fm which shows increased reservoir quality: porosity 13-14% and permeability 100-200 mD.

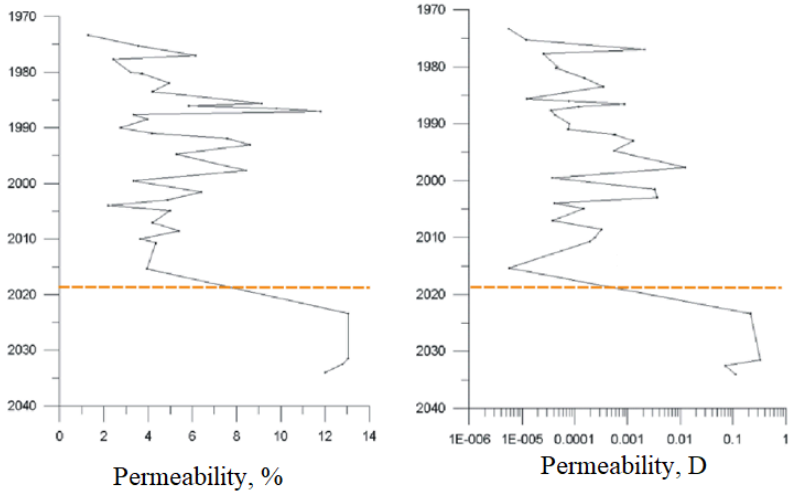

Figure 41. *Porosity and permeability of sandstones, borehole Vydmantai-1. Two sandstones are defined as severely quartz cemented sandstone in the upper part of the reservoir and higher reservoir quality is defined in the lower part of the Deimena Fm.*

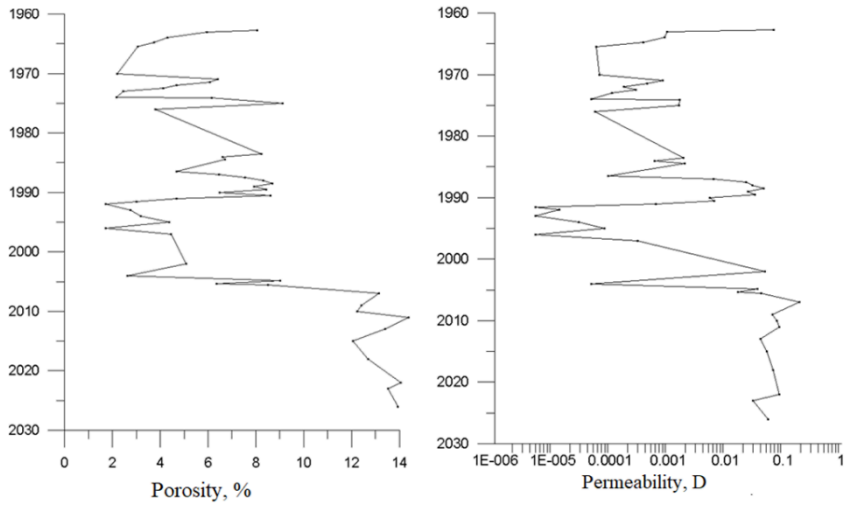

Figure 42. *Porosity and permeability of sandstones, borehole Vydmantai-2. Two sandstones are defined as severely quartz cemented sandstone in the upper part of the reservoir and higher reservoir quality is defined in the lower part of the Deimena Fm.*

It should be noted the geothermal boreholes were drilled close to the Girkaliai oil field. Therefore, abundant drill core information is available about both sites. Also, a high-quality 3D seismic survey was carried out to plan the oil field exploitation strategy. The main tectonic

feature studied in the site is the largest Telšiai fault trading from the Baltic Sea to the Pasvalys and Biržai region.

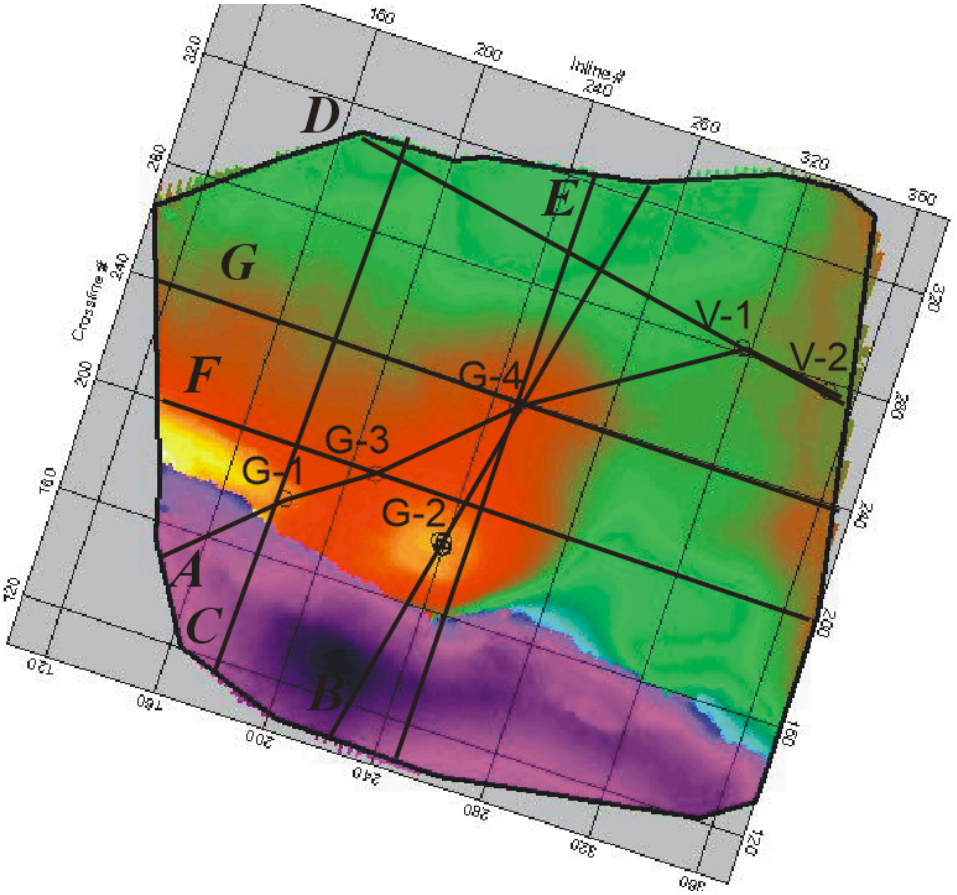

Figure 43: *3D survey in Girkaliai-Vydmantai block (depth of the crystalline basement, colour scale). Please note the large Telšiai fault established on the foot wall of the fault.*

Figure 44. *1 – Strongly quartz cemented sandstones, oil production borehole Girkaliai-5 (Giruliai Fm.); 2 – moderately cemented sandstone stained with oil, borehole Girkaliai-5 (Pajūris Fm). 30º deviated well. The Vydmantai boreholes are located outside the oil field contour.*

Table 3*. The main reservoir parameters of boreholes Vydmantai-1.*

	Girulių Fm			Ablingos Fm			Pajūrio Fm		
Borehole	Ef.thick. m	Porosity %	Permeability D	Ef.thick. m	Porosity %	Permeability D	Ef.thick. m	Porosity %	Permeability D
Vydm-1	5.2	5.0	0.001	10.2	7.2	0.006	20.8	9.0	0.1
Vydm-2	4.8	8.5	0.01	7.8	6.4	0.005	27.0	13.0	0.2

The typical average grain size of sandstones is estimated at c. 16 mm in west and middle Lithuania. The Vydmantai samples show a smaller grain size that, in turn, prompts intense quartz cementation?

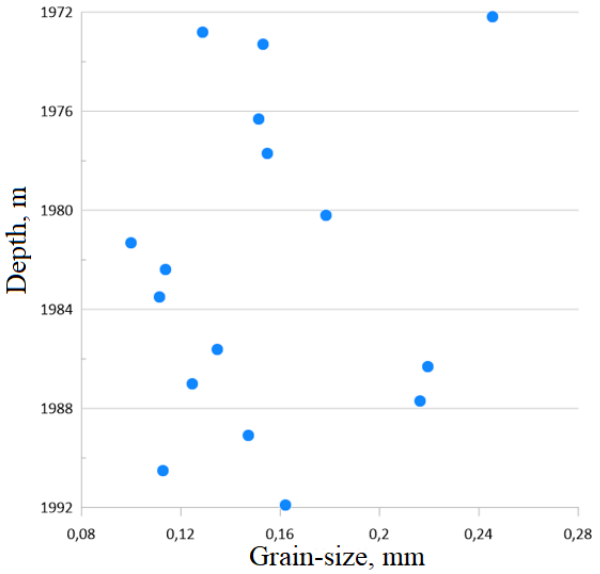

Figure 45. *The grain size is smaller than most of the Lithuanian Cambrian sandstones. The average grain size is estimated 0.13 mm.*

The chemical composition was studied in the Vydmantai wells. Salinity was documented as low as 28 g/l in the Kemeri aquifer and as high as 173 g/l in the Deimena aquifer. The water is classified as the type Na-Cl in both aquifers.

Temperature 74°C was measured in the Deimena aquifer. Chemical analysis is presented below:

I. *Density* – 1.119 g/cm^3
II. *Hardness (very hard)* – 1405 mol/m^3
III. *Mineralization* – 170.4 g/L
IV. *Cl* – 106.4 g/L
V. SO_4 – 0.019 g/L
VI. HCO_3 – 0.095 g/L
VII. *Na* – 36.4 g/L
VIII. *K* – 0.87 g/L
IX. *Mg* – 3.8 g/L
X. *Ca* – 21.9 g/L
XI. Fe^+3 – 11.46 mg/L
XII. Fe^+2 – 40.1 mg/L
XIII. *J* – 2.9 mg/L
XIV. *Br* – 803 mg/L
XV. *B* – 20 mg/L

The concluding figures summerise the main reservoir parameters of boreholes Vymantai- and Vydmantai-2. Two shale layers divide the reservoir into three compartments. Considering the reservoir quality, the Upper 1 and Lower 2 sandstones are defined. The upper part is classified as

the fractured reservoir that shold be subject to hydrofracturing (stimulation), while the lower part is classified as a moderate quality porous type reservoir.

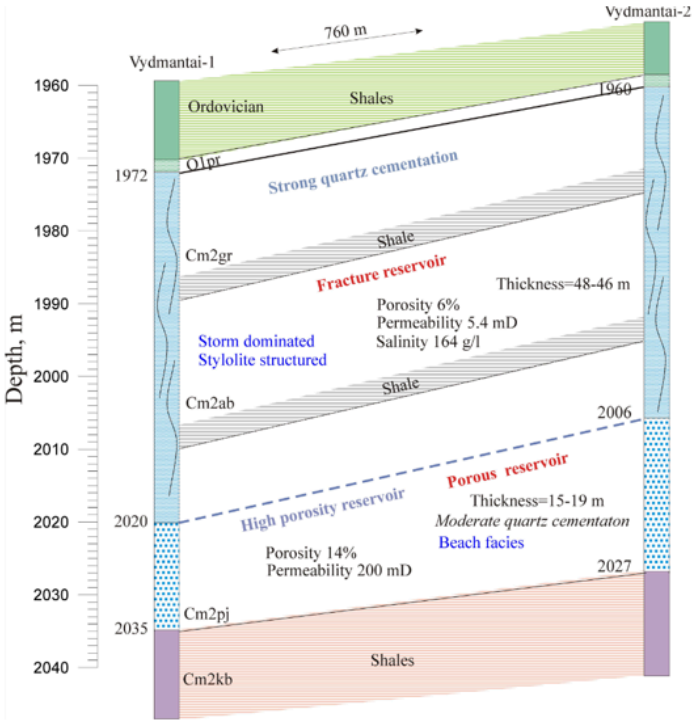

Figure 46. *Overview of the boreholes Vydmantai- and Vydmantai-2.*

4.8 Kemeri geothermal aquifer (lower Devonian): Distribution, depth, and thickness of the Kemeri geothermal aquifer

The Kemeri-Rezekne-Pärnu Fms of the Lower-Middle Devonian is the second-largest geothermal aquifer in the Baltic Artesian Basin. Due to the poor reservoir quality of the Pärnu Fm and the absence of the Rezekme Fm in Lithuania (except in the northeasternmost corner of the country, 7 m thick sandstones mapped in Ignalina NPP area). Only the Kemery Fm is discussed in the present chapter (Sorokin, 1979; Valiukevičius, 1994; Kleesment and Mark-Kurik, 1997; Lukševičs et al., 2012).

The depth of the top of the Kemeri Fm (global Pragian Stage) ranges from -138 m in Visaginas wells to -1028 m in the well Nida-1 (**Figure 47**). It is notable, that the basal part of the Ķemeri Fm is marked by conglomerates impregnated by pyrite and dolomite cement evidencing short break sedimentation after deposition of the Gargždai Fm composed of shales, sandstones, siltstones, and dolostones.

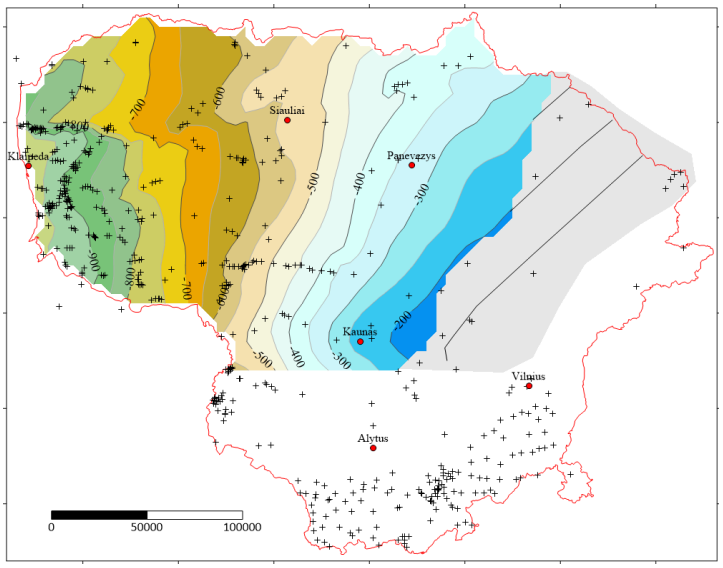

Figure 47. *Depth of top of the Kemery RSt. Wells of the database (cross symbol).*

The thickness of the Kemeri aquifer ranges from 100 m in the southwest to 190 m in the northwest of Lithuania (**Figure 48**). The maximum thickness is confined to the Jelgava Depression in northwest Lithuania and central Latvia. The thickness attenuates to the southeast towards the Belarus Anteclise. The wide range in thickness points to significant variation of the aquifer capacity.

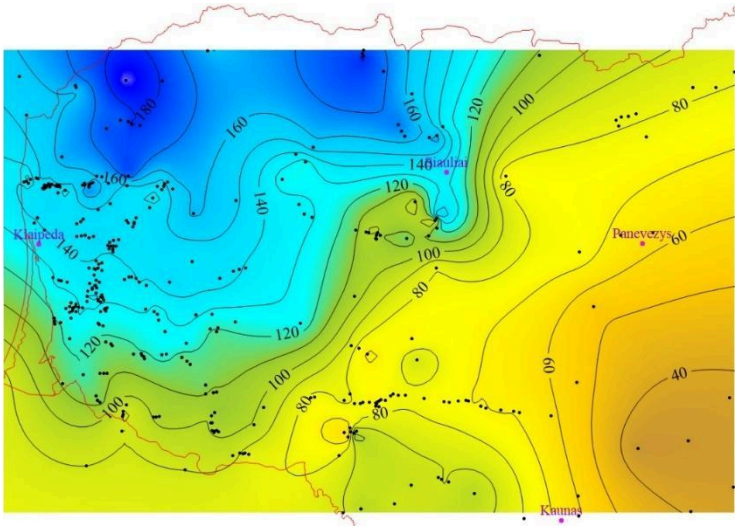

Figure 48. *Thickness of the Kemeri Fm. There is no sin-sedimentary faulting is recognised. while most tectonic activity was registered in Baltic basin (and Lithuania) in the earliest Devonian time (Gargždai Fm.). Deep wells are indicated on the map (black dots).*

4.9 Stratigraphy of the Kemeri RSt. succession in Lithuania

The age of the Kemery aquifer is defined as the Pragian Stage (**Table 3**). In Lithuania, the Viešvilė RSt is characterised by predominating sand lithological alternating to the shales. The aquifer comprises the Šešuvė and Viesitė Fms. For the sake of simplicity, the term Kemery Fm was used in the report. The aquifer is underlain by the lower Gargždai RSt (Lochkovian Stage) and overlain by the Pärnu RSt (lower Eifelian Stage) with a significant break in sedimentation, due to regression of the Rezekne RSt (upper part of the Emsian Stage) in Lithuania territory. The Pärnu RSt is strongly cemented by dolomites and contains dolostones and marlstones that are classified as a no-reservoir part of the aquifer in Lithuania.
In Latvia and Estonia, the thickness of the Rezekne RSt attains 15-35 m and thickness of the Pärnu RSt varies from 10 to 65 m. The marlstones are abundant in the easternmost area.

Table 4. *Stratigraphical chart of Lithuania.*

Stage	Regional stage	Formations
Pragian	Viešvilė RSt *(Kemeri Fm)*	*Viesitė Fm*
		Šešuvė Fm

The friable sandstones, locally strongly cemented layers by dolomite and anhydrite, alternated with shales. The sandstones intercalate to shales at about net-to-gross 0.63-0.68 and increase to 0.75 in Latvia. Sandstones are mostly fine- and very-fine grained, massive and cross-layered. Terrigenous sediments are of grey and reddish colours (**Figure 49**).

Figure 49. *Friable sandstone (Oldred Sandstone), borehole Palanga-138a. Gray and old-red colours are documented in the well. Fine sandstones are cemented by dolomite and an admixture of clay minerals.*

Figure 50. *Transition of the gray to red coloured shales. Kemeri formation, well Vydmantai-1. This boundary reflects a transition from aridic sedimentation to a more humid sedimentation environment.*

The composition is as follows: 81–96 % of detrital quartz (mean value 92 %), 3–12 % detrital potash feldspars (mean value 8 %), 0.2–2.0 % detrital micas (muscovite), 0.2–2.0 % chlorite and locally with glauconite <2.0 %. Some feldspar grains are weathered (0.2–5 %).

Carbonates and clay are the main cementing fractions of sandstones. The detrital grains are overground by thin authigenic quartz of a few percent volume and indicated moderate burial temperatures (**Figure 51**). Gypsum cement is present in some sandstone layers rather. For example, gypsum is present at 1-2% in the well Palanga-318a, whereas no gypsum was identified in the well Vydmantai-1, located only a few kilometres away. The detailed study of the drill cores revealed some differences in both boreholes, such as higher content of organic matter in the Kemeri shales in the borehole Vydmantai-1 and more intense weathering of the potassium feldspars in the same well. In scarce boreholes drilled in west Lithuania, the lower and upper parts of the reservoir are characterised by the red colour of shales, whereas shales are of gray and dark gray colour in the middle part of the section.

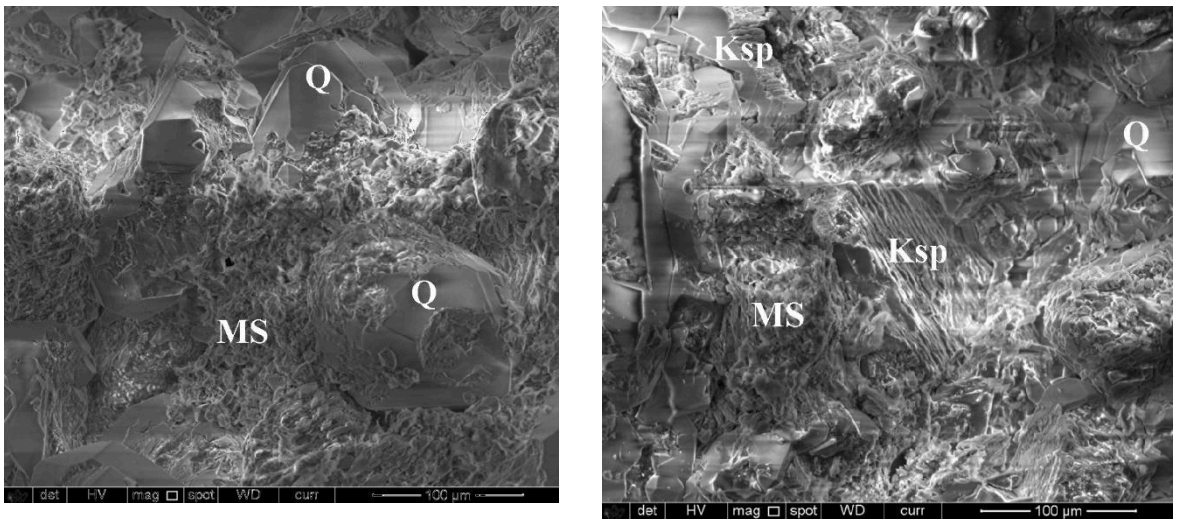

Figure 51. *A - Quartz grains (Q) are overgrown by authigenic quartz and pores are damaged by the abundant drilling mud (MS). An ideal (crystalline) shape of quartz grain is a distinct feature; B - Diagenetic illite (I) between quartz (Q) and potassium feldspar (Ksp) grains. Kaolinite is observed in the lowermost part of micrograph. Borehole Klaipėda-4.*

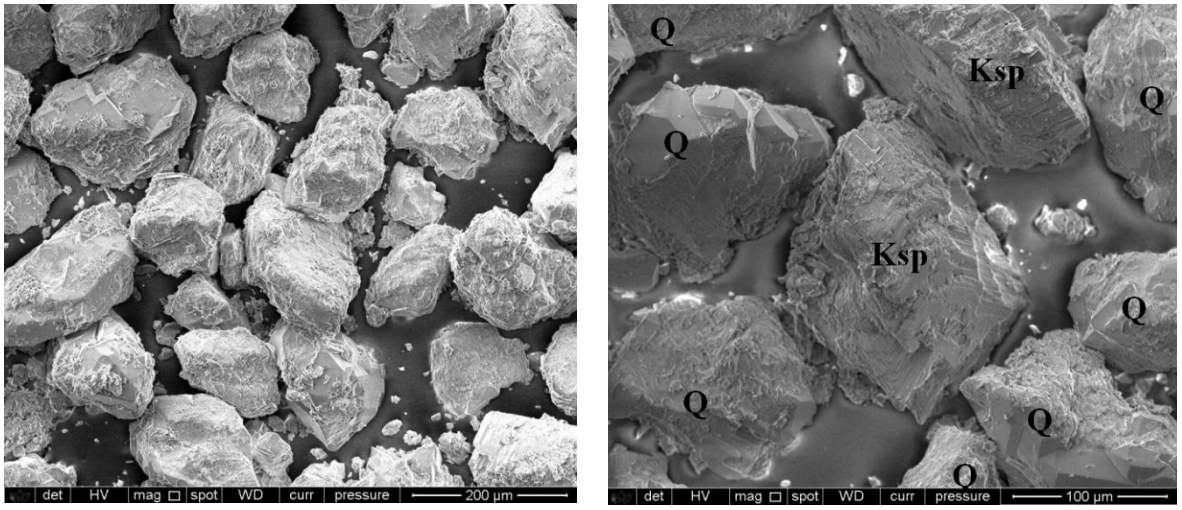

Figure 38. *C - disintegrated sandstone. Grain size is mainly in the range 0.1-0.3 mm (fine and medium sandstone). Please note abundant clay admixture (in situ and drilling mud). D – Quartz and potassium feldspar grains (0.15-0.20 mm large).*

There is an abundant grain size database available from west Lithuanian boreholes. The well Vydmantai-1 is the best-studied borehole represented by 110 sandstone and siltstone samples. The sandstones are classified as silty fine and silty medium sandstone. Fraction 0.10-0.25 mm predominates in studied sandstones. The average value of measured samples is calculated at 0.11 mm. The average grain size composition is shown in **Figure 52**. Three major sedimentation cycles are identified in the grain size distribution.

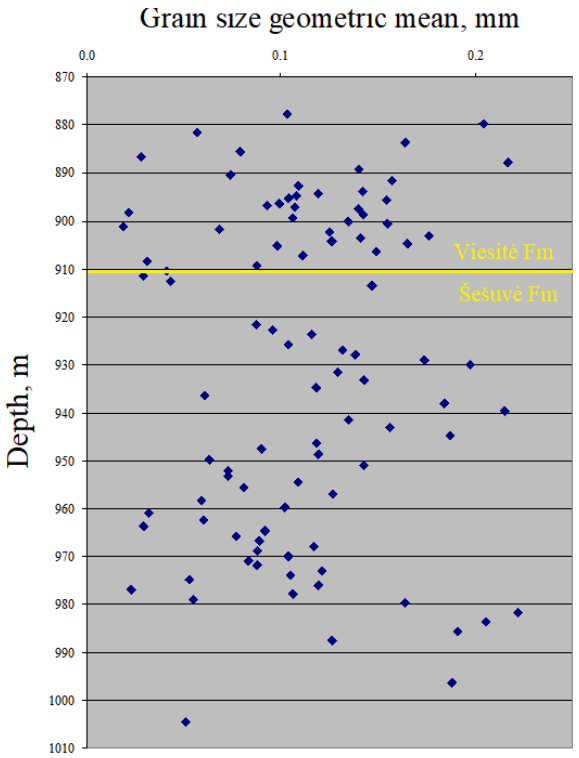

Figure 52. *Geometric mean of grain size of sandstones and siltstones of Kemeri Fm., well Vydmantai-1. Three sedimentation cycles are defined on the diagram. Compared to the Kemeri sandstone, the Cambrian sandstones have a larger average diameter (16 mm). Therefore, the Cambrian and lower Devonian sandstones show very different grain-size structure that, in turn, control the reservoir properties.*

The gamma-ray well log interpretation suggests complex intercalation of sandstones (effective part of the section) and siltstones/shales (non-effective part of the section) (**Figure 53**). The deposition environment is interpreted as a (1) deltaic complex, (2) braiding- and meandering-river system, and (3) shallow sea system. The intercalation of sandstones and shales is a key parameter in exploiting aquifer reserves of the Kemeri sandstones (**Figure 55 A.B.C**). On the other hand, some regularity should in the architecture of the Kemery reservoir (*e.g.*, the distinct boundary between two stratigraphic formations).

Four boreholes were drilled in the Klaipėda Geothermal Plant (Petrauskas et al., 2019). They show a similar 'stochastic' arrangement of the layered reservoir (**Figure 53, Figure 55**). All Klaipeda geothermal wells are located on- or close to the major seismic line NW-SE. Unfortunately, the Geological Survey of Lithuania does not have this data to ask for (possibly they are stored at the company AB Geonafta).

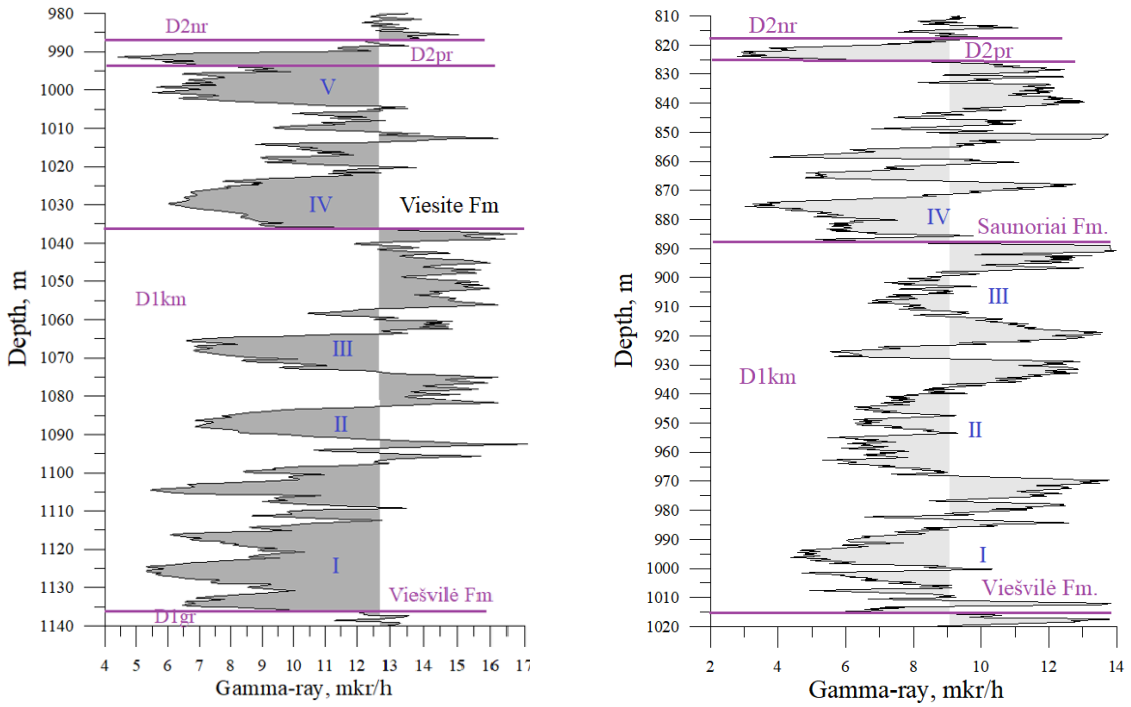

Figure 53. *A - Gamma-ray well log of borehole Kaipėda-1. Net-to-gross estimated 0.57% (effective thickness 82 m); B – Mamiai-1 located on the southern flank of the Jielgava Depression. Net-to-gross assessed 0.56% (effective thickness 106 m). Despite the strong heterogeneity of the two wells, Net-to-Gross was calculated identically which should be taken into account in the reservoir model. The Viešvilė and Saunoriai Fms. are well correlated on the gramma-gray log. The particular sandstones/shales layers do not show any regularity (e.g., sandstone V is not present in the uppermost part of the Kemery reservoir).*

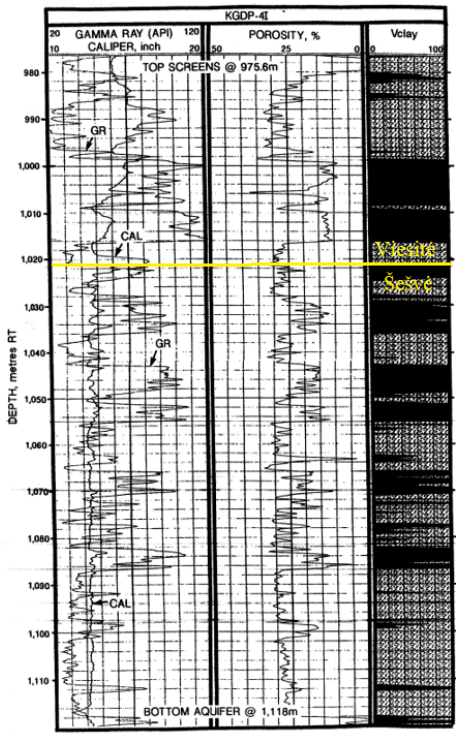

Figure 54. *C - Logging data and interpretation of well KGDP-1 4I (Logging data and interpretation) (Klaipeda geothermal site. injection well). There is some small fault suggested between wels KGDP1 and KGDP4 in the southern part of the profile.*

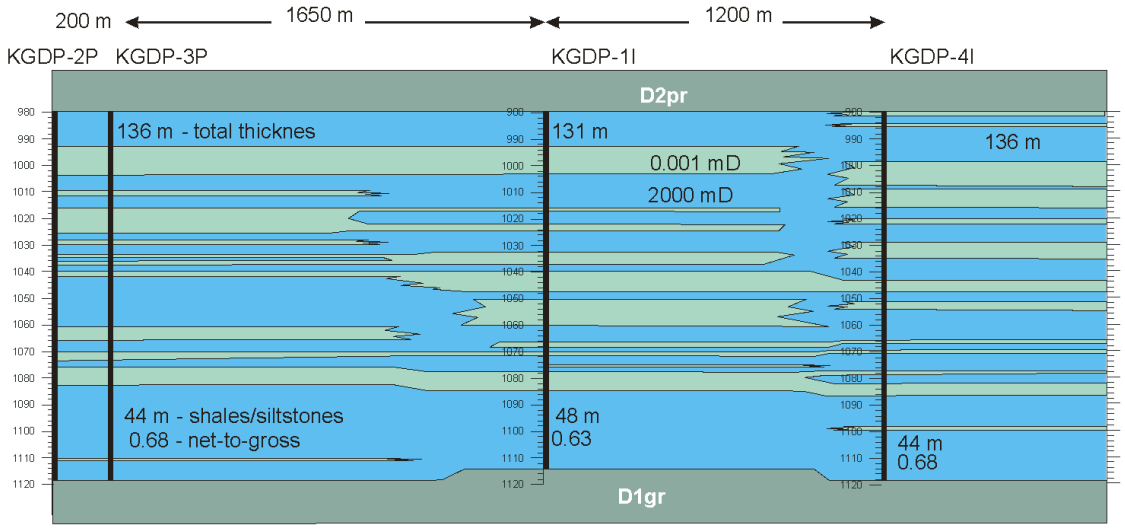

Figure 55. *Architecture of the Kemeri reservoir of the Klaipėda Geothermal Plant. Blue – sandstones. green – shales. Please note the irregular distribution of the terrigenous deposition system. Some long-term cyclicality is recognised in west Lithuania*

4.10 Reservoir properties of the Kemeri RSt.

The Kemeri reservoir is composed of fine-grained sandstones with abundant shale interlayers. Their reservoir properties are measured in only several deep wells in west Lithuania, mainly the deep geological mapping boreholes (*e.g.*, Nida-1), also geothermal boreholes Vydmantai-1,2 and Klaipėda Plant wells.

The average sample porosity is documented at 27.2% and permeability 995 mD (**Figure 56**). It should be noted that drill core recovery is very poor and most of the highest-porosity sandstones were lost during the drilling.

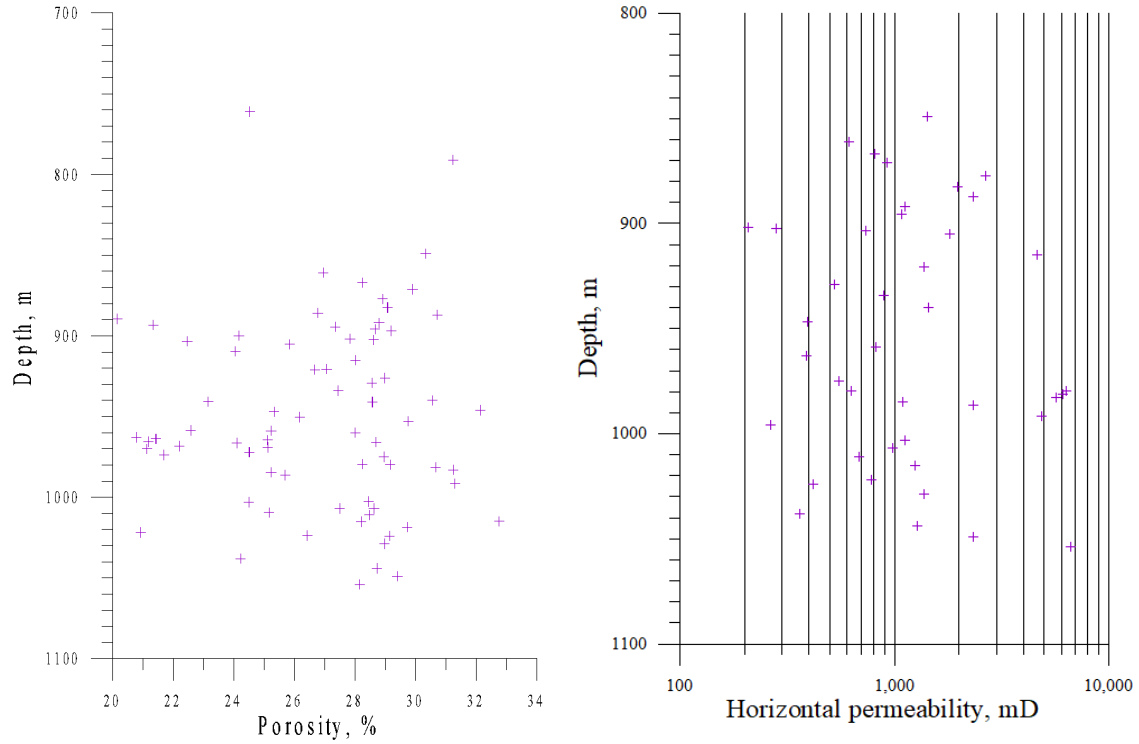

Figure 56. *Porosity and horizontal permeability plots of west Lithuania (depth. 760-1170 m).*

There is a poor correlation between porosity and permeability. It is most likely related to a heavy saturation by drill mud (**Figure 57**). The permeability is typically more affected than the porosity does.

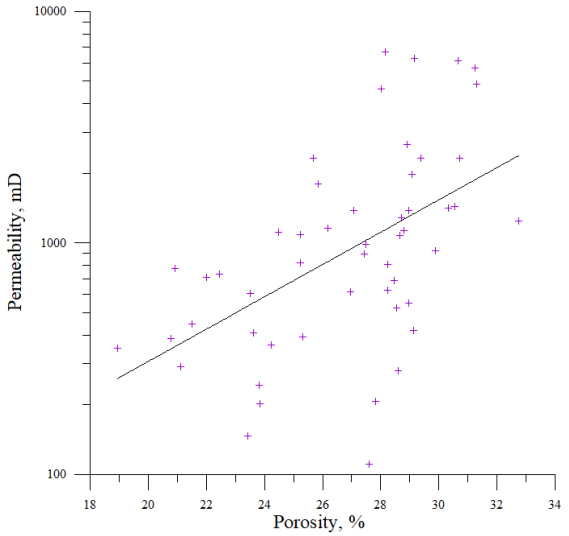

Figure 57. *Porosity and horizontal permeability, west Lithuania. Positive statistical correlation* r^2*=47%.*

4.11 Reservoir properties defined by well testing

The hydrodynamic well testing provides rather accurate results on the performance of the reservoir despite the very complex architecture of the Kemeri Fm. There are only a few well testing data available in west Lithuania (neither in the east). Furthermore, the hydrodynamic testing of borehole Vydmantai-1 and Palanga-318a failed due to technical inconsistency of the experiment (inerpreted abnormally low permeabilities, because of low-power compressor used).
The best experiment was carried out in the wells Vilkyčiai-3 and Vilkyčiai-5 (waste water utilisation). Two sandstone layers were tested in both wells (well perforated) (**Figure 58**).

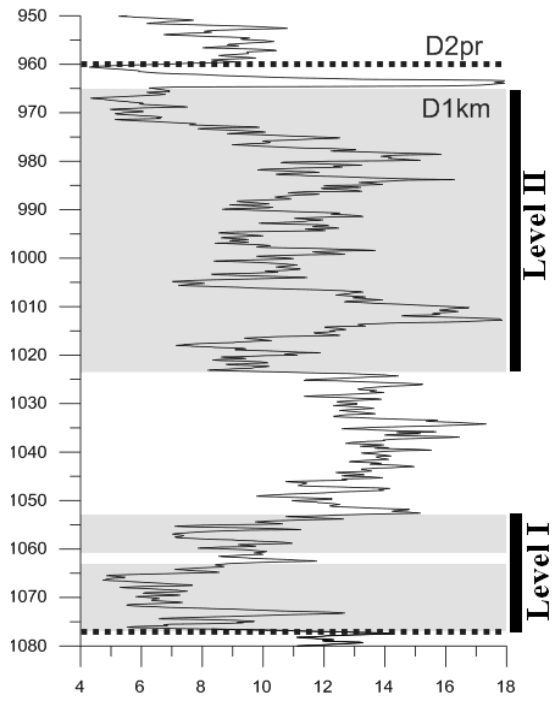

Figure 58. *Gamma-ray log of well Vilkyčiai-3. Perforated levels I and II are indicated.*

The well testing results of both wells are given in **Table 4**. It is interesting to note, the productivity ranges from 29 to 51 $m^3/h/atm$, while injectivity was defined as only 0.76-1.17 $m^3/h/at$:

Table 3*. Well testing results in wells Vilkyciai-3, -5 (of the year 1993).*

Parameters	**Results**
Water density, g/cm^3	1.043
Pressure	10.9 (at 1065 m)
well Vilkyčiai-3. level ***I****. depth 1050-1074 m*	
Productivity k_{ef}, $m^3/h/at$	33.64
Hydraulic conductivity k*h/M, $mkm^2*cm/MPa*s$	11872
Permeability k, *mD*	**4950**
Injectivity, $m^3/h/at$	0.76
well Vilkyčiai-3. level ***II****. depth 946-1029 m*	
Productivity k_{ef}, $m^3/h/at$	51.1
Hydraulic conductivity, k*h/M, $mkm^2*cm/MPa*s$	18033
Permeability k. *mD*	**2280**
Injectivity, $m^3/h/at$	0.86
well Vilkyčiai-5. level ***I****. depth 1053-1077 m*	
Productivity k_{ef}, $m^3/h/at$	29.4
Hydraulic conductivity k*h/M, $mkm^2*cm/MPa*s$	10391
Permeability k, *mD*	**4720**
Injectivity, $m^3/h/at$	0.81
well Vilkyčiai-5. level II. depth 965-1024 m	
Productivity k_{ef}, $m^3/h/at$	40
Hydraulic conductivity k*h/M, $mkm^2*cm/MPa*s$	14118
Permeability k. *mD*	**2206**
Injectivity, $m^3/h/at$	1.17

The experiment provides the most essential parameter on water injectivity and productivity of two wells. The ratio was recorded as low as 2.23 and 1.7% in the well Vilkyciai-3 and 2.8% and 2.9% in the well Vilkyciai-5! It points to severe damage to the reservoir and a very high skinning effect of the well. Based on the hydrodynamic experiment, the permeability of the upper layer is as high as 4.950 and 4.720 mD and the lower layer shows lower quality 2.280 and 2.206 mD. Furthermore, the samples measured in the laboratory show much lower permeability which is explained in terms of saturation of the drilling mud.

4.12 Temperature variations in the Kemeri RSt.

The temperature of the Kemeri aquifer varies from 8°C in the shallow basin periphery to 45°C in westernmost Lithuania (**Figure 59**). The most peculiar feature recognised on the geothermal map is the West Lithuanian Geothermal Anomaly that is delineated at 30°C. Tauragė, Šilalė, Klaipėda, Gargždai, Šilutė, etc. towns have reasonable potential for using geothermal district heating in west Lithuania.

The overlapping two maps, temperature and thickness, show the best prospects in the northern part of the geothermal anomaly (Klaipėda, Gargždai, Rietavas) due to the increase in thickness of the aquifer (**Figure 60**). The thickest reservoir has no economic geothermal potential in Salantai, Skuodas, Mažeikiai, Naujoji Akmenė, etc.

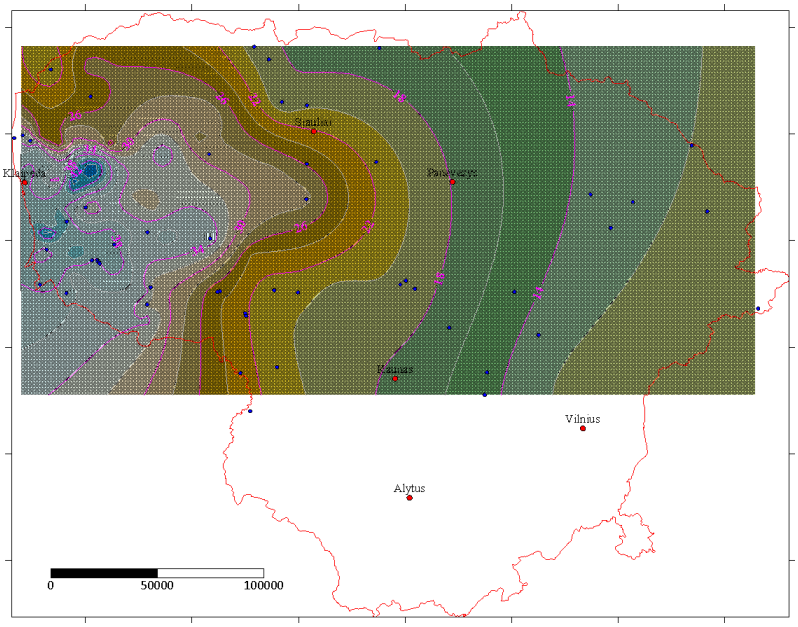

Figure 59. *Temperatures of the Kemeri geothermal aquifer, see doted points.*

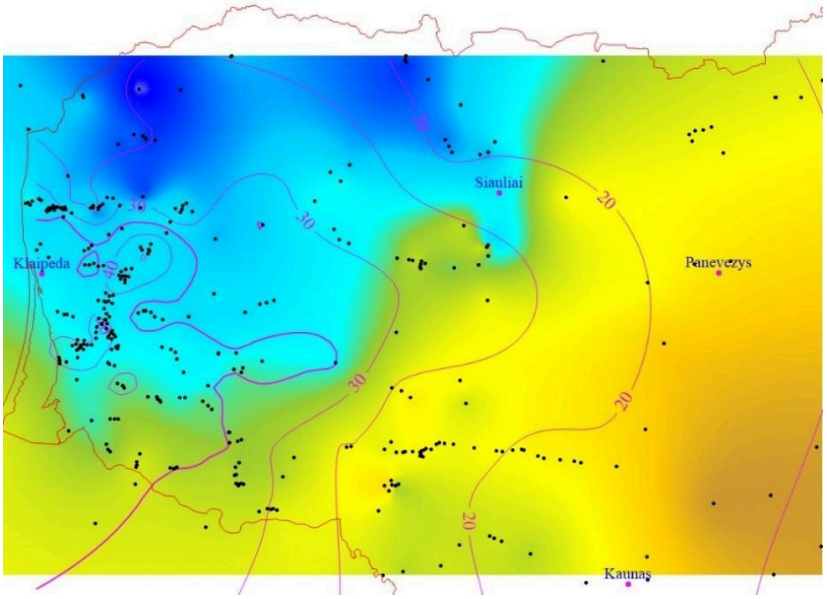

Figure 60. *Overlapping of two maps of temperature and thickness of the top of the Kemeri Fm. Temperature contour line >35°C is marked (bold line)*

There is a positive correlation between temperatures and depth of the top of the Kemeri Fm (**Figure 61**). The highest temperature was measured in wells Vilkyčiai-7,11 (52 and 48°C), Vežaičiai-6,4 (44 and 47°C), Ablinga-2 (47°C). The high temperature measured at the depth of 340-460 m is not commented in the text.

4.13 Water chemical composition of Kemeri aquifer

The salinity of the Kemeri aquifer ranges from sweet water in south Estonia to 10-100 g/L in west Lithuania (**Figure 62**). The meteoric war infiltration is active in the eastern and northern part of the artesian basin. The compactional water flow is defined in the southwestern part of the basin, including west Lithuania, Kaliningrad district, and the southern part of Baltic Sea. In Lithuania, the highest mineralization is documented in the Klaipėda geothermal wells.

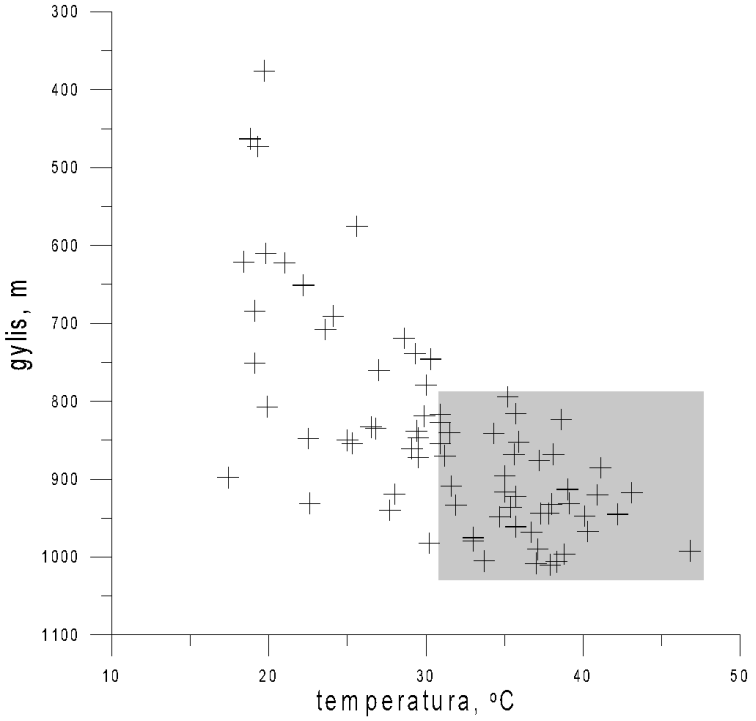

Figure 61. *Temperature of the Kemery aquifer. The West Lithuanian Geothermal Anomaly is marked (shaded).*

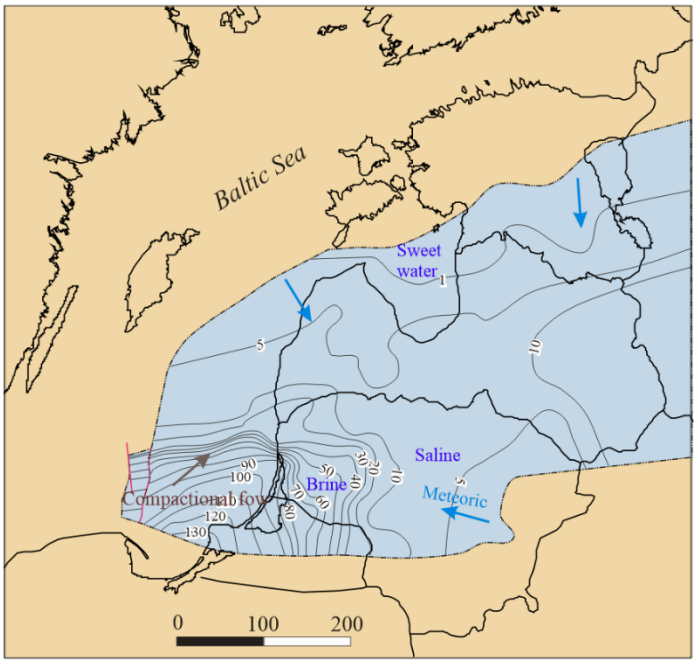

Figure 62. *Kemeri-Rezekne-Pärnu RSt geothermal aquifer of the Baltic basin (salinity, g/L), data shown in isolines.*

The active meteoric water infiltration zone is registered as shallow as <500 m (negative anomaly $\delta^{18}O$ -10.2 to -13.0‰). In the west Lithuania, the isotopic composition is more mature ($\delta^{18}O$ -4.5‰) (Mokrik et al., 2009). It is notable, the iron concentration of this Old Red formation varies from 1 mg/L shallow to 40 mg/L deep (and the highest anomaly 96 mg/L in well Barzdėnai-1).

The two hydrochemical zones are defined in Lithuania. The collision zone (mineralization of 15 g/L) between the meteoric flow in the east and compactional flow in the west is well traced along the Seda-Kuršėnai-Raseinai-Jurbarkas-Šakiai (**Figure 63**).

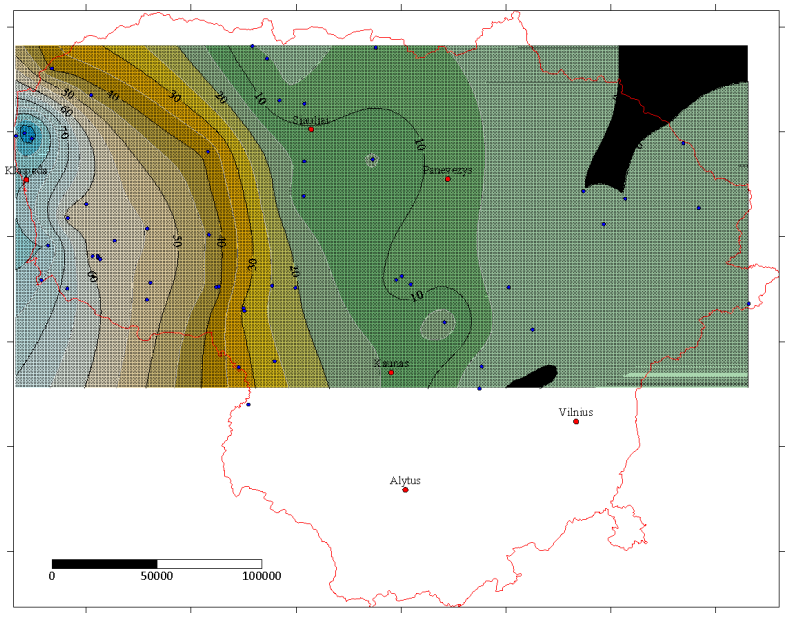

Figure 63. *Salinity (g/L) of the Kemeri geothermal aquifer samples. Studied wells indicated (dots).*

Two hydrochemical zones are defined on the plot mineralization vs. depth (**Figure 64**). Most of the territory of Lithuania is characterised by low salinity. The sharp boundary is mapped at the burial depth of c. 680 m.

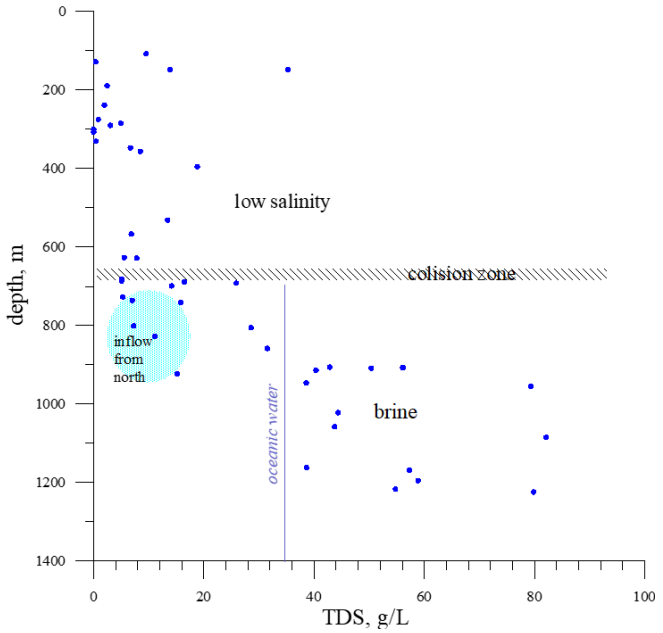

Figure 64. *Mineralization vs. depth of the Kemeri aquifer. Two hydrochemical zones are distinct in Lithuania. Water inflow of low-salinity water is noted in the north. The oceanic water is marked on the plot (blue line).*

It is notable, the highly enriched sulphate water is documented below the depth of c. 200 m (**Figure 65**), similar to Cambrian water registered at the death of c. 600 m (**Figure 34**). Furthermore, they show a similar attenuation trend with a depth. No data from Kaliningrad District are available to extrapolate the trend at the larger depths. The concentration of sulphates is compatible with oceanic water (indicated on the plot).

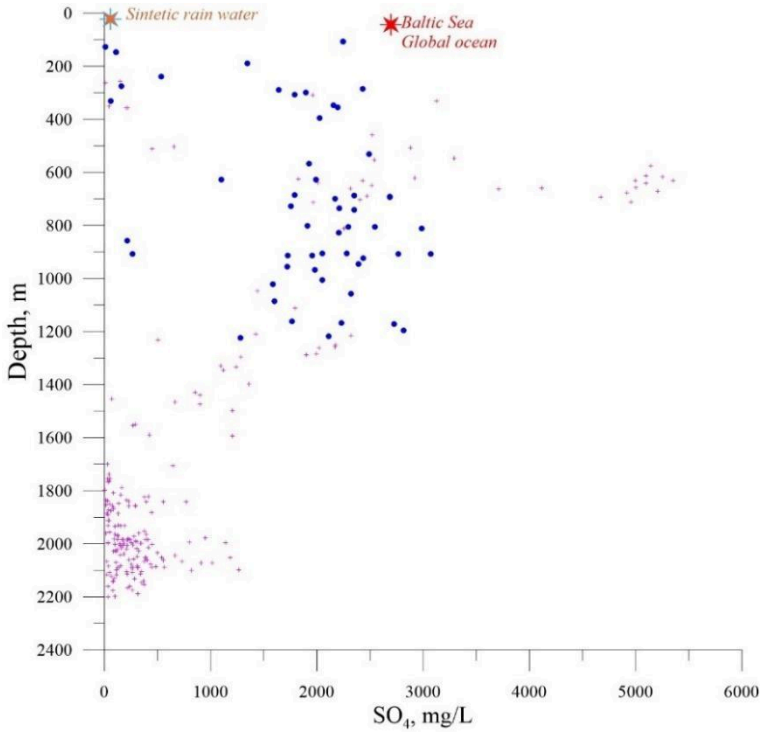

Figure 65. *SO_4 concentration of the Kemery water with depth.*

The chlorite shows a steady increase to 8.0 g/L (oceanic water 18.9 g/L), while the sodium concentration shows a negative correlation with depth (min 0.036 in well Salantai-60 in west Lithuania). The amount of sodium increases with the depth and reaches 16.5 g/L in the well Naumiestis-1 (oceanic water 10.55 g/L) and a very low potassium concentration was measured in Lithuania (0.3 g/L similar to oceanic water). A similar depth increasing trend is documented: maximum concentration in well Vabalai-1 (calcium 9.4 and magnesium 2.8 g/L). In comparison to the oceanic water, the significant depletion in magnesium and calcium is noted in the Kemeri aquifer.

The overlapping of the two maps shows a clear correlation between temperature and water mineralization (**Figure 66**). The hydro chemical boundary is delineated at 15 g/L and roughly correlates to 20°C isotherm. It has no background mechanism to explain this correlation and is merely an automatic overlapping of two maps.

4.14 Geothermal potential of the Kemeri aquifer

The opposing parameters are combined to define the most prospective area in Lithuania: (1) the increasing thickness of the aquifer to the north and (2) the increasing temperature to the southwest (**Figure 67**). The best parameters are calculated in the Traubai, Gargždai, and Klaipėda areas. The methodology for assessing the geothermal aquifer is discussed above.

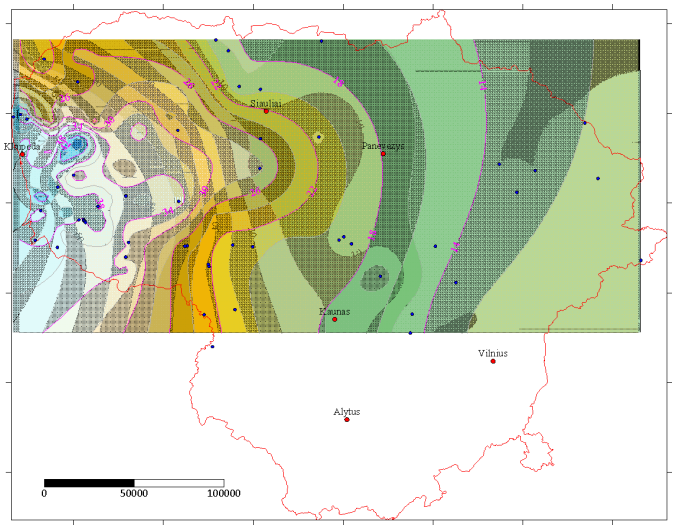

Figure 66. *Temperature overlying the salinity map of the Kemeri aquifer. Studied wells are indicated*

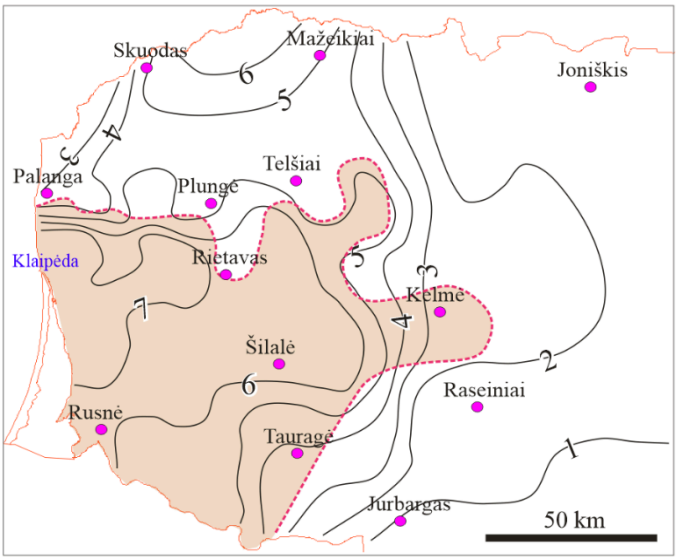

Figure 67. *Geothermal capacity of a geothermal doublet (MW_{th}).*

4.15 Upninkai-Šventoji geothermal aquifer (Middle Devonian-lowermost Devonian): Distribution, depth, and thickness of the Šventoji-Upninkai geothermal aquifer

The depth of the Šventoji-Upninkai geothermal aquifer ranges from -100 m to -664 m in Lithuania (**Figure 68**). Please note the reactivation of the tectonic movements along the largest-scale Telšiai fault. The low inclination of the top of the aquifer in the eastern part of the basin is related to the erosion of the Devonian deposits, including significant erosion during the Quaternary glaciation.

The thickness of the reservoir ranges from 140 m to 255 m (**Figure 69**). The similar thickness pattern is discussed in the Chapter concerning the Kemery aquifer (**Figure 34**). It rather stable trend of the tectonic movements in Lithuania and adjacent Latvia.

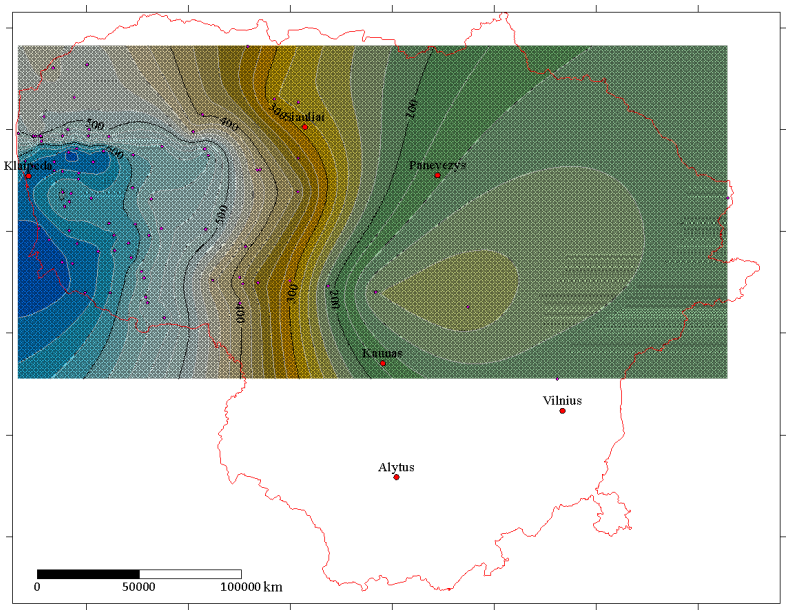

Figure 68. *Depth (m) of top of the Šventoj Upninkai geothermal aquifer*

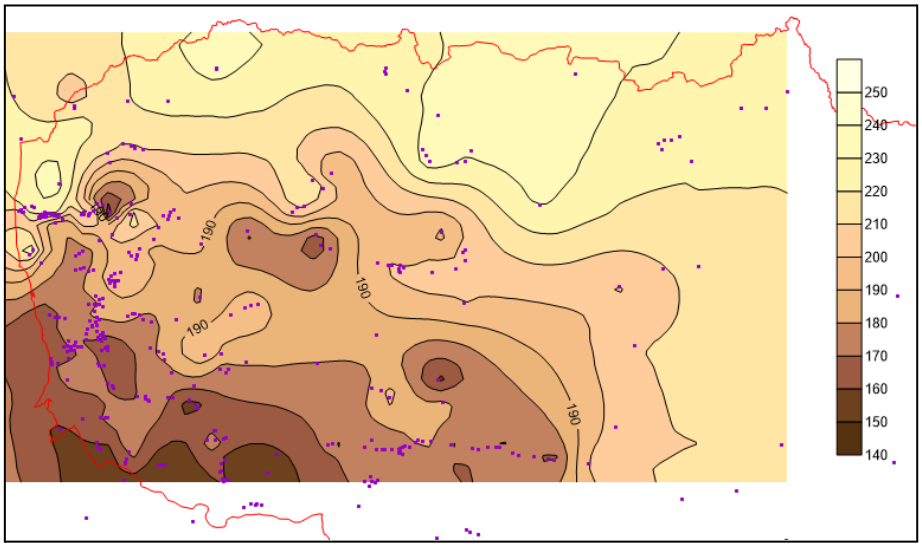

Figure 69. Thickness of the Upninkai-Šventoji aquifer. The Jelgava Depression is an important sub-regional depression, as discussed in the Kemeri RSt chapter.

4.16 Stratigraphy Upninkai-Šventoji geothermal

The Šventoji-Upninkai aquifer is represented by the intercalation of sandstone and shale at about 55% ratio (**Figure 70**). The bedding thickness varies from 2 m to 7 m which considerably complicate the reservoir management.

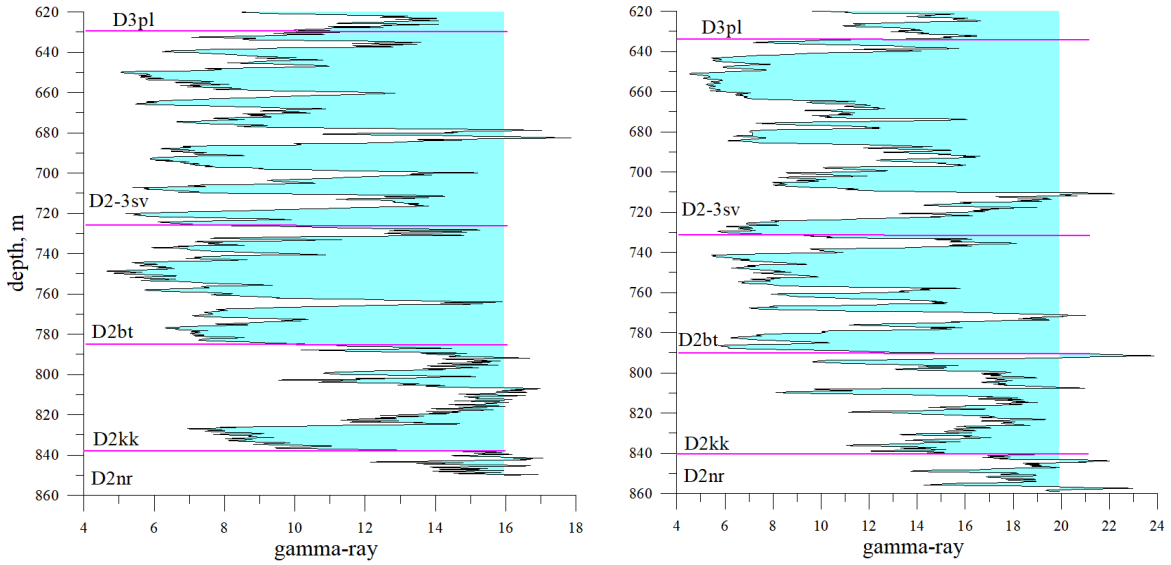

***Figure 70**. Gamma-ray log in the Šventoji-Upninkai aquifer. A - Well Klaipeda-1. thickness 211.6 B - Well Purmaliai-1. thickness 222 m. Stratigraphic formations are well discernable on the wire log curve. The Kukliai and Butkūnai Fms. Show a rather similar pattern of sandstone-shale package. Šventoji Fm. indicates thinner layering in well Klaipėda-1 compared to the 4 cycles in well Purmaliai. The effective thickness is estimated at 100 m (net-to-gross 0.48% in the well Klaipėda-1 and 0.46% in the well Purmaliai).*

Sandstones are fine-grained, quartzous with some 5-10% feldspar grains, friable. Based on the interpretation of the sedimentary logging of a few available boreholes in west Lithuania, sandstones were deposited in the tidal plane environment. Cross-bedding is oriented southeast in west Lithuania.

4.17 Reservoir properties

The lithology of the Šventoji-Upninkai aquifer is similar to the Kemeri RSt. Therefore, we can assume similar reservoir parameters for the Kemeri and Šventoji-Upninkai aquifer. The average porosity of sandstones is about 28%, the permeability is about 2-4 D.

4.18 Temperature distribution

The temperature of the Šventoji-Upninkai reservoir increases to the west. The West Lithuanian Geothermal Anomaly is well discernible on the temperature map. The anomaly is delineated at the contour line 25°C (**Figure 71**). The "hottest" area is defined in the Šilutė and Vilkyčiai area.

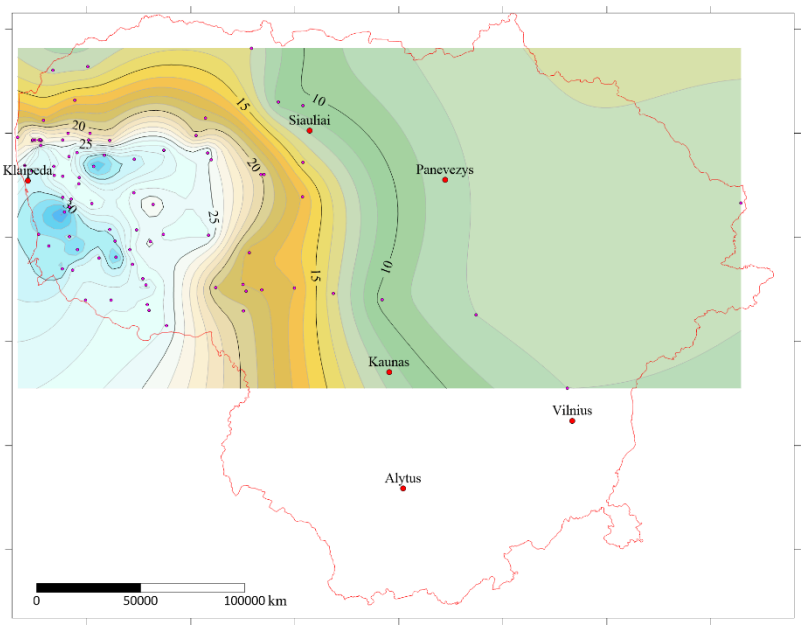

Figure 71. *Temperatures of the Kemeri geothermal aquifer.*

The temperature logging was carried out in most of the oil exploration wells in west Lithuania. The temperatures are listed below (**Table 5**):

Table 5. *Average temperatures in west Lithuanian oil fields*

Oil field	D_3šv-up
Girkaliai	*30*
Genčiai	*30*
Kretinga	*23*
Nausodis	*27*
Plungė	*23*
Ablinga	*35*
Vėžaičiai	*28*
Šiūpariai	*32*
South Šiūpariai	*32*
Degliai	*31*
Sakučiai	*33*
Šilalė	*30*

4.19 Water chemical composition of the Šventoji-Upninkai aquifer

Most of the Šventoji-Upninkai aquifer contains huge potable water resources. West of the Nevežys River, the salinity increases >1 g/L. Mineralization of saline water varies from 1.5 to 30.5 g/L in west Lithuania.

Most of the drilled boreholes are located in the potable water zone mapped at a depth of >240 m (**Figure 72**). There is scarce information available on the high salinity zone.

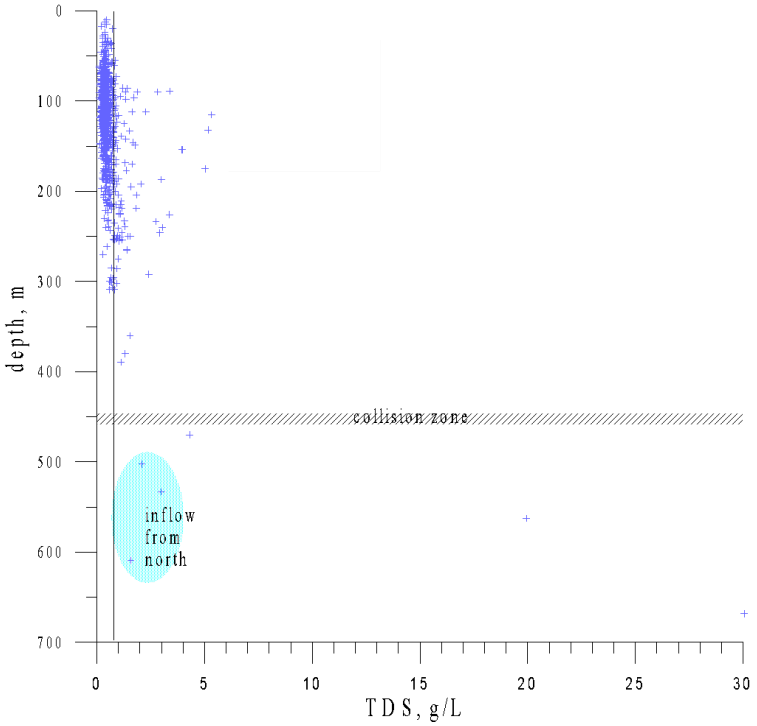

Figure 72. *Mineralization vs. depth of the Šventoji-Upninkai aquifer. Two hydrochemical zones are distinct in Lithuania. Water inflow of low-salinity water is noted in the north.*

Salinity increases to the west (**Figure 73**). No chemical boundary was defined in the boreholes from the east to west of Lithuania. Anion and cation concentration increase steadily to the basin centre with no discernible hydrochemical boundaries.

The saline water is distributed in southwest Lithuania (**Figure 73**). The eastern boundary is controlled by the Nenėžis River and turns to the west. Two water flows are defined in the east and north. The eastern boundary is well controlled by abundant hydrogeological boreholes, while the northern transition is not well mapped, as the Šventoji sandstones are overlain by high quality aquifers in northwest Lithuania (Upper Permian, Žagarė Fm). It is well obervarved in the borehole location map (**Figure 73**).

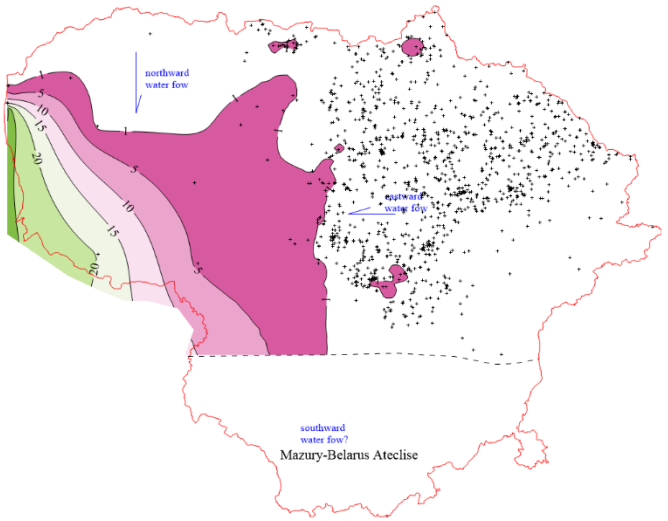

Figure 73. *Water mineralization of the Šventoji-Upninkai aquifer. The Nevėžis River is confined to the major hydrochemical boundary of the Šventoji-Upninkai aquifer.*

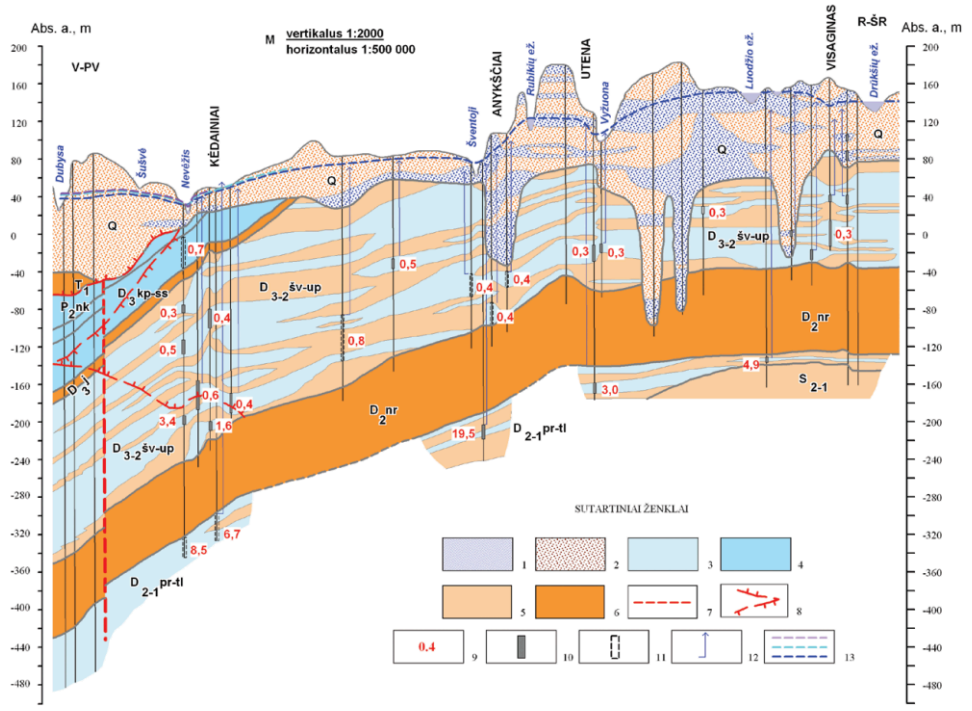

Figure 74. *Šventoji-Upninkai aquifer shows very complicated layered architecture. The profile shows transition boundary of the potable water in the east and saline water in the west (Dubysa boundary), the western part of the profile (after Juodkazis et al., 2011).*

The chemical composition of water shows very different hydrochemical type of the Šventoji-Upninkai aquifer (green tods) and Cambrian aquifer (red crosses) (**Figure 75**). The cation cluster shows similar trend controlled by Mg-Na cations; please note enrichment in magnesium cnocentration in the Šventoji-Upninkai aquifer. The anions are controlled by HCO_3-Cl trend. Two water flows are directed from the east (brown trend) and the north (blow trend) are indicated. The Cambrian water type shows a very different trend (pink).

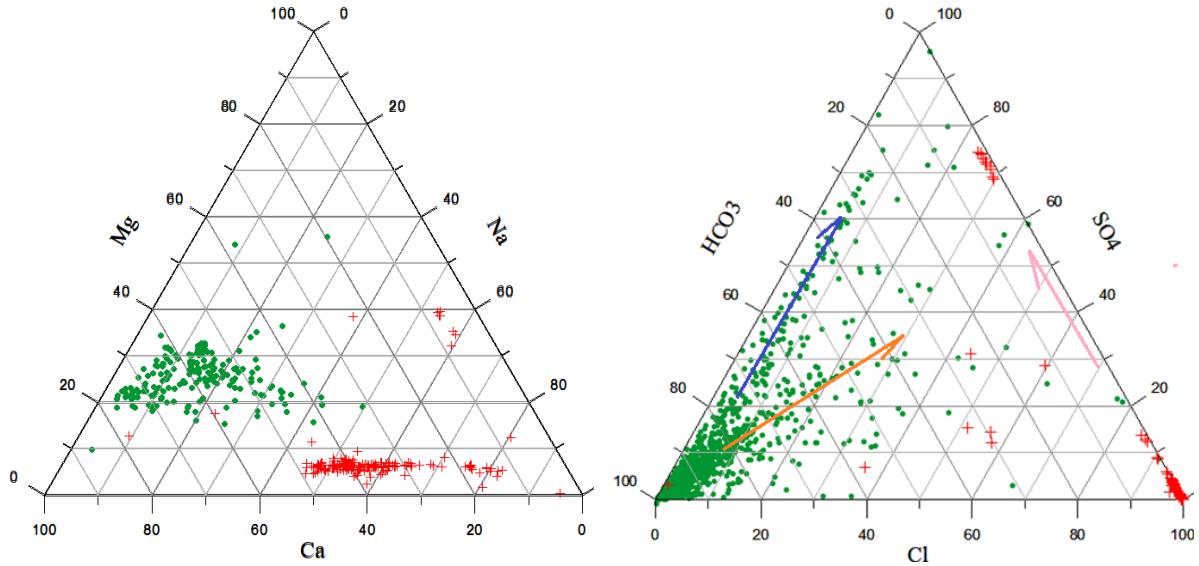

Figure 75. *Water mineralization ternary diagrams. The Cambrian water is shown for comparison.*

5 Summary

Cambrian geothermal aquifer

- The temperature of the prospective area ranges from 40°C in middle Lithuania to 94°C southwest Lithuania
- The effective thickness of the reservoir ranges from a low to 15 m (total 78 m) in westernmost Lithuania to 50 m in middle and northwest Lithuania
- Reservoir properties vary from excellent (porosity mean 15-22% and permeability 250 to 900 mD) to severely cemented sandstones (porosity mean 5-8% and permeability 6 to 9 mD). The local anomalies of increased permeability are randomly distributed in the studied wells
- The authigenic quartz cementation (average grain size 0.16 mm, classified as fine-grained sand) dominates the reservoir quality of sandstones in middle and west Lithuania
- The mineralization of water ranges from 0.25 g/L (Šalčininkai region) to 203.0 g/L (well Žalgiriai-1). pH index varies from 7.9 in north Lithuania (*e.g.*, Šiauliai) to 4.5 in southwest Lithuania.
- Two hydrochemical/hydrodynamic zones are defined, i.e., (1) the zone dominated by meteoric water infiltration influenced zone showing water mineralization from potable water in the south western most corner of Lithuania to 80 g/L and (2) the high salinity compactional water zone of 100-203 g/L in the west. It correlates with an increasing concentration of bulk anions and cations. It is associated with significant pH variation from neutral to acid water.
- The inventory of the active oil exploitation and exploration wells shows the standard design of the past 50 years that can be deployed for converting the boreholes to geothermal exploitation

Kemeri aquifer (lower Devonian)

- The temperature of the prospective area ranges from 35°C to 51°C in western Lithuania
- The thickness of the reservoir in west Lithuania ranges from 90 m in the south to 190 m in the north.
- The aquifer is composed of friable fine-grained sandstones with the admixture of clay minerals and carbonates that is considered the sensitive system
- There is no discernible difference between particular wells in terms of porosity and permeability
- Despite the very complex architecture of the reservoir, a rather consistent ratio of the net-to-gross ratio is defined at ca. 0.65.
- It correlates with only minor variations in the average porosity at 28% and permeability 2000-5000 mD in west Lithuania
- The two injection experiments in the wells Vilkyčiai-3,5 and the long-lasting injection of the geothermal brain in Klaipėda wells shows the very sensitive reaction of the reservoir (*e.g.*, ratio production/injection rates 8.7 and 5.3 in upper and lower sandstones in well Vylkyčiai-3).
- The mineralization of water ranges from 0.8 g/L (*e.g.*, Vilnius) to 98.4 g/L (Klaipėda, Geological database). pH index varies from 7.4 in north Lithuania (*e.g.*, Šiauliai) to 5.9 in Klaipėda.

6 Introduction: Geothermal Power Plants in Europe (2023)

In 2023, geothermal energy continues to play a crucial role in Europe's renewable energy landscape, with significant advancements in both power generation and district heating systems. Although no new geothermal plants became operational in 2023, the region has approximately 50 new power plants in the planning stage and 185 plants under investigation, primarily in countries such as Croatia, France, Germany, Italy, and Turkey. Europe boasts an installed capacity of 3.5 GWe from 143 operational plants, producing around 20 TWh annually, with 7 TWh generated within the EU.

Geothermal power plants consistently exhibit the highest capacity factors among all electricity sources, exceeding 90% efficiency, with some operating close to 100% of the time. Alongside power generation, the expansion of geothermal district heating and cooling systems is on the rise, with over 360 projects in development. As the demand for low-temperature systems and networked geothermal solutions grows, geothermal energy is becoming a dominant force in Europe's push for sustainable energy, especially in district heating systems across several countries.

No new plants in 2023 (as of 2022). Planned: Approximately 50 geothermal power plants, 8 new projects have started development in 2023. Under Investigation: 185 geothermal powerplants are being investigated, mainly in Croatia, France, Germany, Italy and Turkey but also in countries not yet producing such as Greece and Spain., see **Figure 75**.

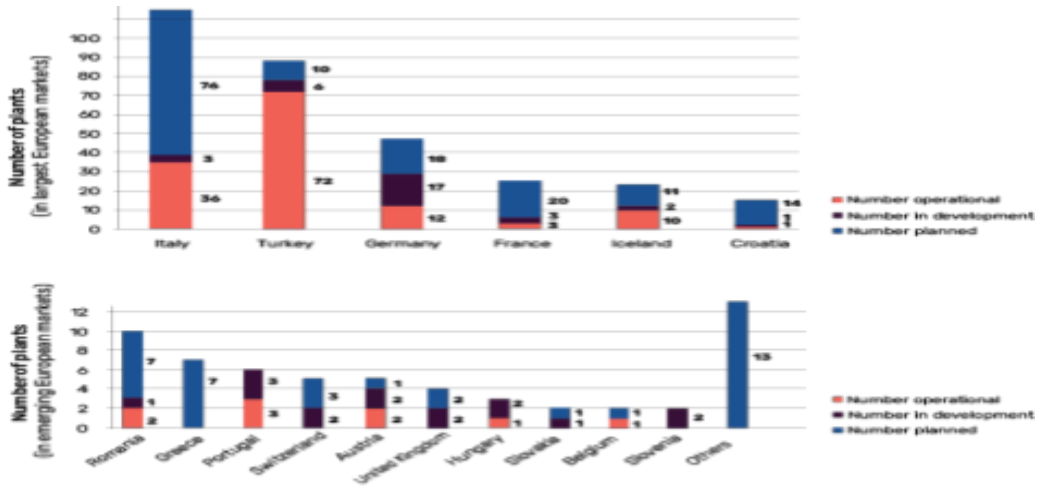

Figure SEQ Figure * ARABIC 76: *Figure showing geothermal power plant distribution in EU.*

In year 2023 Capacity 3.5 GWe in geothermal electricity, 143 operational plants. Generating 20 TWh/year, about 7 TWh/year in the EU. In 2023, as for the last 110 years, geothermal powerplants achieved the highest load factor of all electricity sources. Capacity factor higher than 90%, some operating close to 100% of the hours within a year.. Power Plants with the highest capacity factor in Europe is show in **Table 5.**

*Table SEQ Table * ARABIC 6: Power plan with highest capacity factor in EU.*

Country	Plant's name	Year of commissioning	Installed Capacity in 2023 (MWe)	Gross electric production (GWh)	Capacity factor
Italy	Bagnore 4	2014	40	351,93735	100%
Italy	Piancastagnaio 5	1996	20	174,1763704	99%
France	Géothermie Bouillante 2 / Hydrothermal	2005	11	94,01	98%
Italy	Piancastagnaio 4	1991	20	166,76277	95%
Turkey	Mis-III JES	2019	48	396,40964	94%
Iceland	Nesjavellir	2005	120	984	94%
Italy	Piancastagnaio 3	1990	20	163,56843	93%
Iceland	Krafla	1997	60	487,4	93%
Turkey	Pamukören JES 5	2020	32	258,05104	92%
Iceland	Svartsengi (CHP - Sudurnes)	2007	8,4	67,6	92%
Romania	CE Iosia Nord	2012	0,05	0,4	91%
Italy	Nuova Castelnuovo	2000	14,8	118,28616	91%

6.1 Main geothermal district heating: Reservoirs with existing systems and temperatures

Over 360 geothermal district heating and cooling projects are in development or under investigation, see **Figure 76**. This could result in more than a doubling of capacity within the next 4 to 5 years. The trend towards systems with lower temperatures, lower temperature systems combined with large heat pumps.

6.2 Networked geothermal dominates district heating systems (2022)

Major trend in reducing the temperature of district thermal networks. More than 2000, 5th generation DHC systems are located in Germany, Sweden, Switzerland, France, Denmark, Austria, Italy, Belgium and the Netherlands. Geothermal is the main source (39%) in combined systems. Networked geothermal is also a major source of growth in new medium-to-low temperature district heating and cooling systems.

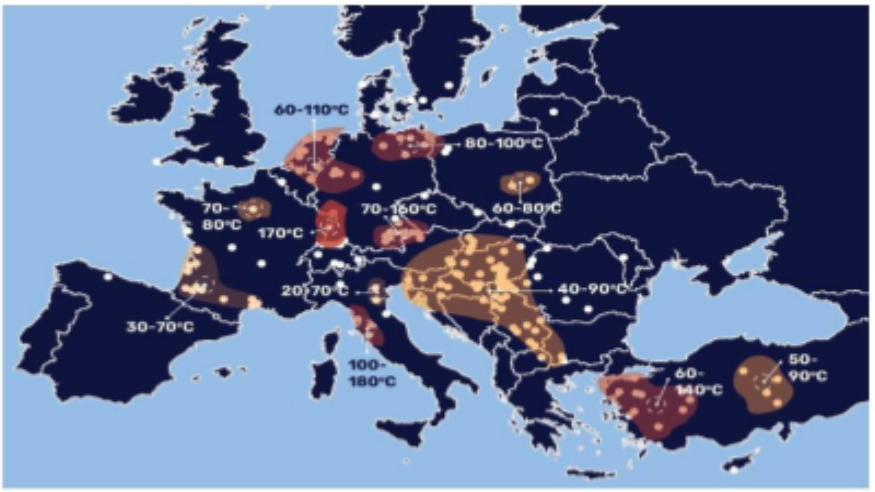

*Figure SEQ Figure * ARABIC 77: Map view of district heating or cooling plant in EU.*

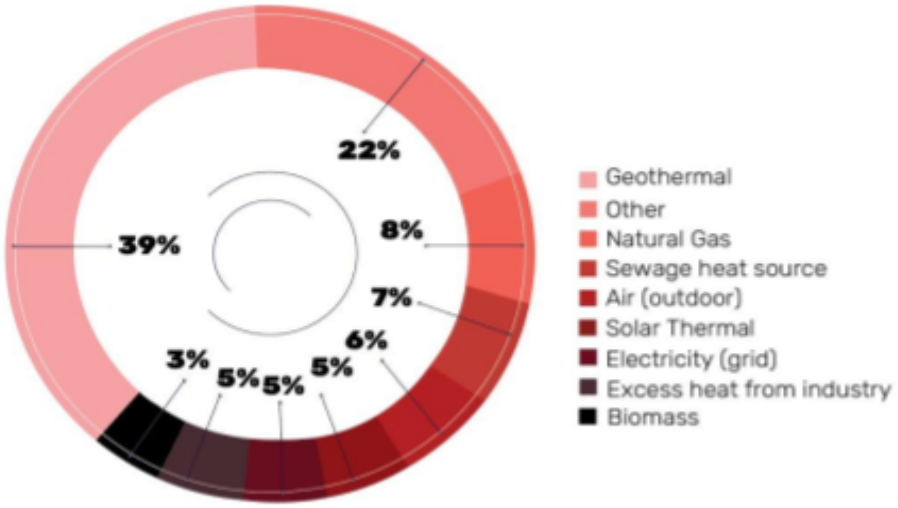

Figure SEQ Figure * ARABIC 78: *Figure showing the spread of different heating sources in EU.*

6.3 Operational heat plants with the highest installed geothermal capacity

Geothermal district heating first developed in high-temperature fields. These were large systems and sometimes associated with a combined heat and power applications.

Table SEQ Table * ARABIC 7: *Currently Operational Plants with highest installed capacity in EU.*

Country	Plant's name	Year of commissioning	Installed Geothermal Capacity in 2023 (MWth)	Gross heat production GWh th/y
Iceland	Reykjavik - Capital area	1930	1000	3823,7
Iceland	Nesjavellir	1998	300	1,8
Turkey	Izmir (Balcova + Narlidere)	1983	243	/
Iceland	Hellisheiði	2006	200	/
Turkey	Afyonkarahisar (Afjet)	1996	179	/
Iceland	Sudurnes (CHP-Svartsengi and Reykjanes)	1976	150	718,5
Turkey	Afyonkarahisar (Sandıklı)	1998	120	/
Turkey	Kutahya (Simav)	1991	110	/
Iceland	Akureyri	1977	94	333,33
Poland	Lesser Poland, Podhale Region	1993	71,4	181,27

6.4 Heat plants in development with the highest expected geothermal capacity

The trends for large geothermal district heating and cooling system development are to: Drill multiple wells. Require insurance to de-risk Greenfields. Employ portfolio business models. Focus more on closed-loop deep geothermal projects, Respond to aggregated demand such as multiple greenhouses in the horticulture sector.

6.5 Top 10 Geothermal Countries 2023 - Installed Geothermal power capacity in GWe

The global geothermal energy sector continues to grow, with several countries leading in installed geothermal power capacity. This section highlights the top 10 geothermal nations in 2023, ranked by their installed capacity in gigawatts electric (GWe), see **Table 7**and **Table 8**. These countries exemplify the successful utilization of geothermal resources for sustainable energy production, showcasing advancements in technology, policy, and investment driving the sector's expansion. +16 GWe total installed capacity in2023, Top 10 countries account for 93% of the total installed capacity

Table SEQ Table * ARABIC 8: *Panned Geothermal Plants with highest installed capacity in EU.*

Country	Plant's name	Status/type	Year of commissioning (expected)	Expected Capacity (MWth)
Denmark	Copenhagen	Permit granted, seismic survey completed, negotiations phase	2028	240
Austria	Vienna City	Development phase 1	2026-2030	120
Denmark	Aarhus	Under construction (drilling)	2025-2029	110
Croatia	Prelog, Međimurje County	Planning		89
Austria	Vienna City	Development phase 2	2030-2040	80
Austria	Lower Austria, Thermenregion	Under investigation	2030-2035	60
Denmark	Vestforbrænding	Negotiations ongoing	2027	50
Romania	Oradea (Crișana region, North West) - NUFARUL		2025	50
Greece	Neo Erasmio - Maggana; Nea Kessani	Additional wells and DH network under construction	2024-2026	48,7
Netherlands	Aardwarmte Delfland			45,91

Table SEQ Table * ARABIC 9: *Outlook to 2030: 64 projects at different stages of investigation in 2023*

Country	Projects	Country	Projects	Country	Projects
Austria	9	Belgium	7	Bosnia	1
Bulgaria	3	Croatia	10	Cyprus	1
Czechia	1	Denmark	6	Estonia	2
Finland	3	France	24	Germany	102
Greece	6	Hungary	17	Iceland	1
Ireland	3	Italy	21	Lithuania	3
Luxembourg	1	Netherlands	22	Poland	21
Portugal	2	Serbia	8	Slovakia	10
Romania	6	Spain	1	Sweden	3
Switzerland	7	Turkey	3	UK	12

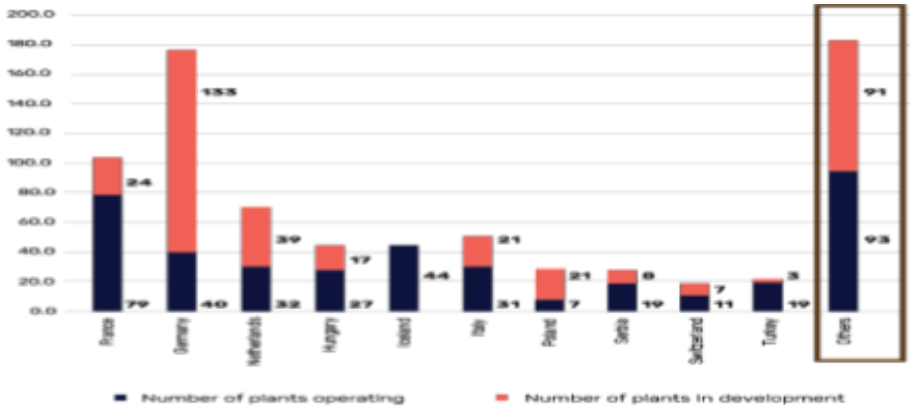

Figure SEQ Figure * ARABIC 79: *Largest geothermal district heating and cooling operating and in development (largest and emerging European markets)*

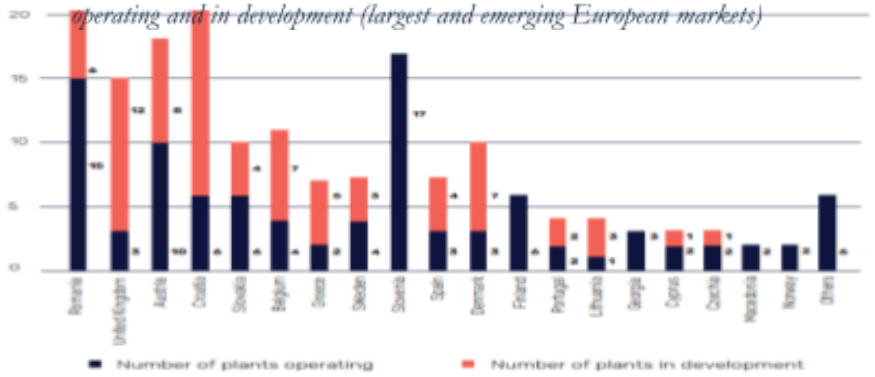

Figure SEQ Figure * ARABIC 80: *Largest geothermal district heating and cooling operating and in development (largest and emerging markets)*

7 An overview of geothermal resources extraction methods

When discussing geothermal wells in terms of their orientation and layout, they can generally be classified into vertical, horizontal, and other specialized types. Vertical and horizontal wells are the most common, each suited to different site conditions and space availability. Directional wells offer flexibility in accessing geothermal resources, while coaxial wells provide efficient heat exchange for deeper systems. In closed-loop systems, both vertical and horizontal, are widely used for their reliability and low environmental impact, while open-loop systems offer high efficiency where water resources are available. Each type of well and system is chosen based on specific project requirements, geological conditions, and available space.

7.1 Vertical Wells

The wells are drilled in vertical direction, and they are perpendicular to the subsurface layers as shown in the **Figure 81**. They are typically used for both residential and commercial geothermal systems. These types of wells are often used when there is limited surface area available. The depth can range from a few hundred to several thousand feet. While multiple vertical wells can be drilled to create a geothermal field. The vertical wells are common in both closed-loop and open-loop geothermal systems. The main advantage of these type of wells are that they require less surface area and are consistent performance due to stable underground temperatures.

Figure 81. *Schematics of a Vertical well taken from ref. [4].*

7.2 Horizontal Wells

Horizontal wells deviate from a vertical borehole to extend horizontally within the subsurface layer. As implied from the nomenclature, horizontal wells start from the lateral position. Additionally, the procedure for horizontal drilling entails guiding a drill bit to traverse a path predominantly oriented between 85 and 95 degrees relative to the vertical direction as shown in **Figure 81.** Horizontal wells are drilled when the surface area is ample, and drilling depth is limited by geological conditions or cost. They are often used in closed-loop systems and are suitable for residential properties with large yards and in areas with shallow geothermal resources. The main advantages of drilling horizontal wells are lower drilling costs compared to vertical wells and easier to install in certain geological conditions.

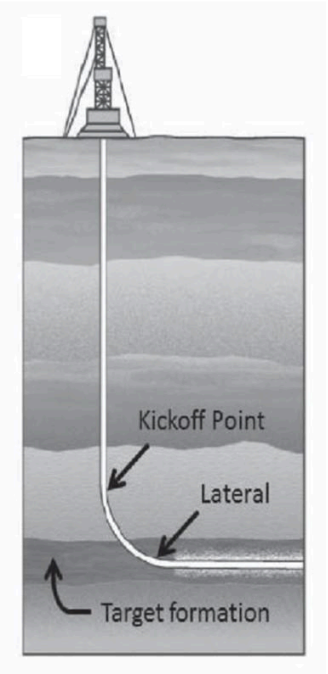

Figure 82: *Schematics of a Horizontal well taken from ref. [4].*

7.3 Directional Wells

Directional wells are generally drilled when access to geothermal resources that are not directly below the drilling site or to maximize reservoir contact. Directional wells are drilled at various angles, not just vertically or horizontally as depicted in **Figure 83**. This technique allows for more flexible placement of wells and better access to geothermal reservoirs. The design utilizes steerable drill bits and downhole motors and include both shallow and deep directional drilling. These types of wells are often drilled in enhanced geothermal systems (EGS) and when the geothermal resource is spread out horizontally. The main advantage is that they offer greater flexibility in well placement and increase the productivity of geothermal reservoirs.

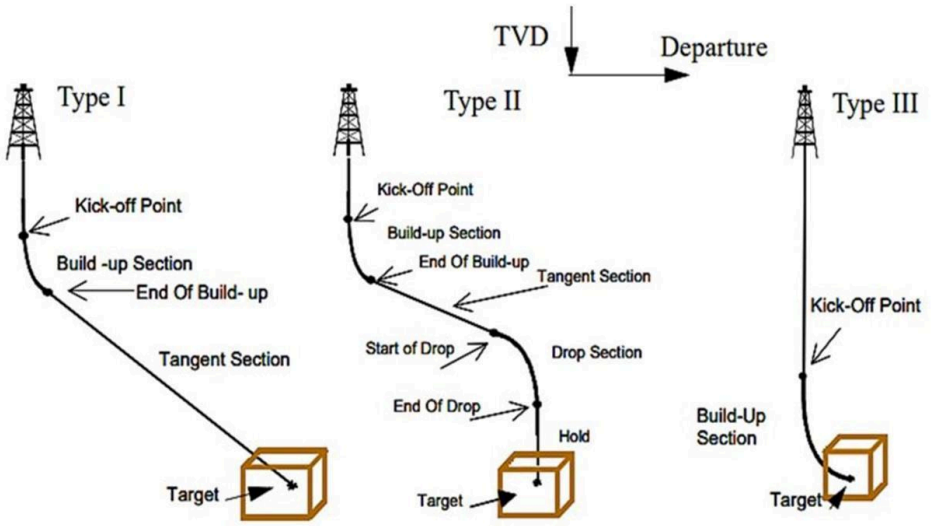

Figure 83: *Figure showing different Types of directional wells, taken from ref. [5].*

7.4 Coaxial Wells

Coaxial wells are a specialized type of geothermal well designed for efficient heat exchange, particularly in deep geothermal systems. The key feature of coaxial wells is their double-walled pipe configuration, which allows for effective heat transfer between the geothermal fluid and the surrounding geological formations. The coaxial wells use a double-walled pipe system where one pipe is placed inside another. The geothermal fluid flows down through the outer pipe and returns via the inner pipe or vice versa as depicted in **Figure 84**. The main advantage of coaxial wells is they provide efficient heat transfer and have simplified installation in certain geological settings.

7.5 Closed-Loop Systems

Vertical closed-loop systems where vertical wells in a loop of pipes is inserted into the drilled holes, and a heat transfer fluid circulates through these pipes. The pipes are typically made of polyethylene and wells are backfilled with grout to ensure good thermal contact with the surrounding soil or rock.

In horizontal closed-loop systems the pipes are laid out horizontally in trenches dug in the ground. It requires a large land area and can be installed in various configurations (e.g., straight, slinky, or grid). **Figure 85** depicts the closed loop system.

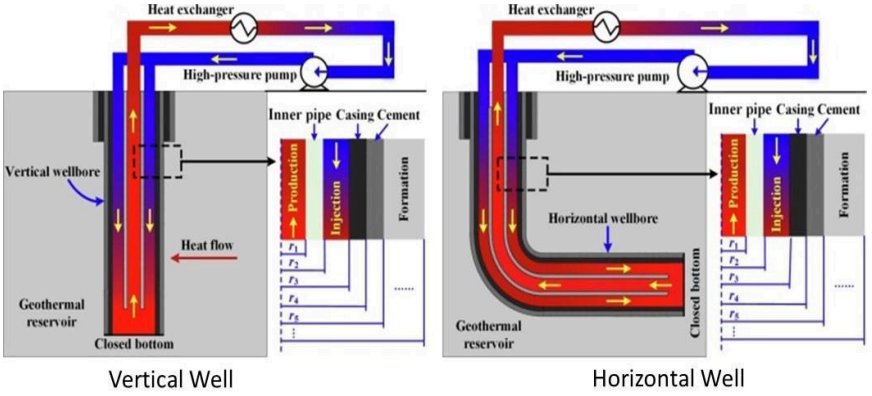

Figure 84: *Figure showing schematics of a Coaxial well's fluid flow and heat transfer with different assembly [6].*

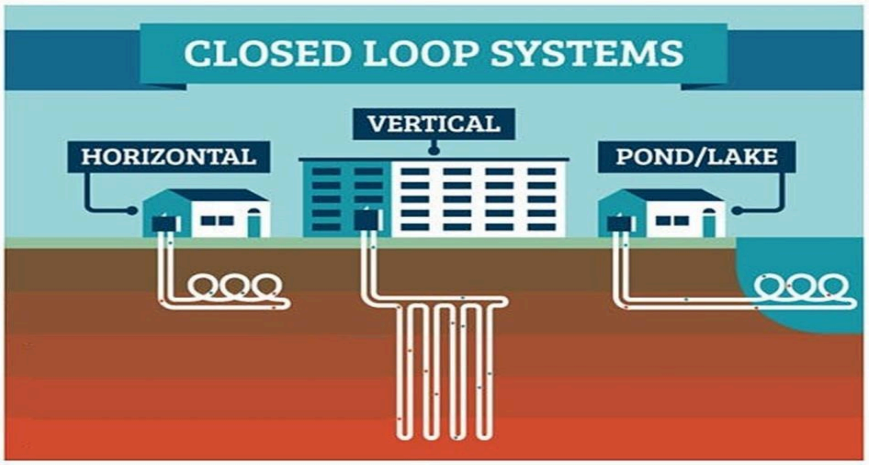

Figure 85: *Figure showing schematics of a Closed loop system [7]*

7.6 Open-Loop Systems

In open-loop system a direct use of groundwater or surface water is done for geothermal extraction. Open-loop systems pump water from a well or a body of water, use it for heat exchange, and then discharge it back into the ground or another body of water. The open-loop system requires a sufficient supply of clean water and includes a pump, heat exchanger, and discharge system as shown in **Figure 86**. The main advantages of this type of system are that they offer higher efficiency due to direct use of water. They offer lower installation cost compared to closed-loop systems in some cases.

7.7 Tapping the geothermal energy

Geothermal energy is often located deep within the Earth. Therefore, drilling allows access to these deep geothermal reservoirs where temperatures are sufficiently high for energy production. The key components include well drilling methods to access geothermal reservoirs, pumps to bring the geothermal fluid to the surface, heat exchangers to transfer heat, and various auxiliary systems to enhance efficiency and adaptability.

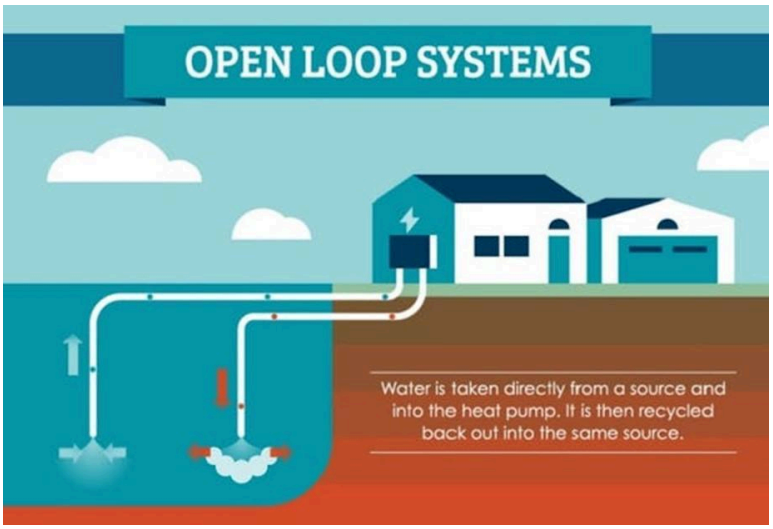

Figure 86: *Figure showing schematics of an Open loop system [7]*

7.7.1 Well Drilling Methods

Well drilling methods for geothermal resource extraction are essential for tapping into the Earth's heat. These methods, like those used in oil and gas drilling, are adjusted to handle the high temperatures and unique geological conditions of geothermal resources. From traditional rotary drilling to advanced directional and coiled tubing techniques, these methods ensure efficient and effective access to geothermal energy. Each method involves specialized equipment and processes designed to handle the unique challenges of geothermal drilling, such as high temperatures, hard rock formations, and the need for precise directional control.

i. **Rotary Drilling:** This is the most common method used in geothermal drilling, similar to oil and gas drilling which involves a rotating drill bit to crush and penetrate the rock formations. The main components include derrick floor, drill bit, drill pipe and circulating

drilling mud. The drilling mud is circulated to cool the bit, stabilize the borehole, and carry cuttings to the surface. The other most important techniques include.

Mud Rotary Drilling: It utilizes drilling mud to cool the drill bit, stabilize the borehole, and bring cuttings to the surface.

Air Rotary Drilling: It uses compressed air instead of drilling mud, suitable for hard rock formations and areas with less groundwater.

ii. **Percussion Drilling:** This type of drilling is older method of drilling which is widely used for hard formations which uses a heavy bit that is repeatedly lifted and dropped to crush the rock. It is widely used for shallow and hard geothermal applications and less common for deep geothermal wells. The main components include percussion bit, cable tool, and hoisting mechanism. In this drilling technique water is added to create a slurry, which is then bailed out to remove cuttings. Moreover, this drilling process is slow and labor-intensive but effective for certain geological conditions.

iii. **Directional Drilling:** This method is also known as Extended Reach Drilling (ERD) and the most widely used which allows for drilling at various angles, not just vertical. More efficiently used to reach geothermal reservoirs that are not directly beneath the drilling site. The main components include steerable drill bits, downhole motors, and measurement-while-drilling (MWD) tools.

iv. **Advanced Drilling Techniques:** The recent and more advanced techniques in the geothermal drilling industry are.

i. **Coiled Tubing Drilling:** In this technique a continuous length of flexible steel tubing is used instead of traditional drill pipe, allowing for faster and more efficient drilling. The main components include coiled tubes which is a continuous steel tube wound on a large spool. Other components include downhole motors and drilling bits similar to those used in rotary drilling. In addition to this it also includes injector head which pushes the coiled tubing into the wellbore. While working the coiled tubing is unwound from the spool and pushed into the well. The drilling fluid or air is circulated through the tubing to remove cuttings and cool the bit. This type of drilling is particularly useful for re-entry drilling and workover operations.

ii. **Enhanced Geothermal Systems (EGS) Drilling:** This type of drilling technique involves creating artificial geothermal reservoirs in hot, dry rock formations by injecting water to stimulate the formation. The drilling includes doublet wells one injector and one producer to create circulation system of water. The main components include high-pressure pumps which are used to inject water into the formation. Other components are fracturing tools which are used to create and maintain fractures in the rock. In this process an injection well is drilled into the hot rock formation. The high-pressure water is injected to create fractures in the rock and production well is drilled to intersect the fractured zone, allowing the injected water to circulate and extract heat.

7.8 Pumps

Pumps in the doublet wells play an important role for injection and production of the reservoir fluids. The most common types of the pumps used are.

i. **Line Shaft Pumps:** This type of pumps is used for medium-depth geothermal wells. The motor is located at the surface, and the shaft extends down to the pump, which is submerged in the well to produce the fluids. The advantages of these pumps are high efficiency, reliable, and easy to maintain.

ii. **Submersible Pumps:** In the submersible pumps the entire pump, including the motor, is submerged in the well. Commonly used for deep geothermal wells. They are suitable for deep wells, reduces the risk of shaft bending or misalignment.

iii. **Downhole Pumps:** The subsurface pumps are of two types.

i. **Electric Submersible Pumps (ESPs):** They are utilized for very deep wells where line shaft pumps are impractical.

ii. **Geothermal Heat Pumps (GHPs):** They are used in ground-source heat pump systems for heating and cooling buildings.

7.8.1 Heat Exchangers

Heat exchangers are the equipment used for exchanging of heat. The most common types of heat exchangers are.

i. **Direct-Contact Heat Exchangers:** This type of heat exchangers are open heat exchangers which allow direct contact between geothermal fluid and the working fluid, facilitating efficient heat transfer. They are typically used in binary cycle power plants.

ii. **Surface Heat Exchangers:** In these types of heat exchanger, the geothermal fluid passes through a series of tubes or plates where heat is transferred to a secondary fluid. The most common types of surface heat exchangers are.

i. **Shell and Tube Heat Exchangers:** These are the most common heat exchangers used in the industries where one fluid is passed through the shell and other fluid is flowing through the tubes. They are most used in larger power plants.

ii. **Plate Heat Exchangers:** These are compact and efficient heat exchangers generally used in smaller applications.

7.9 Heat Pumps

Heat pumps are needed in extraction of heat from geothermal fluid and transfers it to the desired application, like heating a building or preheating water. The cycle involves the evaporation and condensation of a refrigerant to absorb and release heat. The main components include evaporator, compressor, condenser, and expansion valve. The advantage of geothermal heat pumps is highly efficient because they leverage the stable temperatures of the ground or water and reduced operating cost. Moreover, geothermal heat pumps produce fewer greenhouse gas emissions compared to traditional heating and cooling systems, contributing to environmental sustainability.

7.10 Geothermal Technologies for energy generation and storage

In previous section we discussed geothermal resources by temperature. Furthermore, based on type of conversion, which is part of the geothermal power plant design, operation mechanism, and on the state of the subsurface fluid (steam or water) and its temperature, the technologies for building a geothermal power plant could be classified as follows:

i. **Binary Cycle Power Plant:** In this type of geothermal system the use of geothermal fluid is to heat a secondary fluid with a lower boiling point in a heat exchanger, which then vaporizes and drives a turbine to generate electricity. The working of this type of plant is like a closed loop system, schematics shown in the **Figure 87**. The advantage is that it can utilize lower temperature geothermal resources (e.g. hot water).

ii. **Flash Steam Power Plants:** In this system the geothermal fluid is depressurized or "flashed" to produce steam, which drives a turbine and generate electricity. The working of this type of system is also like a closed loop system, schematics shown in **Figure 88**. The main advantage is that this system is efficient for high-temperature geothermal resources.

iii. **Dry Steam Power Plant:** In this system the geothermal fluid is steam with pressure and temperature which drives a turbine and generate electricity. The working of this type of system is like an open loop system, schematics shown in **Figure 89**. The main advantage is that this system is efficient for high-temperature and pressure geothermal resources.

iv. **Enhanced Geothermal Systems (EGS):** This system involves creating artificial reservoirs by injecting water into hot dry rock formations, extracting the heat as the water returns to the surface. The main components include injection and production wells and requires reservoir stimulation techniques to extract the efficient heat from the system, schematics of EGS are shown in **Figure 90**.

v. **Direct Use Applications:** The direct use of geothermal resources is the use of underground hot water to heat buildings, grow plants in greenhouses, dehydrate onions and garlic, heat water for fish and shrimp farming (aquaculture), pasteurize milk, and for many other applications. In some cities pipe the hot water under roads and sidewalks to melt snow, schematics of this type of system is shown in **Figure 91**.

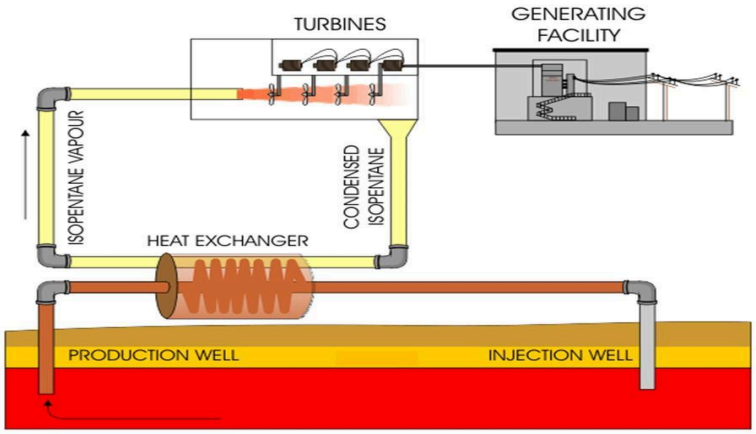

Figure 87: *Figure showing a schematics of Binary cycle power plant [8]*

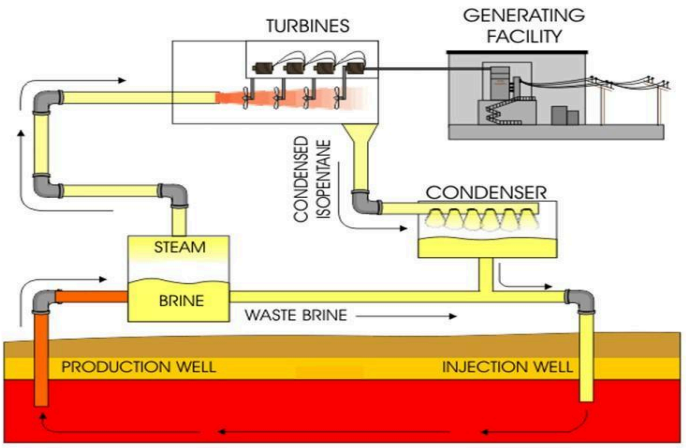

Figure 88: *Figure showing a schematics of Flash steam power plant [8]*

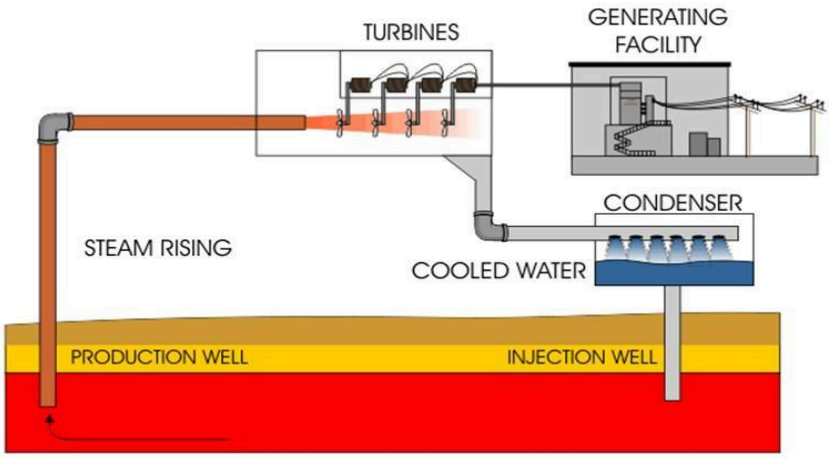

Figure 89: *Figure showing a schematics of Dry steam power plant [8]*

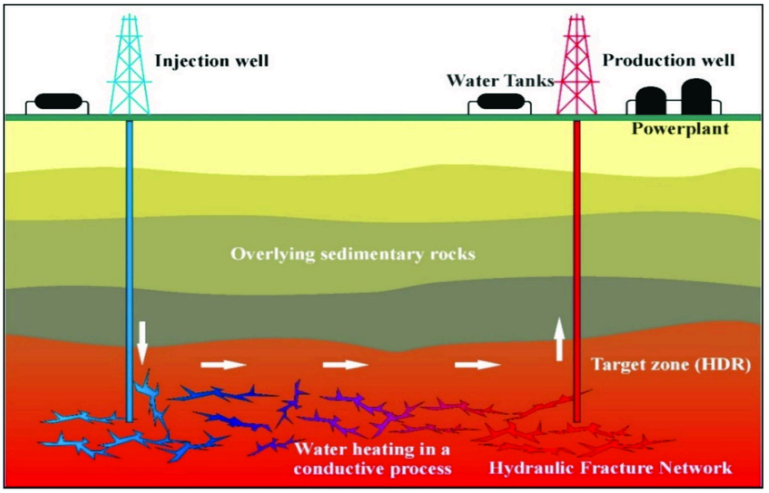

Figure 90: *Figure showing a schematics of Enhanced geothermal power plant [9]*

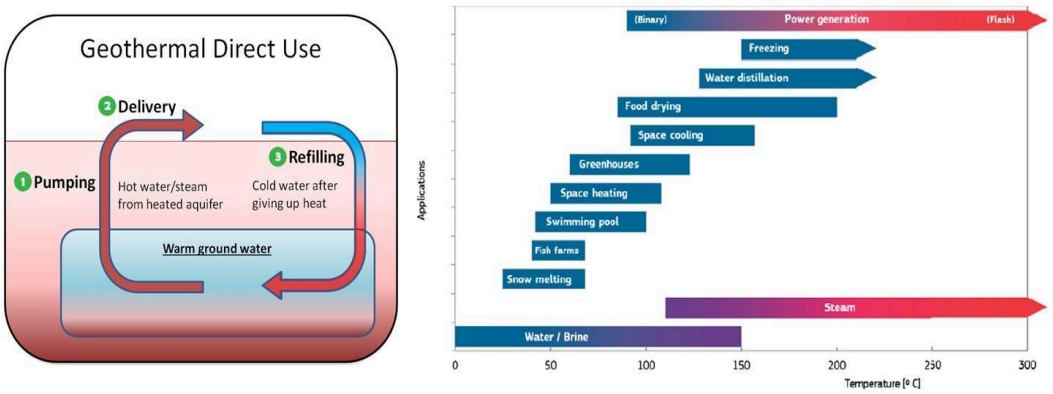

Figure 91: *Direct use geothermal plant, Figure modified from ref. [10],[11].*

7.11 Cost estimates of geothermal technologies

The previous section describes about the equipment's used for geothermal extraction for closed loop system which requires cost estimates. This section describes the approximate cost needed for each inventory.

7.12 Geothermal Wells

Cost estimates or economic feasibility of geothermal projects are mainly depended on drilling and completion cost of the well. Therefore, they must be estimated on the individual well basis. In absence of the enough data two references had been cited to estimate the cost model based on the correlations between measured depth (m) and average well drilling and completion cost and the total well cost (M$) has been evaluated. The model 1 has been obtained from reference 12 and model 2 has been obtained from the reference 13 which are given as below.

Model 1: Total well cost (M$): $1.65 * 10^{-5} * MD^{1.607}$

Model 2: Total well cost (M$): $1.72 * 10^{-7} * MD^{2} + 2.3 * 10^{-3} * MD - 0.62$

The output from the models is given in the ***Figure 92***. There exists a small difference in the estimated cost due to the input of the available data and the trend fit. To capture the sensitivity in the model differences a good fit relation has been developed which represents the change in the trend as higher depth. The best fit model 3 is given below.

Model 3: Total well cost (M$): $2.655 * 10^{-7} * MD^{2} + 1.65 * 10^{-3} * MD - 0.485$

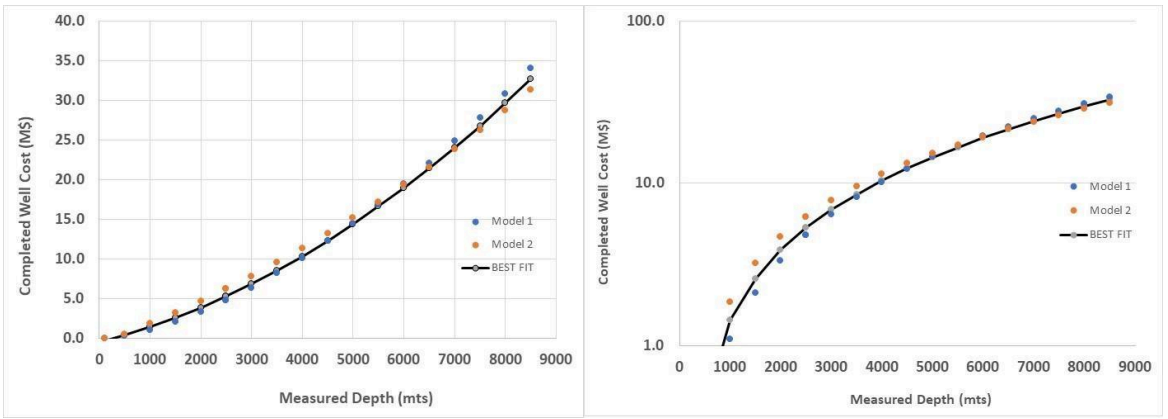

Figure 92: *Total cost (M$) of the geothermal wells and measured depth (m).*

Other equipment's

An estimated costs of the other inventories used in geothermal systems is given in the ***Table 10****. These costs are notional cost. Actual cost is function of rates and actual project size for heat delivery.*

Table 10 *Cost estimates for the geothermal inventories.*

Inventories		Minimum $	Maximum $	Reference (Accessed on 4 July 2024)
Ground Heat Pumps		15,000	40,000	https://homeguide.com/costs/geothermal-heat-pump-cost
Industrial Heat Exchangers	Plate Type Heat Exchangers	5,000	50,000	Based on discussion with experts and Information from experience
	Shell and Tube HE	5,000	100,000	
Circulation Pumps	Electric Submersible Pumps (ESP)	5,000	10,000	https://www.absolutewaterpumps.com/submersible-pumps/outlet-diameter/6%22
	Line Shaft Pumps	2,000	7,000	

7.13 Active exploration and oil production wells in west Lithuania

More than 250 oil exploration wells were drilled in Lithuania. Most of the wells reached the Cambrian succession. Some wells were terminated to Silurian succession in Middle Lithuania. The oil production climaxed in 2001 and gradually declined in recent years **Figure *93***.

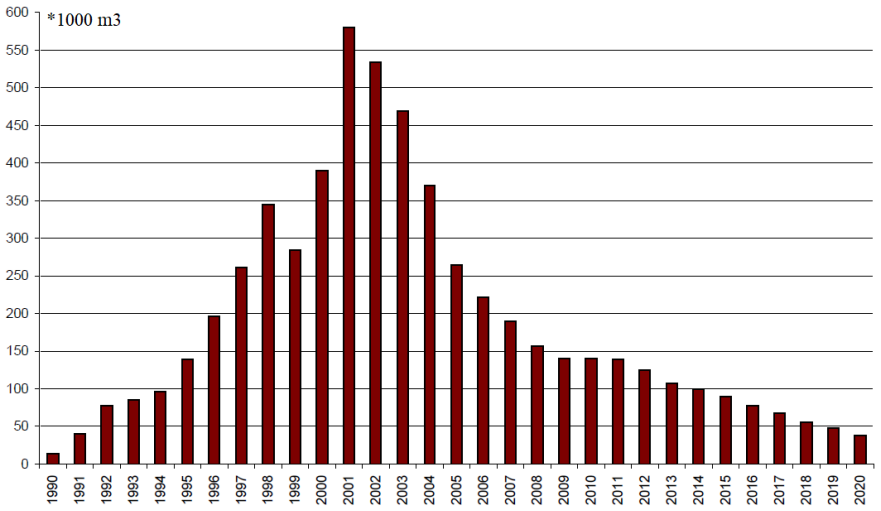

Figure 93: *History of oil production in Lithuania. The oil exploration can be continued for at least of dozen years and cannot be converted to geothermal boreholes.*

Most of the wells are distributed along the Telšiai and Gargždai master faults. The primary target in middle Lithuania is targeted on the Upper Silurian „reefs". According to the Lithuanian Geological Survey, there are 89 active oil exploitation wells in Lithuania.

Two basic well designs were used for the oil exploration and exploitation wells (***Table 11***). The diameter of the exploration and exploitation wells was typically 146 mm. The drilling design

was somewhat changed in 2001. The diameter of the production liner was adapted to 178 mm in Lithuania.

Table 11: Design of the oil exploration and exploitation wells in the Gargždai Elevation (data of inventory of 51 wells):

Type	*Diameter, mm*	*Shoe depth, m*	*Cementation, m*
Structural casing	529	3-8	Top to bottom
Conductor string	324	123-313	Top to bottom
Surface pipe	219	511-890	Top to bottom (rarely from 360 m)
Production liner	146	1918-2252	From shoe to depth of 1910-245

Remark: conduction ensures the safe operation of the Upper Permian and some underlying vuggy and high-porosity limestones and dolomites and is cemented (top to down); surface pipe isolates sedimentary deposits reaching down to the Šventoji-Upninkai sandy aquifer and is cemented (top to down); production liner isolates the Cambrian succession and overlying sedimentary deposits; depth of cementation varies from several meters to as thick as ~1500 m.

Table 12: *Design of the oil exploration and exploitation wells in the Telšiai fault zone (data of inventory of 29 wells):*

Type	*Diameter, mm*	*Shoe depth, m*	*Cementation, m*
Structural casing	529	3-8	Top to bottom
Conductor string	324	117-226	Top to bottom
Surface pipe	219	437-676	Top to bottom (rarely from 97 m)
Production liner	146	1918-2252	From shoe to depth of 1954-430

Most of the oil exploration wells were abundant after drilling in middle and west Lithuania. The total number of wells labelled as "*oil exploration*" is about 250 in the GeoLIS database [94]. Regulation of both active and abundant wells is subject to "DĖL ANGLIAVANDENILIŲ GRĘŽINIŲ PROJEKTAVIMO, ĮRENGIMO, KONSERVAVIMO IR LIKVIDAVIMO TVARKOS APRAŠO PATVIRTINIMO" TAR, 2023-07-10, Nr. 2023-14226), 2023 m. liepos 10 d. įsakymas Nr. D1-227. (ON THE APPROVAL OF A DESCRIPTION OF PROCEDURES FOR THE DESIGN, INS TALLATION, CONSERVATION AND DISPOSAL OF HYDROCARBON WELLS). TAR, 2023-07-10, Nr. 2023-14226), 2023 m. July 10 d., Nr. D1-227.

The abundant and active (converted) wells can be used for (1) production–injection geothermal installation (*e.g.*, the distance between wells Nilkyčiai-3 and Vilkyčiai-5, located outside the oil closure, is 2.272 m) or used as (2) deep single borehole heat exchangers (DBHEs). In the later part, the heat capacity can be estimated in the range of 150-250 kW (Kolo et al., 2024).

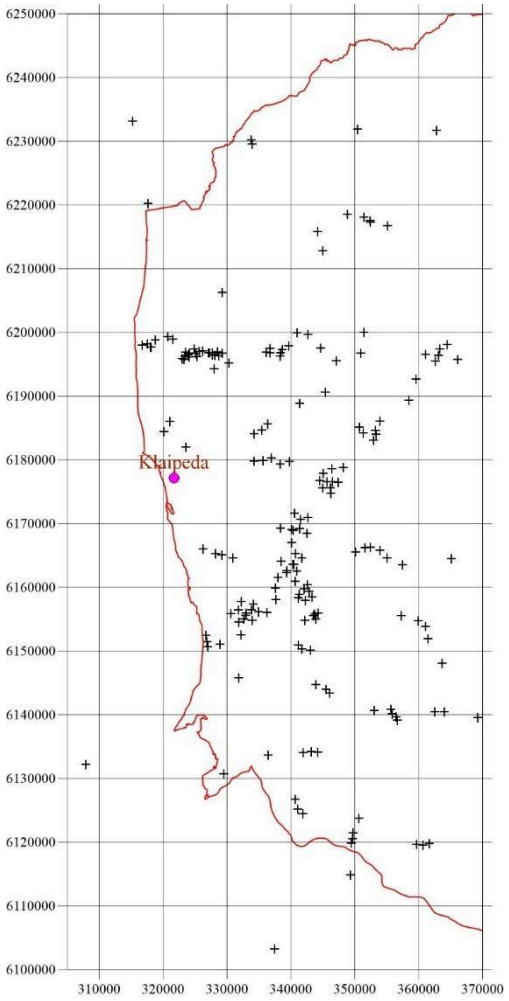

Figure 94:*:The oil exploration and exploitation wells are mainly clustered along the Telšiai and Gargždai fault zones in westernmost Lithuania. The wells, located closest to the seashore and Curonian Lagoon, sow the worst reservoir quality in west Lithuania (e.g., Traubai, Klaipėda, Purmaliai, Girkaliai). On the other hand, the geothermal potential is the highest in the seaside area.*

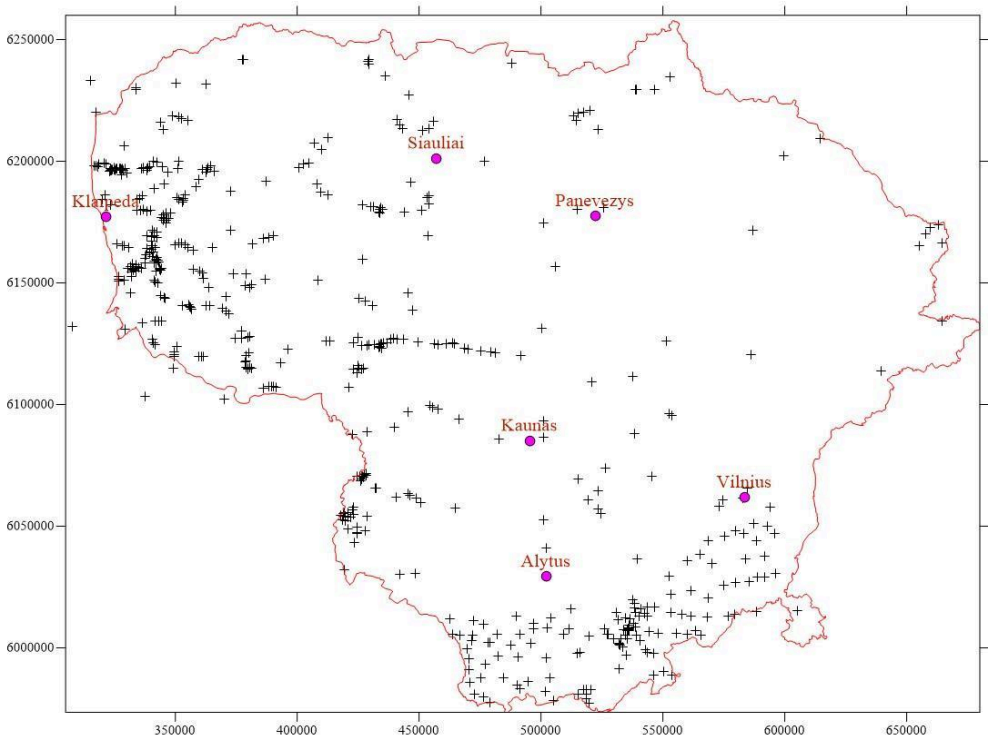

Figure 95: *The map of the deep boreholes of Lithuania, including wells studied the geothermal field. Two distinct well groups are distinct, e.g., well drilled for deep geological mapping of the crystalline basement in southeast Lithuania and oil exploration and exploitation wells in west Lithuania.*

8 Introduction

Lithuania, despite being located on the stable and thick East European Craton of Early Precambrian origin, exhibits a notable geothermal anomaly in its southwestern region [1]. This anomaly is linked to Middle Proterozoic cratonic granitoid intrusions, which are abundant in radiogenic, heat-generating elements [2-5]. These intrusions primarily consist of massive biotite and monzogranites, with smaller amounts of biotite syenogranites and porphyritic quartz monzodiorites. The granitoids are predominantly alkali-calcic and shoshonitic, enriched with incompatible elements such as potassium (K), rare earth elements (REE), uranium (U), and thorium (Th). Located at depths exceeding 2 km beneath the Cambrian formation, see **Figure 96**. the most significant geothermal anomaly in this region is associated with the Zemaicių Naumiestis Batholith (ZNB), which spans 30 × 45 × 4 km, see **Figure 97**. Similar intrusions are found along Lithuania's southern coast, where the thick sedimentary cover and increased geothermal gradient create promising zones for geothermal energy utilization. The thermal insulation provided by these sedimentary rocks also contributes to the elevated heat flow, resulting in geothermal gradients as high as 45 °C/km [1,4,5].

Western Lithuania hosts two primary hydrothermal complexes within the Cambrian (80 m thick) and Lower Devonian (180 m thick) sandstones. The Kemery Formation (Lower Devonian) sandstones, with an average porosity of 26% and permeability ranging from 2000 to 4000 mD, display excellent flow properties but only achieve reservoir temperatures up to 45 °C. In contrast, the Cambrian sandstones, with reservoir temperatures ranging from 14 to 96 °C, exhibit significant west-to-east variations in porosity (3 to 24%) and permeability (5–200 mD in West Lithuania to 600–900 mD in Central Lithuania).

These geological formations in Western Lithuania offer varying degrees of suitability for geothermal energy development, influenced by their lithological characteristics, reservoir properties, and temperature profiles. Detailed geological and geothermal surveys are essential for optimizing geothermal projects. While the Cambrian sandstones may have lower flow properties compared to the Devonian reservoirs, their higher temperatures make them more suitable for geothermal development, offering greater energy output and efficiency. Consequently, the Cambrian geothermal complexes in Western Lithuania are considered more promising targets for geothermal energy projects than the Lower Devonian reservoirs for several reasons, listed below. Series of useful maps showing geothermal aspects of various geological sites are listed in **Appendix 1.**

8.1 Higher Reservoir Temperatures

The Cambrian sandstones exhibit a significantly higher range of reservoir temperatures, from 14 to 96 °C, compared to the Lower Devonian Kemeri Formation sandstones, which reach only up to 45 °C. Higher reservoir temperatures are crucial for efficient geothermal energy production, as they directly impact the energy yield and the efficiency of the geothermal systems.

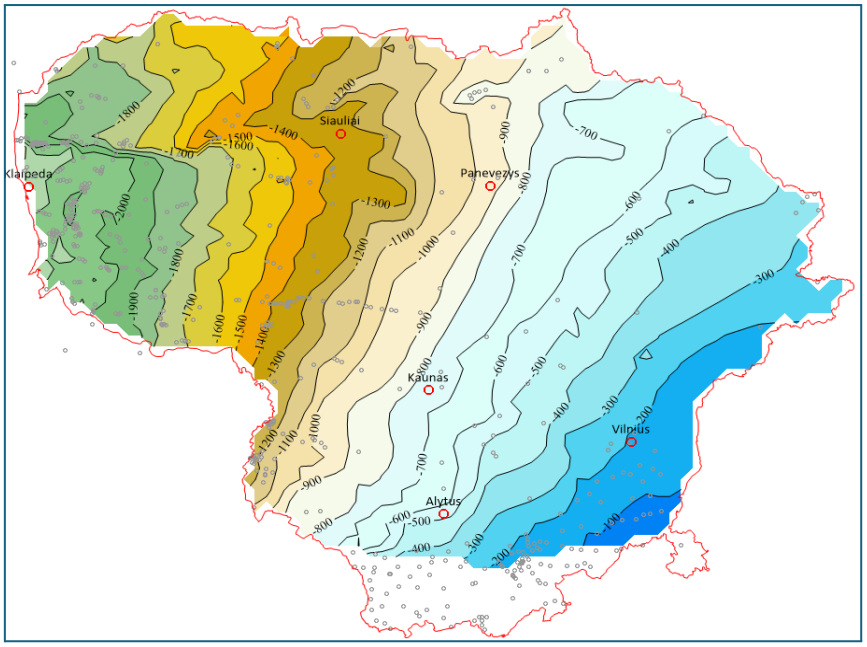

***Figure 96**: Depth (m) of top of the Cambrian succession of Lithuania. Deep wells (grey circles). Tectonic faults are not indicated on the map*

8.2 Regional Variability in Porosity and Permeability

Although the Cambrian sandstones show substantial regional variations in porosity (3 to 24%) and permeability (5–200 mD in West Lithuania to about 600–900 mD in Middle Lithuania), these properties can be advantageous when strategically selecting and optimizing drilling locations. This variability allows for the identification of zones with higher permeability and porosity that can enhance the flow and extraction of geothermal fluids.

8.3 Overall Reservoir Performance

While the Kemeri Formation sandstones of the Lower Devonian exhibit excellent flow properties with high porosity (26%) and permeability (2000–4000 mD), their lower reservoir temperatures limit their potential for high-efficiency geothermal energy production. The Cambrian sandstones, despite having a wider range of porosity and permeability, offer a better balance between these properties and the crucial factor of higher reservoir temperatures.

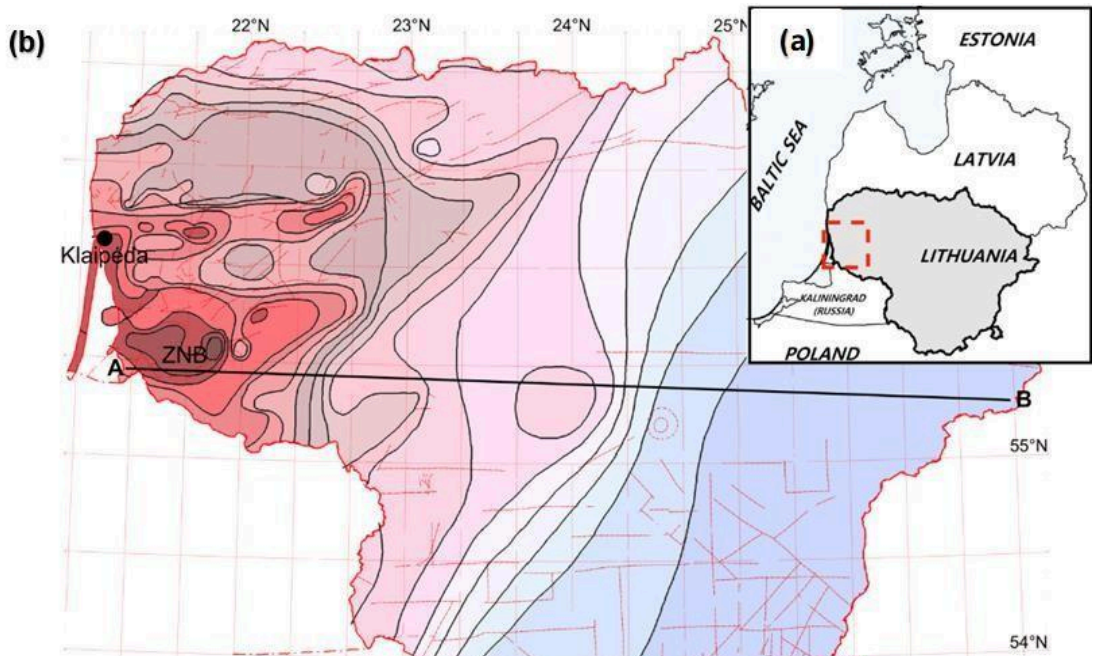

***Figure 97**: (**a**) The study area is shown in dashed red rectangle in the Baltic Sea region context. (**b**) Top Cambrian temperature map with a marked geothermal anomaly at Zemaiciu Naumiestis Batholith (ZNB) (modified from [5]. (**b**) Generalized geological cross-section throughout Lithuanian territory (A–B profile is shown in the map above) [5].*

9 Potential Geothermal Formations in Western Lithuania:

The geological formations in Western Lithuania that are suitable for geothermal development include the following:

9.1 Lower Devonian Kemeri Formation

The lithology of the reservoir consists of sandstones, which exhibit excellent flow properties due to their high porosity, averaging 26%, and permeability ranging from 2000 to 4000 millidarcies (mD). The reservoir temperatures can reach up to 45°C, making it suitable for low-temperature geothermal applications.

9.2 Cambrian Sandstones

The lithology of the reservoir is predominantly composed of sandstones, which exhibit significant regional variations in porosity and permeability. Porosity ranges from 3% to 24%, while permeability varies from 5 to 200 millidarcies (mD) in West Lithuania to approximately 600–900 mD in Middle Lithuania. Reservoir temperatures are notably high, ranging from 14°C to 96°C, offering substantial potential for geothermal applications across a wide temperature range.

9.3 Middle Proterozoic Cratonic Granitoid Intrusions

The lithology of the region consists of granitoids, including biotite and monzogranites, with occurrences of biotite syenogranites and porphyritic quartz monzodiorites. These rocks are rich in radiogenic heat-producing elements, contributing to higher geothermal gradients in the area. This composition provides significant potential for geothermal energy exploitation due to the enhanced heat production capabilities of the rock formations.

9.4 Zemaičių Naumiestis Batholith (ZNB)

The lithology of the region is characterized by granitoids forming a large batholith measuring approximately 30 × 45 × 4 kilometers. This batholith significantly contributes to a major geothermal anomaly due to its size and heat production capabilities. The presence of enhanced geothermal gradients further highlights its high potential for geothermal energy exploitation.

9.5 Silurian and Ordovician Carbonates:

The lithology of the region consists of limestones and dolomites, which exhibit reasonable porosity and permeability, making them suitable for geothermal water flow. Reservoir temperatures vary moderately based on depth, enhancing their applicability. These formations hold potential for geothermal applications, particularly when utilized in combination with other geological formations.

9.6 Upper Devonian Formations:

The lithology of the region comprises various sedimentary rocks, including sandstones and shales, which exhibit varying porosity and permeability. While these characteristics make them suitable for geothermal applications, their effectiveness is enhanced when combined with other

geothermal targets. The moderate reservoir temperatures further support their use in certain geothermal systems, offering potential for integration to achieve enhanced performance.

Although a number of low and high potential sites are present in western Lithuania based on geological classification of data, not all sites have data abundance to carry out a detailed analysis. Cambrian sites have most data available due to oil and gas exploration.

10 Evaluation of Possible Geothermal Sources in Western Lithuania – Cambrian Reservoirs

Western Lithuania hosts numerous hydrocarbon reservoirs, many of which are either depleted or nearing the end of their production lifecycle (see **Figure 98**), also the temperature distribution in the Cambrian geothermal aquifers is shown in **Figure 99**. These reservoirs present a unique opportunity for repurposing into geothermal energy production sites with minimal additional cost. The Cambrian reservoirs, in particular, are of great interest due to the extensive geological and geothermal data accumulated over years of exploration and production. This wealth of information enhances the potential for successful geothermal energy development.

An initial screening was carried out to identifying sites with the highest volume of water extracted based on some historical production data (Table 13) from the deep wells drilled in some of the locations in western Lithuania. Water production data was obtained from reports held by the Lithuanian Geological Survey and oil companies upon request. An important selection criterion was the presence of water production infrastructure, with a higher number of wells increasing the likelihood of extracting more water. Therefore, the number of wells at each site was included in the screening. The status of the wells (e.g., currently open, plugged, or abandoned) was also crucial, with priority given to operational fields producing large amounts of water. This is because re-opening abandoned or plugged wells would incur additional costs. Another key criterion was the temperature of the co-produced water, as it influences the potential geothermal applications of the reservoir.

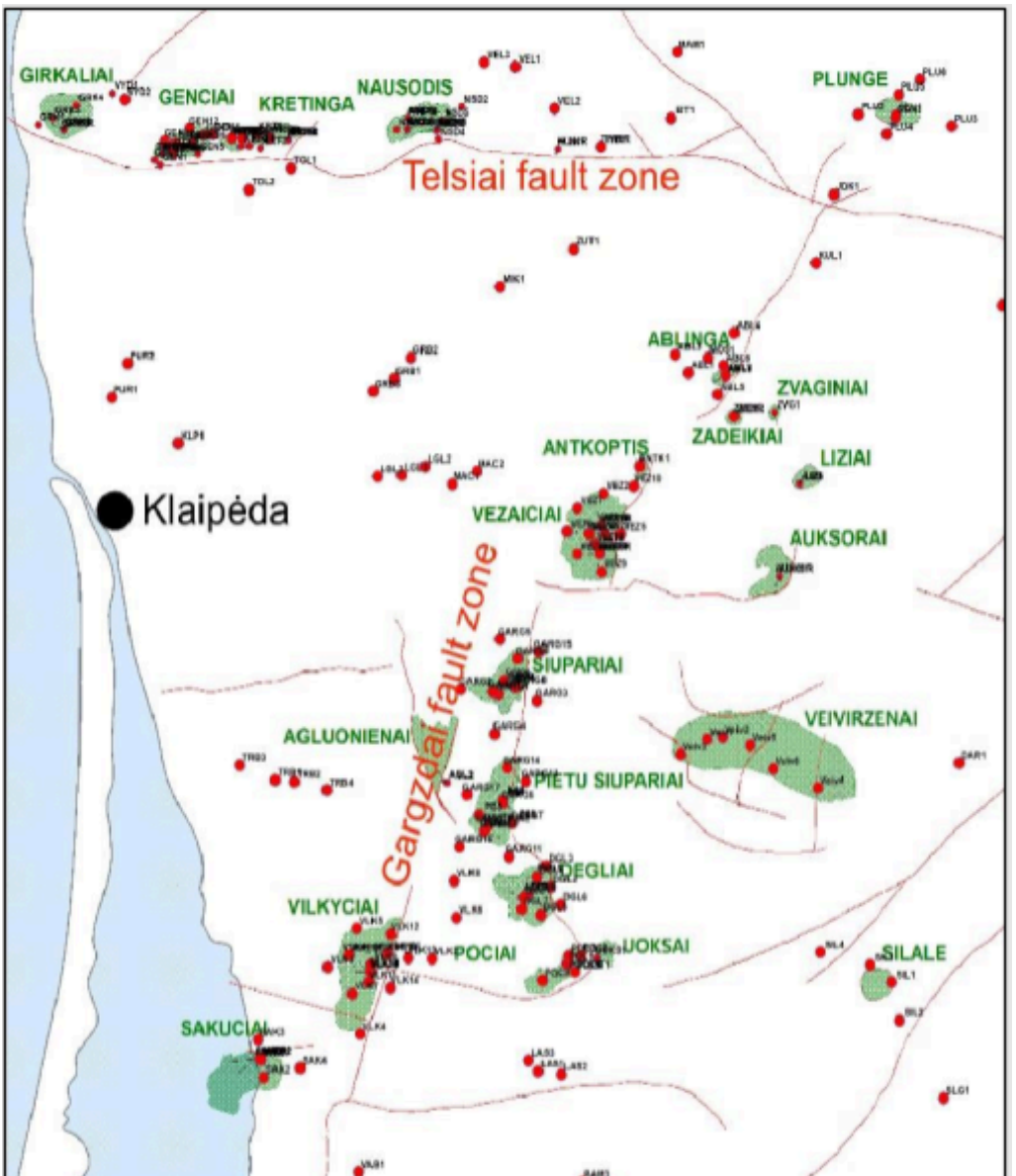

Figure 98: *Map of Cambrian reservoirs used for initial screening. Note that the reservoirs are located along the major fault zones. Klaipeda city for reference.*

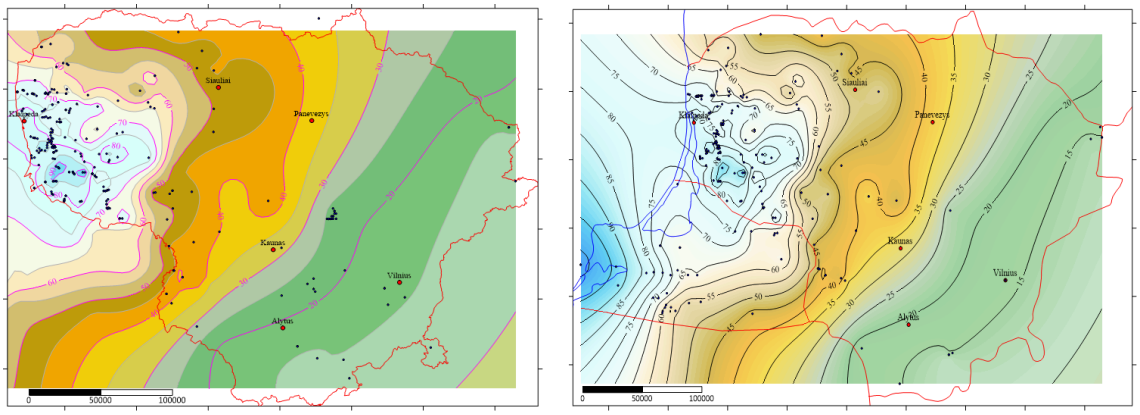

Figure 99: *Map of Cambrian reservoirs used showing geothermal temperatures used in initial screening.*

Table 13: *Water production data from the existing oil fields in Lithuania. Also shown are the number of wells within each reservoir as well as temperature of the formation water measured within the fields.*

Cambrian Reservoir	Water Extracted from the Field since the Start of water production in m3	Water Produced in 2022, m^3/year	No. of Wells	Temperature at the Top of Cambrian, ˚C
Gencai	5,651,869.915	86,236.001	10	74
Vilkyciai	4,129,050.971	64,714.905	15	85.5
South Siupariai	2,955,872.771	0	10	83
Nausodis	2,107,141.674	42,946.523	14	75
Diegliai	1,623,752.633	0	6	82.9
Kretinga	1,319,346.659	8488.2	9	70.2
Siupariai	872,572.994	372.661	6	76.3
Pociai	559,226.701	8377.844	5	84.3
Vezaiciai	543,463.32	10,453.455	12	76

Girkaliai	370,381.596	8571.187	6	71.7
Liziai	365,821.766	3949.233	4	N/A
Sakuciai	152,549.824	3843.274	4	84
Ablinga	61,134.015	0	3	80.8
Agluonenai	45,666.05	419.345	2	N/A
Uoksai	10,358.773	0	1	84.3
Silale	3246.94	0	2	82.4
Auksoras	2522.611	0	1	N/A
Zadeikiai	1794.846	0	1	N/A
North Vezaiciai	1221.246	141.685	1	76

Based on the data presented in **Table 13**, top 3-4 sites targeting the Cambrian geothermal system are identified. Then, the petrophysical properties of each site were mapped, including porosity, permeability, depth, average subsurface temperature, water salinity, injection water temperature, reservoir pressure, expected flow rates, reservoir thickness, and NTG (Net-to-Gross) (Table 1.3.1-2). All of the property ranges listed in **Table 14** were collected from the reports pre- pared by oil companies and submitted to Lithuanian Geology Survey during oil exploration. The reservoir properties indicate that the sandstone reservoirs are rather heterogeneous containing at least four different effective layers of sandstones of varying properties alternating with more clayey layers in between.

Table 14: *Petrophysical properties of the selected five top sites that were used for modelling.*

Reservoir Parameters	**Genčiai**	**Vilkyčiai**	**South Siupariai**	**Nausodis**	**Diegliai**
Effective porosity, % (min-average-max)	6–8–10	4.6–6.5–9.7	5.4–6.2–7.7	0.3–8–15	6–8.5–11.3

Permeability, mD (min-average-max)	0.1–12–219	0.1–10.4–41.4	0.01–16.7–45.14	0.01–9.4–895.6	0.1–10.8–47
Depth, m	1800–1826.4	1975–1992.5	1958–1988	1765–1860.6	1940–1990
Average temperature, °C	73.64	88	83	75	85
Water salinity, mg/L	146,217.33	229,000	-	138,241.18	200,000
Injection water temperature, °C	55	55	55	55	55
Reservoir Pressure, bars	191.66	222	216	190.491	213
Reservoir thickness, m (total and effective)	26.4; 16.19	68; 17.5	30; 16	95.6; 82.28	61; 25
NTG (Net-to-Gross), units	0.61	0.26	0.53	0.86	0.41

10.1 Evaluation of screening sites using Mini-Modelling Methodology

A previous study employed computer-generated models to evaluate the geothermal heat potential at a specific site in Lithuania [6,7]. In this screening work, we adopt a more advanced modelling approach by constructing mechanistic/mini box models that mimic the fundamental characteristics of the geological site through an integrated modeling process. These models were then used to simulate the flow of geothermal fluids within subsurface reservoirs. The modelling process began with the collection of data from logs and core measurements, which were then integrated into a simulation model where dynamic properties were assigned to conduct thermal flow simulations. Geological data was integrated to develop 3D mechanistic models, subsequently used for simulation.

The 3D mechanistic models were constructed using an integrated modelling workflow based on reservoir parameters outlined in **Table 15**. Initially, a 3D static model corresponding to the depth and thickness of the reservoir was created. This model was then populated with reservoir properties such as permeability, porosity, and NTG. Due to software limitations in integrating log data with the static model, a method was used to populate permeability and porosity values in the models, ensuring that the mean, low, and high values of these properties matched those listed in **Table 16**. For each reservoir, three 3D models were developed, representing low, mid, and high case scenarios for the simulation study. Based on published works it was decided to keep well spacing of 1300m for modelling the doublet well pairs.

10.2 Mechanistic Mini Modelling and Experimental Design Workflow

Upon selecting the optimal well spacing, geological screening criteria were employed to construct a series of mechanistic simulation models for each geological site. These models were subsequently utilized to assess the geothermal potential of each site through fluid flow simulations. Next, an experimental design approach was used to identify the most impactful parameter for each geological site. The workflow applied for experimental design approach is rather simple and straight-forward to implement. The steps of this workflow are shown below:

i. Identify the most impactful model/reservoir parameter through sensitivity analysis.
ii. For sensitivity analysis, a parameter range is decided, then prediction is performed.
iii. Using the set of model/reservoir parameters, the impact on prediction accuracy is checked.
iv. Several combinations of different model/reservoir parameters could be tested.
v. Finally, the model/reservoir parameters giving the best prediction accuracy are selected.

Based on the above workflow, the most impactful parameters were identified and used with the high, mid, and low cases to assess the geothermal potential of the site.

Although, some of the selected sites were primarily designed for hydrocarbon production, the wells used in hydrocarbon production lack open-hole sections and are drilled only at the topmost layer, which possesses relatively poor collector properties in the Cambrian layer. Despite these limitations, in order to stay true to the assessment of potential geothermal potential, these models were configured to represent a potential scenario for well doublets repurposed for geothermal fluid extraction with specific well spacing selection.

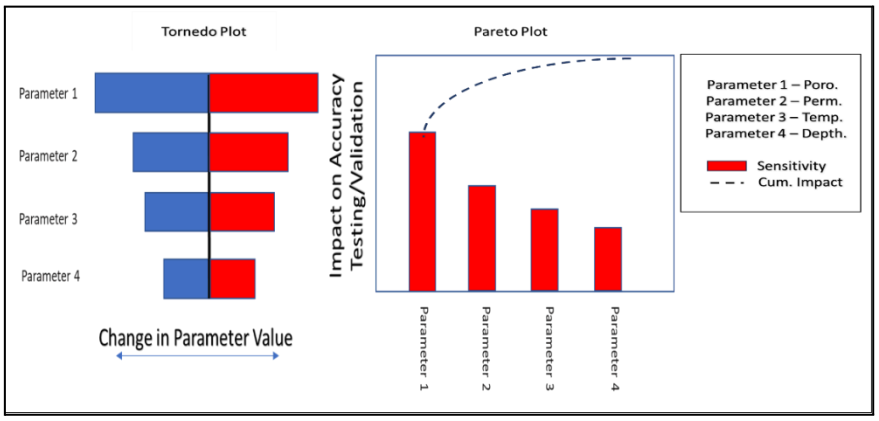

Figure 100: *The experimental design workflow.*

Based on the workflow described above, Tornado and Pareto charts were created for each site. For this analysis, the Static Model provides low/mid/high ranges for parameters such as porosity, permeability, thickness, and NTG to account for the reservoir petrophysical uncertainties for all selected sites. Additional parameters such as Kv/Kh in hardgrounds were also included in the sensitivity analysis. Here, low, mid, and high cases for geological parameters were assumed.

A base case simulation was defined for the selected development site option using a reference case input for all parameters (denoted as the mid case in the mechanistic model). The key project metric, cumulative water production after 50 years, was recorded from the base/reference case. These base case results form the basis for comparison with the results of the parameter sensitivities.

Individual parameter sensitivities were conducted by single parameter changes to the model. For each parameter the values were changed from the lower to the upper limits to gauge the maximum potential impact of that particular parameter. Results of all sensitivities were collated and are presented in the Tornado charts in **Figure 101**. For the example shown in **Figure 101**, a total of four reservoir/fluid parameters were selected to investigate the key uncertainties associated with this development. The example Tornado chart in **Figure 100** shows that the range associated with the uncertainty on Parameter 1 is the most dominating factor, followed by Parameter 2, 3, and 4. The red color indicates the high case realization of the reservoir parameter, and the low case realization is colored blue.

In order to rank and select key parameters for the probabilistic uncertainty evaluations, another step was included to provide consistency across all investigated development scenarios. The Pareto analysis is a technique that provides the required ranking and selection of the most

influential input parameters for particular metrics, e.g., thermal recovery for a geothermal development.

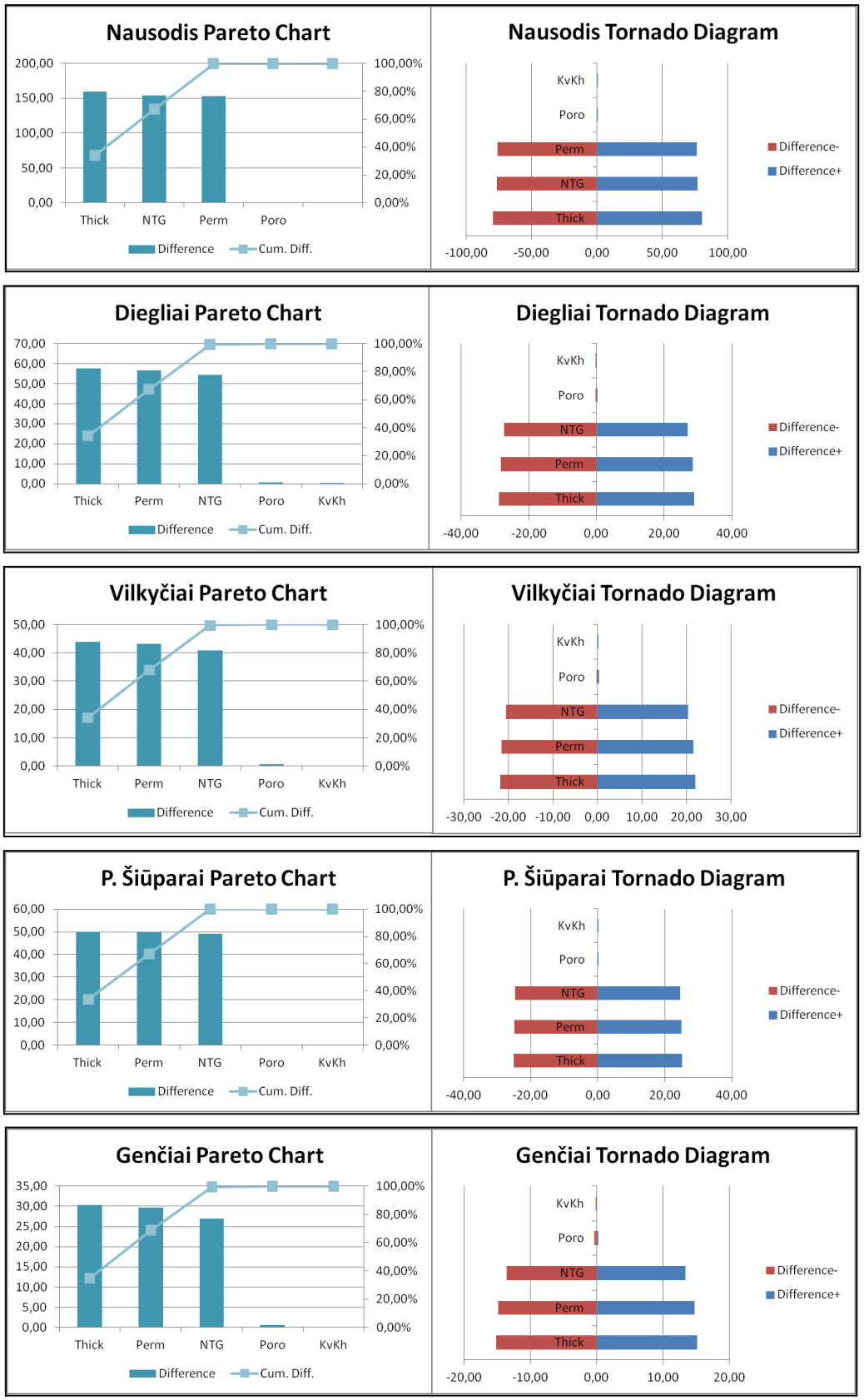

Figure 101: *Tornado and Pareto charts for the five selected sites based on preliminary screening.*

Figure 101 depicts the results of the Tornado and Pareto analysis performed on an example model for geothermal recovery and total production rate sensitivities. The vertical bars shown in the Pareto charts reflect the uncertainty range associated with the individual sensitivities, sorted in descending order. The Pareto chart also shows a curve representing the cumulative normalized uncertainty. Parameters corresponding to 80% of the full uncertainty (blue dashed line in Pareto chart) are considered the most important and are therefore selected for probabilistic forecasting.

The Tornado and Parato charts for the five selected sites, based on preliminary screening, are shown in **Figure 101**. From the Tornado and Pareto analysis, it can be said that for all the selected sites, the most impacting parameters turn out to be thickness, permeability, and NTG. The porosity and Kv/Kh have a very insignificant impact on the total production rates. Next, these selected parameters were used to carry out the probabilistic forecasting for these sites and were used in the creation of the high, mid, and low cases for carrying out the simulation, see **Table 15**.

Table 15: *Petrophysical L-M-H properties selected for sensitivity analysis of the five modelled sites.*

Reservoir Parameters	**Genčiai**	**Vilkyčiai**	**P. Šiūparai**	**Nausodis**	**Diegliai**
Effective porosity, %	7.2–8.0–8.8	5.9–6.5–7.2	5.6–6.2–6.8	7.2–8.0–8.8	7.7–8.5–9.4
Permeability, mD	10.8–12.0–13.2	9.4–10.4–11.4	15.0–16.7–18.4	8.5–9.4–10.3	9.7–10.8–11.9
Kv/Kh, units	0.30–0.33–0.36	0.30–0.33–0.36	0.30–0.33–0.36	0.30–0.33–0.36	0.30–0.33–0.36
Reservoir thickness, m	23.8–26.4–29.0	61.2–68.0–74.8	27.0–30.0–33.0	86.0–95.6–105.2	54.9–61.0–67.1
NTG, units	0.55–0.61–0.67	0.23–0.26–0.29	0.48–0.53–0.58	0.77–0.86–94.6	0.37–0.41–0.45

10.3 Geothermal Output of selected Sites

In accordance with the well spacing and geological screening criteria, models were developed for each site. This section presents results for a specific site (see Table 1.3.1-4), focusing on a screened Cambrian reservoir. An analysis was conducted to examine the trajectory of injected water from injection to production wells and to assess achievable production rates. The findings indicated that with a well spacing of 1300 m, it is theoretically feasible to produce heat at a rate from 38 to 187 GWh annually (power output from 178.8 kW to 854.5 kW). The following equation was used for the power P calculation:

$$P = \frac{Q}{t} \quad (1)$$

This is how power P is defined in physics in general, where Q is energy (heat in our case) and t is the time taken to transfer that much energy. Heat is extracted from the water directly, so the formula used is known as a heat equation:

$$Q = c \cdot m \cdot \Delta T \quad (2)$$

Lastly, the amount of water affected by heat loss is known from the water rate q. However, in order to get the mass, this quantity is multiplied by the water density ρ:

$$m = q \cdot \rho \quad (3)$$

Putting Equations (2) and (3) in Equation (1) we derive a general formula for power through the intrinsic loss of heat from the water:

$$P = c \cdot (q \cdot \rho) \cdot \Delta T \quad (4)$$

Here P is power, c is the specific heat, q is the volumetric flow rate of water, ρ is water density, and ΔT is the temperature change of water. This formula does not include real life heat losses and equipment efficiencies but describes the fundamental heat transfer of water. Furthermore, the results demonstrate the potential for achieving doublet injection and production rates potentially reaching 800 m3/day for some Cambrian reservoirs.

Table 16: *Results of subsurface flow modeling of the five selected sites*

		TRUE	CALCULATED	
Site	Cases	Temperature, °C	Production Rate, m3/d	Potential Energy Produced, MWh
Nausodis	Low	75	647	1.52×10^5
	Mid		799	1.87×10^5
	High		967	2.27×10^5
Diegliai	Low	85	258	9.06×10^4
	Mid		284	9.99×10^4
	High		319	1.12×10^5
Vilkyčiai	Low	88	195	7.56×10^4
	Mid		217	8.37×10^4
	High		242	9.37×10^4
P. Šiūparai	Low	83	225	7.38×10^4
	Mid		247	8.12×10^4
	High		276	9.05×10^4
Genčiai	Low	74	142	3.11×10^4
	Mid		176	3.84×10^4
	High		213	4.64×10^4

The analysis underscores the significance of both the water temperature and production rate in determining the geothermal potential of each site over a 25-year period. Comparing these sites, Nausodis stands out with by far the highest thermal output due to its substantial production rate, which can be explained by a huge reservoir thickness combined with a high NTG value. Diegliai, Vilkyčiai, and P. Šiūparai fall closely to each other, displaying competitive thermal outputs since they have very similar geological properties. The fifth place goes to Genčiai, which exhibits comparatively lower potential due to a low reservoir temperature as well as poor production rates.

11 Possible Geothermal Sources in Western Lithuania – Devonian Reservoirs

An initial Cambrian screening was carried out to identifying sites with the highest volume of water extracted based on some historical production data as described in earlier section. In Lithuania the Devonian complex is not explored extensively similar to Cambrian. In case of Devonian aquifer only three possible sites were ranked based on available data and uncertainties involved in it. The petrophysical properties of each site were mapped, including porosity, permeability, depth, average subsurface temperature, water salinity, injection water temperature, reservoir pressure, expected flow rates, reservoir thickness, and NTG (Net-to-Gross) (**Table 17**).

All the property ranges listed in **Table 17** were collected from the research articles and industrial reports which are published. The reservoir properties indicate that the sandstone reservoirs are unconsolidated and more permeable.

Table 17: *Petrophysical properties of these top sites that were used for modelling.*

Reservoir Parameters	**KGDP-1I**	**Nida**	**Vydmantai - Devonian**
Effective porosity, % (min-average-max)	20.1-25-31.2	11.6-25-31	3.7-16-29
Permeability, mD (min-average-max)	207-2563-6295	290-6434-9850	207-2500-6295
Depth, m	980-1048-1116	1023-1074-1126	827-912-997
Average temperature, °C	38	35-40	34.1
Water salinity, mg/L	92,800	80,000-90,000	27,600-45,700
Injection water temperature, °C	11-15	-	-
Reservoir Pressure, bars	109	111.7	95
Reservoir thickness, m (total and effective)	87; 56	103; 51.5	110.8; [300-115]
NTG (Net-to-Gross), units	0.64	-	0.39

11.1 Evaluation of screening sites using Mini-Modelling Methodology

Due to the limited exploration of Devonian complex, it was observed that there was only one geothermal plant in Klaipeda built in 2000 and was shut down in 2017 due to operational difficulties. The above data set in the **Table 17** does incorporate lot of uncertainties within itself. To fulfil the uncertainty gaps all the data were compiled together, and one field model is developed which captures low, mid, and high case values. The further screening work is similar to Cambrian advanced modelling approach by constructing mechanistic/mini box models that mimic the fundamental characteristics of the geological site through an integrated modeling process.

In initial runs a homogenous model was built with the high case properties but due to high permeability values temperature breakthrough was observed with the 1200m well spacing as depicted in the **Figure 102**. So, temperature sensitivity runs were performed, and it confirmed that at well spacing of 5500m is enough to prevent breakthrough for 30 years run. So, for all future runs it was decided to keep well spacing of 5500 m for modelling the doublet well pairs.

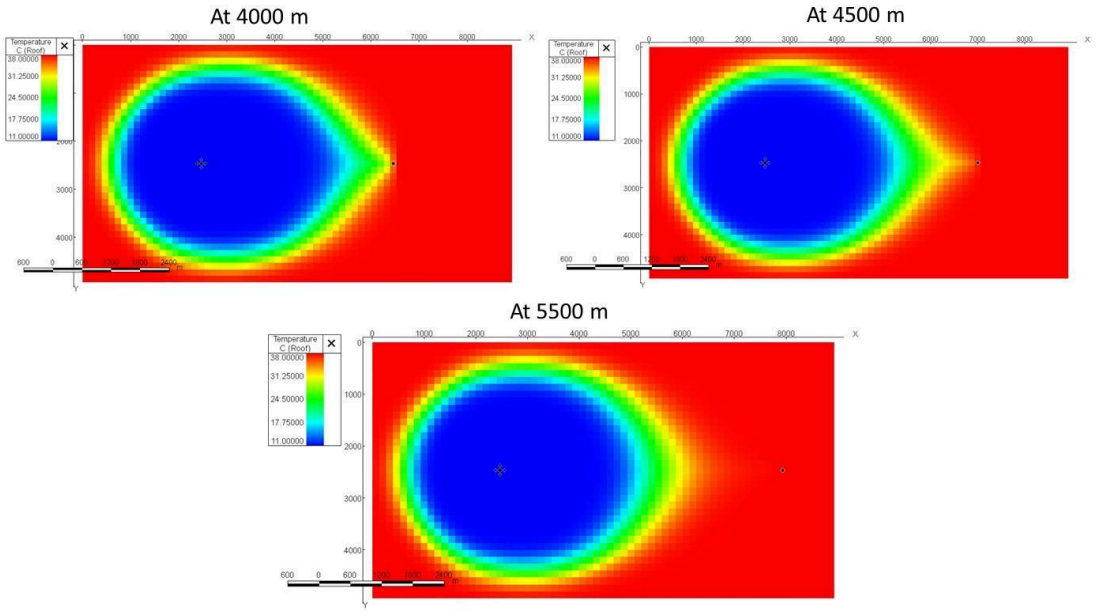

Figure 102: *Temperature front profile of the designed site (Devonian aquifer).*

11.2 Mechanistic Mini Modelling and Experimental Design Workflow

Upon selecting the optimal well spacing, geological screening criteria were employed to construct mechanistic simulation models for geological site. This homogenous model was then subsequently utilized to assess the geothermal potential through fluid flow simulations. Before moving ahead with geothermal production potential, the degree of impact of the uncertainty parameters must be evaluated. This uncertainty can be solved using the Tornado and Pareto plots.

A Tornado diagram is a simple chart that helps to see how much the result changes when one adjusts one factor at a time. It shows the impact of changing each factor while keeping everything else the same. Thus, Tornado diagrams are helpful for understanding which factors are most important in a situation. To use them, we need to estimate the lowest, average, and highest possible outcomes for each factor.

A Pareto chart is a simple graph that combines bars and a line. The bars show individual values from largest to smallest, while the line shows the running total of all values. The aim of the Pareto chart is to highlight the most important parameter among all set of described factors. In a Pareto chart, the bars are arranged from highest to lowest based on how often something happens. Thus, Pareto charts helps to see which areas to work on first to make improvements.

Based on the workflow described above, Tornado and Pareto charts were created for developed site. For this analysis, the Static Model provides low/mid/high ranges for parameters such as porosity, permeability, thickness, and NTG to account for the reservoir petrophysical uncertainties for the site. Additional parameters such as Kv/Kh was also included in the sensitivity analysis. Here, low, mid, and high cases for geological parameters were assumed as referred in **Table 18**. Also, described in the earlier section of Cambrian reservoir the top 5 most parameters were considered but in the Devonian section thickness was almost same for Nida and KGDP. To further, the sensitivity analysis was performed on the remaining parameters by developing the Tornado and Pareto plots.

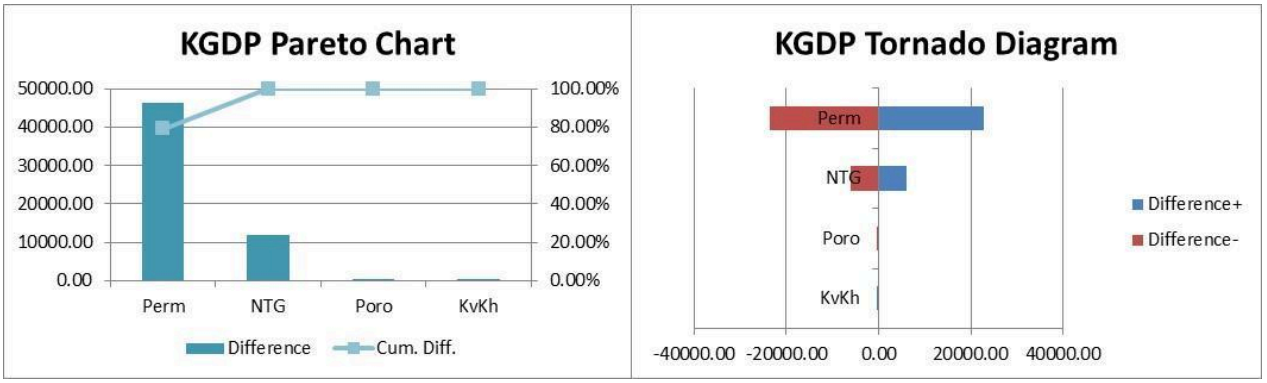

Figure 103: *Tornado and Pareto charts for the designed site based on initial screening.*

As described earlier in section the Pareto chart shows a curve representing the cumulative normalized uncertainty. Parameters corresponding to 80% of the full uncertainty (blue dashed line in Pareto chart) are considered the most important and are therefore selected for probabilistic forecasting.

From the **Figure 103**, the Tornado and Pareto charts of the designed site based on preliminary screening concludes that the most impacting parameters turn out to be permeability, and NTG. The porosity and Kv/Kh have a very minimal impact on the total production rates. Next, these selected parameters were used to carry out the probabilistic forecasting of the designed site and were used in the creation of the high, mid, and low cases for carrying out the simulation, see **Table 18**.

Table 18: *Petrophysical L-M-H properties selected for sensitivity analysis of designed site.*

Reservoir Parameters	**Designed Site (Devonian Aquifer)**
Effective porosity, %	3.75-20-31.2
Permeability, mD	207-3251-6295
Kv/Kh, units	0.30–0.33–0.36
NTG, units	0.39-0.52-0.64

Furthermore, the obtained sensitive parameters (Permeability and NTG) along with the base case value of porosity and Kv/Kh were used to determine the probabilistic average water production flow rate. The obtained low and high case values of the sensitive parameters (Permeability and NTG) were taken as a property to define several intermediate property values which are created by linear interpolation within these two properties to obtain a set of 7. Using this procedure to represent the defined uncertainty range, the likelihood of each set is now evaluated from the normal distribution shown in **Figure 104** (Permeability; and NTG). This resulted in 7 uncertainty ranges for each parameter and generate 7 * 7 cases to be run for calculation of average water production rates.

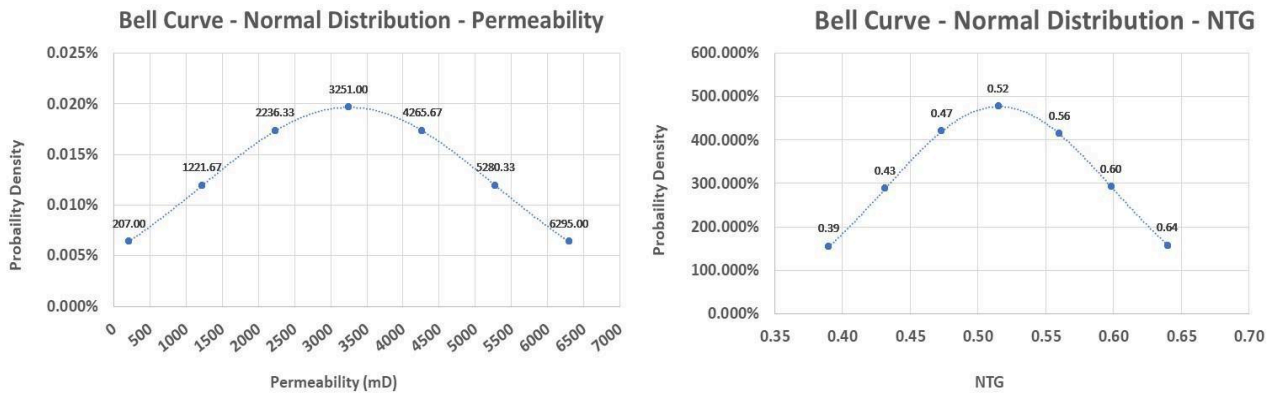

Figure 104: *Bell curve of permeability and NTG for the designed site (Devonian aquifer).*

Over 50 simulations were run for the calculation of average water production rates. Each simulation used a different mix of the uncertainty factors listed earlier. The results are tabulated in the **Table 19**.

Table 19**:** *Average water production based on the sensitivity analysis of designed site.*

With Porosity value of 20% - WATER PRODUCTION (sm3/day)							
PERMZ	69.00	407.22	745.44	1083.67	1421.89	1760.11	2098.33
PERMX	207.00	1221.67	2236.33	3251.00	4265.67	5280.33	6295.00
NTG							
0.39	1215.93	6974.54	12575.02	18102.57	23573.87	29015.16	34382.96
0.43	1344.72	7703.92	13889.13	19998.65	26070.17	32080.20	38013.82
0.47	1473.30	8431.12	15207.63	21897.01	28532.00	35130.60	41679.67
0.52	1601.74	9158.19	16515.77	23791.74	31004.23	38191.41	45350.45
0.56	1730.02	9883.71	17830.10	25690.93	33501.41	41241.51	48948.30
0.60	1858.11	10608.46	19140.89	27583.49	35983.22	44337.41	52631.08
0.64	1986.09	11332.14	20443.48	29491.52	38466.52	47434.96	56269.41

From the above analysis a S-curve for average water production rates is determined to calculate the low, mid, and high average water production rate as depicted in **Figure 105** and values are tabulated in the **Table 20**.

Table 20: *Results of subsurface flow modeling of the designed site (Devonian aquifer).*

		TRUE	CALCULATED	
Site	Cases	Temperature °C	Production Rate m^3/d	Potential Energy Produced, MWh

Devonian Aquifer	Low Mid High	38	4,500 23,700 43,000	1.37×10^6 7.23×10^6 1.31×10^7

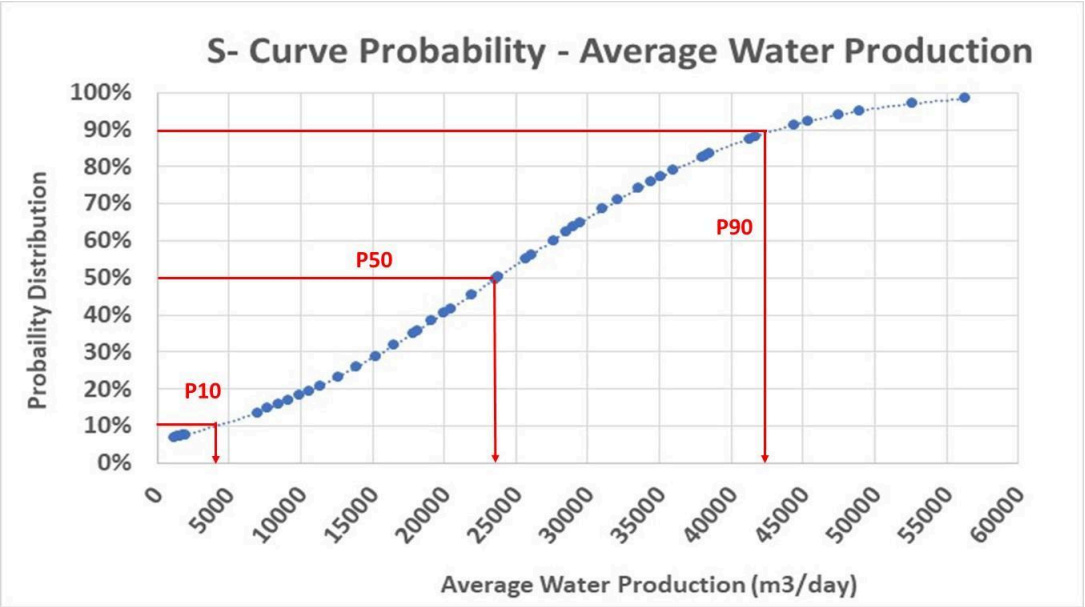

Figure 105: *S-curve of average water production rate for the designed site (Devonian aquifer).*

11.3 Geothermal Output of selected Sites

In accordance with the well spacing and geological screening criteria, models were developed for designed site (Devonian Aquifer). The findings indicated that with a well spacing of 5500 m, it is theoretically feasible to produce heat at a rate from 1370 to 13,100 GWh annually (power output from 6265 kW to 60,000 kW). The analysis underscores the significance of both the water temperature and production rate in determining the geothermal potential of each site over a 25-year period. The high-power production is due to high average water production rates which is due to increased permeability.

12 Legal framework for resource extraction

The use of geothermal energy in the depths of the earth is regulated by the Law of the Republic of Lithuania on the depths of the earth and the Decree of the Minister of the Environment of the Republic of Lithuania in 2015. April 3 order no. D1-273 "On the approval of the description of the procedure for the design, installation and liquidation of geothermal wells".

Article 16, Part 2, Clause 3 of the Law on Subsoil Depths provides that a permit for the use of subsoil resources or subsoil cavities is not required for the use of subsoil geothermal energy. Clause 10 of Article 4, Part 2 of the Law on the Depths of the Earth provides that the Ministry of the Environment of the Republic of Lithuania establishes the procedure for the design, installation, conservation and liquidation of geothermal energy wells.

Pursuant to the provisions of Article 7, Paragraph 1 of the Law on the Depths of the Earth, natural and legal persons or a group of such persons, operating under a joint venture agreement, who have a permit to explore the depths of the earth issued in accordance with the procedure established by this law, have the right to conduct direct and remote investigations of the depths of the earth. Pursuant to Article 7, Part 2, Item 1 of the Law on the Depths of the Earth, the permission to explore the depths of the earth grants the right to conduct the following types of direct and remote explorations of the depths of the earth: geothermal energy search and prospecting.

Pursuant to the provisions of Article 14 of the Subsoil Law, paragraph 5, subsoil resources and subsoil cavities are used only after the procedures set forth in the Law on Environmental Impact Assessment of Planned Economic Activities have been completed.

The description of the procedure for the design, installation, preservation and liquidation of geothermal energy wells, approved by the Minister of the Environment of the Republic of Lithuania in 2015. April 3 by order no. D1-273 "On the approval of the description of the procedure for the design, installation and liquidation of geothermal wells" (hereinafter - the Description), is not applicable to the exploration and (or) use of geothermal energy in the depths of the earth, related to geothermal energy or other wells, the construction of which and their primary purpose does not comply with the provisions of clauses 7.2 and 7.3 of the Description.

The list of legal acts establishing the requirements for geological research and use of the depths of the earth can be found on the website of the Lithuanian Geological Agency (link https://lgt.lrv.lt/lt/teisine-informacija/teises-aktai/).

In the valid tax of the Republic of Lithuania for state taxes Annex 2 of the Law on Natural Resources contains tax rates for used geothermal water

TARIFFS FOR WATER AND SOIL TAX

No.	Resources		Tariffs, Eur
1.	Groundwater, except mineral water:	m^3	
	a) supplied by a water supplier for household needs and space heating		0,03
	b) used by legal entities for commercial purposes, bottled		4,29
	c) other groundwater (not specified in points a and b)		0,10
	d) used by natural and legal entities for agricultural activities, except for groundwater used for processing agricultural products and for the sale of food or non-food products made from them		0,03
2.	Mineral water, except mineral water used in medical institutions	m^3	4,29
3.	Mineral water, used in medical institutions	m^3	2,14
4.	Surface water for industry and agriculture	m^3	0,003
5.	Surface water for cooling condensing thermal power plants	m^3	0,0003
6.	Surface water for fisheries	m^3	0,0001
7.	Surface water for hydropower	m^3	0,00001
8.	Surface water for a nuclear power plant	m^3	0,0004
9.	Surface water for LNG import terminal	m^3	0,00003
10.	Primer	m^3	0,26

view of geothermal resource uses in Lithuania and in neighboring countries, their exploited resource characteristics, scope and technology.

12.1 Lithuania

Together with experts from the "Petroleum Geology Investigators" and the Danish Environmental Protection Agency" funding from the Danish Kingdom was prepared the Baltic geothermal energy project, which assessed the possibility of geothermal energy usage in Lithuania, i.e. to use low temperature (35-40ºC) from highly mineralized geothermal water for municipal buildings heating and other purposes. Klaipeda's area is part of the Baltic Basin, occupying the major Baltic Sea as well as the Estonian, Latvian and Lithuanian land areas. The Baltic Basin is bounded by the Fennoscandian Shield in the north and west and by the Tornquist-Tesseyre main tectonic zone in the south. Towards the east the Baltic Basin appears separated from the major Russian Platform area by a series of north-south trending elevated basement features, sometimes referred to as the Latvian-Lithuanian saddle. The main objective of geothermal installations comprises the Lower Devonian D1km (Kemeri) geological section from 963 m MSL to 1100 m MSL formation, also referred to as "the aquifer zone".

In the Baltic Artesian Basin (BAB), studying the concentrations of the inert gas 81Kr and 4He isotopes of underground water in the deep geological layers revealed that the age of the underground water at a depth of 0.5-1.1 km varies from 0.319 to 1.157 million years. Below a depth of 2 km, the age of the underground water on the coast of Lithuania exceeds even 1.3 million years limit. Such old water, dated by the 81Kr/Kr method, was discovered for the first time in the world. Radiokrypton-81, an inert krypton gas dissolved in water, was analyzed using highly sensitive laser equipment with a magneto-optical trap (ATTA - English "Atom Trap Trace Analysis"). Measurements were made at the US Argonne National Laboratory. So far, the oldest one-million-year-old underground water was discovered in the Nubian aquifer in Egypt, and the Guarani layers in Brazil are also dated to be very old - 850 thousand years old water. The article is published in the journal Geochimica et Cosmochimica Acta. More information: (http://dx.doi.org/10.1016/j.gca.2017.01.033).

12.1.1 Klaipeda

12.1.1.1 UŽDAROJI AKCINĖ BENDROVĖ „GEOTERMA”

The geothermal power plant in Klaipeda is the only geothermal power plant in the Baltic States. The heat extracted from the boreholes was used for heating the city of Klaipeda, and the geothermal water - for balneology, aquaculture, road irrigation, and medicine. Due to technical problems and economic reasons, its activities were stopped in 2017, and the devices were preserved. Research and deliberations are currently underway to revive the work of the power plant. In Klaipeda geothermal plant the two wells producers, - 2P (55°41’03”.85 North 21°12’07”.95 East) and 3P (55°40’58”.30 North 21°12’12”.40 East) and two wells injectors, - 1I (55°40’24”.65 North 21°13’18.19 East) and 4I (55°39’41”.46 North 21°13’18”.70 East) were drilled during the end of the Year 1997 till the end of the Year 1998. The Klaipeda Geothermal Demonstration Plant was launched on December 2001. After quite long period due to arising problems with gypsum precipitations the plant was commissioned just in June 2004. The production and injection after commissioning was about 450 m^3/h of geothermal water. This Study provides more detailed information about one of the 4 wells in Klaipeda, details can be found in APPEDIX 2.

12.1.1.2 Holiday Park

ATOSTOGŲ PARKAS

"Holiday Park" is the largest recreation and wellness complex in Western Lithuania, with 16 swimming pools and 8 saunas for your relaxation and health. The complex is located on the outskirts of Palanga, in Zibininkai. It is a nature refuge in a strategically excellent location, 6 km from the Baltic Sea and the resort of Palanga, 30 km from the port city of Klaipeda. The complex invites to enjoy water entertainment, unique sauna programs, spa, health and treatment procedures, stay in a hotel or in log villas surrounded by a forest, spend time actively on padel and tennis courts, etc. "Holiday Park" was the first in Lithuania to start using mineral geothermal water for health purposes, so only in this complex the procedure "Mineralų jura" in the only certified mineral geothermal water pool in Lithuania, which is combined with the applications of mud with healing properties - sapropel. "Holiday Park" uses up to 20m3 of geothermal water per month for the needs of its wellness complex, which is extracted from the Vilkyciai - 3 well, installed in 1970, the depth of the well is 2154.2 m. Well ID Nr.10880. The address of the borehole is Priekule sen., Vencku village, Klaipeda district municipality. The chemical analysis of the borehole water allows us to make a preliminary conclusion that it is suitable for use in aquaculture, balneology, health care.

More detailed information about gethermal well Vilkyčiai 3 can be found in APPEDIX 2

12.1.1.3 Gradiali

Nestled next to the pine forest in the quiet part of Palanga resort, Gradiali Medical SPA & Wellness is just 500 meters from the sandy Baltic Sea beach. Gradiali Medical SPA & Wellness offers a peaceful and exclusive recreation for everyone. Guests at Gradiali Medical SPA & Wellness are welcome to enjoy a variety of medical procedures, massages, herbal bubble baths, underwater massages, and other procedures. Many treatments use geothermal water from a nearby geothermal well. The distance from Gradiali Medical SPA & Wellness to the center of Palanga and the local bus station is 3 km. The Palanga Airport is 4 km away.

More detailed information about Gradiali gethermal well can be found in APPEDIX 2

12.1.1.4 Vydmantai

The deepest geothermal wells in Lithuania are Vydmantai 1 (2564m), and Vydmantai 2 (2150m,).

Summary of the report of investigation of the geothermal wells (execuation date 2023.11.08).

can be found in APPENDIX 2

12.2 Fish farming and spirulina cultivation

According to Lund, Freeston and Boyd (2011), 22 countries use geothermal resources in fish farming, led by the United States of America, China, Iceland, Italy, and Israel. The most common species farmed in this way are tilapia, salmon, and trout, but tropical fish, lobsters, shrimp, prawns and alligators are also being farmed. In 2010, the total energy used in fish farming was 11 521 TJ/year, equivalent to 47,600 tonnes of annual production (Lund, Freeston and Boyd, 2011).

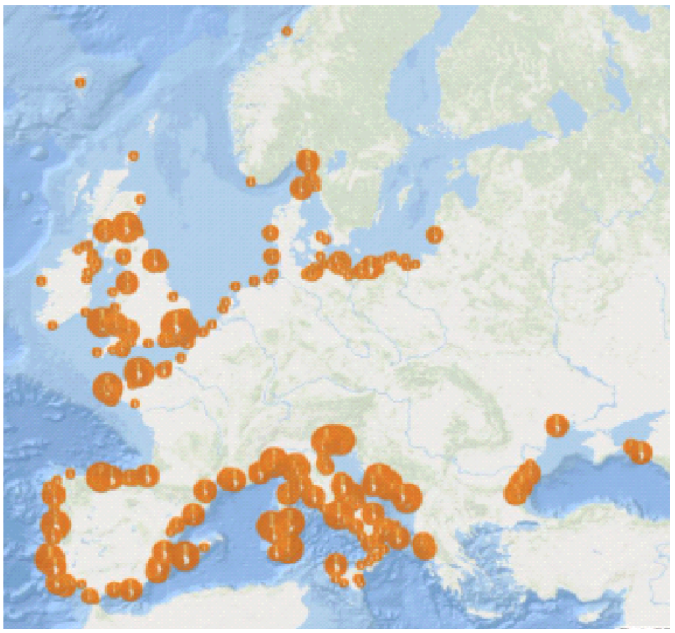

12.3 Geothermal applications in Poland

Geothermal energy in Poland is utilized across various sectors, highlighting its versatility and growing importance. Key applications include district heating plants, health resorts, and recreation centers, which benefit from direct heat use, see **Figure 107**. Additionally, geothermal energy supports specialized industries like wood drying, fish farming, and individual heating systems, reflecting its integration into both large-scale and niche operations. These advancements underline Poland's commitment to leveraging geothermal resources for sustainable energy solutions (Kępińska & Hajto, 2023, WGC2023).

Most prospective areas (heat, EGS,ORC/ binary, etc.) in Poland

Orange – heating Blue – EGS

Green – binary systems

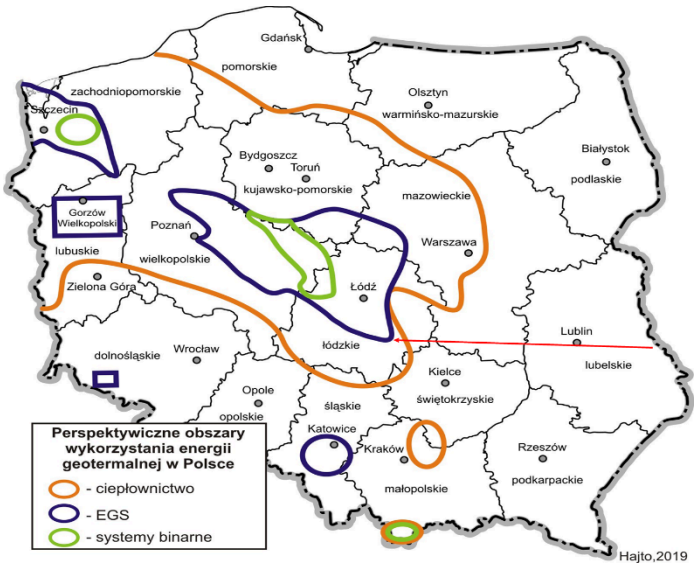

- Geothermal waters T>50°C at depths
  2 km can be found within 40% of Polish area
- These waters are suitable for heating

Figure 107: *Figure showing map of Geothermal application in Poland.*

- **Balneotherapy, bathing:**
  - 12 health resorts, 16 bathing centres
- **Other single uses:**
  - Atlantic salmon farm; Wood drying; Heating up of a football pitch, parking; Extraction of bathing salts, CO_2; cosmetics' production; Food processing; Drinking water
- **Geothermal water parameters:**
  - T = 20–92°C, M = 0.4–150 g/L, Q = several – 550 m^3/h
- **Geothermal heat pumps, GSHPs:** ca. 80 200 units, > 900 MW, > 4 600 TJ

- Total installed geothermal capacity: ~ 1 125 MW
  - (225 MW deep-geo + 900 MW GSHPs)
- **Total heat sales / production: ~ 6 047 TJ**
  - (>1 447 TJ deep-geo, > 4 600 TJ GSHPs)

Four geothermal provinces are defined in Poland: the Polish Lowlands, the Carpathians, the Carpathian Foredeep and the Sudetes (**Figure 108**) Generally, they are natural sedimentary-structural basins filled with geothermal waters with a relatively high temperature range, namely, from 20°C to about 90°C (even up to 100°C) at the depth between 1-4km. Generally, the water flow rates (from a single well) vary from several to around 150 l/s, whereas the total dissolved solids (TDS) of thermal waters differ from 0.4 g/l to as many as 300 g/l, depending on the province.

Figure 108. *Geothermal energy provinces and installations in Poland*

Jolanta Gdaniec and Tomasz Karapuda initiated drilling to as deep as 1,224 m to harvest geothermal energy from the Jurassic sandstone aquifer (well Trzęsacz GT-1). Initially, the well was planned as a geothermal SPA facility. An analogous water park powered by geothermal sources (water temperature about 36°C) operates in the German border town Ahlbeck–3 (Germany) km from Świnoujście (Poland).

Within a year, however, the couple diverted focus to a re-circulating aquaculture system (RAS) to bree the Atlantic salmon indoors, avoiding the open-ocean marine environments where conventional producers have encountered disease, sea lice and conflicts with environmental groups. After securing equipment, a contractor, a plan for the facility as well as bank and EU funding, Gdaniec and Karapuda became president and vice president, respectively, at Jurassic Salmon, a company name inspired by the name of the Lower Jurrasic aquifer.

Salmon is one of the top three species produced by European aquaculture facilities, according to the European Commission, behind mussels and trout. "Jurassic Salmon" 2.2-acre RAS farm is now one of three indoor facilities in the world producing salmon from egg to harvest size. The venture also represents a step forward for Poland, which is not among the top aquaculture producers in the EU, like France, the United Kingdom, Greece, Italy, and Spain.

Officially opened in June 2015, "Jurassic Salmon" has wasted little time in achieving local accolades and important international marketplace benchmarks (**Figure 109**, **Figure 110**). The company received Aquaculture Stewardship Council (ASC) certification in 2015 and granted two "Golden Fish" awards: "*Złotej Rybki*" in Poland, for the company of the year and the investment of the year.

Figure 109. *Jurassic Salmon in Karnice, Poland.*

Figure 110. *Salmon breeding tanks (5m diameter) – post-smolt cycle phase on the Jurassic Salmon farm. Picture of the author.*

The facility is also certified by International Featured Standards (IFS) and the British Retail Consortium (BRC); since the company operates a small processing facility on site, as the fish must be killed and gutted before being sold on.

The process begins with importing batches of 80,000 to 120,000 salmon eggs four times a year, from hatcheries in Norway and Iceland. The adult salmon weighs 5-kilogram.

The geothermal water that the fish are farmed in is treated in a denitrification facility before being released to the environment through a controlled process. Nitrogen and phosphorus compounds are removed from the water, which is then reused in the temperature regulation of the facility before the release to open waters. Fish feces are removed from the water and passed on to an agricultural facility to be used as a fertilizer.

Output at "Jurassic Salmon" is 1,000 metric tons of Atlantic salmon per year (2017). The product is sold to restaurants and distributors who sell within Poland and the rest of the EU. Kowalski is proud high-end restaurants feature Jurassic Salmon on their menus, but he explained that they are now stuck in an awkward phase of growth. The production cycle lasts 20–22 months, starting from the spawning phase of eggs (imported by air from Norway or Iceland) through the growth of fry, smolt grow up to the rearing phase of adults reaching a commercial weight of 5–6 kg.

The flow rate of the well Trzęsacz GT-1 (depth of 1,224 m) is about 180 m^3/h and a working temperature of 25.4°C, salinity of the water of the Lower Jurassic aquifer is rather low 13.5 g/l.

The Jurassic Salmon farm has confirmed the wider use of geothermal water than just for energy needs. After the tests, the adapted and treated Jurassic water turned out to be an excellent environment for salmon farming.

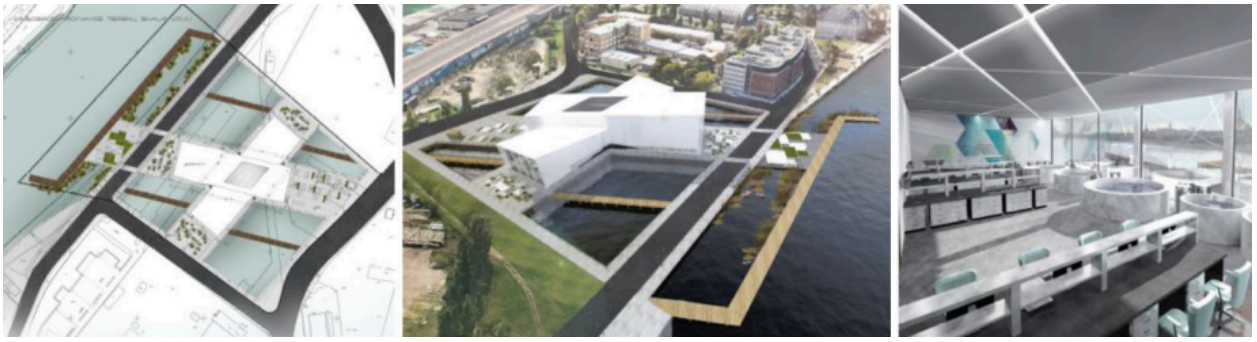

Figure 111. *Project of the Research Centre – Aquaculture Lab located in the postindustrial city fabric of Szczecin on the Odra River bank (Muszalska A., Świątek L. ZUT Szczecin, 2018).*

In comparison with surface water resources, used at traditional farms, geothermal water, due to the hermeticity of the deep underground deposit, is free from chemical pollution or dangerous to fish parasites. RAS systems used on the farm have become a kind of filter for mineralized geothermal waters when they are reintroduced into the environment.

Figure 112*: Janowo: salmon farm, since 2015, please see https://www.portalspozywczy.pl/mieso/wiadomosci/jurassic-salmon-pierwsza-geotermalna-hodowla-lososia-w-polsce- szuka-inwestora,163037.html*

GeoDHs in Poland vs European background, 2022*

** acc. to 2022 EGEC Geothermal Market Report Key Findings (EGEC, 2023)*

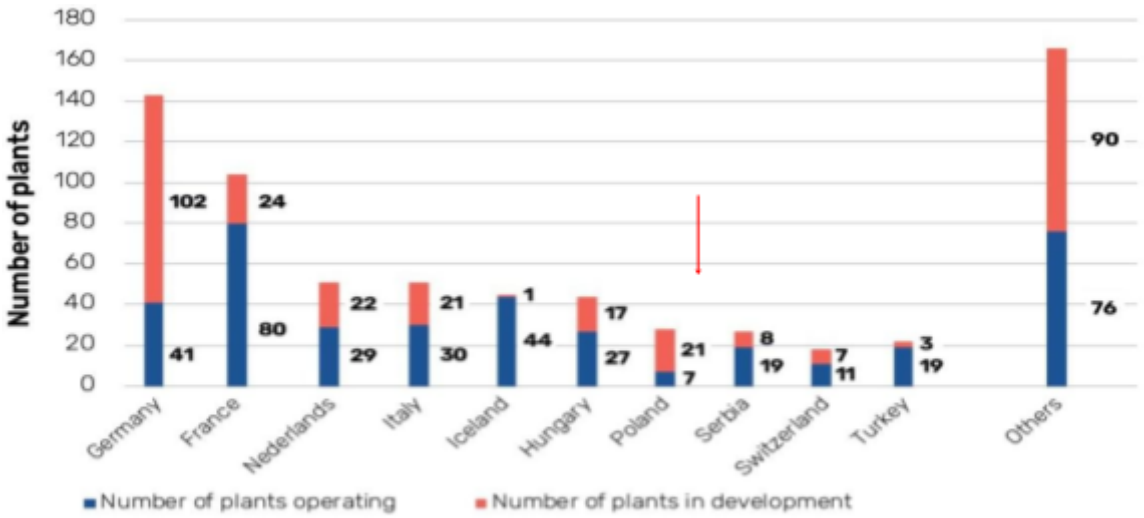

***Figure SEQ Figure * ARABIC 113**: GeoDHs in Poland Vs. EU*

12.4 Main areas of further geothermal uses in Poland

Geothermal energy offers significant opportunities for district heating, serving as a primary application area by connecting to many existing district systems. This integration enhances local energy security, stabilizes heat prices, and contributes to CO_2 emission reductions. Beyond district heating, geothermal energy supports diverse and prospective uses such as agriculture, food processing, aquaculture (fish farming), industrial applications, balneotherapy, recreation, mineral and salt recovery, and innovative fields like biotechnology. It can also be employed in multi-purpose or "cascaded" systems to maximize efficiency. Additional applications include shallow geothermal systems using heat pumps, deep borehole heat exchangers, and underground energy storage solutions such as UTES (Underground Thermal Energy Storage), ATES (Aquifer Thermal Energy Storage), and BTES (Borehole Thermal Energy Storage), which exemplify geothermal's versatility in modern energy solutions.

12.5 Germany

Number of plants (e.g. borehole heat exchanger, collectors in combination with heat pumps): ca. 470.000. Installed capacity: ca. 4.700 MW. Newly installed plants, incl. Ground water heat pumps: ca. 26.000. Supplied heat: ca. 10 TWh/a

The three most promising geothermal areas in Germany for a geothermal application are shown on the map: the North German basin, the Rhine Valley in the southwest, and the Molasse basin in the south (**Figure 114**). No efficient analysis can be made for the central part of Germany, where geothermal use would also be interesting, as there is currently almost no data available for this area (Agemar et al., 2012). In the North German basin, in the areas of Parchim, Perleberg, or Anklam, the necessary temperature of 100oC is reached at around 2200 m. Prospective sites and depths indicated in northeast Germany: Anklam – 2270 m, Perleberg – 2200 m, Parchim – 2130 m. (Figure 114). All other analyzed places show similar results in the North German basin with necessary depths between 2200 m and 2700 m. Here, the temperature of 150oC is reached at around 3900-4200 m.

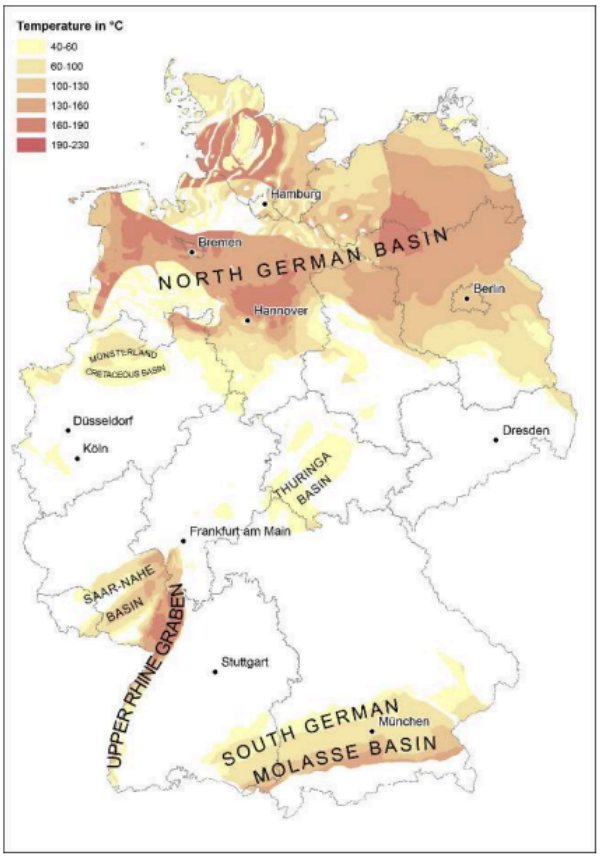

Figure 114: *Regions with hydrothermal resources in Germany and associated temperature ranges (map adapted from Suchi et al., 2014)*

Geothermal heat is utilised in about 190 larger installations using hydrothermal resources. The commercial project development to date focuses on hydrothermal resources in sedimentary systems. The most important geologic systems hosting proven geothermal reservoirs in a depth greater than 1000 m in Germany are the North German Basin, the South German Molasse Basin, and the Upper Rhine Graben (Figure 115). Most of the wells exploit the warm water at the depth of 20-50oC for SPA, most in the southern part of the country. In north Germany, few heat district plants operate in the east (tapping Mesozoic geothermal aquifers) and one ATES system (diamond symbol).

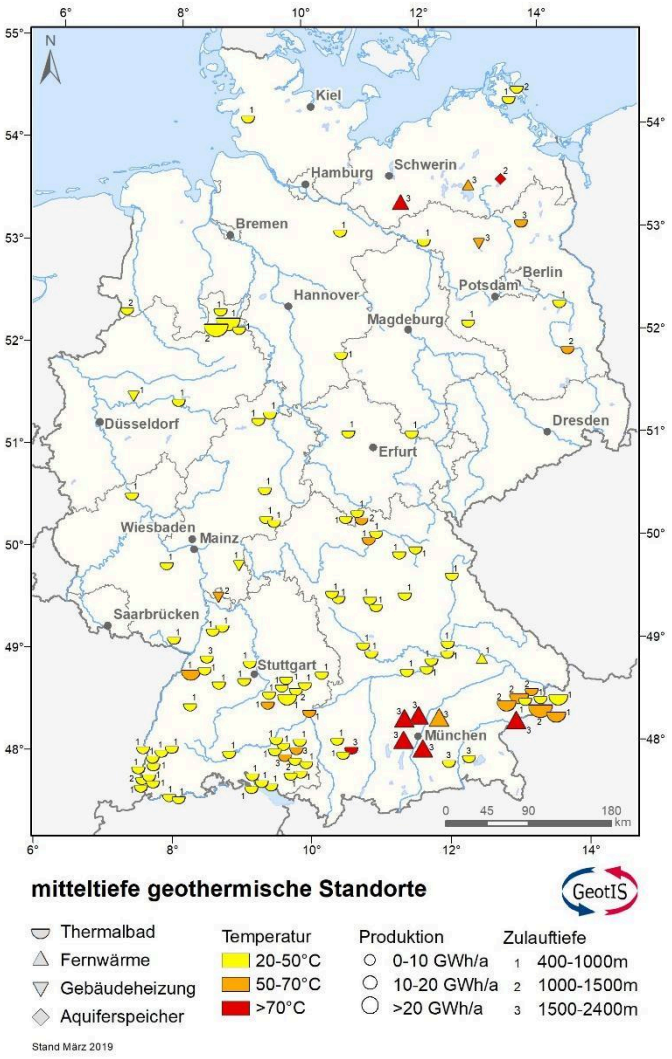

Figure 115: *Depth of the geothermal boreholes in Germany and productivity. The map shows medium-deep geothermal locations with type of use, temperature, production, and depth of wells. The red colour shows production temperatures >70°C (Agemar and Tribbensee, 2019). Please notice the scale of symbols.*

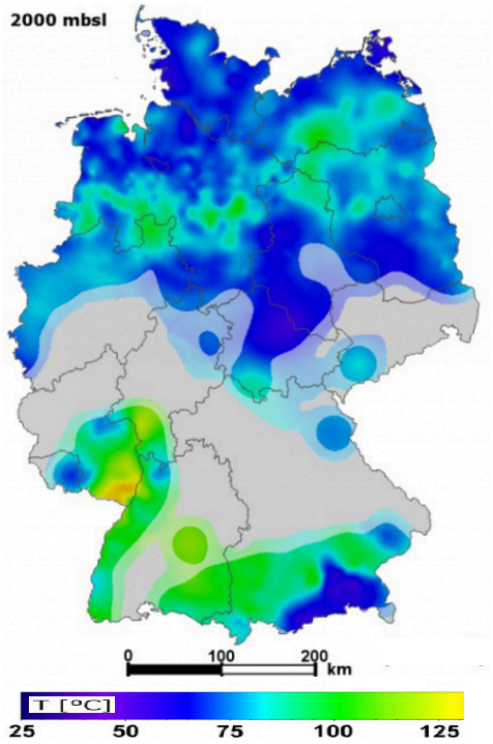

Subsurface temperature distribution at the depth of 2000 m.mbsl. (Agemar et al., 2014).

The similar map shows the temperature distribution at the base of the sedimentary basins in Germany (Figure 3). Three district heating plants we installed in northeast Germany (please note 2 similar DH plants located in Poland). 6 SPA (+2 in Rügen Island) facilities are shown on the map and one geothermal aquifer storage.

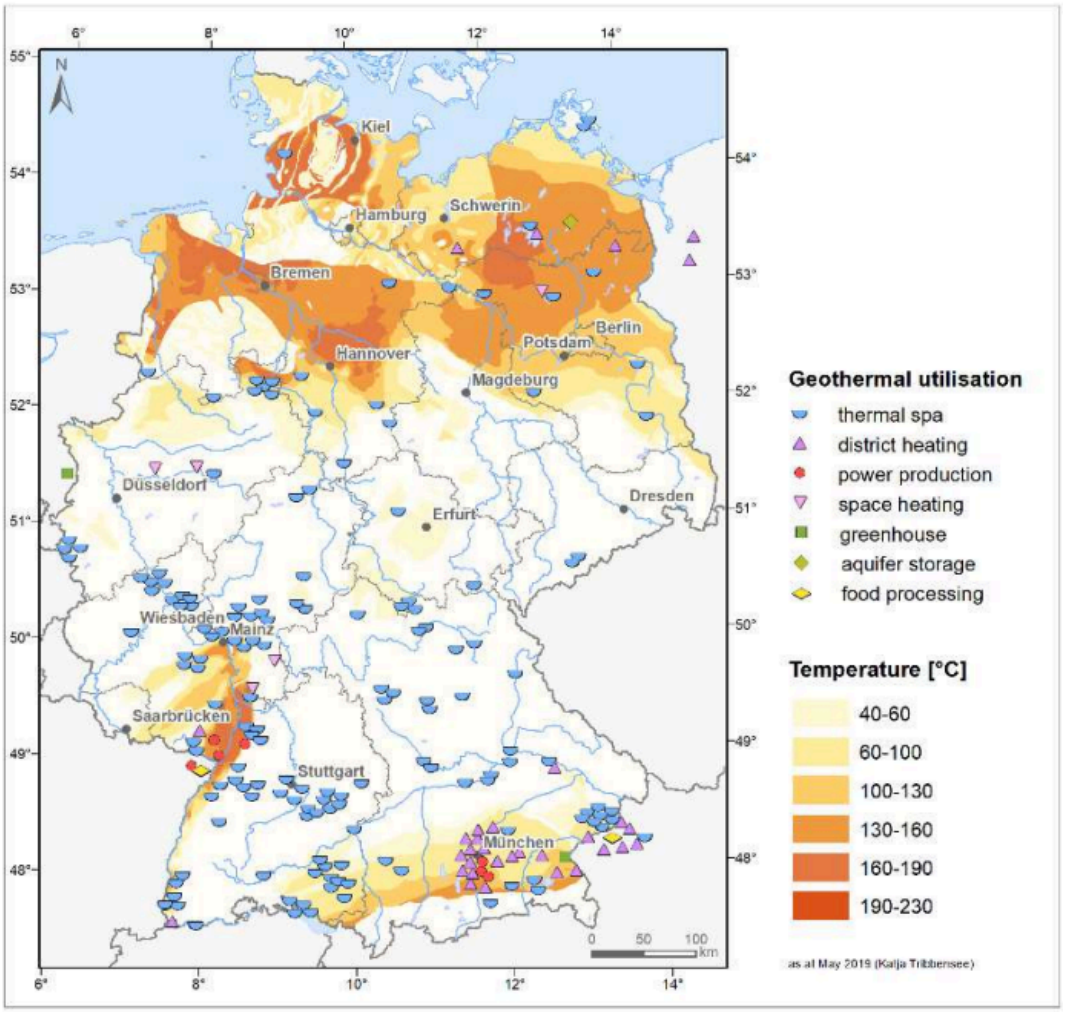

Figure 116: *Sites of deep geothermal utilization in Germany and neighboring countries. The background colors represent predicted temperature ranges of the respectively deepest identified geothermal resources in sedimentary or volcanic rocks (map generated in GeotIS, 2019).*

The thickness of the sedimentary cover ranges from 2,000 m east of Rügen Island (oil exploration well G-14-1 in the Baltic Sea) to 12,000 m in West Pomerania (**Figure 116, Figure 117**). The crystalline basement is overlain by strongly folded Cambrian-Silurian sedimentary rocks representing the East Avalonia microcontinent. The North German Basin was established in the Devonian time and was strongly affected by Rot Rotliegend clastic sedimentation and igneous activity. The Zechstein carbonates and evaporites accumulated in the northern part of Germany and later induced dramatic salt diapirism. The Mesozoic deposits are the most prospective geothermal aquifers in north Germany (marked in yellow on the profile). The thickness reaches c. 2 km.

The Mesozoic deposits of the North German Basin are made up of sandstones, clay and carbonates, with evaporite intercalations. Six **Cretaceous**, **Jurassic** and **Triassic** sandstone aquifers are of interest for direct use of geothermal energy: Valendis-Sandstein, Bentheimer Sandstein, Aalen, Lias and Rhät, Schilfsandstein, and Buntsandstein. Because of the salt tectonics, great variations of depth and thickness, exceeding locally 1000 m, occur along short distances. Therefore, the temperature and energy content of the geothermal resources vary strongly on a regional scale. Table 21 shows the resources of these aquifers.

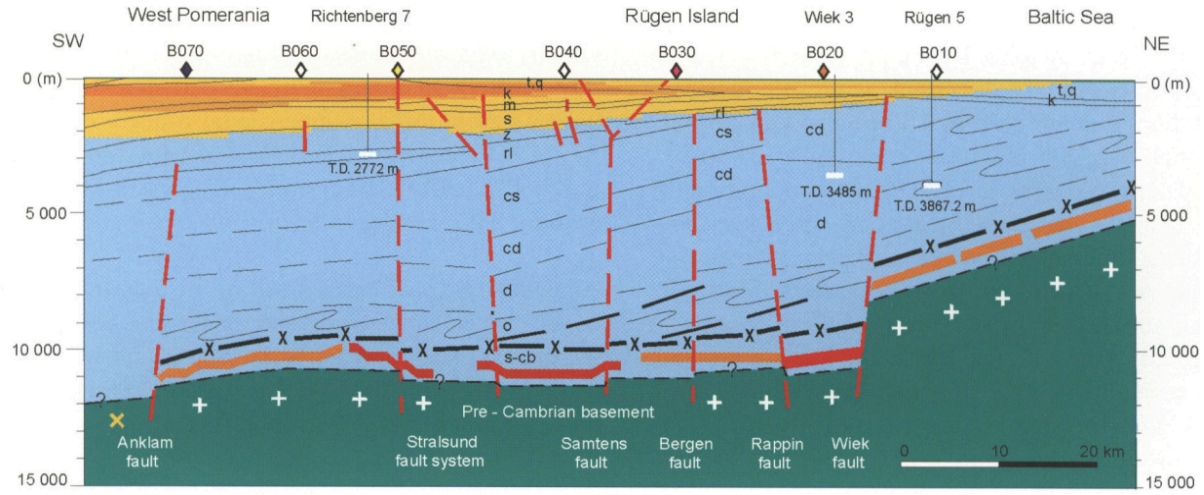

Figure 117: *The geological section between West Pomerania and the Baltic Sea. The interpretation of the deep magnetotelluric data. The excellent conductor correlates with the Cambro-Ordovician 'Scandinavian Alum shale', encountered in Baltic offshore well G14 (not indicated on the profile). The main stratigraphic indexes are shown on the profile. The crystalline basement is highlighted in green. Mesozoic succession is highlighted in yellow.*

Stratigraphical subdivision:

t, q	Tertiary, Quaternary
cr	Cretaceous
j	Jurassic
k	Keuper
m	Muschelkalk
s	Bunter
z	Zechstein
ru	Upper Rotliegend
rl	Lower Rotliegend
p	Permian
c	Carboniferous
cs	Upper Carboniferous
cd	Lower Carboniferous
pc	pre-Carboniferous
d	Devonian
o	Ordovician
s-cb	Silurian until Cambrian

Table 21: *Resources of North German Basin (Schellschmidt et al. 2002):*

Reg.	Aquifer	A km²	T_t °C	Resources 10^{18} J	GJ/m²
A	Valendis Sst.	143	50	0.11	0.79
	Bentheimer Sst.	361	54	0.28	0.78
B	Aalen	66250	43	80.83	1.22
	Lias and Rhät	68125	38	102.87	1.51
	Schilfsandstein	63125	48	37.88	0.60
	Buntsandstein	67500	49	70.88	1.05

**geothermal areas (km^2). A = Western North German Basin, B = Eastern North German Basin*

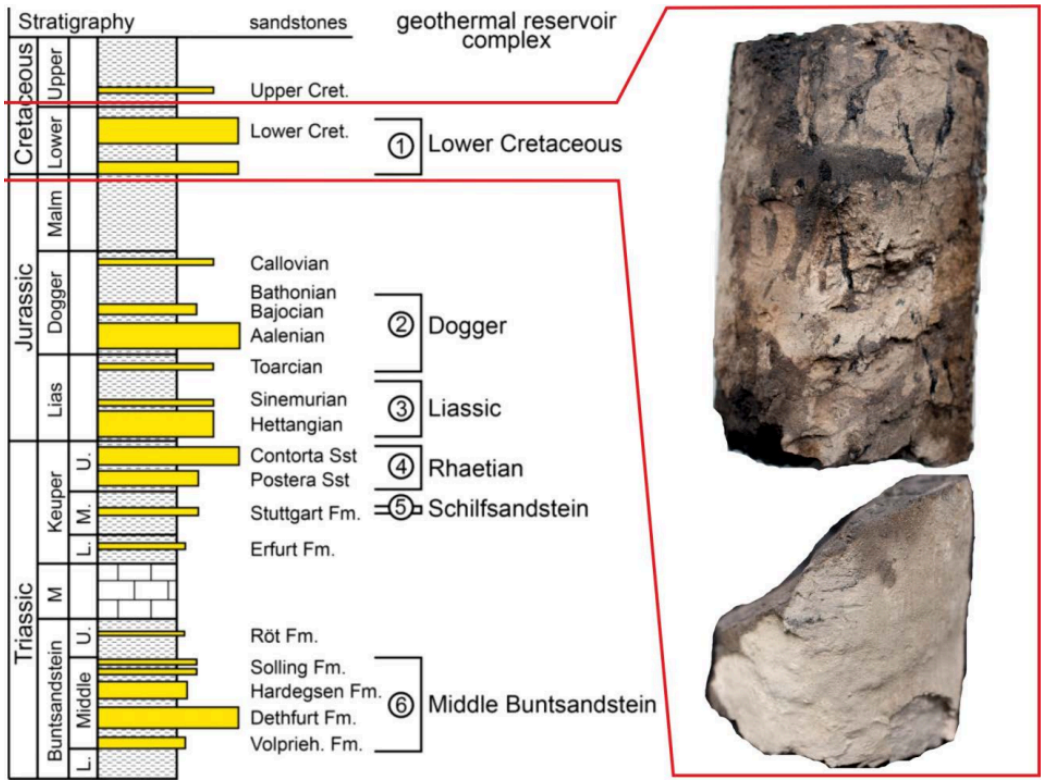

Figure 118: *Mesozoic hydrothermal reservoirs in the North German Basin. Core material from well Darßer Ort, Lower Cretaceous geothermal sandstone (Western Pomerania Lagoon, National Park; 20 km west of Rügen Island).*

Six sandstone geothermal complexes are defined in the Mesozoic succession (**Figure 118**). For the sake of comparison, the shallow lower Cretaceous reservoir of the fluvio-deltaic channel belt is prospective (not used presently). The Lower Cretaceous deposits are dominated by (I) Berriasian fluvio-deltaic strata from an upper and lower delta plain: (a) levee/crevasse-splays complex according to the channel belt, (b) distal crevasse splays and proximal sheetsands, (c) interdistributary bay sheet sands, paralic swamps, (d) delta plain sheetsands and delta front successions and (II) Hauterivian to Barremian shallow marine shoreface sands (Figure 119). So far, these sandstone reservoirs seem to be the most promising ones within the Lower Cretaceous successions of the northeastern North German Basin. Calculated temperatures range from 23°C in 400 m to 43°C in 900 m depth. The potential Lower Cretaceous reservoirs are situated in depths of 160 m to 1000 m. Higher depths up to 1900 m and, therefore, higher temperatures of up to 74 °C are known from salt plug rim synclines as drilled, for example, in well Gt Pritzwalk 2. Porosity values measured in Lower Cretaceous samples show a mean porosity of 23 %. Relevant permeability values range from 100 mD up to 7000 mD (**Figure 120**).

There are no geothermal fish farming initiatives is registered in Germany. However, Neomar has developed the shrimp farm for feed and is seeing improvement in grow-out rates.

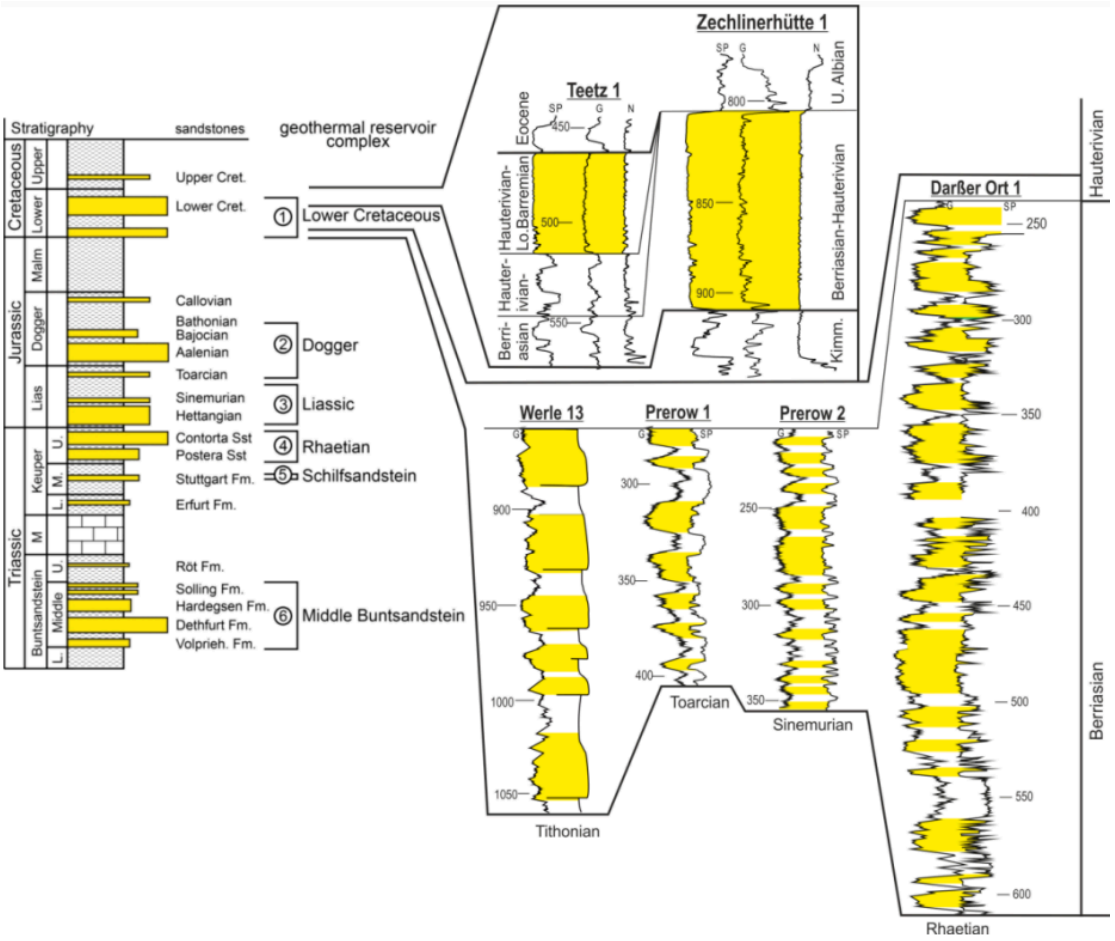

Figure 119: *Left side – Mesozoic geothermal reservoir complexes. Right side – potential Lower Cretaceous geothermal reservoir complexes. Berriasian to Barremian sandstones in the deltaic sandstones in Western Pomerania (bottom) (Franke, 2023)*

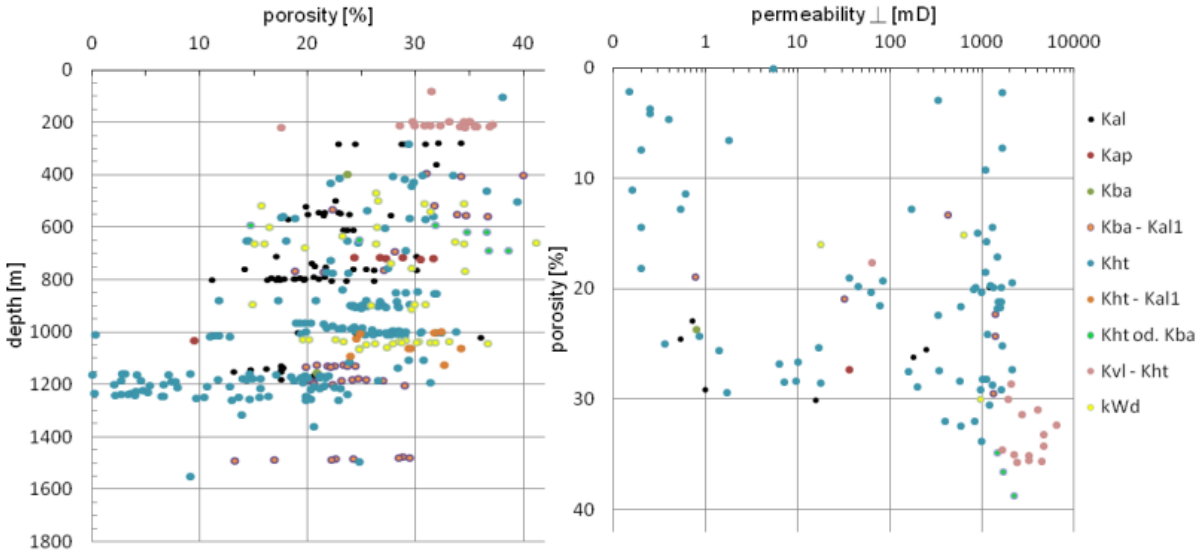

Figure 120: *Left: measured porosity data from Lower Cretaceous lithologies in relation to sample depth (n=380). Right: the relationship between porosity and permeability (n=161). Kal – Albian; Kap – Aptian; Kba – Barremian; Kht – Hauterivian; Kvl – Valanginian; KWd – Wealden-type (Berriasian) (Franke, 2023).*

Figure 121: *Photo. Neomar's shrimp production site near the port of Kiel (https://thefishsite.com/articles/germanys-clearwater-shrimp-ras-champion-oceanloop)*

12.6 Latvia

The fish farm was established in Soviet times near Dobele. No updated information is available.

12.7 Others

The Lithuanian Geothermal Association has no knowledge about the use of the potential of shallow geothermal resources in aquaculture application in Baltic Sea region neighboring countries (Poland, Germany, Latvia, Estonia).

13 Evaluation of suitable technologies for heating water in closed aquaculture systems

To evaluate the three most suitable technologies for heating the water in closed aquaculture systems up to 30°C using geothermal resources, we should consider factors such as the efficiency of heat transfer, the sustainability of the geothermal resource, and the scalability to different volumes of water (1,000 to 10,000 m³) with 2% water renewal. Below are three potential technologies, each evaluated based on these criteria:

13.1 Direct Use of Geothermal Water in Heat Exchangers

Technology Overview: This system involves using geothermal water directly in a heat exchanger to transfer heat to the aquaculture water without mixing the two fluids. The geothermal water's heat is transferred to a secondary loop that circulates through the aquaculture system, maintaining the desired temperature.

Efficiency: High, as heat exchangers can achieve near-complete energy transfer, especially with high-temperature geothermal sources.

Suitability for Volume: This system is highly scalable and can be adjusted to maintain temperature in volumes ranging from 1,000 to 10,000 m³ with minimal heat loss.

Water Renewal: The system can accommodate 2% water renewal without significant heat loss due to the efficient design of heat exchangers.

Advantages

- ❑ High efficiency and precise temperature control.
- ❑ Scalable to large volumes.
- ❑ No direct contact between geothermal and aquaculture water, avoiding contamination risks.

Disadvantages

- ❑ Initial setup costs can be high.
- ❑ Requires geothermal sources with sufficient temperature to achieve the desired heating.

13.2 Geothermal Heat Pumps

Technology Overview: Geothermal heat pumps use the stable temperatures of shallow geothermal resources to heat water. The system consists of ground loops that absorb geothermal heat, which is then transferred to a heat pump that increases the temperature to the desired level before circulating it through the aquaculture system.

Efficiency: Moderate to high, depending on the geothermal gradient and the efficiency of the heat pump system.

Suitability for Volume: This system is also scalable, although efficiency may decrease slightly as volume increases, requiring more extensive ground loop systems.

Water Renewal: Geothermal heat pumps can maintain temperatures with 2% water renewal, but the system might need to be calibrated to account for the energy loss from the renewal.

Advantages:

- ❑ Works well with lower-temperature geothermal sources.
- ❑ Can be used in regions where deep geothermal resources are not available.
- ❑ Lower operational costs once installed.

Disadvantages:

- Moderate efficiency compared to direct use systems.
- Requires a large area for ground loop installation, which might be a limitation.

13.3 Hybrid Geothermal-Solar Heating System

Technology Overview: This system combines geothermal energy with solar thermal collectors to achieve the desired water temperature. Geothermal energy provides a consistent baseline temperature, while solar collectors supply additional heat during peak sunlight hours.

Efficiency: High, due to the dual energy input, especially in regions with strong solar resources.

Suitability for Volume: Suitable for large volumes, as the system can be scaled by increasing the number of solar collectors and adjusting the geothermal input.

Water Renewal: This system can maintain temperatures even with 2% water renewal, thanks to the supplementary heat from solar collectors.

Advantage:

- Combines renewable energy sources, reducing reliance on any single resource.
- Highly efficient and can reduce operational costs with sufficient sunlight.
- Provides more flexibility in temperature management.

Disadvantages:

- Higher complexity and initial investment.
- Efficiency depends on solar availability, which may fluctuate seasonally.

13.4 Summary

- Direct Use of Geothermal Water in Heat Exchangers is the most efficient and reliable for large-scale applications, offering precise temperature control and scalability.
- Geothermal Heat Pumps provide a versatile option for areas with lower geothermal temperatures, with moderate efficiency and lower operational costs.
- Hybrid Geothermal-Solar Heating Systems offer the highest efficiency in regions with strong solar potential, combining two renewable energy sources for optimal performance.

Each of these technologies can maintain the required water temperature of up to 30°C in closed aquaculture systems of 1,000 to 10,000 m^3 volume, with 2% water renewal. The choice depends on the specific geothermal resources available, the geographic location, and the project's scale and budget.

13.5 Computations for heat load calculation

Given statement: Consider a closed aquaculture with volumes of 1000 m^3 and 10,000 m^3 as shown in the process diagram in the **Figure 122**. The water inlet into the aquaculture is around 15 C and outlet temperature of water is 35 C to maintain the aquaculture temperature of 30 C

including the heat loss to the surroundings. This water is regenerated with the 2% renewable volumes (20 m^3 to 2000 m^3) to maintain the oxygen in the aquaculture for farming.

To determine: Three most possible technologies with heat load calculations.

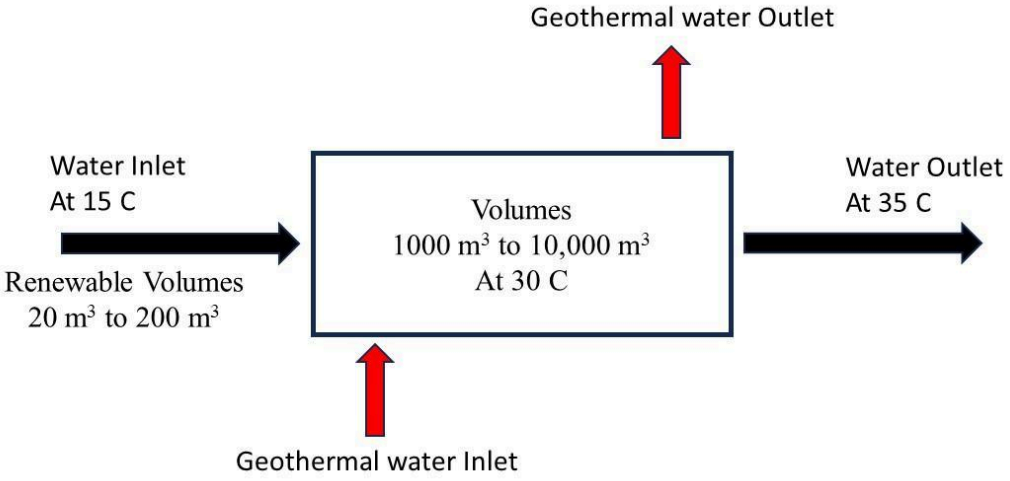

Figure 122: *Closed aquaculture for farming.*

Proofing Statement: The three most promising technologies for closed aquaculture framing are use of heat pumps, geothermal heat exchangers and direct use of geothermal heating as described in the section 1.3.2 respectively. Using these technologies the heat stored below the surface of Earth can be utilized for fish or shrimp farming in the closed aquaculture as described in the Lindal diagram in the figure 1.2.2-11. To maintain the aquaculture system, it is necessary to maintain the heat load requirements as described below.

13.6 Heat Load Calculation:

The heat load required to maintain the water temperature, considering the volume of water low case of 1000 m^3 and high case of 10000 m^3 and 2% daily water renewal rate with low case of 20 m^3 and high case 200 m^3.

$$Q = V \times \Delta T \times Cp \times \rho$$

Where:

Q = Heat load (KW)

V = Volume of water (m^3)

ΔT = Temperature difference (desired temperature - inlet temperature)

Cp = Specific heat capacity of water (4.186 KJ/Kg °C)

ρ = Density of water (Taken as 1000 Kg/ m^3, but it depends on the nature of brine used for aquaculture)

Assuming an inlet temperature of 15°C and a desired outlet temperature of 35°C:

Low case: For 1000 m^3

$Q_1 = 1000 \times (35 - 15) \times 4.186 \times 1000$

= 83,720,000 KJ/day

Q_l = 83,720,000 ÷ 86, 400

Q_l = 969 KW

High case: For 10,000 m³

Q_h = 9690 KW

To keep the system aerated 2% water renewable is considered so there is an addition of fresh water which also consumes the heat for warming up.

Low case: $Q_{rl} = 0.02 \times 1000 \times (35-15) \times 4.186 \times 1000 \div 86{,}400 = 19$ KW

High case: $Q_{rh} = 0.02 \times 10000 \times (35-15) \times 4.186 \times 1000 \div 86{,}400 = 194$ KW

The total head load can be determined as

Total heat load: Low Case: $Q = Q_l + Q_{rl} = 969 + 19 = 988$ KW.

Total heat load: High Case: $Q = Q_h + Q_{rh} = 9690 + 194 = 9884$ KW.

The heat load analysis for closed aquaculture systems highlights significant energy requirements ranging from 988 KW for smaller systems (1000 m³) to 9884 KW for larger systems (10,000 m³), driven by maintaining optimal water temperatures and warming daily water renewals. To meet these demands sustainably, renewable energy technologies such as heat pumps, geothermal heat exchangers, and direct geothermal heating are identified as the most promising solutions. These technologies utilize renewable heat sources efficiently, with direct geothermal heating and large-scale exchangers being particularly suitable for larger operations. Implementing such technologies not only ensures energy-efficient and cost-effective operation but also supports environmentally sustainable aquaculture practices, aligning with global sustainability goals.

13.7 Evaluation of economic, technical aspects of 30 ppt, 100 ppt and 200 ppt salinity extraction

Salinity extraction involves a multifunctional interaction between economic and technical considerations. The extraction of water at lower salinities is achievable both economically and technically with existing technologies, while the extraction at higher salinities presents substantial challenges. These challenges necessitate the use of advanced materials, higher energy consumption, and more sophisticated effluent management strategies. The economic feasibility of such high-salinity extraction projects often hinges on factors such as the availability of subsidies, the market value of the extracted water, and the practicality of managing the resultant brine effluent.

The economic aspect includes the following components.

Capital Investment: Capital investment varies with respect to the amount of salinity, particularly lower salinity (30 ppt) has less corrosive nature of the feedwater, leading to reduced equipment wear and lower material costs. The technology used is often similar to conventional desalination but requires modifications to handle slightly higher salinities than seawater. The investment cost rises due to the need for more robust materials to handle higher salinity (100 ppt and 200 ppt) due to the extreme corrosiveness of the feedwater. Thus, establishing desalination plants,

particularly for the treatment of high-salinity waters (e.g., 100 ppt or 200 ppt), necessitates substantial initial investments. These costs encompass the procurement of specialized equipment, including high-pressure pumps and corrosion-resistant materials.

Operating Cost: Energy costs rise with salinity levels due to the increased operating pressure and the need for more energy-intensive technologies. For instance, at 100 ppt & 200 ppt, energy costs can become a dominant factor in overall operating expenses. Furthermore, higher salinity increases wear and tear on equipment, leading to higher maintenance costs and potential downtime. So, specialized materials, frequent servicing and schedule maintenance are required to prevent corrosion and scaling.

The technical aspect includes the following components.

Technology Performance: The technology consideration plays a vital role for highly saline water desalination process.

1. 30 ppt: This salinity is similar to seawater desalination, with moderate energy consumption (~3-5 KWh/m^3). The performance is relatively high, with standard RO systems achieving 40-50% recovery rates. Thus, most effective for 30 ppt but less efficient at 100 ppt and nearly impractical at 200 ppt without significant energy inputs and specialized equipment.
2. 100 ppt: Operating costs increase due to higher energy requirements (up to 8-10 KWh/m^3) and the need for specialized membranes that can handle higher osmotic pressures. Recovery rates drop to 20-30%. Hence for this salinity Electrodialysis (ED) and Thermal Desalination is suitable for medium salinity but becomes energy-intensive at higher concentrations.
3. 200 ppt: Very high operating costs due to the need for even more energy-intensive processes (up to 15 KWh/m^3 or more). Recovery rates are low (~10-20%), and maintenance costs rise due to the harsh operating conditions. Hence, an emerging technology like Membrane Distillation (MD) and Forward Osmosis (FO) can be more effective that can handle very high salinity levels, potentially up to 200 ppt. This technology is still in the developmental stages and not widely commercialized that can be more cost and energy intensive.

Technology Improvement: Let consider the existing wells are used for handling 30 ppt saline water. Thus, retrofitting the existing wells requires assessing the salinity of the brine and the ability of existing infrastructure to handle higher salinity without excessive wear or reduced performance. Wells designed for lower salinity (e.g., 30 ppt) may require significant upgrades to materials and technologies to extract higher salinity brines.

The disposal of produced water is a challenging aspect. Therefore, effluent management is a key consideration for the water disposal management. The effluent management includes.

Effluent Handling: The effluent salinity is a key parameter to solve the disposal problems.

1. 30 ppt: The disposal problem of 30 ppt brine can be managed with standard desalination practices, typically involving dilution or deep well injection, though environmental regulations must be carefully considered.
2. 100 ppt: Effluent management becomes more challenging due to the higher concentration of salts. Options include enhanced dilution, crystallization, or the use of evaporation ponds, though these methods can be costly and land intensive.
3. 200 ppt: The most challenging due to the high concentration of toxic salts and chemicals. Zero liquid discharge (ZLD) systems are often required, which involve the complete

evaporation of water to leave behind solid salts. This is expensive and energy-intensive but necessary to prevent environmental contamination.

Environmental Impact: The higher the salinity, the greater the potential environmental impact, particularly regarding marine and soil contamination. Hence proper selection of effluent disposal methods and proper effluent management systems must be carefully designed to avoid adverse effects on local ecosystems.

With respect to the above aspects, the heat requirement is also increased based on the brine salinity. The **Table 22** shows the heat calculations necessary for the designed structure. The calculation procedure is already outlined in the section 3.2.

Table 22: *Heat calculation for different salinity of water.*

Sr. No	Salinity	Density		Ql		Qh	
	ppt	gm/cc	Kg/m^3	KJ / day	KW	KJ / day	KW
1	30	1.024	1024	85729280	992	857292800	9922
2	100	1.080	1080	90417600	1047	904176000	10465
3	200	1.160	1160	97115200	1124	971152000	11240

Moreover, based on the above aspects the initial investment for the technologies is described in the **Table 22**.

Table 23: *Cost comparison of different technologies for different salinity of water.*

Sr. No	Technologies	Initial Investment (M$) for 30 years design		References
		Low	High	
1	Reverse Osmosis (RO)	11	110	1
2	Electrodialysis (ED)	66	657	2
3	Thermal Desalination	14 - 25	140 - 250	3
4	Membrane Distillation (MD)	5 - 14	50 - 140	4
5	Forward Osmosis (FO)	30	300	5

The extraction of water at various salinity levels involves complex economic and technical considerations. While desalination at lower salinities (e.g., 30 ppt) is economically and technically feasible with existing technologies, higher salinities (100-200 ppt) present significant challenges. These include increased capital investments, higher operating costs due to energy requirements, and more complex effluent management strategies. Desalination of 30 ppt brine resembles seawater desalination, requiring moderate energy and standard RO systems with recovery rates of 40-50%. For medium salinities (100 ppt), technologies like Electrodialysis (ED) and Thermal Desalination are viable but energy-intensive, with recovery rates dropping to 20-30%. Extremely high salinities (200 ppt) necessitate advanced methods such as Membrane Distillation (MD) and Forward Osmosis (FO), which are in developmental stages, with low recovery rates (~10-20%) and high energy requirements (up to 15 KWh/m^3).

Effluent management becomes increasingly challenging with salinity. At 30 ppt, conventional disposal methods like dilution or injection are manageable, while higher salinities require expensive solutions such as crystallization, evaporation ponds, or Zero Liquid Discharge (ZLD) systems to mitigate environmental impacts. Heat requirements and energy consumption also rise with salinity, as outlined in **Table 22**, where water density and heat load increase proportionally with salinity. Initial investments vary significantly by technology, as shown in **Table 22**, with Reverse Osmosis being cost-effective for lower salinities, while Membrane Distillation and Forward Osmosis are promising but costly options for higher salinity brines. Effective implementation demands careful balancing of technology performance, cost, and environmental impact.

14 Conclusions

I. **Geological Overview of the Baltic Basin**:

- The Baltic Artesian Basin in Lithuania contains significant geothermal potential, with major aquifers such as the Cambrian and Devonian formations.
- The Cambrian aquifer is the most promising in terms of temperature and resource quality, particularly in Western Lithuania, where temperatures reach up to 94°C.

II. **Temperature and Geothermal Resource Distribution**:

- The geothermal gradient across Lithuania varies, with higher heat flow in the western regions, making these areas more suitable for geothermal energy exploitation.
- Temperatures of up to 94°C in the Cambrian and 45°C in the Kemeri aquifer suggest good potential for geothermal heating, with further investigation needed into the distribution of these resources for practical applications.

III. **Geothermal Potential for Aquaculture**:

- Geothermal energy can be used for closed-loop heating systems in aquaculture, maintaining stable water temperatures for farming up to 30°C, which is essential for sustainable aquaculture practices in cold climates.
- Western Lithuania's geothermal resources are particularly well-suited for heating aquaculture systems, providing an economic and sustainable energy source.

IV. **Brine extraction availability**:

- Based on the provided study, the feasibility of extracting highly mineralized brines is significantly influenced by a combination of geological, technical, and economic factors. The study highlights that lower-salinity brine extraction (e.g., ~30 ppt) is both economically viable and technically feasible with current desalination technologies such as Reverse Osmosis (RO). However, as salinity increases to 100 ppt and 200 ppt, substantial challenges arise due to the need for advanced materials, higher energy requirements, and more sophisticated effluent management.
- Geologically, the reservoir properties of the brines in the Baltic Basin, particularly in Western Lithuania, show promising potential with significant thickness and temperature gradients in certain formations, such as the Cambrian aquifers. Technologically, high-salinity brine extraction requires energy-intensive systems like Electrodialysis, Thermal Desalination, or emerging technologies like Membrane Distillation and Forward Osmosis, which are not yet fully commercialized. Economically, the feasibility depends on capital investments, operational costs, and brine disposal methods, with high-salinity systems facing steep costs and complex effluent management solutions such as Zero Liquid Discharge (ZLD).
- The study concludes that while opportunities for high-salinity brine extraction exist, particularly in geothermal-rich areas, they require robust technical and financial planning. Geothermal systems paired with advanced technologies could present a sustainable approach, provided subsidies or market incentives offset the substantial initial and operational investments.

V. **Economic and Technical Feasibility**:

- The document evaluates the economic feasibility of geothermal extraction in Lithuania, highlighting costs associated with drilling, infrastructure, and heat exchange systems.
- Various well designs (vertical, horizontal, and coaxial) and drilling methods are discussed, focusing on their suitability for geothermal resource extraction in different geological contexts.

VI. **Hydro chemical Data and Water Quality**:

- The hydro chemical analysis of geothermal water shows varying levels of salinity across aquifers, with the Cambrian aquifer containing high mineralization levels (up to 203 g/L), impacting the potential for direct use.
- Water chemistry is important for determining the applicability of geothermal resources for fish and shrimp farming, where salinity and mineral content are critical factors.

VII. **Challenges and Considerations**:

- Significant challenges include variations in reservoir quality, particularly due to quartz cementation in deeper formations, which reduces porosity and permeability, impacting geothermal well performance.
- Environmental considerations, such as potential fluid migration and the sustainability of extraction, must be factored into long-term geothermal resource planning.

VIII. **Geothermal Energy for District Heating**:

- Beyond aquaculture, geothermal resources in Lithuania are also well-suited for district heating systems, particularly in Western Lithuanian towns where geothermal anomalies exist, offering a renewable heating alternative to fossil fuels.

REFERENCES

1. Brehme, M., Nowak, K., Banks, D., Petrauskas, S., Valickas, R., Bauer, K., Burnside, N., Boyce, A. 2019. A Review of the Hydrochemistry of a Deep Sedimentary Aquifer and Its Consequences for Geothermal Operation: Klaipeda, Lithuania. Geofluids. 2019. 1-20. 10.1155/2019/4363592.
2. Feldrappe. H.. Hahne. K.. Rhede. D. 2005. Regionale Stellung und Alter der präpermischen "Bunten Serien" in Vorpommern. NE-Deutschland. *Zeitschrift der Deutschen Gesellschaft für Geowissenschaften*. 156. 299-322. 10.1127/1860-1804/2005/0156-0299.
3. Grendaitė. M.; Michelevičius. D.; Radzevičius. S. A large array of inselbergs on a continuation of the sub-Cambrian peneplain in the Baltic Basin: evidence from seismic data. Western Lithuania. *Geol. Q*. 2022. 66. doi: 10.7306/gq.1633.
4. Grendaitė. M.; Michelevičius. D.; Radzevičius. S. Insights into the structural geology and sedimentary succession of the Baltic Basin. Western Lithuania. *Marine and Petroleum Geology*. 2023. 147. 106009. DOI:10.1016/j.marpetgeo.2022.106009.
5. Jankauskas T.. Lendzion K. 1992. Lower and Middle Cambrian acritarch-based biozonation of the Baltic Syneclise and adjacent areas (East European Platform). *Przegląd Geologiczny*. 9. 519-524.
6. Jaworowski. K.; Sikorska M. 2003. Composition and provenance of clastic material in the Vendian–lowermost Cambrian from northern Poland: geotectonic implications. *Polish Geological Institute Special Papers*. 8. 59 p.
7. Jõeleht. A.. Kirsimäe. K.. Shogenova. A.. Šliaupa. S.. Kukkonen. I.T.. Rasteniene. V.. Zabele A. 2002. Thermal conductivity of Cambrian siliciclastic rocks from Baltic paleobasin. *Proc. Acad. Sci. Estonia. Geol.*. 51(1). 5-15.
8. Juodkazis. V.. Suveizdis. P.. Rastenienė. V. 1997. Geothermal and mineral water resources of Lithuania. In: *Mineral and Thermal Groundwater Resources*. 281–316. Springer.
9. Juodkazis, N., Mokrik, R., Gregorauskas, M. 2011. Development of hydrogeodynamical investigations of groundwater resources. Baltica, Vol. 24, Special Issue. Geosciences in Lithuania: challenges and perspectives, 31–42. Vilnius. ISSN 0067–3064.
10. Kleesment. A.; Mark-Kurik. E. 1997. Devonian. In *troduction. Lower Devonian. Middle Devonian. In Geology and Mineral Resources of Estonia*; Estonian Academy Publishers: Tallinn. Estonia. 107–121.
11. Klimas. A.. Gregorauskas M.. 2010. Computer Models. Used for Klaipeda Geothermal Plant Operation Failures Analyse. *Scientific Journal of Riga Technical University*. 45. 7-15.
12. Kreitler. C.W.. 1989. Hydrogeology of sedimentary basins. *Journal of Hydrology*. 106. 29·53.
13. Lukševičs. E.; Stinkulis. Ģ.; Mūrnieks. A.; Popovs. K. 2012. Geological evolution of the Baltic Artesian Basin. *Highlights Groundw. Res. Balt. Artesian Basin*. 7–52.
14. Mokrik R.. & Baublyte A. (2005). Water geochemistry in the Šventoji–Aruküla aquifer system. Lithuania. *Geologija. 52*. 55–64.
15. Mokrik. R.. Baublyte. A. 2005. Water geochemistry in the Šventoji–Aruküla aquifer system. Lithuania. *Geologija*. 52. 55–64.
16. Mokrik. R.. Mažeika. J.. Baublytė. A.. & Martma. T. (2009). The groundwater age in the Middle–Upper Devonian aquifer system. Lithuania. *Hydrogeology Journal. 17*(4). 871–889.
17. Mokrik. R. 1997. *The Palaeohydrogeology of the Baltic Basin. Vendian and Cambrian*. Tartu University Press. 138 p.
18. Mokrik. R. 1997. The Palaeohydrogeology of the Baltic Basin. Vendian and Cambrian.
19. Kowalska, S., Wójtowicz, A., Halas, S., Wemmer, K., Mikołajewski, Z., Buniak, A. 2019. Thermal history of Lower Palaeozoic rocks from the East European Platform margin of Poland based on K-Ar age dating and illite-smectite palaeothermometry. Annales Societatis Geologorum Poloniae, 89. 10.14241/asgp.2019.21. DOI: 10.14241/asgp.2019.21.
20. Molenaar. N.. Čyžiene. J.. Šliaupa. S. 2008. Lack of inhibiting effect of oil emplacement on quartz cementation: Evidence from Cambrian reservoir sandstones. Paleozoic Baltic Basin. *Geological Society of America Bulletin*. 120(9-10). 1280-1295. ISSN: 0016-7606).
21. Molenaar. N.; Cyziene. J.; Šliaupa. S. 2007. Quartz cementation mechanisms and porosity variation in Baltic Cambrian sandstones. *Sedimentary Geology*. 195. 135-159. 10.1016/j.sedgeo.2006.07.009.
22. Mostafa Shamsuzzaman. Md... Kumar Biswas. T.. 2012. Aqua chemicals in shrimp farm: A study from south-west coast of Bangladesh. *Egyptian Journal of Aquatic Research*. 38. Pages 275-285. ISSN 1687-4285. https://doi.org/10.1016/j.ejar.2012.12.008.

23. Mozuta. G. 2022. The Precambrian Geology of Lithuania. Springer. 203. ISBN/GTIN978-3-030-96854-0.
24. Näslund. J.O.. Jansson. P.. Fastook. J.L.. Johnson. J.. & Andersson. L. 2005. Detailed spatially distributed heat-flow data for modeling of basal temperatures and meltwater production beneath the Fennoscandian ice sheet. *Annals of Glaciology*. 40. 95–101. doi:10.3189/172756405781813582.
25. Paskevicius. J. 1997. The geology of the Baltic Republics. Vilnius: Geological Survey of Lithuania. 388 p.
26. Paškevičius. J. 1997. *The Geology of the Baltic Republics*; Vilnius University and Geological Survey of Lithuania: Vilnius. Lithuania. 387.
27. Petrauskas, S., Šliaupa, S., Nair, R., Valickas, R. 2019. The Horizon 2020 SURE Project: Deliverable 6.1 - Field scale RJD stimulation for the Klaipeda site 2019, Potsdam: GFZ German Research Centre for Geosciences, DOI: 10.2312/GFZ.4.8.2019.007.
28. Poprawa. P.. Šliaupa. S.. Stephenson. R.. Lazauskiene. J. Late Vendian–Early Palaeozoic tectonic evolution of the Baltic Basin: regional tectonic implications from subsidence analysis. *Tectonophysics*. 1999. 314(1–3). 219–239.
29. Prasad. S. N.; Sharma. P. V.; 1978. Palaeomagnetism of the Nexø Sandstone from Bornholm Island. Denmark. *Geophysical Journal International*. 54. 669-680. https://doi.org/10.1111/j.1365-246X.1978.tb05501.x.
30. Puronas. V.. Šliaupa. S. 2001. Integrated 2-D modelling of the Baltic Cambrian. *Litosfera*. 5. 14–24.
31. Radeckas. B.. Lukosevicius. V. 2000. Klaipeda Geothermal Demonstration Project. In: *Proceedings Word Geothermal Congress 2000*. Kyushu-Tohoku. Japan. May 28 - June 10. 2000. p. 3547-3550.
32. Rasteniene & Puronas. 2005. Geothermal Atlas of Lithuania. Proceedings World Geothermal Congress. 1-6.
33. Rapolienė. L.. Vasiliauskienė. E.. Šliaupa. S.. Dailidienė. I.. Valiukas. D.. Martinkėnas. A.. Bredelytė. A. 2003. Lietuvos gamtinių išteklių ir juos gydymui bei sveikatinimui naudojančių centrų ir kurortų. ŽEMĖLAPIS. Klaipėdos Universitetas. ISBN 978-609-481-196-8.
34. Šliaupa S. (2012). Vendian sedimentation and low-rate syn-sedimentary tectonic activity in SE Lithuania. *Geologija*. 54(4). 155–170.
35. Šliaupa S. 2009. Hydrogeothermal resources of Lithuania. *Geologijos akiračiai*. 3-4. 11-19. ISSN 1392-0006.
36. Šliaupa S.. Fokin P.. Lazauskienė J.. Stephenson R. 2006. The Vendian-Early Palaeozoic sedimentary basins of the East European Craton. In: Gee D.. Stephenson R.A. (eds.) Eoropean Lithosphere Dynamics. *Geological Society*. London. Memoirs. 32: 449-462. https://doi.org/10.1144/GSL.MEM.2006.032.01.28.
37. Šliaupa. S. & Kežun. J. (2011). Hydrothermal resources of Middle Lithuania. *Geologija*. 53(2). 75–87.
38. Šliaupa. S. Kežun. J. 2011. Hydrothermal resources of Middle Lithuania. *Geologija*. 53(2). 75–87.
39. Sliaupa. S. Cyziene. J. Molenaar. N & Musteikyte. D. 2008. Ferroan dolomite cement in Cambrian sandstones: burial history and hydrocarbon generation of the Baltic sedimentary basin. *Acta Geologica Polonica*. 58. 27-41.
40. Šliaupa. S. 2002. Geothermal Data Base of Lithuania. *Results of the Lithuanian Geological Survey*. 2001. 51-53.
41. Šliaupa. S. 2002. Geothermal Data Base of Lithuania. Results of the Lithuanian Geological Survey. 2001. 51-53.
42. Šliaupa. S.. & Hoth. P. (2011). Geological Evolution and Resources of the Baltic Sea Area from the Precambrian to the Quaternary (pp. 13–51). https://doi.org/10.1007/978-3-642-17220-5_2
43. Šliaupa. S.. Rasteniene. V. (2000). Heat flow and heat production of crystalline basement rocks in Lithuania. Geologija. 31. 24–34.
44. Šliaupa. S.. Hoth. P. 2011. Geological Evolution and Resources of the Baltic Sea Area from the Precambrian to the Quaternary. 13–51. https://doi.org/10.1007/978-3-642-17220-5_2.
45. Šliaupa. S.. Motuza. G.. Korabliova. L.. & Motuza. V. (2005). Hot granites of southwest western Lithuania: new geothermal prospects. *Technika Poszukiwan Geologichnych. Geosinoptika i Geotermia*. 3. 10–23.
46. Šliaupa. S.. Motuza. G.. Korabliova. L.. & Motuza. V. (2005). Hot granites of southwest western Lithuania: new geothermal prospects. *Technika Poszukiwan Geologichnych. Geosinoptika i Geotermia*. 3. 10–23.

47. Šliaupa. S.. Rastenienė. V. 2000. Heat Flow and Heat Production of Crystalline Basement Rocks in Lithuania. *Geologija*. 31. 24-34.
48. Šliaupa. S.; Hoth. P.; Shogenova. A.; Huenges. E.; Rasteniene. V.; Freimanis. A.; Bityukova. L.; Jõeleht. A.; Kirsimäe. K.; Lashkova. L.; Zabele. A. (2003). Characterization of Cambrian reservoir rocks and their fluids in the Baltic States (CAMBALTICA). *Cleaner Energy Systems Through Utilization of Renewable Geothermal Energy Resources: Cleaner Energysystems Through Utilization of Renewable Geothermal Energy Resources*. Cracow. Poland. 31st March - 2nd April 2003. Ed. Bujakowski. W. Krakow: Kajc. 61−73.
49. Šliaupa. S.; Kežun. J. Hydrothermal resources of Middle Lithuania. *Geologija*. 2011. 53. 75–87. ISSN 1392-110X.
50. Sorokin. V.S. 1981. *Devon i karbon Pribaltiki [Devonian and Carboniferous of the Pre-Baltic Region]*; Zinātne: Riga. Latvia. 1–502. (In Russian).
51. Stirpeika. A. 1999. Tectonic evolution of the Baltic Syneclise and local structures in the South Baltic Region with respect to their petroleum potential. Vilnius. 189 p.
52. Stirpeika. A. 1999. Tectonic Evolution of Baltic Syneclise and local structures in the Baltic Region with Respect of their Petroleum Potential. Vilnius. 112 p. (translated PhD of 1979)
53. Suveizdis. P.. Rasteniene. V. Zinevicius. F. 1995. Geothermal Energy Possibilities in Lithuania. In: *Proceedings of Word Geothermal Congress*. Vol.1. Florence. p. 227-232.
54. Suveizdis. P.. Rastenienė. V. 1994. Geothermal investigation in Lithuania. Proceedings of Latvian – Danish seminar on "*Groundwater and Geothermal Energy*". Riga-Copenhagen: Riga Technical University. 315-318.
55. Suveizdis. P.. Rastenienė. V. 1998. Geology and the potential of geothermal energy in Lithuania. *Geologija*. 23. 47-52.
56. Suveizdis. P.. Rasteniene. V.. Zui. V. 1997. Geothermal field of the Vydmantai-1 borehole within the Baltic heat flow anomaly. *Baltica*. vol. 10. pp. 38–46.
57. Tallabacka L.. Mahler A.. Radeckas B.. Freimanis A.. Eihmanis E. A rewiew of the Baltic Geothermal Energy Project. *Geothermal bulletin of LGA*. No 2. 1994. p. 1-8.
58. Urban. G. 1989. Heat flow and radiogenic heat generation of some structures of the crystalline basement of Baltic Syneclise. *Izv. AN Estonii*. 38 (4). 155-160.
59. Urban. G. 1991. New estimates of the heat flow in the geothermal anomaly of the Baltic Seniclise. *Izv. AN Estonii. Geol.*. 40 (1). 24-32. (in Russian)
60. Urban. G. 1991. New estimates of the heat flow in the geothermal anomaly of the Baltic Seniclise. *Izv. AN Estonii*. 40 (1). 24-32. (in Russian)
61. Urban. G. 2004. Heat flow of Baltic Sineclise. IFZ RAN. *Moscow*. 158 p. (in Russian)
62. Urban. G. 2004. Heat flow of Baltic Sineclise. IFZ RAN. Moscow. 158 p.
63. Valiukevičius. J. 1994. Acanthodian zonal sequence of Early and Middle Devonian in the Baltic Basin. *Vilnius Geol.* 17. 115–125.
64. Zui V.I. 2004. Anomalies of terrestrial temperature field of Belarus. Lithosphere. 2 (21). 117–125.
65. Zui. V.. Dubanevich. M.. Vasilionak. E. 2016. Geothermal Field and Geothermal Resources in Belarus. Country Update for Belarus. *European Geothermal Congress* 2016 Strasbourg. France. 19‑24 Sept 2016. 2-13.
66. Alexandre Rivera Diaz, Eylem Kaya, Sadiq J. Zarrouk; Reinjection in Geothermal Fields: A Worldwide Review Update; Proceedings World Geothermal Congress 2015; Melbourne, Australia, 19-25 April 2015.
67. Abdul Rashid Memon, Pijus Makauskas, Ieva Kaminskaitė-Baranauskienė and Mayur Pal; Unlocking Geothermal Energy: A through literature review of Lithuanian Geothermal complexes and their production potential, Energies 2024, 17, 1576.
68. Abdul Rashid Memon, Pijus Makauskas, Ieva Kaminskaitė-Baranauskienė and Mayur Pal; Workflow for assessing geothermal potential of depleted hydrocarbon fields: A study of Cambrian reservoirs in Lithuania, EAGE ECMOR 2024, Oslo, Norway 2-5 September 2024. (Accepted for poster presentation).
69. Duggan-Haas, Don Andrew, Robert M. Ross, and Warren D. Allmon; The science beneath the surface: a very short guide to the Marcellus Shale. Paleontological Research Institution, 2013.
70. www.google.com ...image by well experts (accessed on 01 July 2024)

71. Wang G, Song X, Shi Y, Yulong F, Yang R, Li J; Comparison of production characteristics of various coaxial closed-loop geothermal systems. Energy Conversion and Management. 2020 Dec 1; 225:113437.
72. https://www.hpac.com/heating/article/20929819/how-geothermal-heating-and-cooling-can-improve-building-efficiency (accessed on 01 July 2024).
73. http://www.digtheheat.com/geothermal/index.html (Accessed on 01 July 2024)
74. Yasin, Qamar, Mariusz Majdański, Rizwan Sarwar Awan, and Naser Golsanami. "An analytical hierarchy-based method for quantifying hydraulic fracturing stimulation to improve geothermal well productivity." Energies 15, no. 19 (2022): 7368.
75. Joint Research Centre, Institute for Energy and Transport, Sigfússon B, Uihlein A. 2014 JRC geothermal energy status report: technology, market and economic aspects of geothermal energy in Europe. Publications Office; 2015. Available from: doi/10.2790/959587
76. https://19january2021snapshot.epa.gov/rhc/geothermal-heating-and-cooling-technologies_.html (accessed on 01 July 2024).
77. Beckers, Koenraad F., Maciej Z. Lukawski, Timothy J. Reber, Brian J. Anderson, Michal C. Moore, and Jefferson W. Tester. "Introducing GEOPHIRES v1. 0: Software package for estimating levelized cost of electricity and/or heat from enhanced geothermal systems." In Proceedings, Thirty-Eighth Workshop on Geothermal Reservoir Engineering, Stanford University, Stanford, California, vol. 11. 2013.
78. Lukawski, Maciej Z., Brian J. Anderson, Chad Augustine, Louis E. Capuano Jr, Koenraad F. Beckers, Bill Livesay, and Jefferson W. Tester. "Cost analysis of oil, gas, and geothermal well drilling." Journal of Petroleum Science and Engineering 118 (2014): 1-14.
79. Brehme, M.; Regenspurg, S.; Leary, P.; Bulut, F.; Milsch, H.; Petrauskas, S.; Valickas, R.; Blöcher, G. Injection-Triggered Occlusion of Flow Pathways in Geothermal Operations. *Geofluids* **2018**, *2018*, 4694829. [CrossRef]
80. Grendaite˙, M.; Michelevic˘ius, D.; Radzevic˘ius, S. Insights into the structural geology and sedimentary succession of the Baltic Basin, Western Lithuania. *Mar. Pet. Geol.* **2023**, *147*, 106009. [CrossRef]
81. Sliaupa, S.; Lazauskiene, J.; Laskova, L.; Cyziene, J.; Laskovas, J.; Motuza, V.; Korabliova, L. The petroleum system of Lithuanian offshore region. *Z. Für Angew. Geol.* **2002**, *2*, 41–63.
82. Šliaupa, S.; Motuza, G.; Korabliova, L.; Ciuraite, K.; Puronas, V. Geothermal potential of hot granites of Lithuania. In Proceedings of the World Geothermal Congress 2010, Bali, Indonesia, 25–29 April 2010.
83. Šliaupa, S.; Zinevic˘ius, F.; Mazintas, A.; Petrauskas, S.; Dagilis, V. Geothermal Energy Use, Country Update for Lithuania. In Proceedings of the European Geothermal Congress 2019, Den Haag, The Netherlands, 11–14 June 2019.
84. Kilda, L.; Friis, H. The key factors controlling reservoir quality of the Middle Cambrian Deimena Group sandstone in West Lithuania. Bull. Geol. Soc. Den. 2002, 49, 99–113.
85. Puronas, V. A Reservoir Model and Production Capacity Estimate for Cambrian Geothermal Reservoir in Kretinga, Lithuania; Geothermal Training Programme, Orkustofnun, Grensásvegur 9, IS-108 Reykjavík, Iceland. Reports; Publisher National and University Library of Iceland, Iceland 2002; Volume 11, pp. 187–204.
86. Zinevicius, F.; Sliaupa, S. Lithuania–Geothermal Energy Country Update. In Proceedings of the World Geothermal Congress 2010, Bali, Indonesia, 25–29 April 2010.
87. Klimas, A.A.; Gregorauskas, M.; Malisauskas, A. Computer Models, Used for Klaipeda Geothermal Plant Operation Failures Analyse. Rigas Teh. Univ. Zinat. Rak. 2010, 45, 7.
88. https://medium.com/@desalter/the-true-cost-of-drinking-water-understanding-the-expenses-of-reverse-osmosis-plants-4254b4f3f166
89. Muhammad M. Generous, Naef A.A. Qasem, Usman A. Akbar, Syed M. Zubair; Techno-economic assessment of electrodialysis and reverse osmosis desalination plants; Separation and Purification Technology; Volume 272,; 2021; 118875; https://doi.org/10.1016/j.seppur.2021.118875.
90. Layla Saleh, Toufic Mezher; Techno-economic analysis of sustainability and externality costs of water desalination production; Renewable and Sustainable Energy Reviews; Volume 150; 2021; 111465; https://doi.org/10.1016/j.rser.2021.111465.

91. R. Schwantes, A. Cipollina, F. Gross, J. Koschikowski, D. Pfeifle, M. Rolletschek, V. Subiela; Membrane distillation: Solar and waste heat driven demonstration plants for desalination, Desalination; Volume 323; 2013; Pages 93-106; https://doi.org/10.1016/j.desal.2013.04.011.
92. Sara R. Osipi, Argimiro R. Secchi, Cristiano P. Borges; 13 - Cost analysis of forward osmosis and reverse osmosis in a case study, Editor(s): Angelo Basile, Alfredo Cassano, Navin K. Rastogi, Current Trends and Future Developments on (Bio-) Membranes, Elsevier, 2020, Pages 305-324; https://doi.org/10.1016/B978-0-12-816777-9.00013-7.
93. Kolo, I., Brown, C.S., Nibbs, W. et al. A comprehensive review of deep borehole heat exchangers (DBHEs): subsurface modelling studies and applications. Geotherm Energy 12, 19 (2024). https://doi.org/10.1186/s40517-024-00297-3.
94. https://lgt.lrv.lt/lt/veiklos-sritys/geologines-informacijos-kaupimas-ir-valdymas/informacines-sistemos/geologijos-informacine-sistema-geolis/
95. Agemar, T.; Schellschmidt, R.; Schulz, R. Subsurface Temperature Distribution of Germany. Geothermics, 2012. 44, 65–77.
96. Agemar, T.; Weber, J.; Schulz, R. 2014. Deep Geothermal Energy Production in Germany. Energies, 7, 4397-4416.
97. Franz, M.; Barth, G.; Zimmermann, J.; Budach, I.; Nowak, K. & Wolfgramm, M. 2018. Geothermal resources of the North German Basin: exploration strategy, development examples and remaining opportunities in Mesozoic hydrothermal reservoirs. Geological Society, London, Special Publications, Volume 469, 193 – 222. https://doi.org/10.1144/SP469.11
98. Hoffmann, N; Jodicke, H.; Gerling, P. 2001. The distribution of Pre-Westphalian source rocks in the North German Basin - Evidence from magnetotelluric and geochemical data. Geologie en Mijnbouw / Netherlands Journal of Geosciences, 80 (1): 71-84.
99. Schellschmidt, R., Sanner, B., Pester, S. and Schulz, R.: Geothermal Energy Use in Germany, Proceedings World Geothermal Congress 2010, Bali, Indonesia, (2010), paper 0152, 19p.
100. Suchi, E., Dittmann, J., Knopf, S., Müller, C. and Schulz, R. 2014. Geothermie-Atlas zur Darstellung möglicher Nutzungskonkurrenzen zwischen CO2- Einlagerung (CCS) und Tiefer Geothermie in Deutschland, German, J. Geosci., 165 (3), (2014), 439-453.
101. Weber, J,; Born, H,; Pester, S;, Schifflechner, Ch,; Moeck, I. 2022. Geothermal Energy Use in Germany, Country Update 2019-2021.

APPENDIX: 1 Geological Maps

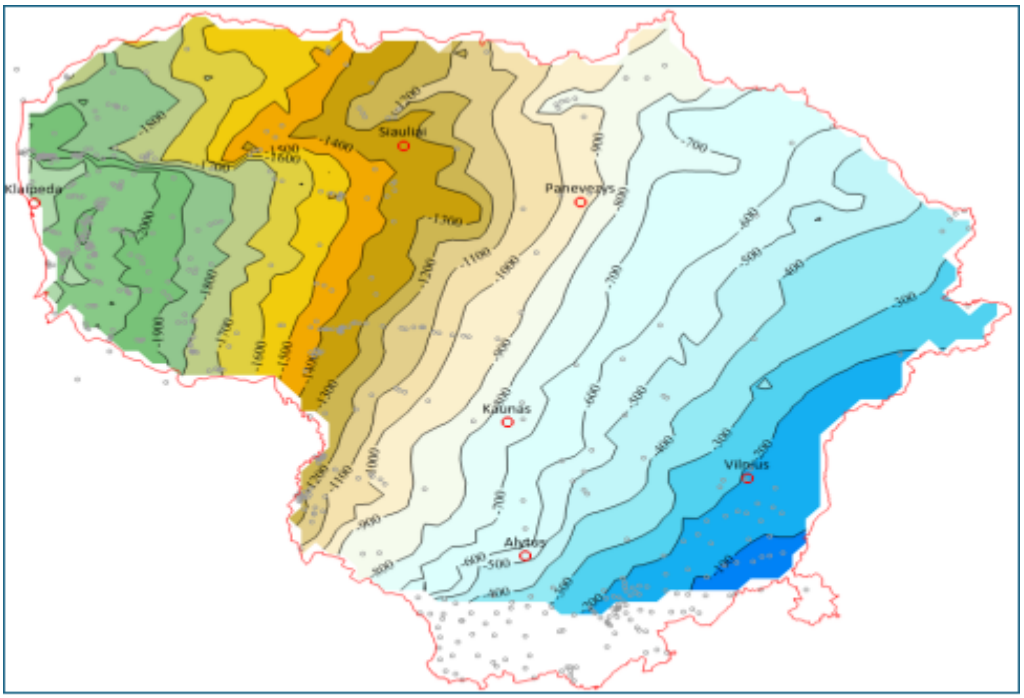

Figure SEQ Figure * ARABIC 123. *Depth (m) of top of the Cambrian succession of Lithuania. Deep wells (grey circles). Tectonic faults are not indicated on the map*

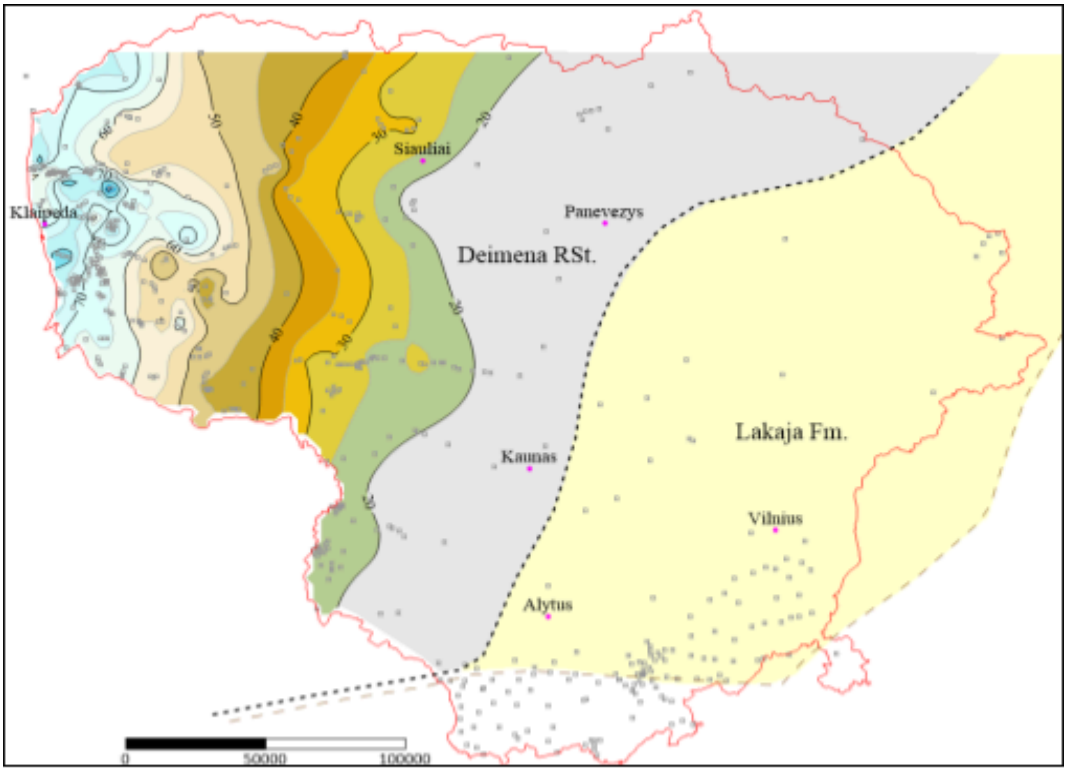

Figure SEQ Figure * ARABIC 124. *Distribution and thickness of the Deimena RSt. (scaled colours). Lakajai Fm. sandstones are sub-cropping in the east (yellow)*

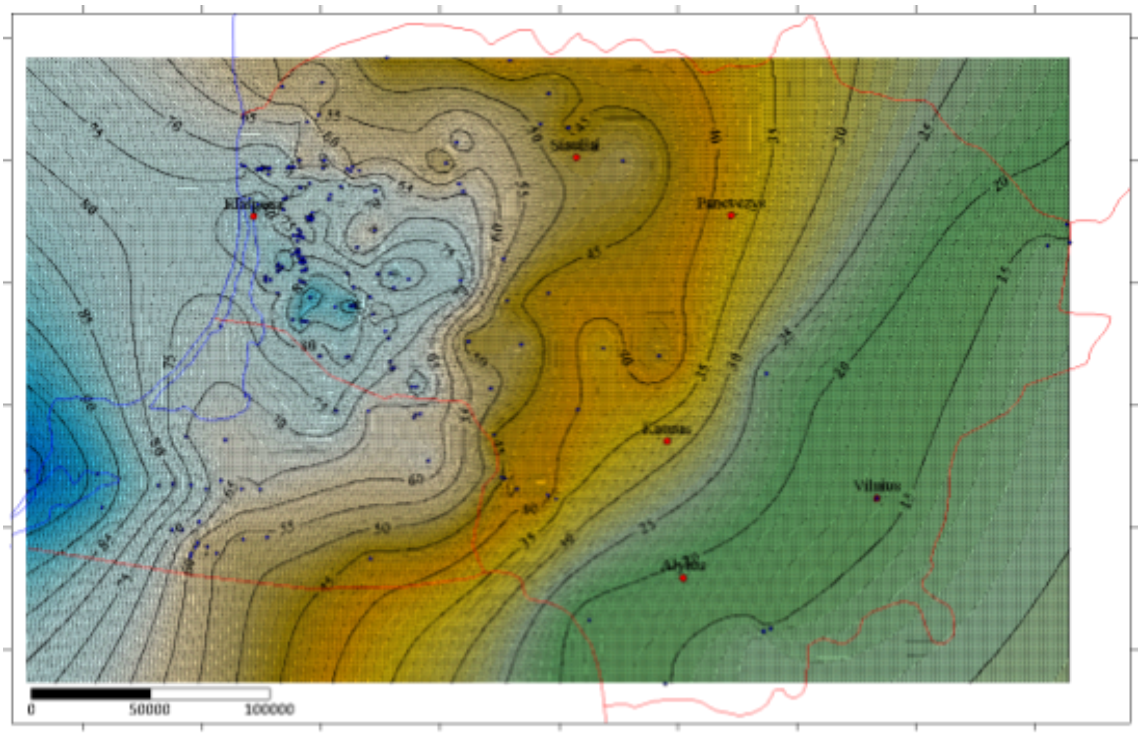

Figure SEQ Figure * ARABIC 125. *Temperatures of Cambrian geothermal aquifer (added Kaliningrad district data)*

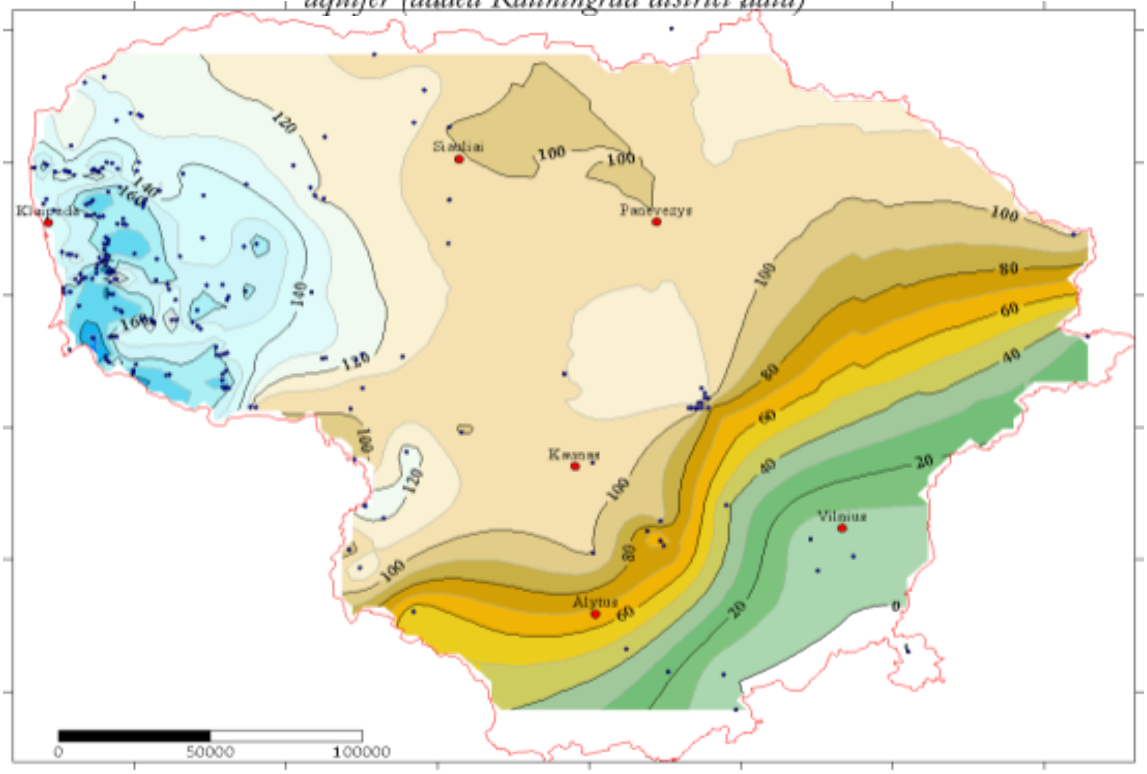

Figure SEQ Figure * ARABIC 126. *Salinity of Cambrian aquifer. Studied wells are indicated (samples N=279)*

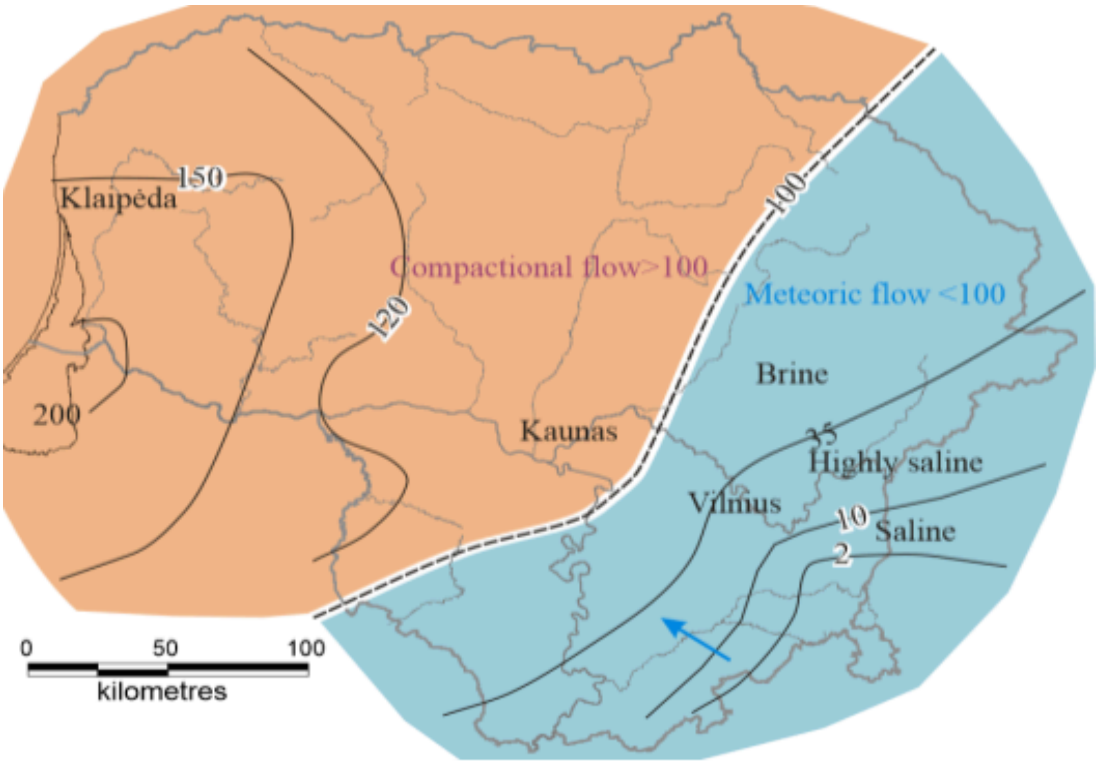

Figure SEQ Figure * ARABIC 127. *Hydrochemical zonation of Cambrian aquifer of Lithuania, water salinity g/L*

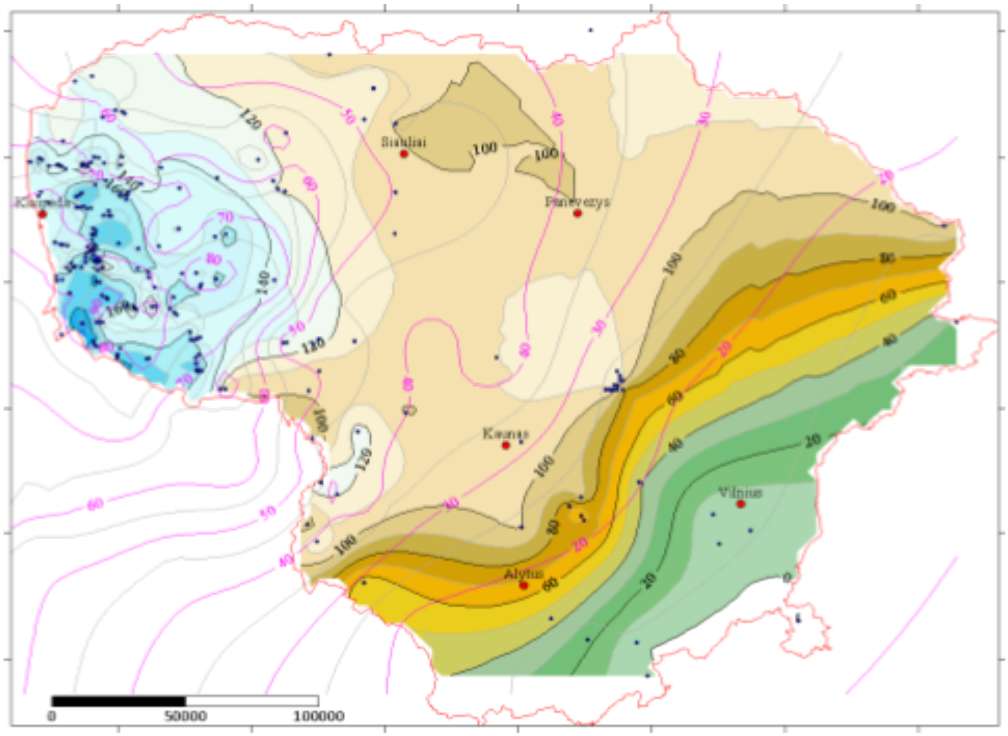

Figure SEQ Figure * ARABIC 128. *Temperature map overlying the salinity map of Cambrian aquifer. Studied wells are indicated*

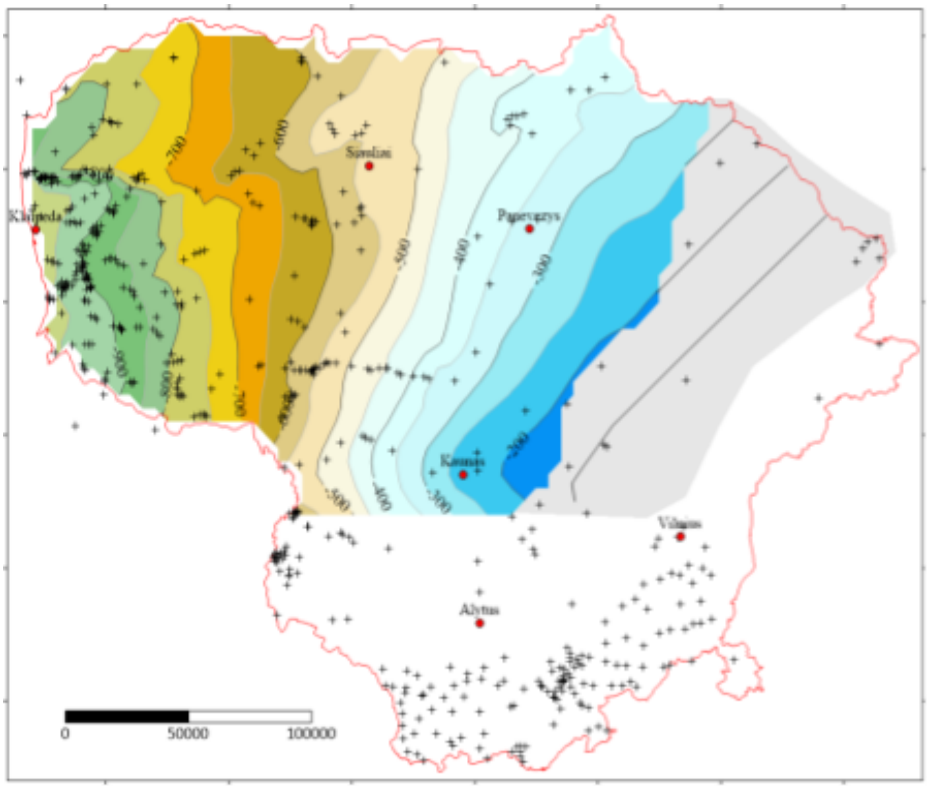

*Figure SEQ Figure * ARABIC 129. Top of Kemery Fm. geothermal aquifer. Wells of database*

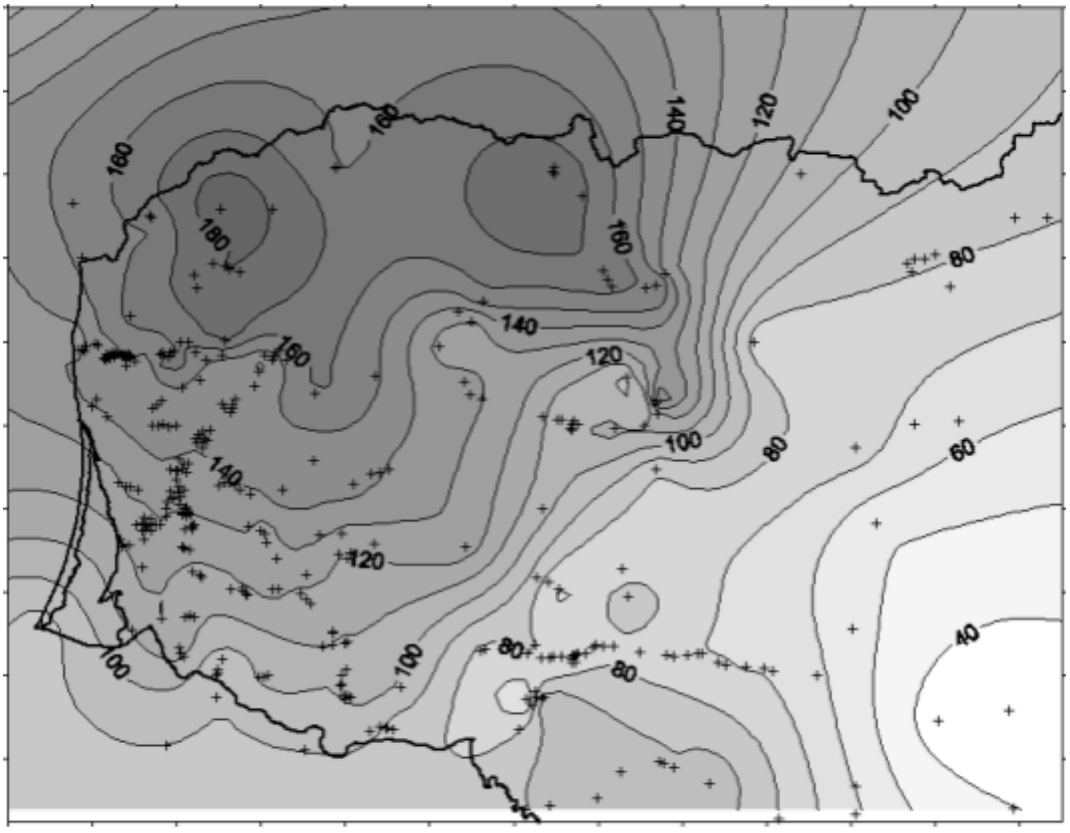

Figure SEQ Figure * ARABIC 131. *Thickness of the Kemeri Fm.*

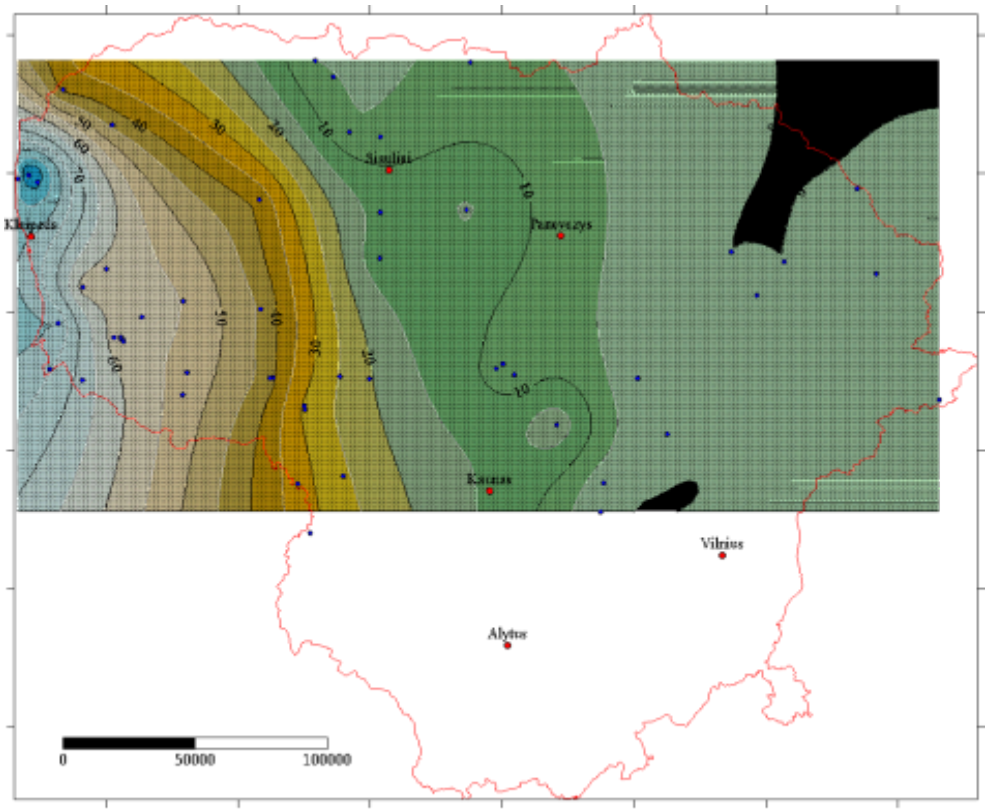

Figure SEQ Figure * ARABIC 133. *Salinity (g/L) of the Kemeri geothermal aquifer samples (N=53)*

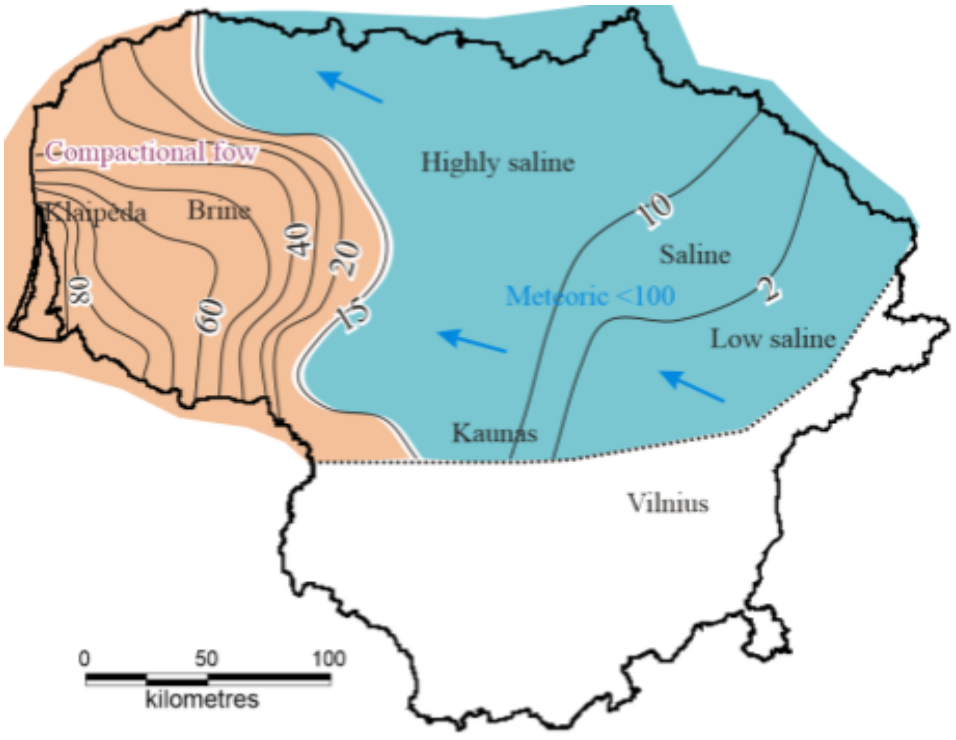

Figure SEQ Figure * ARABIC 132. *Salinity of the Kemeri Fm. geothermal aquifer (g/L)*

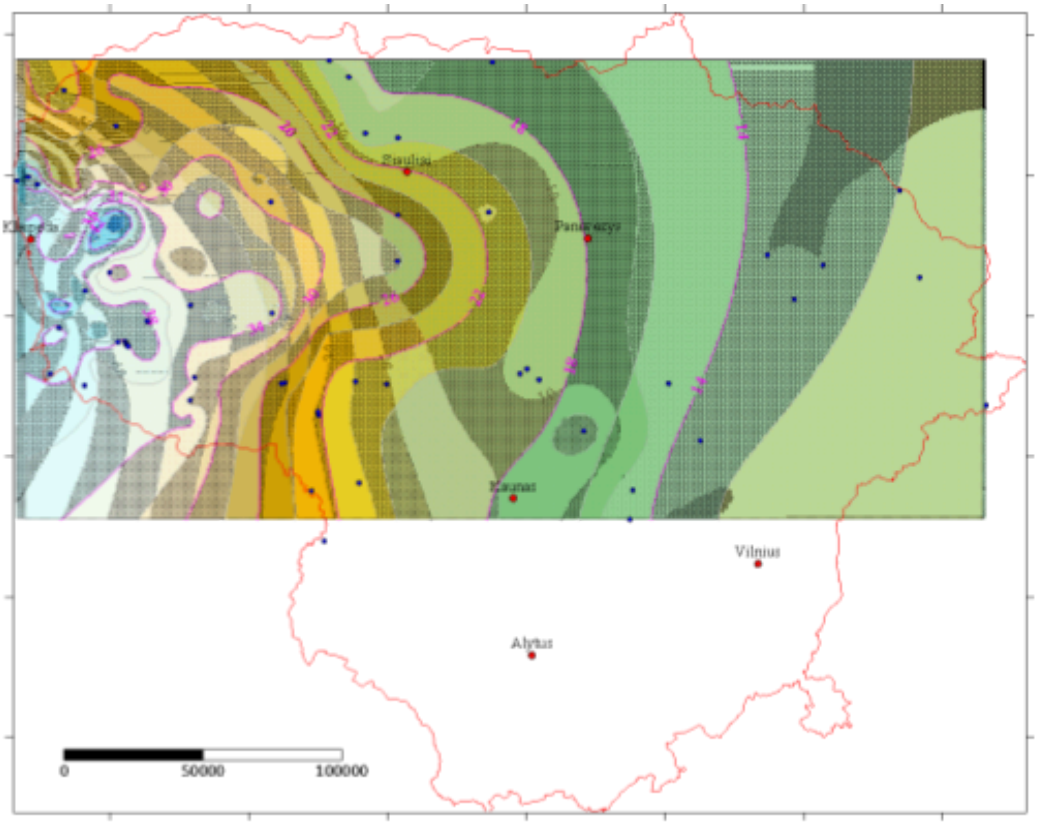

Figure SEQ Figure * ARABIC 134. *Temperature map overlying the salinity map of the Kemeri aquifer. Studied wells are indicated*

15 APPENDIX 2:

15.1.1 **Well Summary**

Well KGDP-3P was suspended after drilling and completion on the 3rd of November, 1997 at 1300 hours after 28 days of drilling operations. After reaching TD at 1,225m RT, the well was plugged back to 1,130m RT, and the 128m thick aquifer zone between 990m-1,118m RT was completed with gravel packed screens with top and bottom at 1,006.5m and 1,118.9m RT, respectively.

The Klaipeda Geothermal Demonstration Project is planned to supply 500 Terajoules of geothermal heat annually into the existing district heating network of Klaipeda, Lithuania. Geothermal aquifer water was pumped through two water production wells from a Devonian sandstone aquifer zone located at approximately 1,000 meters depth and re-injected into the aquifer zone through a water injection well offset by approximately 1.7 kilometers. Geothermal heat was retrieved at the surface using heat exchange and absorption heat pump technologies. The technical concept is based on the Thisted Geothermal Plant in Denmark. Well KGDP-3P is the second of three wells under this project.

15.1.2 **Well Data**

I. **Well Name**: KGDP-3P
II. **Type**: Geothermal Water Producer
III. **Location**: 55°41'03".85 North, 21°12'07".95 East
IV. **Employer**: till year 2022 - JSC Geoterma, Vilnius, Lithuania
V. **Service Contractor**: Dowell Schlumberger (Eastern) Inc., Virgin Islands (GB)
VI. **Drilling Contractor**: Oil And Gas Exploration Company, Krakow, Poland
VII. **Drilling Rig**: Skytop Brewster TR-800
VIII. **Spud Date**: 17th October, 1997
IX. **Completion Date**: 13th November, 1997
X. **Well Status**: Drilled and Suspended. Stopped in 2017 and the devices were preserved
XI. **Total Depth (TD)**: 1,225m RT (Driller), 1,225m (Logger)
XII. **Plugged Back Total Depth**: 1,130m RT
XIII. **Casing**: 27½" (Conductor) @ 11.0m, 20" @ 214.5m, 13⅜" @ 438m, 9⅝" (Liner) between 342m-1,001m
XIV. **Completion String**: 7" Blanks & Screens between 936.7m-1,118.9m

15.1.3 **Well Summary**

Well KGDP-3P is located within Klaipeda, Lithuania, adjacent to the Eastern Boiler House, about four kilometers southeast of downtown Klaipeda. It was drilled as part of the World Bank-financed Klaipeda Geothermal Demonstration Project. The well was spudded on 17th October 1997 and suspended on 13th November 1997. The total depth was reached at 1,225m RT in the Lower Devonian Gargzdai Formation, with the objective early Devonian aquifer unit located between 990m-1,118m RT. The well was plugged back to 1,130m RT, and the aquifer unit was completed with a combination of gravel packed screens and blanks.

15.1.4 **Drilling Operations**

Mobilization

The drilling rig was mobilized from the location of Well KGDP-II. Rig up was completed on the 16th of October 1997, and well KGDP-3P was spudded on 17th October 1997.

Conductor Pipe

A 27½" conductor pipe was pre-installed at 11.0m RT (6m below GL) during the well site construction.

Surface Hole Section

The 26" surface hole was drilled to 218m RT. Similar to KGDP-II, issues with aggressive clay caused problems with mud handling and disposal. A 20" casing was set at 214.5m RT and cemented to the surface.

CASING

Casing materials for well KGDP-3P were supplied by Dalmine S.p.A., Italy. The following casings were used:

I. 20" x 94 lbs/ft Grade K55 BTC Range 3
II. 13⅜" x 54.5 lbs/ft Grade K55 BTC Range 3
III. 9⅝" x 40 lbs/ft Grade K55 BTC Range 3 (liner)
IV. 7" x 23 lbs/ft Grade K55 BTC Range 2 (used as blanks in the completion string)

STRATIGRAPHY AND LITHOLOGY/DESCRIPTION

The document details the geological layers encountered during the drilling of Well KGDP-3P. These include:

I. Red clays with gypsum near the bottom.
II. Limestone and dolomite.
III. Interbedded clay, sand, and calcareous materials.
IV. Glacial deposits of sand, clay, gravel, and pebbles.
V. Predominantly dense, hard dolomite with marl partings and some gypsum.
VI. Sandstone interbedded with clay and siltstone.

WELL COMPLETION

The completion string consists of a liner attached to a combination of 7" blanks and standard screens over the interval from 936.7m to 1,120m RT. Screens have a 0.008" wire spacing. There were initial issues with the completion string standing up at certain depths due to inadequate leveling and loose aquifer sands. The string was re-run after a clean-up trip.

The completion string was gravel packed using formation water as a carrier fluid, with a total of six tons of 40/60 mesh gravel being pumped into the underreamed 10 ⅝" annulus. This process was performed at a circulation pressure of eight bars, and the gravel was mixed at 250 kilograms per cubic meter. The final packing occurred at a pressure of 70 bars.

Source: Well KGDP-3P, Final Well Report, World Bank Loan No. IBRD 4013-L

GEOTHERMAL WATER

This Study presents the laboratory data of Klaipeda borehole KGDP-3P water laboratory tests

Anschrift des Labors: VKTA - Strahlenschutz , Analytik & Entsorgung Rossendorf e. V.
Labor fUr Umwelt- und Radionuklidanalytik PF 510119,
01314 Dresden
Tel.: 0351 I260 3489, Fax: 0351 I260 3190

Auftraggeber: HelmholtzZentrum Potsdam, DeutschesGeoForschungsZentrum GFZ Sektion 4.1 Reservoirtechnologien z.H. Frau Dr. Regenspurg Telegrafenberg 14473 Potsdam

Auftragsnummer: 10038394-C

vom: Auftragsbezeichnung: Analytik hochsalinarer Fluide **PrOfgegenstand:** Tiefenfluid

Probenzahl: 1

Probenahme durch: Auftraggeber

Probeneingang: 09.04.2015

PrOfzeitraum: 09.04 .2015 - 16.04.2015

Bemerkungen: keine

freigegeben:

Name: U. Czeslik

Funktion: Unterschrift: Methodenverantwortliche

VKTI Labor fi.ir Umwelt- und Radionuklidanalytik	Prufbericht		Revision O	
	2010.23		vom	16.04.15

Analysenergebnisse:

Probenummer

: 000562-2015

Kennzeichnung

AG : Klaipeda

Kationen

Parameter	Kenn.	Verfahren	Einheit	Ergebnis	s	s/ci [%]
Natrium		DIN EN ISO 17294-2 (E 29)	mg/I	24700	1290,9	5,2
Kalium		DIN EN ISO 17294-2 (E 29)	mg/I	632	35,76	5 ,7
Calcium		DIN EN ISO 17294-2 (E 29)	mg/I	7560	416 ,61	5,5
Magnesium		DIN EN ISO 17294-2 (E 29)	mg/I	2330	119,85	5 ,1
Eisen		DIN EN ISO 17294-2, mod.	mg/I	18,8	0,968	5,1
Mangan		DIN EN ISO 17294-2 (E 29)	mg/I	1,00	0,064	6 ,4
Aluminium		DIN EN ISO 17294-2 (E 29)	mg/I	0,019	0,001	5 ,4

Spurenelemente

Parameter	Kenn.	Verfahren	Einheit	Ergebnis	s	s/ci [%]
Lithium		DIN EN ISO 17294-2 (E 29)	µg/I	4450	286	6,4
Sor		DIN EN ISO 17294-2 (E 29)	µg/I	13000	673	5 ,2
Silizium		DIN EN ISO 17294-2 (E 29)	mg/I	7,06	0,369	5,2
Titan		DIN EN ISO 17294-2, mod.	µg/I	1,43	0,1	7,3
Chrom		DIN EN ISO 17294-2 (E 29)	µg/I	3 ,61	0,49	13,6
Cobalt		DIN EN ISO 17294-2 (E 29)	µg/I	<0,200		
Nickel		DIN EN ISO 17294-2 (E 29)	µg/I	<0,600		
Kupfer		DIN EN ISO 17294-2 (E 29)	µg/I	<1,00		
Zink		DIN EN ISO 17294-2 (E 29)	µg/I	17,8	1	5,8
A rsen		DIN EN ISO 17294-2 (E 29)	µg/I	<1,00		
Strontium		DIN EN ISO 17294-2 (E 29)	µg/I	160000	8846	5 ,5
Silber		DIN EN ISO 17294-2 (E 29)	µg/I	<1,00		
Cadmium		DIN EN ISO 17294-2 (E 29)	µg/I	1,45	0,25	16,9
Barium		DIN EN ISO 17294-2 (E 29)	µg/I	256	13	5 ,1
Gold		DIN EN ISO 17294-2 (E 29)	µg/I	1,70	0,41	23,9
Quecksilber		DIN EN ISO 17294-2 (E 29)	µg/I	0,081	0,0089	10,9
Blei		DIN EN ISO 17294-2 (E 29)	µg/I	2,26	0,13	5 ,8
Uran		DIN EN ISO 17294-2 (E 29)	µg/I	<0,020		

(1)	nicht akkreditiertes Verfahren	(2)	Nachauftragnehmer
k.S.	keine Summenbildung , da Einzelergebnisse	mod.	modifiziert
i.A.	<NWG in Anlehnung		
s/ci	relative Messunsicherheit	NWG	Nachweisgrenze

Fur ein Vertrauensniveau von 90% isl der Vertrauensbereich durch ci +/- 1,645 s gegeben. Angaben mil < entsprechen der Nachweisgrenze des angewendeten

15.1.4.1.1.1.1.1 *Radiation Protection Centre*

(test and evaluation performed by)

15.1.4.1.1.2 CERTIFICATE OF RADON ACTIVITY CONCENTRATION TEST fN WATER AND CONCLUSION FROM THE VIEW OF RADIATION PROTECTION

July 29, 201 5 No. 15-2015

Vilnius

(place)

Certificate issued to

JSC„ Geoterma", Lypkiu str. 17, 94100 Klaipeda, Lithuania

(Name, code and address of/ e2al or natural per son)

Water produced and operated by

JSC„ Geoterma", Lypkiu str.17, 94100 Klaipeda, Lithuania

Geothermal water sample from drilling well No. 25871, registered land No. 2101-0034-

0007. Drilling well is located at 55°41 '03".85 North latitude and 21°12'07".95 East longitude

(by Greenwich) .

(Name. code and address of leal or natural person)

Sampled by

JSC „Geoterma", Lypkiu str.17, 94100 Klaipeda, Lithuania

(Name. code and address of legal or natural person) (Name, code and address of legal or natural person)

July 21 , 2015 Protocol No. 01-24-55.

(date)

Test performed by

Radiation Protection Centre, code 193288633, Kalvari ju str. 153, LT-08221 Vilnius

(Name, code and address of legal or natural person)

July 28, 2015 Protocol No. RAD151 1.

(date)

CONCLUSION. It was determined by the test that radon (Rn-222) activity concentration in sample is 24,3±3,8 Bq/l.

Analyzed water Qasses the requirements for drinking water of the Lithuanian Hygiene Norm

HN 85:201 1„ Natural ex12osure. Norms of radiation Protection".

(vasselnot passes)

15.1.4.1.1.3

Radiation Protection Centre

LIETUVOS
NACIONALINIS
AKREDITACIJOS
BIURAS

15.1.4.1.1.4	*Data of issue* Measurement of gross alpha activity in non-saline water . Thick source method (ISO 9696:2007, identical)"
	LST ISO 9697:2009 "Water quality. Measurement of gross beta activity in non-saline water. Thick source method (ISO 9697:2008, identical) "
Date of test	Very low background alpha/beta multiple detector IN20/82-82, Nr.81
Results	Geothermal water sample from underground mineral water well No.25871, registered land parcel No.2101-0034-0007. Drilling well is located at 55°41'03".85 North latitude and 21°12'07".95 East longitude (based on the Greenwich).

Gross alpha activity concentration, Bq/l	Expanded uncertainty, Bq/l
5,2	± 0,6
Gross beta activity concentration (without 3H,222Rn and it's decay products) , Bq/l	Expanded uncertainty, Bq/l
	± 2,2

Vydmantai

The deepest geothermal wells in Lithuania are Vydmantai 1 (2564m,) and Vydmantai 2 (2150m,).

Summary of the report of the investigation of geothermal wells (execution date 2023.11.08):

Construction of drilled internal columns:

Vydmantai-1

The construction of the internal columns of the well is as follows:

0-268 m - inner diameter 332 mm (outer 13 3/8" or 340 mm)

268-869 m - Inner diameter 232 mm (outer 9 5/8" or 244 mm)

869-2150 m - inner diameter 128 mm (outer 5 3/4" or 140 mm),

*Interval 1960-2060 m - perforated, i.e. all Cambrian layers - exposed from 2150 m - open borehole.

*The productive Cambrian layer from which the main water inflow takes place is at a depth of 2015-2030 m,

temperature 74-75 degrees C

Vydmantai-2

The construction of the internal columns of the well is as follows:

0-1000 m - inner diameter 232 mm (outer probably 9 5/8" or 244 mm) 1000-2125 m - inner diameter128 mm (external 5 3/4" or 140 mm),

*Interval 1960-2070 - perforated, i.e. all cambric layers - exposed

*The productive Cambrian layer from which the main water inflow takes place is at a depth of 2003-2027 m,

temperature 74-75 degrees C.

*Borehole - open along the entire length of the well.

Research results:

After comparing the results of the new studies with the studies registered during the drilling of wells in 1992,

recorded by gamma and temperature curves - a good coincidence of them is observed, which is justified in the borehole passports

the depths of isolated lithological layers and stratigraphic boundaries, as well as temperature measurements made in wells.

The newly registered cavernometry curve confirmed the internal columns presented in the Vydmantai-2 well's passport

construction, but showed inconsistencies in the diameter of the column, as indicated in the passport, in the Vydmantai-1 well.

The boreholes are not exploited from year 1992. Boreholes owner is JSC" Vydeko"

Engineering networks and distances from the territory:

- Geothermal wells - within the boundaries of managed land parcels;
- AB Litgrid main electricity network to support -1500m;
- AB ESO's high-voltage networks - within the boundaries of managed land parcels;
- AB ESO's electricity input power is 20MW within the boundaries of the managed land parcels;
- AB Amber Grid main gas pipeline - 200m;
- Internal gas pipeline network of AB ESO -100m;
- City water supply and sewage networks - within the boundaries of managed land parcels;
- Water industrial borehole - within the boundaries of managed land parcels;
- Rain nets - within the boundaries of managed sedge plots.

Distances from the territory (plots of land) to:

- Klaipėda city's frost-free sea port - 25 km,
- The sea port of the city of Liepaja (Latvia) - 80 km
- Venspils (Latvia) city seaport - 200km,
- Palanga City Airport - 11km,
- Kaunas airport - 240 km
- Riga city (Latvia) airport - 260km
- Vilnius airport - 330 km
- Kretinga city railway cargo and passenger station (Klaipėda-Vilnius) - 8km
- A11 Šiauliai–Palanga highway -750m

Source:

Well 26327 passports

Tyrimu protokolas Nr. 230324GC019 data: 2023-03-24 ID 67967

Obiektas Grezinvs 10880

Vandens bendroji chemine analize

Analite	mg/l	mg-ekv./	I ekv.%	Analizcs metod as
Aniionai				
Chloridas, Cl	49900	1407	97.6	LST EN ISO 10304-1:2009
Sulfatas, SO 4	1647	34.3	2.38	LST EN ISO 10304-1 :2009
Hidrokarbonatas, HCO 3	<10.0			LST EN ISO 9963-1: 1999
Karbonatas CO3	<0.01			
Nitritas NO 2	<0.05			LST EN ISO 10304-1 :2009
Nitratas NO 3	<0.10			LST EN ISO 10304- 1 :2009
Katiionai				

Natris, Na+	22100	961	66.3	LST EN ISO 14911:2000
Kalis, K	518	13.3	0.917	LST EN ISO 14911 :2000
Kalcis, Ca 2	6302	314	21 .7	LST EN ISO 1491 I :2000
Magnis Mg	1948	160	11.0	LST EN ISO 1491 1:2000
Gelezis ;bendra Fe	10.1			LST ISO 6332: 1995 CN
Amonis NH 4	25.2	1.40	0.097	LST I SO 7150-1: 1998(N)

Itirpusiu mineralinių medžiagų suma = 82445 mg/I

C02 (pusiausvyrinis) = 32.2 mg/I

Sausa liekana 180°C = 82445 mg/I

Source: Vandens tyrimai, 2023-03-24

LIETUVOS GEOLOGIJOS TARNYBA PRIE APLINKOS MINISTERIJOS

GRĘŽINIO PASAS

Grežinio identifikavimo Nr. 70580

Zemes gelmių tyrimo identifikavimo Nr.

Paso pateikėjas	UZDAROJI AKCINE BENDROVE „ARTVA"	Juridinio ar fizinio asmens kodas	120404147
Buveine (adresas)	Vilniaus m. sav. Vilniaus m. Eisiskių pl. 26		
Rangovas	UZDAROJI AKCINE BENDROVE „ARTVA"	Juridinio ar fizinio asmens kodas	120404147
Buveine (adresas)	Vilniaus m. sav. Vilniaus m. Eisiskių pl. 26		
Jungtines veiklos sutarties sudarymo data/numeris			

Duomenų naudojimo apribojimas, metai ------

Grežinio ziocių koordinatės (LKS-94 sistemoje) X 6204713 m Y 317116 m

Grežinio kirtavietės koordinatės (LKS-94 sistemoje) X m Y m

Grežinio adresas

Valstybė	Apskritis	Savivaldybė/Seniūnija	Gyvenamoji vietovė (miestas, miestelis, kaimas)	Gatvė	Namas
Lietuva	Klaipėdos	Palangos m.	Palangos m.	Vanagupės	15

Žemės sklypo (adastrinis numeris) 2501/0021:101 Pastabos

Grežinio pavadinimas

Pirminio dokumento tipas GREŽ. B.

Pirminio dokumento Nr. 6281

Ataskaitos fondinis Nr.*

Knygėlės pakelio Nr.*

Knygos Nr.*

Fond. kortelės Nr.*

Grežinio įrengimo data 2019 07 05

Grežinio ziocių a. a., m 6.33

Grežinio gylis, m 570.0

Grežinio įžeminio ilgis, m

Savininkas (pasikeitus grežinio savininkui, apie tai būtina pranešti Registro tvarkymo įstaigai):

	Vardas	Pavardė	Fizinio asmens kodas
Fizinis asmuo			
Adresas			
Data nuo		Data iki	

Juridinis asmuo	UAB „SVEIKATOS UOSTAS"	Juridinio asmens kodas	303997416
Buveine (adresas)	Palangos m. sav. Palangos m. Vanagupės g. 15		
Data nuo	20190705	Data iki	

Juridinių ir/ar fizinių asmenų grupė, veikianti pagal jungtinės veiklos sutartį

Jungtinės veiklos sutarties sudarymo data/numeris

Data nuo Data iki

Objekto tipas Objektas

*Pildo Lietuvos geologijos tarnybos Žemės gelmių registro tvarkytojas

1

NACIONALINIS MAISTO IR VETERINARIJOS RIZIKOS VERTINIMO INSTITUTAS

J.Kairiuksciog.10,LT-08409Vilnius
Tel. (370-5) 2780470 Faks. (370-5) 2780471
El.pastas: info@nmvrvi.lt

TYRIMŲ PROTOKOLAS Nr. 1-19/14643/1 CH

Savikontrole

Meginio (-ių) gavimo data: 2019-06-27 Tyrimų atlikimo data: 2019-07-15

Uisakovo duomenys:

Uzsakovopavadinimas, adresas: UAB "ARTVA" im.k. 120404147, Eisiskiu pl. 26, Vilnius

Meginio (-ių) aprasymas: Pazeminis mineralinis vanduo (mineralizacija 20g/l), 5L.
Paimta 2019-06-26, 13:30 val., is grzinio Nr.70580, sanatorijos "GRADIALI" vandenvietes, Vanagupes g. 15, Palanga.

Meginio (-ių) paemimo tvarka**: Aktas, 2019-06-27. UAB "ARTVA" vyriausiasis hidrogeologas N.Šeirys

Megini(-ius) pristate: N.Šeirys

TYRIMO REZULTATAI

Alavas (Sn), µg/L	< 5	SDP 5.4.4.Ch.169 (4 leidimas)
Aliuminis (Al), µg/L	< 20	SDP 5.4.4.Ch.169 (4 leidimas)
Arsenas (As), µg/L	4,63 ± 0,56	SDP 5.4.4.Ch.169 (4 leidimas)
Baris (Ba), µg/L	21,8 ± 1,7	SDP 5.4.4.Ch.169 (4 leidimas)
Bendras gyvsidabrio kiekis, µg/L	< 0,1	SDP 5.4.4.Ch.169 (4 leidimas)
Berilis (Be), µg/L	< 0,2	SDP 5.4.4.Ch.169 (4 leidimas)
Bismutas (Bi), µg/L	< 1	SDP 5.4.4.Ch.169 (4 leidimas)
Ceris (Ce), µg/L	< 1	SDP 5.4.4.Ch.169 (4 leidimas)
Cezis (Cs), µg/L	< 1	SDP 5.4.4.Ch.169 (4 leidimas)
Chromas (Cr), µg/L	< 5	SDP 5.4.4.Ch.169 (4 leidimas)
Cinkas (Zn), µg/L	< 20	SDP 5.4.4.Ch.169 (4 leidimas)
Kadmis (Cd), µg/L	< 0,2	SDP 5.4.4.Ch.169 (4 leidimas)
Kobaltas (Co), µg/L	1,15 ± 0,10	SDP 5.4.4.Ch.169 (4 leidimas)
Lantanas (La), µg/L	< 1	SDP 5.4.4.Ch.169 (4 leidimas)
Litis (Li), µg/L	74,8 ± 6,4	SDP 5.4.4.Ch.169 (4 leidimas)
Manganas (Mn), µg/L	130 ± 11	SDP 5.4.4.Ch.169 (4 leidimas)
Molibdenas (Mo), µg/L	2,01 ± 0,27	SDP 5.4.4.Ch.169 (4 leidimas)
Nikelis (Ni), µg/L	<2	SDP 5.4.4.Ch.169 (4 leidimas)

Rubidis, µg/L	61.8±5,7	SDP 5.4.4.Ch.169 (4 leidimas)
Selenas (Se), µg/L	<1	SDP 5.4.4.Ch.169 (4 leidimas)
Sidabras (Ag), µg/L	<1	SDP 5.4.4.Ch.169 (4 leidimas)
Stibis (Sb), µg/L	<0,2	SDP 5.4.4.Ch.169 (4 leidimas)
Stroncis (Sr), mg/L	21,5±2,6	SDP 5.4.4.Ch.169 (4 leidimas)
Švinas (Pb), µg/L	<I	SDP 5.4.4.Ch.169 (4 leidimas)
Talis (Tl), µg/L	<0,I	SDP 5.4.4.Ch.169 (4 leidimas)
Tolis (Th), µg/L	<1	SDP 5.4.4.Ch.169 (4 leidimas)
Uranas (U), µg/L	1,30± 0,10	SDP 5.4.4.Ch.169 (4 leidimas)
Vanadis (V), µg/L	9,7± 1,4	SDP 5.4.4.Ch.169 (4 leidimas)
Boras (B), mg/L	2,59±0,33	SDP 5.4.4.Ch.169 (4 leidimas)
Kalcis (Ca), mg/L	1247±118	SOP 5.4.4.Ch.169 (4 leidimas)
Kalis (K), mg/L	140±10	SOP 5.4.4.Ch.169 (4 leidimas)
Magnis (Mg), mg/L	379±34	SDP 5.4.4.Ch.169 (4 leidimas)
Natris (Na), mg/L	4051±308	SOP 5.4.4.Ch.169 (4 leidimas)
Varis (Cu), mg/L	<0,02	SOP 5.4.4.Cl1.169 (4 leidimas)
Jodidas, mg/L	<0,20	SOP Ch.31:2019:1:

Paaiskinimas : Nr....CH - Chem inil!tyrim4 skyrius.
"<"-reiskia, kad analites koncentlacija meginyje yra mazesne nei galima nustatyti ir kiekybiskai ivertinti duotuoju analizes metodu.
± isplestine matavim4 neapibrėztis, apskaiciuota is standartines neapibrezties, naudojant aprepties daugikli k=2, kuris esant noll naliajam skirstiniui duoda apie 95% pasiklio vimo lygmeni.
* - NAB neakredituota sritis.

Tyrimij rezultatai yra susij tik su pateiktu meginiu.
** Institutas meginiq neima ir uz jq paemim<i neatsako.
Institutas neprisiima atsakomybes U Z uzsakovo pateiktus duomenis.
Be [illegible] boti [illegible]

Well -Vilkyčiai-3 prospective for geothermal utilization

There is a number of active wells for oil exploitation in west Lithuania. In total, 86 wells are registered by the Lithuanian Geological Survey. There are a few wells that can be potentially applied for fish farming, while other wells are still exploited.

The first oil exploration well Vilkyčiai-1 was drilled in 1969. The top of the structure is defined at -1931 m in the well Vilkyciai-1 There are 15 wells shown on the map (**Figure 129)**. Based on the seismic survey, most of the wells are situated on the crestal part of the Vilkyčiai Uplift based on the seismic survey. The oil-water contact is defined -1973 m in the Vilkyčiai oil field.

The well Vilkyčiai-3 was drilled in 1970 close to the contact oil field, outside the oil contact. The top of the Deimena reservoir is situated at -1983.2 m in this well. Similar parameters are recorded in the well Vilkyčiai-5, outside the oil field limits.

The design of the well is typical for the west Lithuanian. The conductor of 8 m is followed by 215 m deep casing to friable Lower Cretaceous green sand. The second pipe isolated the Šventoji-Upninkai aquifer, but not the underlying Lower Devonian Kemery aquifer. The exploitation pipe was inserted to as deep as 2156.0 m (**Figure 129**).

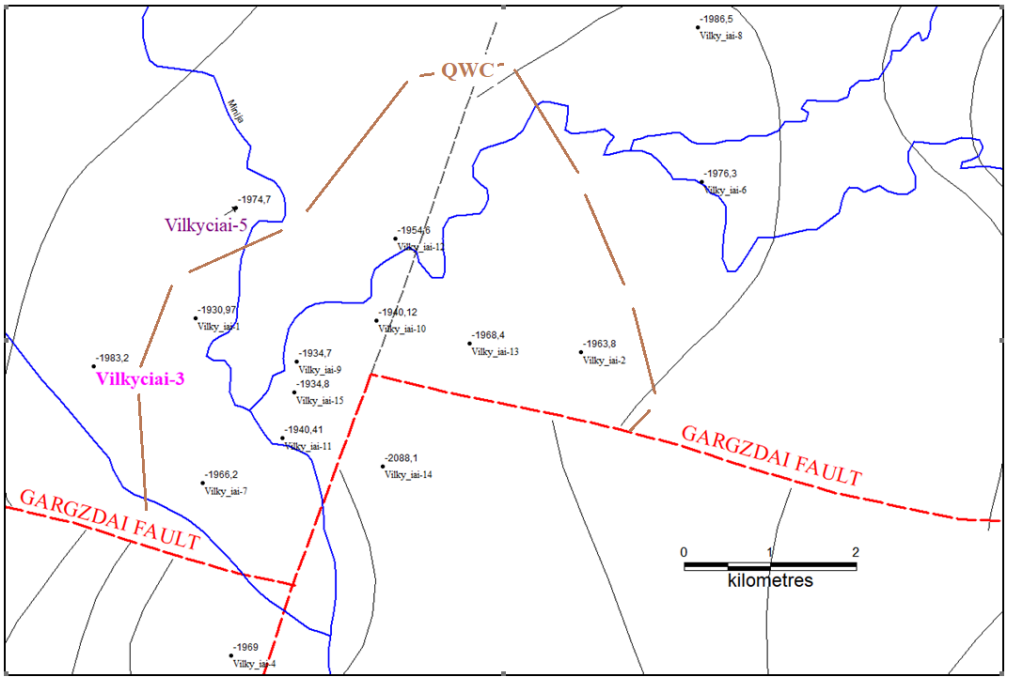

Figure 135: *Wells drilled in the Vilkyčiai oil field. Well Vilkyčiai-3 and Vilkyčiai-5 are located on the Vilkyčiai Uplift on the western flank, beyond the oil contour (brown line). The Gargždai fault was shown (red line).*

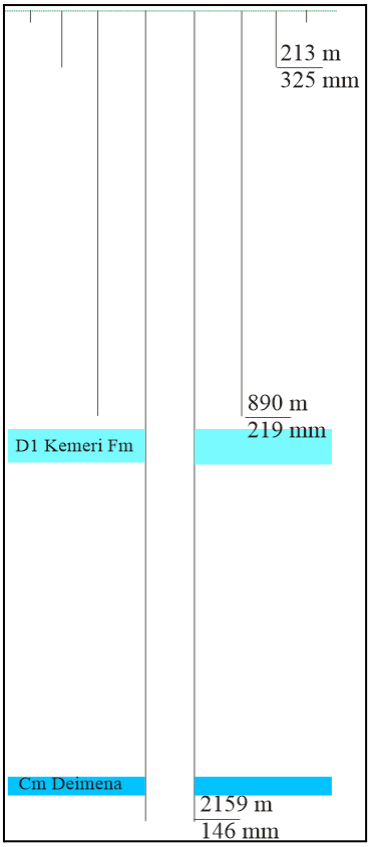

Figure 136: *Construction of the well Vilkyčiai-3. Well is cased by the exploitation of steel pipe. The Deimena section was perforated for well testing. Later, the perforation was carried out in Kemeri section in 1993(discussed below).*

X.1. Deimena aquifer (Cambrian)

In the well Vilkyčiai-3, the depth of the Deimena RSt is defined at 1983.9-2066.20 m and the thickness 76.9 m, as recorded in drill cores and well logging. The crystalline basement was drilled at the interval 2134.2-2154.2 m (24.5 m). Based on the interpretation of the well logging, the top of the basement is strongly weathered (1.5 m thick).

Based on the well logging interpretation, the effective thickness of the low-quality sandstone of 20 m was recorded in the well (0.26%) which is in concert with the Lithuanian-scale effective thickness map.

Gamma-ray and NGR logs show two distinct reservoir parts referred to as the Upper Sandstone (interval 1983.9-2035.5 = 51.6 m) and Lower Sandstone (interval 2035.5-2066.20 = 30.7 m). The upper reservoir is represented by bedded sandstones (a few centimeters- and 10-centimeter-thick) and thin-bedded sandstones (**Figure 130**).

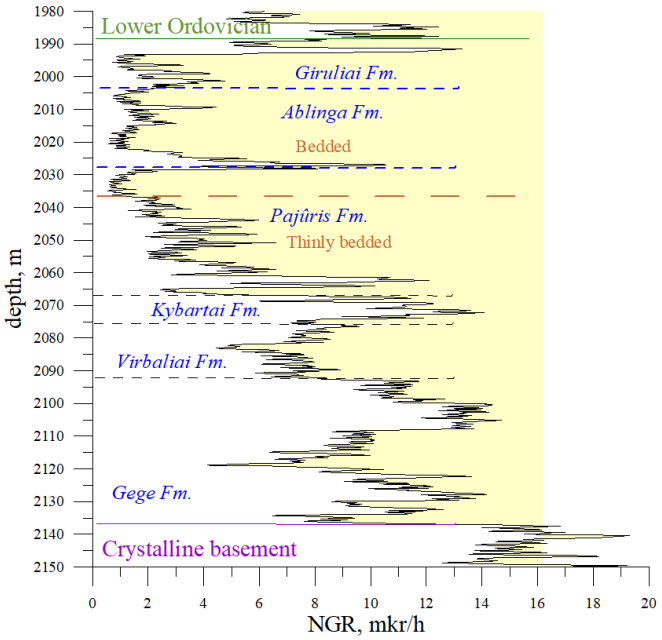

Figure 137: Stratigraphy and lithology of sandstones and interlaying shales of Cambrian succession, well Vilkyčiai-3. Upper bedded sandstone and thinly bedded sandstone in the lower part of the reservoir.

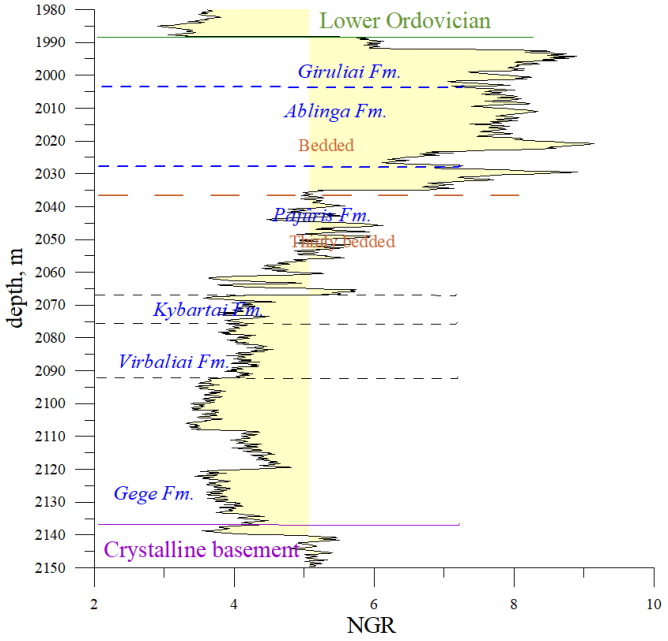

Figure 138: Two distinct sandstones are defined in the Deimena reservoir (boundary defined at the depth of 2035.5 m). The prospective upper reservoir was defined based on well logging interpretation and correlates with well testing results (see below).

Only the upper part of the Deimena RSt was drilled by coring, while the lower part was studied using logging methods (**Figure 132**). Also, the hydrodynamic testing of the well was carried out int. 1994-2004 m (Giruliai Fm.). The calculated permeability shows the rather high quality 52.4 mD (testing duration 34 min.). It correlates with permeability measured in the core samples.

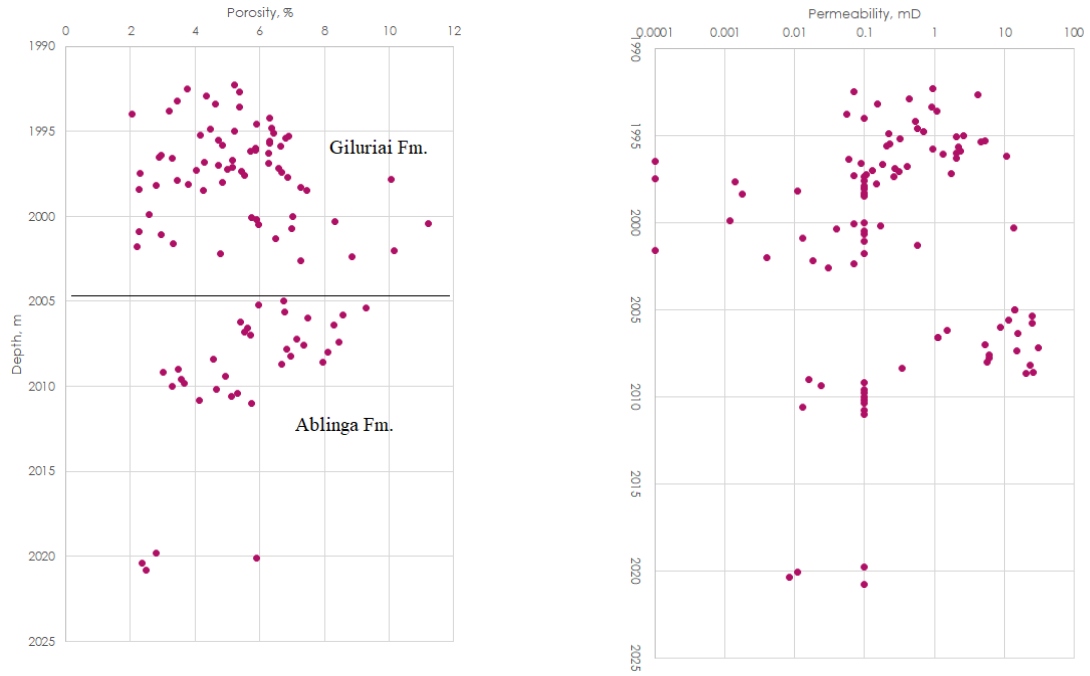

Figure 139: . Porosity and permeability of sandstones, well Vilkyčiai-3. Average porosity was calculated 5.46% and permeability 2.98 mD (strongly cemented sandstone by quartz comprising 2 layers of 3-4 m thick). No coring was carried out below 2020.8 m.

The chemical composition of the Deimena water was measured at the depth of 1992-1998 (Giruliai Fm.) and 2023-2038 m (Pajūris Fm.). The type of water is classified as Na-Ca-Cl and shows strong depletion in SO_4, as typical for west Lithuanian wells.

Table A2.1. Chemical composition of the water of Deimena RSt. (int. 1992-1998 m in the Giruliai Fm. and 2023-2038 m in the Pajūris Fm.).

Interval	Density g/cm3	TDS g/L	pH	Cl mg/L	SO_4 mg/L	HCO3 mg/L	Na mg/L	K mg/L	Mg mg/L	Ca mg/L
1992-1998	1.0603	148.9	-	88402	306	42	28853	900	2456	20645
2023-2038	1.118	1697	5.9	103225	284	60	29328	773	2851	26419

X.1. Kemeri aquifer of lower Devonian

The thickness of Kemeri Fm. is thrice as large compared to the Deimena reservoir. There are no drill cores and information on the Kemery reservoirs is solely based on well logging. The thickness reservoir was defined at 143 m (922.0-1065.0 m).

The old wells re-open with no special technical operations. As far as the Vilkyčiai-3 and Vilkyčiai-5 are located outside the oil contour, the wells were perforated in 1993. The well testing was performed to study the quality of the Kemery reservoir.

Two reservoir layers are defined in the reservoir succession (**Figure 134**). The effective thickness was assessed at **41 m** (total thickness 51 m) and **50 m** (total thickness 67 m) based on

the interpretation, respectively. The total effective thickness was defined at 91 m (net-to-gross was calculated 0.64 which is typical for Kemeri reservoir in west Lithuania).

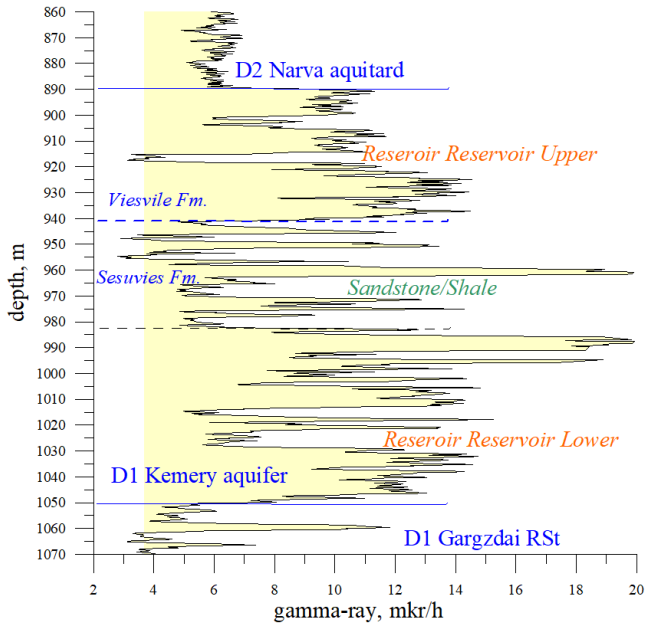

Figure 140: . Gamma-ray logging curve. Two distinct aquifers are defined in the Kemery Fm. (thickness 51 m and 67 m). The net-to-gross ratio was calculated at 0.64.

The well testing defined very high reservoir quality. The permeability was defined as high as 4950 mD in the Upper sandstone and 2280 mD in the Lower sandstone. However, the injectivity is drastically different compared to high productivity. The well productivity was estimated at 33.64 $m^3/h/at$ and 51.1 $m^3/h/at$, while injectivity is poor at 0.76 $m^3/h/at$ and 0.86 $m^3/h/at$. It implies the drastic skin effect in the well due to drilling mud infiltration and damage to the reservoir, similar to the Klaipeda geothermal wells.

Assuming the drawn down as low as 400 m, the production (discharge) of the Lower sandstone is calculated 1286 m^3/h and 945 m^3/h. (total 2261 m^3). The large discharge is related to excellent permeability, large depth, and low viscosity. The diameter of the well is rather small (144 mm). The dramatic difference in the re-calculated volume of injected water should be strongly stressed: 112 m^3/h and 50 m^3 (total 162 m^3/h).

The calculated heat extraction from two sandstone layers was calculated at 3.5 MW_{th} and 1.6 MW_{th}. (total 5.1 MW_{th}) assuming 400 m drawdown and $\Delta 26^oC$.

Remark: well testing points to severe damage to the reservoir quality (fine-grained friable sandstones). This particular well can be easily converted to geothermal exploitation of hot, provided the new injection well was drilled beside the old production well connected with exchanger. Some part of the water supplied from the well can be used for re-recycling of the fish breading pond. Another alternative is using only saline water for the fish pond with no extra heating from the how brine. In any case, the 'wastewater' problems should be clearly considered.

To my knowledge, there is no comprehensive publication on the application of the geothermal for farming set in the sedimentary basin subject to igneous and hydrothermal activity. The Polish case should be analysed in particular.

The temperature of the Kemeri geothermal aquifer was measured 48°C (well Vilkyčiai-11), and 52°C (Vilkyčiai-7). The first well Vilkyčiai-1 drilled in the oil field shows technical

inconsistencies. In general, the Vilkyčiai site shows the highest temperature measured in west Lithuania and the much lower temperature was defined in the Klaipėda geothermal site.

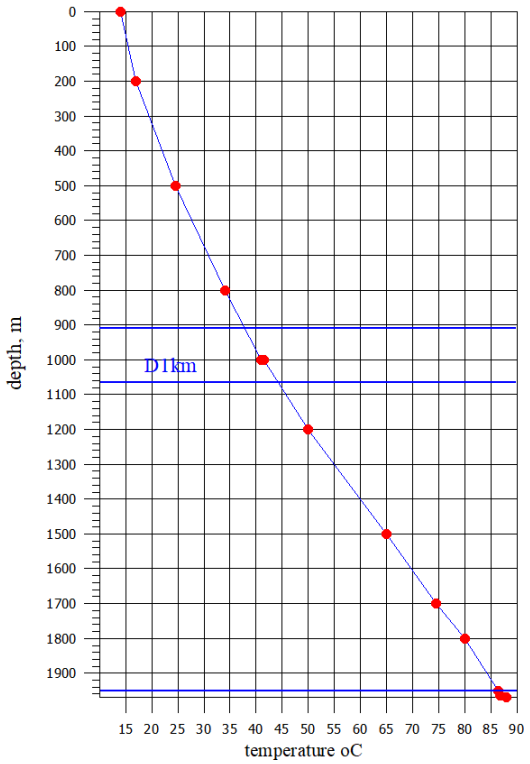

Figure 141: Regular measurements of temperature and measurement of temperature in the Deimena reservoir. Please note higher thermal gradient was defined in the Silurian shales. The temperature 41°C was measured in the Kemery interval and is similar to Klaipėda wells.

The mineralization of the Kemery water is somewhat lower compared to the Klaipėda geothermal plant which shows the highest salinity in Lithuania (82 g/L compared to 100 g/L mineralization). The sulfur and carbon elements are significantly enriched which correlates with the high concentration of other elements (Br=270 mg/L, B=7.95 mg/L). Rather low concentration of SiO_2 and moderate content of Fe are noted. pH was estimated at 5.71.

Table A2.2. The chemical composition of the Kemeri water is presented below (mg/L):

Depth	*TDS*	*Na*	*K*	*Mg*	*Ca*	*Cl*	*SO_4*	*HCO*	*Fe*	*Br*	*SiO_2*	*B*
~1000	82445	22100	518	1946	6302	49900	1647	<10	10.1	270	<2	7.95